DEVELOPMENT OF A PHYSIOLOGICALLY-BASED PHARMACOKINETIC MODEL FOR JET FUELS IN THE RAT

by

SHEPPARD ALLEN MARTIN

(Under the Direction of Jeffrey W. Fisher)

ABSTRACT

The pharmacokinetic behavior of the majority of jet fuel constituents has not been previously described in the framework of a physiological-based pharmacokinetic (PBPK) model for inhalation exposure. Exposure-related effects have been reported in multiple organ systems, though exposure methods were different across studies, utilizing either vaporized or aerosolized fuels. Uncertainties in the kinetics associated with both exposure types previously represented a barrier to model development and interpretation of toxicity data. While assessments of pharmacokinetics and metabolic interactions have been conducted for binary to quaternary hydrocarbon mixtures, few models exist for higher-order fuel or solvent mixtures. The purpose of this work was first to elucidate the characteristics of the dynamic chamber environment and assess the effect on pharmacokinetic behavior of aerosolized jet fuels, in comparison to vaporized fuels. Using this information, individual PBPK models were developed to assess chemical behavior and then combined into the first PBPK model for petroleum-based and synthetic jet fuels. The resulting models were capable of predicting individual chemical and fuel kinetic behavior following both vaporized and aerosolized chemical exposures. To support model development, exposures to individual n-alkanes n-octane and n-tetradecane were

conducted at 89 mg/m^3 aerosol+vapor and 100-5000ppm vapor, respectively. Exposures to JP-8 and S-8 were conducted at ~900-1000 mg/m^3, and to a 50:50 blend of both fuels at ~200 mg/m^3 aerosol+vapor. A novel computational description of the respiratory tract was developed, with concentrations directed to either gas-exchange or respiratory tract tissue compartments, describing vapor and aerosol uptake respectively. Visceral tissue compartments were described using perfusion and diffusion-limited equations connected by blood. The model described the kinetics of individual chemicals and fuel constituents at multiple aerosol and vapor concentrations, utilizing a chemical "lumping" strategy to estimate parameters for unspeciated fuel fractions. The model more accurately simulated data for aromatic and lower molecular weight (MW) n-alkanes than for some higher MW chemicals. Metabolic interactions were more pronounced at high total fuel concentrations (~2700 - 1000 mg/m^3) than at low concentrations (400 - 200 mg/m^3). This model serves as the most detailed assessment of fuel pharmacokinetics to date.

INDEX WORDS: Jet Fuel, n-Alkane, Aromatic, Hydrocarbon Mixture, Rat, PBPK Model

DEVELOPMENT OF A PHYSIOLOGICALLY-BASED PHARMACOKINETIC MODEL FOR JET FUELS IN THE RAT

by

SHEPPARD ALLEN MARTIN

BS, University of Georgia, 2003

MPH, University of Georgia, 2006

A Dissertation Submitted to the Graduate Faculty of The University of Georgia in Partial Fulfillment of the Requirements for the Degree

DOCTOR OF PHILOSOPHY

ATHENS, GEORGIA

2010

DEVELOPMENT OF A PHYSIOLOGICALLY-BASED PHARMACOKINETIC MODEL FOR JET FUELS IN THE RAT

by

SHEPPARD ALLEN MARTIN

Major Professor: Jeffrey W. Fisher

Committee: James V. Bruckner
W. Matthew Henderson
David R. Mattie
Luke P. Naeher

Electronic Version Approved:

Maureen Grasso
Dean of the Graduate School
The University of Georgia
May 2010

DEDICATION

To my family and friends for their support and kind gestures during this period in my life.

ACKNOWLEDGEMENTS

I would like to express my gratitude to current and former students and staff that provided guidance or assistance in support of my time in graduate school: Christine Kendrick, Kristyn Flynt, Ella Willingham, Tammy L. Ray, Joanne Mauro, Drs. Raphael T. Tremblay, Jerry L Campbell, Jr., Eva D. McLanahan, Babatope Fatuyi, Oluseye Ogunmoroti, and Satheesh Anand. My committee members, Drs. James Bruckner, Matthew Henderson, David Mattie, and Luke Naeher provided support, thought provoking questions, and encouragement in meetings and in conversations on campus. I would most like to thank my advisor, Dr. Jeffrey Fisher, whose confidence in my abilities, expert tutelage, and constant encouragement kept me driving forward to this point.

Funding for this work was provided by the Air Force Office of Scientific Research (AFOSR) grant #: FA9550-07-1-0132.

TABLE OF CONTENTS

Page

LIST OF TABLES

Page

LIST OF FIGURES

Page

CHAPTER 1

INTRODUCTION AND LITERATURE REVIEW

Rarely are humans exposed to only high doses of single chemicals, as has been reflected in the majority of laboratory animal studies. In reality, humans are exposed to complex mixtures of exogenous chemicals containing pharmaceuticals, food additives, solvents, and a myriad of other potential toxicants at home and in occupational settings. The single largest occupational chemical exposure for military service personnel is Jet Propellant-8 (JP-8); a complex mixture of hydrocarbons used to fuel aircraft, ground vehicles (armored vehicles and Humvees), and small scale equipment such as tent heaters. The chemical composition of neat JP-8 is essentially the same as that of the commercial domestic jet fuel, Jet-A, suggesting potential relevance for this work in the civilian fuels arena(NRC, 2003, Ritchie *et al.*, 2001b, Ritchie *et al.*, 2003). JP-8 does differ from Jet-A in the addition of comparatively low concentrations of performance additives, such as de-icers and rust inhibitors, however the presence of toxic aromatic, aliphatic, and naphthenic constituents remains in both fuels. In addition to the US Air Force standard fuel JP-8 (and similar Navy JP-5), the U.S. Department of Defense (including U.S. Air Force, Navy, and Army) is phasing in a 50:50 blend of JP-8 and a synthetic jet fuel (S-8) produced from coal, natural gas, or biomass (DOD, 2008). While chemical comparisons and flight performance tests have been conducted using the petroleum-based, synthetic, and blended fuel, the tissue kinetic behavior of aerosolized JP-8, S-8 and the blended fuel has not previously been reported in the literature and is original to this work (Chavanne, 2007, Hemighaus, 2007, Hernandez, 2007, Moses, 2008, Moses, 2009).

In light of these recent changes and the relative paucity of pharmacokinetic data in the literature on jet fuels, the pharmacokinetics of JP-8, S-8, and the 50:50 JP-8:S-8 blend were determined using inhalation exposure. Additionally, custom-made simple mixtures of prominent jet fuel constituents, and prominent individual chemicals were examined using inhalation exposure. The resulting data was used to develop a physiologically-based pharmacokinetic (PBPK) model to describe JP-8, S-8, and blended JP-8:S-8 pharmacokinetics. These PBPK models will inform the specific pharmacokinetic and toxicologic literature on complex mixtures and individual hydrocarbon constituents. Additionally, model development and publication of the tissue data sets may aid in performance of future risk assessments and review or modification of current exposure limits for petroleum-based and synthetic jet fuels.

PURPOSE OF STUDY

The overarching purpose of this work was to develop a complex mixture PBPK model for exposure to both aerosolized and vaporized jet fuels, using the most detailed assessment of chamber chemical composition to date. In support of this goal, a nose-only inhalation exposure chamber was developed and characterized (Martin *et al.*, 2010, Tremblay *et al.*, 2010b). PBPK models for individual constituents and jet fuel were then developed; based either on existing published data or on data generated in this dissertation project. It was hypothesized that a detailed characterization of the fuel exposure atmospheres, along with inclusion of validated models that were capable of describing aerosolized and vaporized fuel data, would facilitate development of a single PBPK model to address fuel dosimetry, potential metabolic interactions, and provide predictions of the internal tissue dose following exposures at concentrations reported in the fuel literature.

SCOPE OF DISSERTATION

This dissertation includes a detailed literature review (Chapter 1) of the current state of jet fuel and hydrocarbon mixture modeling; providing insight into the achievements of the past and areas where renewed focus has been brought to the field. In the next chapter (Chapter 2), the design and characterization of an inhalation exposure system (Figure 1) for the study of aerosolized and vaporized jet fuel and jet fuel constituents, is described. The jet fuel PBPK model is described in the next chapter (Chapter 3), along with predictions and applications. This work serves as the most detailed assessment of jet fuel pharmacokinetics and fuel model development to date. The chapter covers aerosol and vapor deposition and uptake, with comparison to data collected under both exposure regimens, distribution to organs of interest, and the influence of competitive metabolic inhibition on the clearance behavior. In order to lay the foundation for fuel exposure studies and PBPK model development, the author sought to improve his understanding of solvent exposure characterization and associated sampling methodologies (Chapter 4). Existing occupational hygiene and chamber sampling methodology was used to assess ambient exposure to the industrial solvent trichloroethylene (TCE), in an Athens-area community concerned about releases of the toxicant into the environment near homes and an elementary school. The benefit of this work was to familiarize the author with sampling techniques and to foster an understanding of analytical chemistry in the determination of chemical concentrations using adsorbent tube and filter methods. This work was published in 2007. It serves as the first publication of this dissertation research project (Martin *et al.*, 2005). Of note, the publication date listed from the journal is the result of the publisher's attempt to retain timelines following a period when no journal volumes were published. The actual publication year was 2007.

The current state of model development is then discussed (Chapter 5) in the context of the path forward, as it pertains to the fuel mixture and individual chemical PBPK models described herein. The implications of this modeling effort on exposure limits and risk assessment for complex mixtures are also covered.

LITERATURE REVIEW

Approximately 300 billion/gal/year of petroleum was consumed in the U.S. in 2008, the most recent data reported by the Energy Information Administration. Of that total, 25 billion/gal/year was consumed in the form of kersosene-based aviation fuel, with the remainder as gasoline (140 billion/gal/year), diesel (52 billion/gal/year), and various other petroleum products (84 billion/gal/year) (EIA, 2008). Of the 5 billion/gal/year of jet fuel consumed by the U.S. Department of Defense in 2008, the largest consumers were the U.S. Air Force and U.S. Navy, accounting for 2.5 and 1.3 billion/gal/year, respectively (DOD, 2008). Current U.S. Air Force use is specific to Jet Propellant-8 (JP-8) while Navy use is either JP-5 or JP-8 depending on application. Exposure of flightline personnel to these and other complex hydrocarbon mixtures is most common while conducting tasks such as refueling, foam installation, maintenance, tank entry, and after cold starts, while other personnel may be exposed during dust suppression activities where fuel is aerosolized, or pesticide application where JP-8 is a vehicle (NRC, 2003, Ritchie *et al.*, 2003). As the primary routes of exposure for military personnel are via inhalation and dermal contact, the majority of toxicologic studies have focused on identification of exposure induced toxicity to the integumentary, auditory, nervous, and respiratory systems, and for identification of biomarkers in breath or urine that may be useful in exposure assessment (Chao *et al.*, 2006, Egeghy *et al.*, 2003, Kaufman *et al.*, 2005, Monteiro-

Riviere *et al.*, 2001, Rhodes *et al.*, 2003a, Ritchie *et al.*, 2001a, Serdar *et al.*, 2004, Serdar *et al.*, 2003).

Inhalation of jet fuel has been reported to result in CNS symptoms including dizziness, nausea, altered mobility, and other neurological endpoints in the human (Knave *et al.*, 1979, Knave *et al.*, 1978, Knave B, 1976, Porter, 1990, Smith *et al.*, 1997b, Tunnicliffe *et al.*, 1999), as well as the rodent (Ritchie *et al.*, 2001a, Rossi *et al.*, 2001). A comprehensive literature review detailing fuel neurotoxicity studies has been compiled for aviation fuels, where high brain:blood partition coefficients and the lipophilic nature of prominent jet fuel components, contribute to uptake of these compounds and their metabolites to the brain (Ritchie *et al.*, 2001b).

A review of the respiratory effects of jet fuels was included in a larger review by Ritchie *et al.* (2003). Several authors have reported irritation, release of biomarkers of exposure from cells in the rat or mouse lung, or direct observable toxicity (apoptosis) to Type II cells of the lung(Drake *et al.*, 2003, Hays *et al.*, 1995, Pfaff *et al.*, 1995, Stoica *et al.*, 2001, Whitman and Hinz, 2001, 2004, Witzmann *et al.*, 1999).

Immunosuppression has been widely reported in laboratory animals after short and long-term exposure, across multiple concentrations, by inhalation as well as the dermal route (Harris *et al.*, 1997, Harris *et al.*, 2000, Ramos *et al.*, 2007, Ullrich, 1999). The implications are that short duration repeated exposures have the potential to significantly alter the in vivo immune system of mammals. Similar immune system effects have not been reproduced in humans occupationally exposed to jet fuels (Rhodes *et al.*, 2003a). The findings of Rhodes *et al.* (2003a) were that white blood cells, neutrophils, and monocytes were elevated in highly exposed personnel with no changes in other immune cell counts. Unfortunately, with the exception of this work, there is very little epidemiological data available fully asses the potential for

immunotoxicity in exposed human personnel. In notable recent studies, inhaled S-8 has also been shown to induce cellular and immunotoxic effects at low exposure concentrations (Wong *et al.*, 2009, Wong *et al.*, 2008). This is the first S-8 toxicity data to have been reported for animals exposed via inhalation.

Aliphatic fuel constituents may also alter reproductive endocrine hormones related to conception in women (Reutman *et al.*, 2002). Modulation of lutenizing hormones in female personnel may have long term implications for military personnel of child-bearing age. This effect has not been noted in the rodent exposure literature. However, benzene and other solvents, such as toluene, have been identified as having reproductive toxicity in women and may lead to reduced birth weight and subfecundity (Chen *et al.*, 2000, Plenge-Bonig and Karmaus, 1999, Sallmen *et al.*, 1995, Smith *et al.*, 1997a). Significant affects on male reproductive capability have not been noted in fuel exposed personnel, though aircraft painters with solvent exposure were reported to have significantly reduced sperm motility (Lemasters *et al.*, 1999). Toluene, a fuel constituent, has been noted for its reproductive toxicity in the male; specifically in oxidative damage to the spermatozoa (Nakai *et al.*, 2003).

Several authors have investigated biomarkers for evaluation of dosimetry in the exposed human. Exhaled breath, blood, and urine concentrations of naphthalene, benzene, and other solvents and metabolites have been monitored and assessed in exposed flightline personnel (Chao *et al.*, 2006, Egeghy *et al.*, 2003, Lockey *et al.*, 1999, Serdar *et al.*, 2004). This work may have future implications for development of a human PBPK model for fuel exposure.

Adding to the list of potential exposures involving complex hydrocarbon mixtures, the U.S. Air Force is in the process of transitioning from use of JP-8 as the sole fuel, to a 50:50 blend of petroleum-based JP8 and a synthetic jet fuel (S8) derived from the Fischer-Tropsch

process. Completion of the certification process is slated for the year 2011. It is proposed that 50% of jet fuel production will be from domestic sources by 2016 (Arnold Engineering Development Center Public Affairs, 2008). When blended 50:50 with petroleum-based JP-8, it is suitable for use in military engines and may be produced from domestic sources (Arnold Engineering Development Center Public Affairs, 2008, Hemighaus, 2007, Hernandez, 2007). The inhalation pharmacokinetics of S-8 and blended JP-8:S-8 have not been reported prior to this dissertation project.

While JP-8 is comparatively rich in aromatic compounds with noted health effects, the S-8 fuel replaces the aromatic fraction with higher concentrations of branched (iso)- and straight-chain aliphatics with comparatively little toxicologic data available on the majority of components within the fuel. On an individual basis, there is a limited amount of in vitro data describing effects of iso-alkanes on Syrian Hamster Embryos (SHE). 2-methylheptane and 2-methyloctane were reported to potentiate the effect of benzo(a)pyrene on SHE cells, while 2-methyloctane and 2-methylnonane reduced intercellular communication (Rivedal *et al.*, 1992). The inhalation pharmacokinetics of these iso-alkanes has also been reported, though at high concentrations, 100ppm 12hr/day/3days (Zahlsen *et al.*, 1993). Limited metabolism data is available (Mortensen *et al.*, 2000). However, the kinetics of simple or complex mixtures is lacking in the literature for the majority of S-8, and JP-8, iso-alkane constituents. To successfully describe the kinetics of fuel and fuel constituents, a computational modeling approach that accounts for some or all chemicals with reported individual and mixture derived kinetic data, as well as for the remainder of the less defined constituents in the exposure atmosphere, is required.

PBPK Modeling

Physiologically-based pharmacokinetic (PBPK) models are complex systems of equations and related constants. These equations are coded in specialized software programs to simulate the kinetic behavior of chemicals in physiological systems. Model equations describe select physiological compartments such as the brain, lungs, and liver, using parameters including blood flow to the tissue (Qt), tissue volume (Vt), ventilation rate (QP), metabolism (Km, Vmax), and partition coefficients (PC). Selection of specific compartments to include in the model, by extraction from generalized tissue compartments, is generally based on the importance of the organ or tissue in the pharmacokinetic or pharmacodynamic behavior of the chemical of interest (Figure 2). Compartmental parameters may be obtained from pre-existing published works in the physiology, biology, and toxicology literature, or fit to approximate a dataset of interest (Brown *et al.*, 1997, Delp *et al.*, 1998, Delp *et al.*, 1991, Schoeffner *et al.*, 1999). Examples of parameter fitting include adjustment of binding constants or metabolic parameters to fit *in vivo* data. The resulting models describe the adsorption (uptake), distribution, metabolism, and/or excretion (ADME) related processes that may, or may not, be related to a toxic effect, but may influence the time-course of the chemical(s) *in vivo*. PBPK models may be used for several purposes, such as extrapolations across species (interspecies), across individuals (intraspecies), and for different routes of exposure (route-to-route).

PBPK models may also utilized or be coupled with external algorithms or systems of equations such as those used in computational fluid dynamics (CFD) and the study of quantitative structure activity relationships (QSAR) to create CFD-PBPK and QSAR-PBPK models, respectively (Frederick *et al.*, 2001, Frederick *et al.*, 2002, Gerde and Scott, 2001). Both conventional PBPK models and these coupled-PBPK models have applications in the derivation

of a tissue dose metric. To predict disposition of a chemical entering the body in the form of an aerosol droplet or adsorbed to particulate matter (such as diesel exhaust), a CFD model coupled to a PBPK model may provide lung deposition information useful in prediction of the tissue dose at a particular lung bifurcation, where impaction or deposition-related toxicity has been noted in the literature. Once deposition has occurred, multiple methods for assessing the uptake of chemical, such as permeability area (PA) terms or mass-transfer coefficients (MTC), may be evaluated to describe tissue levels (Figure 3). The ability to simulate the tissue dose associated with a known toxicological response can then be used to test relevant hypotheses about the kinetic behavior or mechanism of action of the toxicant, inform the understanding of a physiological compartment, and modify uncertainty factors in the risk assessment process, or to justify the dose metric used to gauge tissue concentrations where toxicity has been reported (Benignus *et al.*, 2007, Benignus *et al.*, 2006, Bushnell *et al.*, 2007, Kenyon *et al.*, 2008).

PBPK Modeling of Jet Fuel and other Complex Hydrocarbon Mixtures

While there have been many studies investigating different aspects of the toxicologic response to jet fuels, investigation of the inhalation pharmacokinetics of vaporized or aerosolized jet fuel exposure has for the most part been limited to a two research groups. Campbell and Fisher (2007) conducted vapor exposures to the jet fuel JP-8 and collected tissues from rats exposed using "whole-body" methodology. A PBPK model was developed to interpret the observed kinetic behavior of two select aromatic constituents in relation to the remaining "lump," or mass, of fuel in the exposure atmosphere. The model described metabolic interactions during exposure and provided a detailed comparison of tissue time-course data

collected following exposure to a single chemical or to a mixture of interacting chemicals (Campbell Jr and Fisher, 2007).

Tissue pharmacokinetic data was collected by Fechter *et al.* (2007) following exposure rats to aerosolized JP-8. Tissue concentrations of hydrocarbons in blood and brain were investigated for potential association with auditory toxicity. The authors determined that fuel and flightline levels of noise in co-exposure, resulted in potentiation of the effect of noise exposure on hearing loss. Auditory toxicity was not reported after exposure to fuel-only. This work has implications for occupationally related hearing loss.

As part of a series of works on white spirits (WS), Hissink *et al.* (2007) reported on the pharmacokinetics of this mixture and development of PBPK models for n-decane and 1,2,4-trimethylbenzene as constituents of the mixture. The PBPK models utilized perfusion-limited compartmental descriptions throughout and fitted the metabolic parameters to data collected after inhalation exposure, instead of published in vitro values (Mortensen *et al.*, 2000). The fitted values included a Vmax of 20 and km of 0.1 for n-decane, which are inconsistent with the experimental in vitro data and the concept of metabolic inhibition within complex hydrocarbon mixtures, posing questions for the relevance of this model structure in assessment of jet fuel pharmacokinetic behavior.

Investigation of gasoline and simple mixtures of hydrocarbon constituents present in gasoline has been reported (Dennison *et al.*, 2004, Dennison *et al.*, 2003). Exposures to Benzene, Toluene, n-hexane, ethylbenzene, and xylene (BTHEX) as individual chemicals and in a series of custom mixtures aided in development of a PBPK model that predicted chamber loss data collected from closed-chamber gas-uptake studies using gasoline. Individual constituents were used to build and validate PBPK models for BTHEX chemicals. Custom mixtures of the

BTHEX chemicals were created to gauge the effect of five of the chemicals on one chemical at a different concentration, and then repeating the process with each chemical, until all chemicals had been evaluated in this manner. Essentially, the authors assessed the effect of competitive inhibition of metabolism by using a smaller suite of chemicals that compete for the same enzyme, and determining metabolic parameters for each chemical under these conditions. A final PBPK model for gasoline was parameterized using the fitted metabolic data and biochemical parameters (partition coefficients) that were averaged from the BTHEX group. The total gasoline concentration in the chamber was modeled as a single chemical "lump"(Verhaar *et al.*, 1997). The resulting gasoline PBPK model successfully approximated the chamber loss data. Most importantly, while no blood or tissue data was provided for comparison of tissue simulations, this remains the most detailed assessment of gasoline to date.

PBPK Modeling of Individual Hydrocarbons

There are published physiologically-based pharmacokinetic (PBPK) models for individual exposures of rats to n-hexane, n-decane, 1,2,4-trimethylbenzene, m-xylene, toluene, ethylbenzene, naphthalene, and select other aromatics present in JP-8 and/or S-8 (Ali and Tardif, 1999, Béliveau *et al.*, 2003, Campbell Jr and Fisher, 2007, Merrill *et al.*, 2008, Perleberg *et al.*, 2004, Quick and Shuler, 1999, Willems *et al.*, 2001). There is an additional unpublished model for nonane and a recent revised unpublished model based on the same work (Robinson, 2000b, Robinson and Merrill, 2007). However, PBPK model development for the n-alkanes n-hexane to n-nonane (C7-C9) and the series n-undecane to n-pentadecane (C11-C15) has not been previously published.

As the most prominent individual constituents, on a percentage basis, it is imperative that the kinetics of some or all of the fuel n-alkanes be understood in reference to model development. As initial steps in this process, three PBPK models have been previously developed and published for exposure to n-decane vapor. The interest in n-decane was as a representative marker of exposure to due its high relative concentration in aviation fuels. Simulations from the individual chemical models by Perleberg *et al.* (2004) and Merrill *et al.* (2008) tracked well with tissue data collected across several organs, including fat, liver, brain, kidney, and spleen, following exposure. Both models utilized a combination of flow-limited and diffusion limited compartmental descriptions to describe time-course data from the decane exposures. Differences between the two models were the inclusion of metabolism and intertissue diffusion in the Merrill *et al*. (2008) model but not the Perleberg *et al.* (2004) model, and some adjustment of the in vitro determined partition coefficients by the authors in work by Perleberg *et al.* (2004). n-Decane has also been investigated as a representative marker in more complex chemical mixtures, such as white spirit (WS), by Hissink *et al.* (2007), Lof *et al*. (1999) in the rat, and Pedersen *et al*. (1984) and Pedersen *et al*. (1987) in the human . The rat WS PBPK model developed by Hissink *et al*. (2007) simulated data from exposure to decane in the brain and blood. The kinetic data reported by Lof *et al*. (1999) from inhalation exposure to dearomatized white spirit in the rat, included data on n-noneane, n-decane, and n-undecane concentrations in blood, brain, and fat following 1,2,3 weeks and 3 weeks+2, 4, 6, 24hrs post-exposure. This data may be useful for external comparisons and testing the predictive capacity of the jet fuel model developed here to additional complex mixtures.

Investigation of n-nonane kinetics has also been conducted by several authors (Nilsen *et al.*, 1988, Robinson, 2000b, Robinson and Merrill, 2007, Zahlsen *et al.*, 1992, Zahlsen *et al.*,

1990). In the interest of developing a PBPK model for n-nonane as a marker of jet fuel exposure, Robinson (2000a) investigated the pharmacokinetic behavior of n-nonane using a flow-limited model structure following vapor inhalation. In later work, a reinvestigation of the kinetic data utilized a combination of diffusion and perfusion limitation, as well as a low intertissue diffusion rates between fat and the rapidly perfused tissue compartments. Earlier work with n-nonane, reported peak end of exposure tissue concentrations, but did not provide more detailed time-course data following exposures of 1000ppm 12hr/day/14days (Zahlsen *et al.*, 1990), 100ppm 12hr/day/3 day (Zahlsen *et al.*, 1992), and concentrations up to 5000ppm for 8 hours (Nilsen *et al.*, 1988). Both studies examined end of exposure and repeated exposure kinetics, neither included detailed tissue time-course data.

n-Octane kinetics and toxicity have been investigated only by a small group of authors. Tissue time-course data has been collected by Zahlsen *et al*. (1992) at 100 ppm 12hr/day/3day in the adult rat. Identification and characterization of primary metabolites, as well as limited information potential liver toxicity of n-octane has been reported by Olsen *et al*. (1986), Jones and Traeger (1987), and in a series of works by Khan and Pandya (Khan *et al.*, 1980, Khan and Pandya, 1980, 1985, Pandya and Khan, 1982). Mortensen *et al*. (2000) reported in vitro km and vmax values using rat liver microsomes exposed to n-octane. There have been no reports of dermal or immune system toxicity resulting from exposure. Additionally, Holmberg *et al*. (1977) developed a "classical" pharmacokinetic (PK) model for n-octane the mouse, but no PBPK models have been reported in rodents or humans.

Due in part to their higher vapor pressure, greater potential for exposure via the respiratory route, and noted CNS effects, PBPK models for aromatics are more common in the literature. Several authors have published on the kinetic behavior and/or PBPK model

development for aromatic hydrocarbons in the rat, including: ethylbenzene (Campbell Jr and Fisher, 2007, Tardif *et al.*, 1997), Toluene (Ali and Tardif, 1999, Béliveau *et al.*, 2003, Haddad *et al.*, 1999, Tardif *et al.*, 1993), m-xylene (Campbell Jr and Fisher, 2007, Haddad *et al.*, 1999, Tardif *et al.*, 1993), and 1,2,4-trimethylbenzene (Emond and Krishnan, 2006).

The efforts described in this dissertation and the past work noted from the literature, have culminated in a PBPK model for aerosolized and vaporized jet fuels that will be described herein. Following design and characterization of an inhalation exposure system (Chapter 2, (Martin *et al.*, 2010)) to improve our understanding the inhalation exposure atmosphere, PBPK models were developed for three jet fuels (Chapter 3), using novel respiratory descriptions and chemical lumping strategies. Due to the complex interplay of factors driving local uptake and elimination, as well as systemic disposition and metabolic clearance, one must either describe in complex detail each process and factors that govern them, or develop a parsimonious solution that broadly describes the processes and retains physiologic significance. Development of a modeling strategy to simultaneously describe deposition and uptake of aerosol droplets and vapors from fuel and individual hydrocarbons, as well as the description of tissue disposition of marker chemicals contributes significantly to the field of PBPK modeling and will serve to influence future fuel and complex hydrocarbon mixture PBPK models (Chapter 4).

In preparation for work with fuels, laboratory and exposure characterization skills were honed through study of an environmental exposure of citizens to trichloroethylene (TCE) in air (Martin *et al.*, 2005). The community in question was in the shadow of a metal degreasing plant that utilized TCE. To test air concentration of emitted TCE charcoal sorbent tubes were collected and analyzed. The experience and training in the operation of sampling and analytical equipment was then utilized for assessment of air concentrations of jet fuel in controlled

exposure chambers. This work provided basic skills and introductory experience in toxicology that would also prove useful in writing papers, technical reports and this dissertation.

REFERENCES

Ali N, Tardif R. (1999). Toxicokinetic modeling of the combined exposure to toluene and n-hexane in rats and humans. J Occup Health, 41, 95-103.

Arnold Engineering Development Center Public Affairs. (2008). Arnold contributes to first supersonic flight using synthetic fuel. The Official Website of the U.S. Air Force. [Online] Available at: http://www.af.mil/news/story.asp?id=123092762. November 24, 2009.

Béliveau M, Tardif R, Krishnan K. (2003). Quantitative structure–property relationships for physiologically based pharmacokinetic modeling of volatile organic chemicals in rats. Toxicol Appl Pharmacol, 189, 221-232.

Benignus V, Coleman T, Eklund C, Kenyon E. (2006). A general physiological and toxicokinetic (GPAT) model for simulating complex toluene exposure scenarios in humans. Toxicol Mech Methods, 16, 27-36.

Benignus V, Boyes W, Kenyon E, Bushnell P. (2007). Quantitative comparisons of the acute neurotoxicity of toluene in rats and humans. Toxicol Sci, 100, 146.

Brown R, Delp M, Lindstedt S, Rhomberg L, Beliles R. (1997). Physiological parameter values for physiologically based pharmacokinetic models. Toxicol Ind Health, 13, 407.

Bushnell P, Oshiro W, Samsam T, Benignus V, Krantz Q, Kenyon E. (2007). A dosimetric analysis of the acute behavioral effects of inhaled toluene in rats. Toxicological sciences: an official journal of the Society of Toxicology, 99, 181.

Campbell Jr J, Fisher J. (2007). A PBPK modeling assessment of the competitive metabolic interactions of JP-8 vapor with two constituents, m-xylene and ethylbenzene. Inhalation toxicology, 19, 265-273.

Chao Y, Kupper L, Serdar B, Egeghy P, Rappaport S, Nylander-French L. (2006). Dermal exposure to jet fuel JP-8 significantly contributes to the production of urinary naphthols in fuel-cell maintenance workers. Environ Health Perspect, 114, 182.

Chavanne B. (2007). USAF Wants Fleet Certified For Synthetic Fuel Blend by 2011. Aviation Week: Aerospace Daily and Defense Report [Online] Available at:. [Online] Available at: http://www.aviationweek.com/aw/generic/story_channel.jsp?channel=defense&id=news/FUEL102907.xml. 29 October 2007.

Chen D, Cho S, Chen C, Wang X, Damokosh A, Ryan L, Smith T, Christiani D, Xu X. (2000). Exposure to benzene, occupational stress, and reduced birth weight. Br Med J, 57, 661.

Delp M, Manning R, Bruckner J, Armstrong R. (1991). Distribution of cardiac output during diurnal changes of activity in rats. American Journal of Physiology- Heart and Circulatory Physiology, 261, H1487.

Delp M, Evans M, Duan C. (1998). Effects of aging on cardiac output, regional blood flow, and body composition in Fischer-344 rats. J Appl Physiol, 85, 1813.

Dennison J, Andersen M, Yang R. (2003). Characterization of the pharmacokinetics of gasoline using PBPK modeling with a complex mixtures chemical lumping approach. Inhalation Toxicol, 15, 961-986.

Dennison J, Andersen M, Clewell H, Yang R. (2004). Development of a physiologically based pharmacokinetic model for volatile fractions of gasoline using chemical lumping analysis. Environ. Sci. Technol, 38, 5674-5681.

DOD. (2008). Report to Congress on Synthetic Fuel Utilization. Department of Defense. http://www.dod.mil/ddre/doc/Jul08_Synthetic_Fuel_Utilization_Report_to_Congress.pdf.

Drake M, Witzmann F, Hyde J, Witten M. (2003). JP-8 jet fuel exposure alters protein expression in the lung. Toxicology, 191, 199-210.

Egeghy P, Hauf-Cabalo L, Gibson R, Rappaport S. (2003). Benzene and naphthalene in air and breath as indicators of exposure to jet fuel. Br Med J, 60, 969.

EIA. (2008). Product Supplied. Energy Information Administration. http://tonto.eia.doe.gov/dnav/pet/pet_cons_psup_dc_nus_mbbl_a.htm.

Emond C, Krishnan K. (2006). A Physiological Pharmacokinetic Model Based on Tissue Lipid Content for Simulating Inhalation Pharmacokinetics of Highly Lipophilic Volatile Organic Chemicals. Toxicol Mech Methods, 16, 395-403.

Fechter L, Gearhart C, Fulton S, Campbell J, Fisher J, Na K, Cocker D, Nelson-Miller A, Moon P, Pouyatos B. (2007). JP-8 jet fuel can promote auditory impairment resulting from subsequent noise exposure in rats. Toxicol Sci, 98, 510-525.

Frederick C, Gentry P, Bush M, Lomax L, Black K, Finch L, Kimbell J, Morgan K, Subramaniam R, Morris J, Ultman J. (2001). A Hybrid Computational Fluid Dynamics and Physiologically Based Pharmacokinetic Model for Comparison of Predicted Tissue Concentrations of Acrylic Acid and Other Vapors in the Rat and Human Nasal Cavities Following Inhalation Exposure. Inhalation Toxicol, 13, 359-376. doi:10.1080/08958370117942.

Frederick CB, Lomax LG, Black KA, Finch L, Scribner HE, Kimbell JS, Morgan KT, Subramaniam RP, Morris JB. (2002). Use of a Hybrid Computational Fluid Dynamics and Physiologically Based Inhalation Model for Interspecies Dosimetry Comparisons of Ester Vapors. Toxicol Appl Pharmacol, 183, 23-40.

Gerde P, Scott B. (2001). A model for absorption of low-volatile toxicants by the airway mucosa. Inhalation Toxicol, 13, 903-929.

Haddad S, Tardif R, Charest-Tardif G, Krishnan K. (1999). Physiological modeling of the toxicokinetic interactions in a quaternary mixture of aromatic hydrocarbons. Toxicol Appl Pharmacol, 161, 249-257.

Harris D, Sakiestewa D, Robledo R, Witten M. (1997). Immunotoxicological effects of JP-8 jet fuel exposure. Toxicol Ind Health, 13, 43-55.

Harris D, Sakiestewa D, Robledo R, Young R, Witten M. (2000). Effects of short-term JP-8 jet fuel exposure on cell-mediated immunity. Toxicol Ind Health, 16, 78.

Hays A, Parliman G, Pfaff J, Lantz R, Tinajero J, Tollinger B, Hall J, Witten M. (1995). Changes in lung permeability correlate with lung histology in a chronic exposure model. Toxicol Ind Health, 11, 325-336.

Hemighaus G. (2007). Synthetic Fuels for Aviation. ASTM Stand News. ASTM International. [Online] Available at: http://www.astm.org/SNEWS/APRIL_2007/p_hemighaus_apr07.html. 17 July 2009.

Hernandez SAJ. (2007). SECAF certifies Fischer-Tropsch synthetic fuel blends for B-52H. Air Force Materiel Command - News. Air Force Materiel Command. [Online] Available at: http://www.afmc.af.mil/news/story.asp?id=123063849. 14 June 2009.

Hissink A, Krüse J, Kulig B, Verwei M, Muijser H, Salmon F, Leenheers L, Owen D, Lammers J, Freidig A. (2007). Model studies for evaluating the neurobehavioral effects of complex hydrocarbon solvents III. PBPK modeling of white spirit constituents as a tool for integrating animal and human test data. Neurotoxicology, 28, 751-760.

Holmberg B, Jakobson I, Sigvardsson K. (1977). A study on the distribution of methylchloroform and n-octane in the mouse during and after inhalation. Scand J Work Environ Health, 3, 43.

Jones J, Trager W. (1987). The separation of the intramolecular isotope effect for the cytochrome P-450 catalyzed hydroxylation of n-octane into its primary and secondary components. J Am Chem Soc, 109, 2171-2173.

Kaufman LR, Lemasters GK, Olsen DM, Succop P. (2005). Effects of Concurrent Noise and Jet Fuel Exposure on Hearing Loss. J Occup Environ Med, 47, 212-218.

Kenyon E, Benignus V, Eklund C, Highfill J, Oshiro W, Samsam T, Bushnell P. (2008). Modeling the toxicokinetics of inhaled toluene in rats: influence of physical activity and feeding status. J Toxicol Environ Health A, 71, 249.

Khan S, Mukhtar H, Pandya K. (1980). n-Octane and n-nonane induced alterations in xenobiotic metabolising enzyme activities and lipid peroxidation of rat liver. Toxicology, 16, 239-245.

Khan S, Pandya K. (1980). Biochemical studies on the toxicity of n-octane and n-nonane. Environ Res, 22, 271.

Khan S, Pandya K. (1985). Hepatotoxicity in albino rats exposed to n-octane and n-nonane. J Appl Toxicol, 5,

Knave B, Olson B, Elofsson S, Gamberale F, Isaksson A, Mindus P, Persson H, Struwe G, Wennberg A, Westerholm P. (1978). Long-term exposure to jet fuel. II. A cross-sectional epidemiologic investigation on occupationally exposed industrial workers with special reference to the nervous system. Scand J Work Environ Health, 4, 19-45.

Knave B, Mindus P, Struwe G. (1979). Neurasthenic symptoms in workers occupationally exposed to jet fuel. Acta Psychiatr Scand, 60, 39-49.

Knave B PH, Goldberg JM, Westerholm P (1976). Long-term exposure to jet fuel: an investigation on occupationally exposed workers with special reference to the nervous system. Scand J Work Environ Health, 2, 152-164.

Lemasters G, Olsen D, Yiin J, Lockey J, Shukla R, Selevan S, Schrader S, Toth G, Evenson D, Huszar G. (1999). Male reproductive effects of solvent and fuel exposure during aircraft maintenance. Reprod Toxicol, 13, 155-166.

Lockey G, Olsen J, M D, Tabor S, Wilson M, New G, R G. (1999). Comparison of internal dose measures of solvents in breath, blood and urine and genotoxic changes in aircraft maintenance personnel. Drug Chem Toxicol, 22, 181-200.

Lof A, Lam H, Gullstrand E, Ostergaard G, Ladefoged O. (1999). Distribution of Dearomatised White Spirit in Brain, Blood, and Fat Tissue after Repeated Exposure of Rats. Pharmacol Toxicol, 85, 92.

Martin SA, Simmons MB, Ortiz-Serrano M, Kendrick C, Gallo A, Campbell J, Fisher J. (2005). 2007/04/24. Environmental exposure of a community to airborne trichloroethylene. Arch Environ Occup Health, 60, 314-6.

Martin SA, Tremblay RT, Brunson KF, Kendrick C, Fisher JW. (2010). Jan 28 [Epub ahead of print]. Characterization of a nose-only inhalation exposure system for hydrocarbon

mixtures and jet fuels. Inhalation Toxicology (in press), doi:10.3109/08958370903456645.

Merrill E, Gearhart J, Sterner T, Robinson P. (2008). Improved Predictive Model for n-Decane Kinetics Across Species, as a Component of Hydrocarbon Mixtures. Inhalation Toxicol, 20, 851-863.

Monteiro-Riviere N, Inman A, Riviere J. (2001). Effects of short-term high-dose and low-dose dermal exposure to Jet A, JP-8 and JP-8+ 100 jet fuels. J Appl Toxicol, 21, 485-494.

Mortensen B, Eide I, Zahlsen K, Nilsen O. (2000). Prediction of in vivo metabolic clearance of 25 different petroleum hydrocarbons by a rat liver head-space technique. Arch Toxicol, 74, 308-312.

Moses CA. (2008). Comparative Evaluation of Semi-Synthetic Jet Fuels. Final Report. Coordinating Research Council, Inc. CRC Project No. AV-2-04a. New Braunfels, Texas.

Moses CA. (2009). Comparative Evaluation of Semi-Synthetic Jet Fuels. Addendum: Further Analysis of Hydrocarons and Trace Materials to Support Dxxxx. Coordinating Research Council, Inc. CRC Project No. AV-2-04-a. New Braunfels, Texas.

Nakai N, Murata M, Nagahama M, Hirase T, Tanaka M, Fujikawa T, Nakao N, Nakashima K, Kawanishi S. (2003). Oxidative DNA damage induced by toluene is involved in its male reproductive toxicity. Free Radic Res, 37, 69-76.

Nilsen O, Haugen O, Zahlsen K, Halgunset J, Helseth A, Aarset H, Eide I. (1988). Toxicity of n-C9 to n-C13 alkanes in the rat on short term inhalation. Pharmacol Toxicol, 62, 259-266.

NRC. (2003). Toxicologic Assessment of Jet-Propulsion Fuel 8. National Research Council of the National Academies. Washington, DC. The National Academies Press.

Olson C, Yu K, Hobson D, Serve M. (1986). The metabolism of n-octane in Fischer 344 rats. Toxicol Lett, 31, 147.

Pandya K, Khan S. (1982). Effect of n-octane and n-nonane administration on alkaline phosphatase activity in tissues of female rats. Biochem Pharmacol, 31, 201-203.

Pedersen L, Larsen K, Cohr K. (1984). Kinetics of White Spirit in Human Fat and Blood during Short-Term Experimental. Acta Pharmacol Toxicol, 55, 308-316.

Pedersen L, Rasmussen S, Cohr K. (1987). Further Evaluation of the Kinetics of White Spirit in Human Voluneteers. Pharmacol. Toxicol, 60, 135-139.

Perleberg U, Keys D, Fisher J. (2004). Development of a physiologically based pharmacokinetic model for decane, a constituent of jet propellent-8. Inhalation Toxicol, 16, 771-783.

Pfaff J, Parton K, Lantz R, Chen H, Hays A, Witten M. (1995). Inhalation exposure to JP-8 jet fuel alters pulmonary function and substance P levels in Fischer 344 rats. J Appl Toxicol, 15, 249-256.

Plenge-Bonig A, Karmaus W. (1999). Exposure to toluene in the printing industry is associated with subfecundity in women but not in men. Br Med J, 56, 443.

Porter H. (1990). Aviators intoxicated by inhalation of JP-5 fuel vapors. Aviation, space, and environmental medicine, 61, 654-656.

Quick D, Shuler M. (1999). Use of in vitro data for construction of a physiologically based pharmacokinetic model for naphthalene in rats and mice to probe species differences. Biotechnol Prog, 15, 540-555.

Ramos G, Limon-Flores A, Ullrich S. (2007). Dermal exposure to jet fuel suppresses delayed-type hypersensitivity: A critical role for aromatic hydrocarbons. Toxicol Sci, 100, 415-422.

Reutman S, LeMasters G, Knecht E, Shukla R, Lockey J, Burroughs G, Kesner J. (2002). Evidence of reproductive endocrine effects in women with occupational fuel and solvent exposures. Environ Health Perspect, 110, 805.

Rhodes A, LeMasters G, Lockey J, Smith J, Yiin J, Egeghy P, Gibson R. (2003). The Effects of Jet Fuel on Immune Cells of Fuel System Maintenance Workers. J Occup Environ Med, 45, 79-86.

Ritchie G, Rossi J, Nordholm A, Still K, Carpenter R, Wenger G, Wright D. (2001a). Effects of repeated exposure to JP-8 jet fuel vapor on learning of simple and difficult operant tasks by rats. J Toxicol Environ Health, Part A, 64, 385-415.

Ritchie G, Still K, Alexander W, Nordholm A, Wilson C, Rossi J, Mattie D. (2001b). A review of the neurotoxicity risk of selected hydrocarbon fuels. Journal of Toxicology and Environmental Health, Part B, 4, 223-312.

Ritchie G, Still K, Rossi J, Bekkedal M, Bobb A, Arfsten D. (2003). Biological and health effects of exposure to kerosene-based jet fuels and performance additives. Journal of Toxicology and Environmental Health, Part B, 6, 357-451.

Rivedal E, Mikalsen S, Roseng L, Sanner T, Eide I. (1992). Effects of hydrocarbons on transformation and intercellular communication in Syrian hamster embryo cells. Pharmacol. Toxicol, 71, 57-61.

Robinson P. (2000b). Pharmacokinetic Modeling of JP-8 Jet Fuel Components: I. Nonane and C9-C12 Aliphatic Components. AFRL-HE-WP-TR-2000-0046. Operational Toxicology Branch, Human Effectiveness Directorate, Air Force Research Laboratory.

Robinson P, Merrill E. (2007). A Harmonized Physiologically-Based Pharmacokinetic Model for Nonane as a Component of Jet Fuel. Henry M. Jackson Foundation for the Advancement

of Military Medicine. AFRL-RH-WP-TR-2008-0067. Wright-Patterson Air Force Base, OH.

Rossi J, Nordholm A, Carpenter R, Ritchie G, Malcomb W. (2001). Effects of repeated exposure of rats to JP-5 or JP-8 jet fuel vapor on neurobehavioral capacity and neurotransmitter levels. J Toxicol Environ Health, Part A, 63, 397-428.

Sallmen M, Lindbohm M, Kyyronen P, Nykyri E, Anttila A, Taskinen H, Hemminki K. (1995). Reduced fertility among women exposed to organic solvents. Am J Ind Med, 27, 699-714.

Schoeffner D, Warren D, Muralidhara S, Bruckner J, Simmons J. (1999). Organ weights and fat volume in rats as a function of strain and age. J Toxicol Environ Health Part A, 56, 449-462.

Serdar B, Egeghy P, Waidyanatha S, Gibson R, Rappaport S. (2003). Urinary biomarkers of exposure to jet fuel (JP-8). Environ Health Perspect, 111, 1760.

Serdar B, Egeghy P, Gibson R, Rappaport S. (2004). Dose-dependent production of urinary naphthols among workers exposed to jet fuel(JP-8). Am J Ind Med, 46, 234-244.

Smith E, Hammonds-Ehlers M, Clark M, Kirchner H, Fuortes L. (1997a). Occupational exposures and risk of female infertility. J Occup Environ Med, 39, 138.

Smith L, Bhattacharya A, Lemasters G, Succop P, II E, Medvedovic M, Joyce J. (1997b). Effect of Chronic Low-Level Exposure to Jet Fuel on Postural Balance of US Air Force Personnel. J Occup Environ Med, 39, 623.

Stoica B, Boulares A, Rosenthal D, Iyer S, Hamilton I, Smulson M. (2001). Mechanisms of JP-8 jet fuel toxicity. I. Induction of apoptosis in rat lung epithelial cells. Toxicol Appl Pharmacol, 171, 94-106.

Tardif R, Lapare S, Krishnan K, Brodeur J. (1993). Physiologically based modeling of the toxicokinetic interaction between toluene and m-xylene in the rat. Toxicol Appl Pharmacol, 120, 266-273.

Tardif R, Charest-Tardif G, Brodeur J, Krishnan K. (1997). Physiologically based pharmacokinetic modeling of a ternary mixture of alkyl benzenes in rats and humans. Toxicol Appl Pharmacol, 144, 120-134.

Tremblay RT, Martin SA, Fisher JW. (2010). Feb. [Epub ahead of print]. Novel Characterization of the Aerosol and Gas Phase Composition for Aerosolized Jet Fuel Atmospheres. Inhalation Toxicology (in press), doi: 10.3109/08958370903456637.

Tunnicliffe W, O'Hickey S, Fletcher T, Miles J, Burge P, Ayres J. (1999). Pulmonary function and respiratory symptoms in a population of airport workers. Br Med J, 56, 118-123.

Ullrich S. (1999). Dermal application of JP-8 jet fuel induces immune suppression. Toxicol Sci, 52, 61-67.

Verhaar H, Morroni J, Reardon K, Hays S, Gaver Jr D, Carpenter R, Yang R. (1997). A proposed approach to study the toxicology of complex mixtures of petroleum products: the integrated use of QSAR, lumping analysis and PBPK/PD modeling. Environ Health Perspect, 105, 179.

Whitman F, Hinz J. (2001). Sensory irritation study in mice: JP-4, JP-8, JP-8+100. IERA-RS-BR-SR-2001-0005. Risk Assessment Division, Air Force Institute for Operational Health, Brooks City-Base, TX. IERA-RS-BR-SR-2001-0005. Risk Assessment Division AFIfOH, Brooks City-Base, TX.

Whitman F, Hinz J. (2004). Sensory irritation study in mice: JP-5, JP-TS, JP-7, DFM, JP-10. IOH-RS-BR-SR-2004-0001. Risk Assessment Division, Air Force Institute for

Operational Health, Brooks City-Base, TX. IERA-RS-BR-SR-2004-0001. Risk Assessment Division AFIfOH, Brooks City-Base, TX.

Willems B, Melnick R, Kohn M, Portier C. (2001). A physiologically based pharmacokinetic model for inhalation and intravenous administration of naphthalene in rats and mice. Toxicol Appl Pharmacol, 176, 81-91.

Witzmann F, Bauer M, Fieno A, Grant R, Keough T, Kornguth S, Lacey M, Siegel F, Sun Y, Wright L. (1999). Proteomic analysis of simulated occupational jet fuel exposure in the lung. Electrophoresis, 20,

Wong S, Vargas J, Thomas A, Fastje C, McLaughlin M, Camponovo R, Lantz R, Heys J, Witten M. (2008). In vivo comparison of epithelial responses for S-8 versus JP-8 jet fuels below permissible exposure limit. Toxicology, 254, 106-111.

Wong S, Thomas A, Barbaris B, Lantz R, Witten M. (2009). Pulmonary evaluation of permissible exposure limit of syntroleum S-8 synthetic jet fuel in mice. Toxicol Sci, 109, 312-320.

Zahlsen K, Nilsen A, Eide I, Nilsen O. (1990). Accumulation and distribution of aliphatic (n-nonane), aromatic (1, 2, 4-trimethylbenzene) and naphthenic (1, 2, 4-trimethylcyclohexane) hydrocarbons in the rat after repeated inhalation. Pharmacol Toxicol, 67, 436-440.

Zahlsen K, Eide I, Nilsen A, Nilsen O. (1992). Inhalation kinetics of C6 to C10 aliphatic, aromatic and naphthenic hydrocarbons in rat after repeated exposures. Pharmacol Toxicol, 71, 144-149.

Zahlsen K, Eide I, Nilsen A, Nilsen O. (1993). Inhalation kinetics of C8 to C10 1-alkenes and iso-alkanes in the rat after repeated exposures. Pharmacol Toxicol, 73, 163-168.

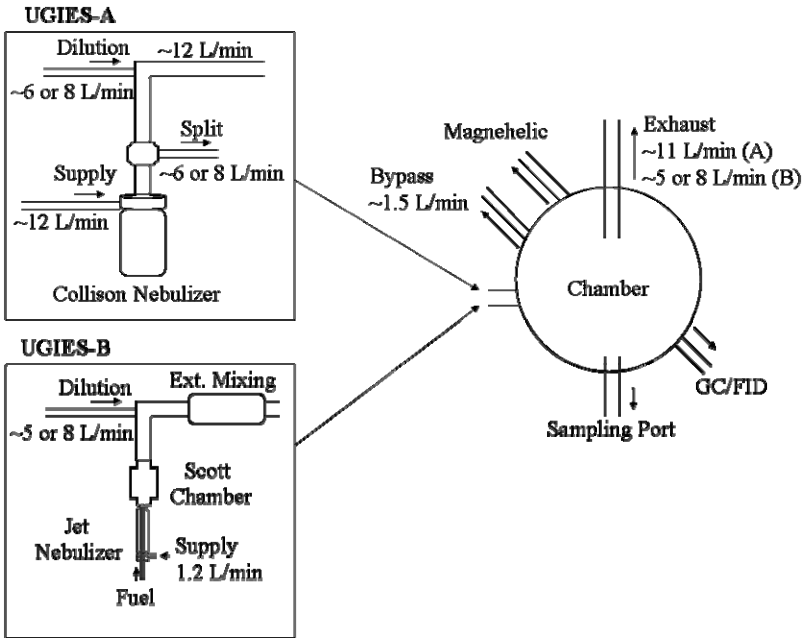

Figure 1.1. University of Georgia Inhalation Exposure System (Martin *et al*, 2010)

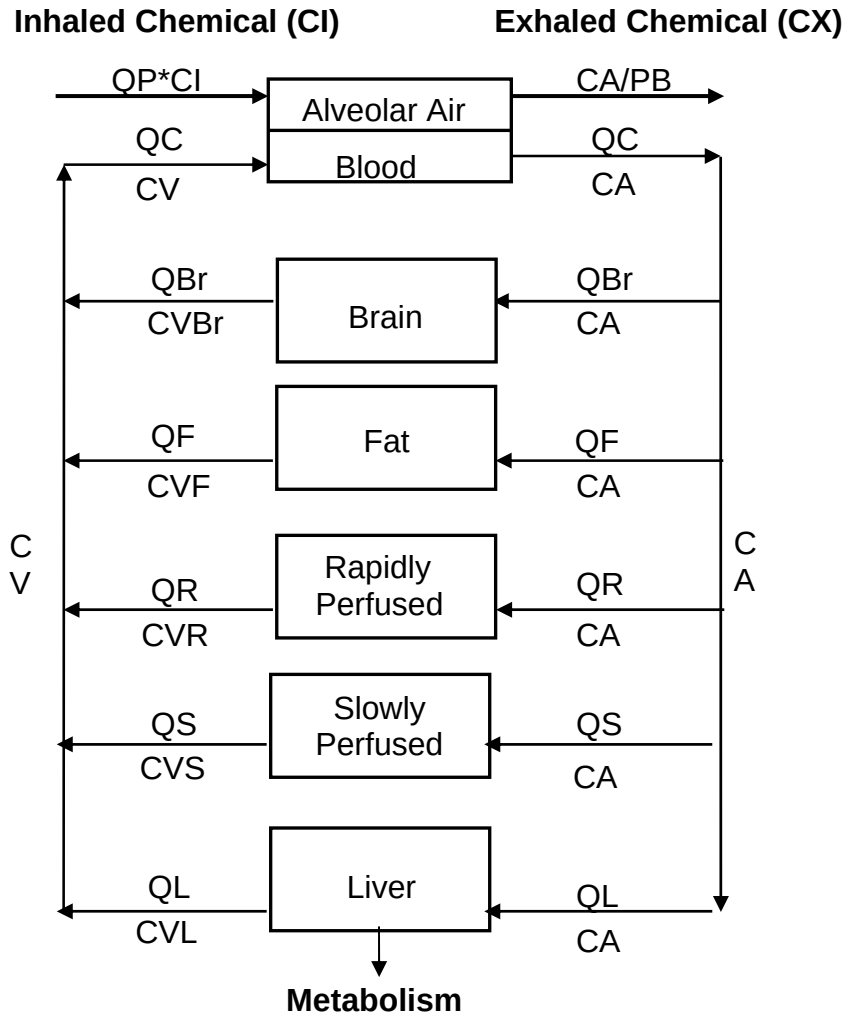

Figure 1.2. General PBPK Model Schematic

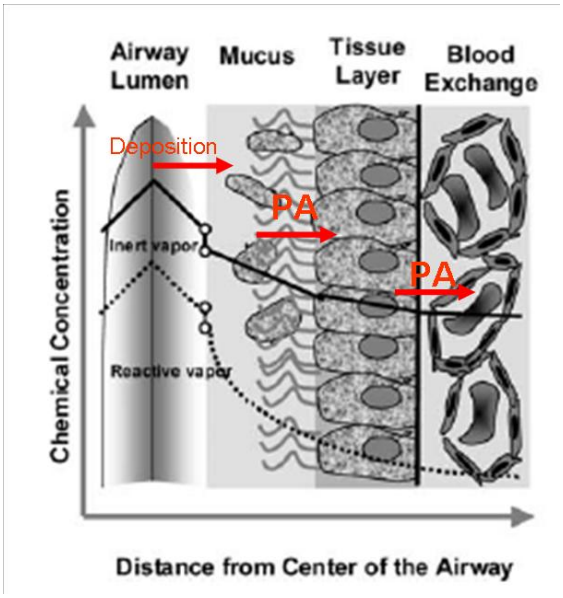

Figure 1.3. Respiratory Diagram. Interaction of inhaled vapor or aerosol in the lumen with mucus and tissue (Adapted from Bogdanffy and Sarangapani, 2003). Aerosols deposit and diffuse to tissue and blood.

CHAPTER 2

CHARACTERIZATION OF A NOSE-ONLY INHALATION EXPOSURE SYSTEM FOR HYDROCARBON MIXTURES AND JET FUELS

Martin, S.A., Brunson, K.F., Kendrick, C., Tremblay, R.T., Fisher, J.W. *Inhalation Toxicology*. 2010. Reprinted with Permission of the publisher.

ABSTRACT

A directed-flow nose only inhalation exposure system was constructed to support development of physiologically-based pharmacokinetic (PBPK) models for complex hydrocarbon mixtures, such as jet fuels. Due to the complex nature of the aerosol and vapor-phase hydrocarbon exposures, care was taken to investigate the chamber hydrocarbon stability, vapor and aerosol droplet compositions, and droplet size distribution. Two generation systems for aerosolizing fuel and hydrocarbons were compared and characterized for use with either jet fuels or a simple mixture of eight hydrocarbons. Total hydrocarbon concentration was monitored via online gas chromatography (GC). Determination of aerosol/vapor (A/V) ratios, and total and individual hydrocarbon concentrations were carried out by analysis of thermal desorption (TDS) tubes using gas chromatography/mass spectrometry (TDS-GC/MS). Droplet size distribution was assessed via 7-stage cascade impactor. Droplet mass median aerodynamic diameter (MMAD) was between 1-3 μm depending on the generator and mixture utilized. A/V hydrocarbon concentrations ranged from ~200-1300 mg/m^3, with between 20 and 80% aerosol content, depending on the mixture. The aerosolized hydrocarbon mixtures remained stable during the 4-hour exposure periods, with coefficients of variation (CV) of less than 10% for the total hydrocarbon concentrations. There was greater variability in the measurement of individual hydrocarbons in the A/V phases. In conclusion, modern analytical chemistry instruments allow for improved descriptions of inhalation exposures of rodents to aerosolized fuel.

INTRODUCTION

Occupational exposures to jet fuels and fuel constituents have been reported in humans. Detrimental effects include central and peripheral nervous system effects (NS) such as dizziness, nausea, and numbness, as well as skin irritation, altered immune cell counts, and decreased performance on evaluations of postural stability (Chatterjee *et al.*, 2006, Knave *et al.*, 1979, Knave *et al.*, 1978, Knave *et al.*, 1976, Porter, 1990, Rhodes *et al.*, 2003a, Smith *et al.*, 1997b). In laboratory animals, several target organs for fuel toxicity have been identified, such as the nervous, integumentary, respiratory, and immune systems. Detrimental effects from exposure include decreased performance on neurological performance batteries, irritation of fuel exposed dermal patches, and respiratory tract toxicity, as well as immunosuppression following inhalation or dermal exposure (Baldwin *et al.*, 2007, Harris *et al.*, 1997, Harris *et al.*, 2000, McDougal *et al.*, 2007, Monteiro-Riviere *et al.*, 2001, Nordholm, 1999, Ramos *et al.*, 2002, Ritchie *et al.*, 2001a, Robledo and Witten, 1998, Rossi *et al.*, 2001, Ullrich, 1999).

JP-8 is a complex mixture of aliphatic and aromatic hydrocarbons. In neat JP-8, aromatic content is roughly 18 %, with the remainder consisting of aliphatics and their isomers, as well as the performance additives diethylene glycol monomethyl ether (DiEGME), DCI-4A, and Statis 450; a deicing agent, a corrosion inhibitor, and an anti-static material, respectively. The aliphatic fraction is comprised primarily of normal and branched-chain isomers of C8-C17 (Dietzel *et al.*, 2005). Prominent aromatics are toluene, ethylbenzenes, xylenes, naphthalenes, and the trimethylbenzene isomers. Synthetic-JP-8, commonly known as FT-JP-8 or S-8, is derived from coal or natural gas using the Fischer-Tropsch process and is devoid of aromatics (Hemighaus, 2007). A 50:50 blend of JP-8:S-8 has been tested in a wide range of military aircraft, including

transport planes and fighter aircraft, to determine its feasibility as an alternative to foreign petroleum (Chavanne, 2007, Hernandez, 2007).

Most inhalation toxicology studies with fuel have been conducted with either a chamber housing the animals (whole body exposures) or with systems in which only the head or nose of the animal is exposed to chemicals (referred to as a nose-only exposure). The generation systems used for jet fuel exposures to rodents have varied widely over the last three decades with the most distinct categories being vapor-only exposures and vapor-plus-aerosol fuel exposures. Traditionally, characterization of vapor-only and vapor-plus-aerosol jet fuel exposure was limited to mg total hydrocarbon per cubic meter of air (mg/m^3) for both vapor and aerosol. Recently, a small number of studies have reported more detailed analysis of the chamber chemical concentrations (Dietzel *et al.*, 2005, Fechter *et al.*, 2007, Tremblay *et al.*, 2008).

To develop physiologically-based pharmacokinetic (PBPK) models for jet fuel, and for individual hydrocarbons inhaled with jet fuel, we designed and fabricated a nose-only exposure system for aerosolized jet fuel. This allowed us to: 1) Control fuel exposure conditions, 2) Carefully characterize the exposures using modern analytical methods and 3) Conduct pharmacokinetic studies in rats for the development of a future fuel PBPK model; the overarching goal of this work.

We describe a nose-only inhalation exposure system for aerosolized jet fuel using two different apparatus to generate the aerosol vapor mixture: a Collison nebulizer and a single-pass nebulizer. The Collison nebulizer has been described in the literature for chemical and bioaerosol generation needs (May, 1973, Tillery *et al.*, 1976). Single-pass nebulizers have been used for several years for aerosolization of various chemicals or pharmaceuticals and have been well described (Dennis *et al.*, 1990, McCallion *et al.*, 1996, Rau, 2002, Wolff and Niven, 1994).

However, the single-pass nebulizer used in this work is less well known and is described in detail.

MATERIALS AND METHODS

We characterized the chemical composition present in the exposure systems using a combination of thermal desorption (TDS) tubes and a gas chromatograph-flame ionization detector (GC/FID). Chamber total hydrocarbon concentrations are presented as the sum of aerosol and vapor content in mg/m^3. We used a 7-stage cascade impactor to assess the droplet size distribution; mass median aerodynamic diameter and geometric standard deviation (MMAD, GSD). Measures of individual chemical concentrations and aerosol:vapor ratios in all exposures utilized the TDS tube method described in the companion paper by Tremblay *et al.* (2010b).

Chemicals

n-Decane, n-undecane, n-dodecane, n-tridecane, n-tetradecane, n-pentadecane, naphthalene were at least 99% purity (Acros Organics, Morris Plains, NJ). Toluene was 99+ % purity and n-hexane was 95-97% purity (JT Baker, Phillipsburg, NJ). 2-methylnaphthalene was 95-97% purity (Acros Organics, Morris Plains, NJ). Jet propellant-8 (JP-8) (POSF 4658 with JP-8 additives), and Synthetic Jet Propellant-8 (S-8), derived from coal or natural gas using the Fischer-Tropsch process, (POSF 4734 Fischer-Tropsch Synthetic Fuel) were obtained from Wright-Patterson Air Force Base, Dayton, OH.

University of Georgia Inhalation Exposure System-A (UGIES-A) was used to generate an aerosolized exposure to a custom hydrocarbon mixture (Figure 1). The hydrocarbon mixture was composed of equal masses (1:1:1:1:1:1:1:1, by mass) of prominent hydrocarbons found in

JP-8. These hydrocarbons were: n-decane, n-undecane, n-dodecane, n-tridecane, n-tetradecane, n-pentadecane, 2-methylnaphthalene, and naphthalene (Table 1). Exposures occurred for 4-hour periods at two concentrations, ~1338 and 645 mg/m^3 (Table 2). Inhalation Exposure System-B (UGIES-B) was configured to generate JP-8 and S-8 jet fuels, or a blend of JP-8 and S-8 (50:50, v:v) (Figure 1). The blend of JP-8:S-8 was tested because of the recent interest in certification of this fuel mixture for military use (Chavanne, 2007). Exposures occurred for 4-hour periods at concentrations of ~907, 1072, 189 mg/m^3, respectively (Table 2).

Nose-Only Inhalation Exposure Chamber

A 12-port directed-flow nose-only inhalation exposure chamber (Jaeger-NYU) was purchased from a commercial supplier (CH Technologies, Westwood, NJ). The chamber construction and specifications are described elsewhere (Jaeger, 1994, Salem and Katz, 2006). In brief, the exposure chamber has inner and outer cylindrical manifolds connected by 12 threaded and removable jets that extend radially from the wall of the inner manifold through the wall of the outer manifold, into the animal restraint apparatus such that they are directly in-line with the nose of the rat. Rats or other experimental animals can be housed in vented polycarbonate nose-only cones with rear plungers that allow the tail to extend for thermoregulation and excreta to drain into attached cups for sample collection. The inner manifold serves as an internal mixing chamber for the chemical exposure air entering at the base. The outer manifold entrains exhaled breath into an exhaust air stream. This particular nose-only chamber design has been successfully used to expose rats to aerosolized jet fuel (Fechter *et al.*, 2007). In the current work, four of the twelve ports were utilized for monitoring devices, with the remaining eight ports available to house rats. Monitoring devices included a heated transfer

line for analysis of total hydrocarbons by a gas chromatograph (GC) equipped with a flame ionization detector (FID), a magnehelic pressure gauge, a cascade impactor, and a thermal desorption (TDS) tube. A fourth port housed a gas line for bypassing the exposure system.

Rats were exposed during the collection of chamber air samples reported in this paper. Animal use was conducted under conditions approved by the University of Georgia Institutional Animal Care and Use Committee.

Generation of Aerosolized Hydrocarbons

Schematics of the exposure systems are shown in Figure 1. The system was housed in a chemical fume hood. HEPA+charcoal filtered laboratory room air (Carbon-Cap Filters, Whatman, Inc., Florham Park, NJ) was used for both the dilution air supply and the air supply used to aerosolize hydrocarbons. Room air temperature was maintained using the wall thermostat. An air compressor (Werther International, Inc., Houston, TX) and metal bellows pumps (MB-41, Senior Operations, Inc, Sharon, MA) were used for both UGIES-A and -B. Exposure air was passed from the generators through either stainless steel or Tygon F-4040-A Fuel and Lubricant Tubing (Cole Parmer, Vernon Hills, IL) before entering the exposure chamber. The F-4040-A Tygon was chosen based on the need for an inert, flexible material. Additionally, it has been reported as suitable to reduce the potential for electrostatic deposition of aerosols (not monitored here) in sample lines (Brockman, 1993). Air flow rates of the UGIES-A and -B were monitored with Gilmont 150mm series and Matheson FM-1050 series rotameters. The flow meters were point calibrated with a digital bubble meter (Gilian Gilibrator 2, Sensidyne, Inc, Clearwater, FL) prior to generation of the n-alkane/PAH mixture and fuels. The internal chamber air temperature during exposures was approximately 21°C (Universal

Enterprises Inc., PDT550 Digital Thermometer, Beaverton, OR). Humidity was not measured. Once in the chamber, aerosolized chemical was directed into the twelve ports, where it was available for inhalation, sampled by the monitoring equipment, or vented to the exhaust air stream. Exhaust air from the systems was removed by a Gast air pump (Model 0523-V191Q-G588DX, Gast Manufacturing, Inc., Benton Harbor, MI) and cleaned via glass wool and activated charcoal before venting to the outside air.

UGIES-A – COLLISON NEBULIZER

Collison Nebulizer

A six-jet bell shaped Collison nebulizer (BGI, Inc. Waltham, MA) was utilized to generate exposures of n-alkane and polyaromatic hydrocarbons (PAH). Screws were added to the base of the Collison nebulizer to provide greater control of hydrocarbon exposure concentrations. By insertion of the screws, the six-jet Collison nebulizer unit was converted into a one-jet model, with five jets providing clean air. Flow to the Collison nebulizer was 12 L/min. The liquid level of hydrocarbons was maintained at approximately 0.95 cm from the base of the bell, as per the manufacturer's recommendations, with a syringe pump (New Era Pump Systems, Inc. Wantagh, NY) replacing lost liquid from the bell through a supplied external adapter (CN-42, BGI, Inc., Waltham, MA).

Generation System UGIES-A

UGIES-A is represented in a schematic in Figure 1. The outlet of the Collison nebulizer was connected to approximately 46 cm of 1.59 cm ID stainless steel tube by Swagelock fittings (Swagelock, Solon, OH) with Teflon ferrules at connection points. To add further control of the

exposure concentration, a gate valve was attached 10cm from the exit point of the Collison nebulizer; in-line with the nebulizer and chamber. The gate valve was also connected to a waste bottle containing glass wool with a rotameter and separate bellows pump. During the n-Alkane/PAH aerosol generations, the gate valve was used to remove (split off) a fraction of exposure air and replace with dilution air downstream. For the 1338 and 645 mg/m^3 n-alkane/PAH exposures, the gate valve removed approximately 6 and 8 L/min of air, respectively. Fine control of exposure concentrations was via adjustment of dilution air flow. The 46 cm length of tube was bent at a smoothed 90° angle with a steel 0.6 cm ID steel bung welded at the center of the bend. A piece of chemical resistant tubing was attached to the bung and connected to a rotameter and air pump, providing HEPA+charcoal filtered dilution air. The 90° steel tube was then attached to a 13 cm Swagelock fitting on the underside of the chamber. One chamber port was occupied by a cored plug that housed chemical resistant tubing connected to a two-way solenoid valve (Parker-Hannifin, Inc., Richland, MI). In the first position the solenoid was open, drawing 1.5-2 L/min from the bypass. In the next position, the solenoid paused the vacuum draw from that port, and flow was shifted to a hose connected to a cascade impactor that was inserted into a chamber port. The solenoid was only activated when the cascade impactor was attached and power was supplied to the solenoid. The exhaust stream was maintained at approximately 11 L/min, which when coupled to the 1.5-2 L/min bypass flow for impactor sampling, as well as 0.1 L/min GC/FID flow, resulted in approximately 12 L/min of total exhaust flow. A 0.4 L/min, 1 minute, sampling condition for the adsorbent (TDS) tubes was shown to have no major impact on chamber internal stability via monitoring with the GC/FID. Internal pressure was maintained at 0 to -2.54 cm H_20 via a magnehelic differential pressure gauge (Dwyer Instruments, Inc., Michigan City, IN). The resulting total path length for UGIES-A, after the Collison nebulizer

connection, was approximately 60 cm for the n-alkane/PAH mixtures, before entry into the chamber.

UGIES-B – SINGLE-PASS NEBULIZER

Single-Pass Nebulizer

A single-pass nebulizer (C-Flow, 800-1-020-02-01, Savillex, Inc., Minnetonka, MN) was used to aerosolize JP-8, S-8, and the 50:50 JP-8:S-8. This concentric nebulizer is constructed from a perfluoroalkoxy copolymer resin (Teflon PFA, DuPont, Co., Wilmington, DE) that is resistant to jet fuel. Factory use of the nebulizer is in inductively coupled plasma-mass spectroscopy (ICP-MS) systems as an injection source for chemical and biological matter. Unlike the Collison nebulizer, this apparatus serves as a single-pass system, such that all liquid entering the unit is expressed from the nozzle. A Scott-type PFA "Double Pass" spray chamber (Osgar, 2009, Savillex, 2005) was attached. The model described in this work is self aspirating, operating on the Bernoulli principle, drawing chemical through the rear of the unit, expressing it through a center channel toward a small opening at the directional front of the unit. Air forced through the back of the unit, moves toward the front opening through an area surrounding the center channel, and proceeds out of an annulus into the attached PFA spray chamber (SC). Flow through the single-pass nebulizer was 1.2 L/min. The interaction of supply air through the nebulizer exit point and chemical drawn through the center capillary produces aerosol droplets. Droplets proceed through the SC, where larger droplets are removed and drain out through an attached tube. The drain tube prevents pooling of droplets in the SC. Connection of the SC to UGIES-B was via an approximately 4 cm section of chemical resistant tubing that was fitted around the SC outlet and into a steel fitting at the proximal side of UGIES-B. To

avoid any chance of starvation of the nebulizer for fuel, a syringe pump (New Era Pump Systems, Inc. Wantagh, NY) was connected to a 10 mL screw cap scintillation vial with Teflon septa. The feed line for the single-pass nebulizer, a fill adapter (taken from the Collison Nebulizer, (CN-42, BGI, Inc., Waltham, MA), and a 22.5 gauge needle were inserted a separate points in the septa with the feed line and fill adaptor side by side at the base of the 10ml vial. The feed line insured a constant supply of fuel, the fill adaptor allowed maintenance of fluid level in the vial with replacement via syringe pump, and the 22.5 gauge needle prevented pressure drop in the 10 ml vial, but was small enough to avoid significant loss of volatiles from the constantly replenished fuel supply.

Generation System UGIES-B

UGIES-B is represented in a schematic in Figure 1. The outlet of the single-pass nebulizer and SC assembly was connected to the 46 cm bent steel tube at the same junction point as was the Collison (UGIES-A). The 46 cm tube was equipped as previously described with the dilution/make-up flow connection. Dilution air was metered into the system at approximately 5 or 8 L/min, depending on the concentration of jet fuel (JP-8, S-8, or lower concentration 50:50 JP-8:S-8) used. As dilution flow required to achieve the desired concentration was somewhat different between the exposure levels, to avoid highly negative atmospheric pressure a plug was removed from the chamber, essentially returning it to ambient pressure. However, as the system is directed-flow, all air entering the chamber is forced out of the twelve radial jets before entrainment into the exhaust stream. Total exhaust flow, including the bypass, was approximately 6.5 or 9.5 L/min. GC/FID flow remained at approximately 0.1 L/min. The 0.4 L/min, 1 minute, TDS tube sampling time was not shown to significantly alter the chamber

concentration. To increase residence time and reduce the percent aerosol to levels reported in aerosolized fuel toxicity studies the exposure system was modified (Dietzel *et al.*, 2005). The exit point of the 46 cm steel tube was connected by 224 cm of 1.59 cm I.D. chemical resistant Tygon Fuel tubing to an o-ring sealed 4.7 L external mixing chamber fabricated at UGA. Diluted chemical exiting the external mixing chamber was connected to the base of the chamber by 350 cm of 1.11 cm I.D. chemical resistant tubing attached to the 13 cm steel Swagelock section on the base. Further chamber adjustments were performed through manipulation of dilution air entering the system.

CHARACTERIZATION OF HYDROCARBON MIXTURES

Total Hydrocarbon Concentration

Total hydrocarbon concentration (THC) of jet fuel was monitored by an Agilent GC/FID model 6890 (Agilent Technologies, Santa Rosa, CA) equipped with internal pneumatic gas sampling valve and heated transfer line (Barnstead Inc, Dubuque, IA) connected through a cored chamber port plug. The 0.64 cm probe extended ~ 2.5 cm until just ahead of the port jet to simulate the position of the nose of a rat and capture an "inspired air" sample. Both the GC pneumatics and transfer line were maintained at 200°C to prevent condensation on system components and ensure vaporization of droplets prior to contact with the pneumatics. The inlet and oven were also maintained at 200°C, with the FID at 260°C. The column was a DB5 with dimensions 15 m x 0.53mm, 15 µm (J&W Scientific, Agilent Technologies, Inc., Santa Rosa, CA). The system utilized HP Chemstation computer software to provide a single visual peak and display area counts at ~2 minute intervals yielding approximately 110 points. Target peak areas represented target concentrations from an n-hexane standard curve similar to earlier work

(Perleberg *et al.*, 2004). Following completion of jet fuel studies, peak areas were converted into mg/m^3 using a calibration curve.

Calibration of total fuel concentrations in the chamber was carried out using Tedlar bags (SKC, Inc. Eighty-Four, PA) and n-hexane to create a standard curve. The Tedlar standard bags were filled to 80% capacity with HEPA+charcoal filtered air and then n-hexane was injected into the bag using a gas tight syringe. The n-hexane in the Tedlar bags was pumped through the heated transfer line and auto-sampling valve to the GC/FID, replicating sample collection from the exposure chamber.

For the n-alkane/PAH mixture, the GC/FID was used only for monitoring chamber stability and targeting a desired peak area during the exposure, not for calculation of chamber concentration. Inability to use the GC/FID for total concentration of the mixture was likely due to the lower overall volatility and high percentage of aerosol droplet constituents, leading to inconsistent volatilization in the transfer line. Because the chemical composition of the n-alkane/PAH mixture was known, total and individual hydrocarbon concentrations were collected via the adsorbent tube method described in the next section.

The responses of jet fuel or hexane spiked on the GC/FID were not significantly different; allowing quantification of the total jet fuel concentration using the n-hexane calibration curve. Issues similar to those for quantification of the n-alkane/PAH mixture were not apparent in work with the jet fuels. Data are represented as mean concentration (mg/m^3), standard deviation, and coefficient of variation (CV). Time weighted average (TWA) concentrations were also determined for the fuels. A TWA was calculated as $\sum(Ci*ti)/(\sum ti)$, where Ci is the average concentration over an approximate 10 minute interval and ti is the approximate 10 minute duration.

Individual Hydrocarbon Concentration and Profile

Quantification of individual hydrocarbons in all studies and discrimination of aerosol and vapor-phase constituents were determined via a novel adsorbent tube method (Tremblay *et al.*, 2010b), using Carbotrap 300 thermal desorption (TDS) tubes (Supelco, Inc., St. Louis, MO). Determination of individual chemical concentrations present on the TDS tubes was via comparison to calibration curves developed using authentic standards. To determine overall aerosol or vapor concentration ratios for jet fuels, a neat jet fuel standard was used and spiked onto TDS tubes. TDS-GC/MS (Gerstel Inc, Baltimore, MD and Agilent Technologies 6890/5973, Santa Rosa, CA) analysis was conducted by the method of Tremblay *et al*. (2010b) and is described fully in the companion paper.

For the n-alkane/PAH mixture work, the tube flow rates were checked immediately before and after sampling with a blank TDS tube and the bubble meter. Tubes were collected sequentially. Each tube was connected to the chamber to sample either vapor concentration (Tube 1) or total concentration (Tube 2). Tube 1 was placed in-line to the exit point of a Gelman glass fiber filter holder that was then connected to the chamber through a cored plug to collect a vapor-only sample. Tube 2 was connected to the chamber through a cored exposure port plug and collected aerosol-plus-vapor. Immediately following the sampling period, the TDS tubes were removed and capped in a manufacturer supplied enclosure prior to analysis.

To improve ease of use in collection of jet fuel exposure data with Carbotrap tubes, a digital mass flow controller (MFC) replaced the bubble meter in the sampling train. TDS tubes (Supelco, Inc., St. Louis, MO) were connected by chemical resistant tubing to a MFC (Pneucleus Technologies, Hollis, NH) and a bellows pump. The MFC was calibrated daily with the bubble

meter to reproduce the desired flow rate. Atmospheric conditions during the 4-h run did not change significantly to affect the mass to flow relationship.

The concentration ratios obtained from the "filtered" Tube 1 to the "non-filtered" Tube 2 provided the aerosol/vapor ratio (Tremblay *et al.*, 2010b). A pair of tubes was collected at approximate 40 minute intervals, with 7-8 tube pairs collected for each of the n-alkane/PAH mixture, S-8, and JP-8 fuel studies. For the JP-8:S-8 fuel blend, 5 pairs of tubes were collected. A complete description of the TDS-GC/MS sampling method and attributes is provided in the companion paper by Tremblay *et al*. (2010b).

To calculate the chemical constituent characteristics:

Aerosol Concentration (mg/m^3), C*ati* = C*tti* – C*vti*

Vapor Ratio (mg/m^3) = C*vti* / C*tti*

Aerosol Ratio (mg/m^3) = (C*tti* – C*vti*) / C*tti,*

where C*tti* is the concentration obtained from the "non-filtered" Tube 2 sample per chemical, C*vti* is the concentration obtained from "filtered" Tube 1, and C*ati* is the aerosol concentration obtained from the difference between C*tti* and C*vti*. To determine the aerosol or vapor ratios, either the vapor or aerosol concentration was divided by the total concentration, C*tti*.

Droplet Size Distribution

A 7-stage cascade (CI) impactor (0.25 – 5 μm) (Intox, Moriarty, NM) was used to determine droplet mass median aerodynamic diameter (MMAD) and geometric standard deviation (GSD). A light layer of Apiezon (M&I Materials, Ltd, Manchester, UK) grease dissolved in toluene (1 gram per 100 mL) was applied to mylar disks sized to the exact dimensions of the steel plates supplied with the 7-stage impactor, and allowed to dry prior to use

(Reboulet, 2006). A 25 mm glass fiber filter (225-702, SKC, Inc, Eighty-Four, PA) was used on the final stage. Samples were collected at 1.5-2 L/min for approximately 10 min. Impactor disk weights were quickly recorded using an AX26 microbalance (Mettler-Toledo, Inc., Columbus, OH). For the n-alkane/PAH mixtures and the JP-8 generation, the impactor disks were collected three times during the exposure, and twice with S-8 exposures. The Intox Cascade Impactor Reduction Program (Intox, Inc, Moriarty, NM) was used to calculate the aerosol droplet MMAD and GSD, with input parameters of pre- and post-exposure impactor plate weights, flow rate to the impactor, chamber air temperature, and the barometric pressure. The program also recalculated cutoff points depending on flow rate.

For the JP-8:S-8 fuel blend, it was determined that the mass of hydrocarbons on each stage was too low to reliably determine the droplet size distribution. A second method to measure droplet size was performed. Fuel exposed mylar disks were immediately transferred to 10 mL solid phase micro-extraction GC/MS (SPME-GC/MS) glass vials and capped with PTFE/silicon septa 18 mm screw caps (Supelco, Inc. St. Louis, MO). It was determined earlier that the grease coating on the disk interfered with GC/MS analysis and uncoated mylar disks were used in this instance. A modification of the tissue extraction method by Campbell and Fisher (2007) was used for the analysis of the disk hydrocarbon content. A polydimethylsiloxane SPME fiber (100 um, 1 cm, Supelco, St. Louis, Mo) was inserted into the headspace above each individual disk or final stage filter for 5 min before desorption into the GC/MS. Unlike the original method, no water or internal standard was used.

RESULTS

The nose-only inhalation chamber was interfaced with two systems for generating aerosolized hydrocarbons. The Collison nebulizer was used in UGIES-A to aerosolize a known mixture of fairly high molecular weight hydrocarbons. The Collison nebulizer performed adequately for this specific hydrocarbon mixture. This nebulizer would be a poor choice for jet fuel because jet fuel contains many lower molecular weight hydrocarbons. The Collison nebulizer preferentially depletes the light hydrocarbons early in the generation of aerosolized fuel (Tremblay *et al.*, 2010a). Therefore a single-pass nebulizer is preferred for the aerosolization of jet fuel. Also, the increased generation system length increased residence time in UGIES-B and lowered the overall percent aerosol in the chamber. The aerosol fraction was lowered to 36% for JP-8, 30% for S-8 and 27 % for the 50:50 JP-8:S-8 mixture.

In preliminary studies, the Collison nebulizer (UGIES-A) generated aerosolized hydrocarbon mixtures ranging from 90 to 6000 mg/m^3 using one jet and all six jets, respectively and controlling the dilution air flow. For the single-pass nebulizer (UGIES-B) a range of 189 to ~1100 mg/m^3 was generated by controlling dilution air flow.

Evaluation of Total Chamber Concentrations (Aerosol Droplet and Vapor-Phase)

The n-alkane/PAH mixture exposures were maintained at total hydrocarbon concentrations (aerosol droplet and vapor-phase concentrations) of 1338 and 645 mg/m^3 for 4-hours with coefficients of variation (CV) of 4 and 5%, respectively (Table 2). The S-8, JP-8, and 50:50 JP-8:S-8 mixture total hydrocarbon concentrations were maintained at 1072, 907, and 189 mg/m^3, with coefficients of variation of 3%, 4%, and 3%, respectively (Table 2). In addition to the arithmetic average for the total hydrocarbon concentration fuel concentrations, a time

weighted average (TWA) was calculated at approximate 10 minute intervals. The TWAs were 1038, 847 and 183 mg/m^3, for S-8, JP-8, and the 50:50 JP-8:S-8 mixture, respectively.

CV values for individual hydrocarbon total concentrations (aerosol droplet and vapor-phase) for the n-alkane/PAH mixture exposures (Tables 3A, 3B, Column 2) ranged from 3 to 14%, with the exception of n-pentadecane in the 645 mg/m^3 exposure (21%, Table 3B, Column 2). CV values for selected individual hydrocarbon total concentrations (aerosol droplet and vapor-phases) for the jet fuel exposures were more varied (Tables 4A, 4B, 4C Column 2). The individual total hydrocarbon concentrations were an order of magnitude or more lower than corresponding individual hydrocarbons in the n-alkane/PAH mixture. All CV values were 20% or under with the exceptions of naphthalene (34%) in the 907 mg/m^3 JP-8 exposure (Table 4A, Column 2), and n-pentadecane (30%) in the 1072 mg/m^3 (Table 4B, Column 2) S-8 exposure.

Evaluation of Individual Hydrocarbons in the Vapor-Phase

All CV values for individual hydrocarbons in the vapor-phase were under 20% for the n-alkane/PAH mixtures (Tables 3A, 3B, Column 3), with the exceptions of n-pentadecane (22%) in the 1338 mg/m^3 exposure (Table 3A, Column 3), as well as n-tetradecane (27%) and n-pentadecane (37%) in the 645 mg/m^3 exposure (Table 3B, Column 3). For the jet fuels (Tables 4A, 4B, Column 3), the CV values for selected individual hydrocarbons in the vapor-phase for the 907 mg/m^3 JP-8 exposure were well under 20% with the noted exception of n-pentadecane (158%) and 2-methylnaphthalene (155%), and for the 1072 mg/m^3 S-8 exposure, n-pentadecane (156%). In the 50:50 JP-8:S-8 mixture 189 mg/m^3 exposure, CV values for several individual hydrocarbons of the vapor-phase (n-dodecane, n-tridecane, n-pentadecane, 2-methylnaphthalene, and naphthalene) were above 20% (Table 4C, Column 3).

Evaluation of Individual Hydrocarbons in the Aerosol-Phase

CV values for the individual hydrocarbons comprising the aerosol droplets of the n-alkane/PAH mixture were all below 20%, the exception of n-pentadecane (21%), in the 645 mg/m^3 exposure (Table 3B, Column 3). In the jet fuel exposures, the CV values for selected individual hydrocarbons found in the aerosol droplets were above 20% for 8 of 14 selected individual hydrocarbons in the JP-8 (Table 4A, Column 3), 6 of 8 individual selected hydrocarbons found in the S-8 (Table 4B, Column 3) and 11 of 14 individual selected hydrocarbons found in the blended fuel (Table 4C, Column 3).

Characteristics of the aerosolized hydrocarbon mixtures and fuels

The aerosolized 1338 and 645 mg/m^3 n-alkane/PAH mixtures were, on the average, 72 and 76% aerosol respectively, and the remainder vapor-phase (Tables 1, Column 5). On an individual hydrocarbon basis, the percent in the aerosol-phase ranged from 29-32 percent for n-decane to 76% and greater for n-tridecane, n-tetradecane, n-pentadecane, 2-methylnaphthalene and naphthalene. For the two n-alkane/PAH mixture exposures of 1338 and 645 mg/m^3, the Collison nebulizer produced similar individual hydrocarbon profiles in the vapor and aerosol-phases. Also, the expected concentration differences of the individual hydrocarbons were observed, given that the 1338 mg/m^3 exposure was nearly twice the 645 mg/m^3 exposure (Tables 3A, 3B). The less volatile hydrocarbons were prominent in the aerosol droplets.

Comparison of the change in individual chemical concentrations generated in UGIES-A during the 1338 and 645 mg/m^3 exposure indicated that the general chamber profile was maintained during a ~50% reduction in total concentration (Tables 3A, 3B). With the exceptions of n-decane in the 645 mg/m^3 exposure, present at 59% of the 1338 mg/m^3 exposure n-decane

concentration, and n-tetradecane and n-pentadecane at approximately 35-40% of the 1338 mg/m^3 exposure concentration, the average reduction in concentration was 48% for the individual chemicals. The hydrocarbons selected represent approximately 15% of the chemical constituents present in a neat sample of JP-8 (Potter and Simmons, 1998).

For the 907 mg/m^3 JP-8 and 1072 mg/m^3 S-8 exposures, fuels were present at 36 and 30% aerosol droplets, respectively, with the remainder as vapor. For the 189 mg/m^3 blended fuel exposure, 27% was present as aerosol. On an individual hydrocarbon basis (Tables 4A, 4B) the more volatile hydrocarbons were prominent in the vapor-phase and the less volatile chemicals in the aerosol droplet phase. The total concentrations of several individual hydrocarbons were low (under 1 mg/m^3) in the 189 mg/m^3 50:50 JP-8:S-8 mixture exposure (Table 4C). The hydrocarbons selected represent approximately 20% of the chemical constituents present in JP-8 (Potter and Simmons, 1998).

The system was able to produce the expected reduction in individual chemical concentrations of jet fuel hydrocarbons during the 50:50 JP-8:S-8 mixture exposure. Exposure to this mixture was conducted at approximately 80% lower total concentration than two standard fuels, JP-8 and S-8. The individual chemical concentrations were approximately 10-20% of the corresponding hydrocarbon concentrations in the JP-8 and S-8 exposures.

Droplet Size Distribution

n-Alkane/PAH mixture exposure air was found to contain droplets with average MMAD between 2 and 3µm. Jet fuel aerosol droplet MMAD was between 1 and 3 µm (Table 3). Three sets of impactor disks were collected for the 1338 mg/m3 n-alkane/PAH exposure, yielding MMAD:GSD measurements of 2.71:2.38, 2.50:2.34, and 1.46:1.34 um. Three sets of impactor

disks were collected for the 645 mg/m3 study, with MMAD:GSD values of 2.52:2.36, 3.96:2.36, and 3.14:2.52 um.. For fuels, two sets of impactor disks were collected for S-8 (MMAD:GSD values of 1.39:1.83 and 1.38:1.92 μm). Three sets of impactor disks were collected for JP-8 (MMAD:GSD values of 3.09:2.27, 3.36:2.39, and 3.40:2.83 μm). The aerosol concentration in the blended 189 mg/m^3 was too low to reliably collect impactor samples. SPME-GC/MS analysis of blended fuel on the impactor disks allowed for determination of the chemical signal detected on each stage. The chemical signal data from a set of impactor disks was entered into the impactor reduction program, resulting in an MMAD of 0.95 and GSD of 1.77 μm (Table 2).

DISCUSSION

This paper provides the details of our aerosolized exposure system that can be used to collect pharmacokinetic data in rats with jet fuels. We have reported on a whole body jet fuel exposure system for jet fuel vapors (Campbell Jr and Fisher, 2007) and the characterization of a nose only exposure system at the University of Arizona for aerosolized fuel (Dietzel *et al.*, 2005). Our interest in better understanding the internal chamber environment containing aerosolized fuels is to relate the inhalation of selected hydrocarbons in the aerosol and vapor-phases with those found in the rat in blood or tissues. The identification and quantification of individual marker hydrocarbons within the complex hydrocarbon mixtures of vapor and aerosol droplets is critical to the interpretation of pharmacokinetic studies with fuels. Typically, the internal chamber environments in aerosolized jet fuel toxcicity studies are characterized only by the sum of hydrocarbons in the vapor and aerosol-phases rather than individual constituents (Harris *et al.*, 1997, Mattie *et al.*, 1991, Ritchie *et al.*, 2001a). This work and the companion

paper (Tremblay *et al.*, 2010b) serve as the most detailed characterization of the aerosol and vapor-phase profile of JP8, S8, and an n-alkane/PAH mixture in an inhalation chamber to date.

The nose-only inhalation system for jet fuel presented in this paper relies on the use of gas chromatography, mass spectrometry and gravimetric measurements of droplet size. Data are presented for two types of generation systems, with either fuel or a predetermined mixture of hydrocarbons. For the fuel exposures, the targeted exposure concentration ranges, based on total hydrocarbon concentration, were selected because of previous toxicity tests in these concentration ranges (Ritchie *et al.*, 2001a, Robledo *et al.*, 2000, Rossi *et al.*, 2001). The n-alkane/PAH mixture studies were carried out to evaluate the performance of the inhalation system and to collect pharmacokinetic data on important marker hydrocarbons found in neat fuel, aerosolized fuel, and in exposed rats. The n-alkane/PAH mixture contained equal amounts of each hydrocarbon. We evaluated the ability of the exposure system to provide an internal chamber environment that was representative of the liquid mixture of hydrocarbons and was able to provide similar hydrocarbon profiles for two concentrations of the n-alkane/PAH hydrocarbon mixture. The concentration of the individual hydrocarbons (as vapor and aerosol droplets) in the chamber ranged two fold of each other (Table 3A, 3B) for both the 1338 and 645 mg/m^3 exposures. The composition of the vapor-phase and aerosol droplet was similar for both exposures, with the higher vapor pressure, lower molecular weight hydrocarbons prominent in the vapor-phase and vice versa for the less volatile and higher molecular weight hydrocarbons. Thus, the exposure of the rats to a predetermined mixture of aerosolized hydrocarbons results in a complex exposure pattern that is governed by the physical/chemical properties of the hydrocarbons and the design of the exposure system.

UGIES-A was able to meet our needs for aerosolization of a mixture of hydrocarbons with relevance for PBPK model development. The Collison nebulizer itself was used to simulate a particular exposure environment (high aerosol, n-alkane/PAH exposure with prominent hydrocarbons in jet fuel). It has been used to aerosolize jet fuels in prior studies (Whitman and Hinz, 2001, 2004). However, based on the goals of this work, UGIES-A was not suitable for conducting jet fuel exposures. Preferential stripping out of the aromatics and light hydrocarbons early in the generation period, and the recycling or concentrating of the heavier hydrocarbons in the reservoir, altered the chamber chemical profile during a 4-hour period. The single-pass nebulizer in UGIES-B was used to aerosolize jet fuel into the chamber and collect data for PBPK model development. Its incorporation into the exposure system also allowed for generation of a chamber environment containing a lower aerosol fraction.

Jet fuel contains many hydrocarbons, none in concentrations greater than a few percent. Unlike the 1338 mg/m^3 n-alkane/PAH mixture, the concentrations of n-alkanes (n-decane to n-pentadecane) in aerosol droplets were 10 to 100 times lower in 907 mg/m^3 JP-8 and 1072 mg/m^3 S-8 chamber air, while naphthalene and 2-methylnaphthalene were 2-3 orders of magnitude lower. In the vapor-phase, many hydrocarbons in both JP-8 and S-8 were 2-10 times lower than the 1338 mg/m^3 mixture with the exceptions of naphthalene and 2-methylnaphthalene, which were several orders of magnitude lower in fuel. When the exposures to JP-8, S-8 and JP-8:S-8 mixture were characterized as mg of total individual marker hydrocarbon (vapor and aerosol droplet phases) per m^3 the CV values were very good except for pentadecane (Table 4B, column 2) in the S-8 and naphthalene in the JP-8 (Table 4A, column 2) and JP-8:S-8 mixture (Table 4C, column 2). However, when CV values for individual hydrocarbons were calculated for the vapor and aerosol-phases, several CV values were much greater than 20% for the vapor and aerosol

droplets. These results demonstrate the challenges in characterizing a chamber for use with aerosolized jet fuel (Tremblay *et al.*, 2010a, Tremblay *et al.*, 2010b). To develop a PBPK model for inhalation of individual hydrocarbons found in aerosol droplets and in vapor, approaches that assume a dynamic distribution of individual hydrocarbons in the chamber might be necessary; such as Monte Carlo.

Higher CVs can be explained by examination of the data and range of concentrations for the individual chemicals in question. The high CV values were generally observed for the same individual constituents in the JP-8, S-8, and JP-8:S-8 mixture exposures. Increased variability in the aerosol-phase of the n-alkanes n-octane, n-nonane, n-decane, and to a lesser extent n-undecane, as well as the aromatics toluene, m-xylene, ethylbenzene, 1,2,4-trimethylbenzene was mainly due to their low concentration compared to their presence in the vapor-phase and low % aerosol. The differential between two similar values, in this case total concentration for the individual chemical and the vapor-phase concentration for that chemical, is more sensitive to subtle changes in either of the two larger values. In the case of n-pentadecane, and the naphthenic hydrocarbons, higher variability was found in the vapor-phase. The vapor-phase concentration of these constituents was considerably lower than in the aerosol-phase. The lower molecular weight n-alkanes n-octane, n-nonane, n-decane and the aromatic constituents that were more variable in the aerosol-phase are considerably less variable in the vapor-phase, as indicated by their lower CV values. Taken together, the lower molecular weight constituents have less variability as the vapor fraction increases and higher molecular weight constituents generally have less variability as the aerosol fraction increases, and vice-versa. These conditions are amplified in the blended fuel exposure air where there is 80% lower total concentration.

Indications of enrichment of aromatic and lower molecular weight alkanes compared to the neat fuel were found. In the JP-8 exposure, the ratio of chamber air concentrations to total concentration of neat fuel were 3-6 fold higher for the aromatics (toluene, m-xylene, ethylbenzene) compared to neat fuel and about 1.5-5 fold higher for n-octane to n-decane (Tremblay *et al.*, 2010b). For the higher molecular weight hydrocarbons, this ratio was 0.04 (naphthalene) to 0.96 (n-dodecane), indicating some depletion of the less volatile constituents in the chamber compared to neat JP-8 fuel. However, the ratios of chamber air constituent concentrations to neat fuel were constant over time, another indication of chamber stability using the single-pass nebulizer. The altered ratios compared to neat jet fuel likely occur in other systems using similar exposure technology (Fechter *et al.*, 2007). Thus, care should be taken when comparing toxicity findings when liquid fuel is administered to laboratory animals compared to inhalation studies. Somewhat higher chamber concentrations of n-decane and n-undecane compared to the other constituents of the n-alkane/PAH mixture are likely the result of some loss to the system of higher molecular weight constituents via aerosol droplet deposition. Volatilization of these constituents from the droplet would add to the vapor-phase and total concentration, while higher molecular weight hydrocarbons would be slower to volatilize and are less likely to add to the vapor-phase based on their vapor pressure.

Earlier studies in the literature that have investigated the toxicity of JP-8 generally did not report the standard deviation of exposure concentration or variability; only mean concentration. As a result, comparison of the stability in the exposure concentration presented in this work and others in the literature is difficult. However, Ritchie *et al*. (2001a) reported concentrations of $500 \pm 10\%$ mg/m^3 and $1000 \pm 10\%$ mg/m^3 JP-8 vapor in a whole body exposure study investigating CNS effects for exposures of 6hr/day for 5d/wk for 6 wks. Also, Baldwin *et al*.

(2007) reported interday total JP-8 aerosol-plus-vapor concentrations and standard deviations for a nose-only exposure CNS effect study of 1318.5 ± 1318.5 mg/m^3 for a 5 day period, 1755.6 ± 1856.1 mg/m^3 for a 10 day period, 1568.8 ± 910.1 mg/m^3 for a 15 day period, and 1774.1 ± 1133.7 mg/m^3 for a 20 day period. While not provided in the original publication, the calculated CVs for this study would be as follows: 5 day - 100%, 10 day - 106%, 15 day - 60%, and 20 day - 64%. Determination of the stability of individual JP8 or S8 constituents in a chamber across a 4 hour period has not been previously reported.

The droplet MMAD and GSD reported are in the respirable range for the rat and generally range from 1-3 μm across all exposures. The conditions present by design in a cascade impactor, where there is lower pressure in the lower stages, could influence volatilization and determination of droplet size. In effect, this would skew the data such that the values reported are upper limits for MMAD and GSD, rather than more definitive values that could be obtained from an aerodynamic particle sizer. The analysis via SPME-GC/MS would also follow the same trend. The cascade impactor has been used in prior work with jet fuels and offers a point of comparison (Whitman and Hinz, 2001, 2004).

In conclusion, with the increased interest in biofuels and blended petroleum-biofuels, as well the use of a 50:50 blend of JP-8 and S-8 for military aircraft, a better understanding of the composition of each jet fuel is paramount. In performing inhalation toxicity experiments with these potential fuels, efforts to characterize the complex mixture are necessary to interpret the toxicity findings. To develop risk assessment tools such as PBPK models, state of the art analytical methods are required to characterize laboratory animal exposures.

ACKNOWLEDGEMENTS

This work was supported by Air Force Office of Scientific Research (AFOSR) grant FA9550-07-1-0132. The authors would like to thank Drs. Rudolph Jaeger, Jerry L. Campbell Jr., Eva D. McLanahan, W. Matthew Henderson, Babatope Fatuyi, Oluseye Ogunmoroti, Mr. James Reboulet, Mrs. Libby Myers for their help during this work, also Dr. Anne Marie Zimeri for kindly editing this document.

DECLARATION OF INTEREST

The authors report no declarations of interest. The authors alone are responsible for the content and writing of the paper.

REFERENCES

Acros Organics N.V. (2000). Material Safety Data Sheet Naphthalene, Scintillation Grade 99+%. [Online] Available at: http://avogadro.chem.iastate.edu/MSDS/naphthalene.htm. Accessed August 12, 2009.

Baldwin C, Figueredo A, Wright L, Wong S, Witten M. (2007). Repeated Aerosol-vapor JP-8 Jet Fuel Exposure Affects Neurobehavior and Neurotransmitter Levels in a Rat Model. J Toxicol Environ Health, Part A, 70, 1203-1213.

Brockman J. (1993). Sampling and Transport of Aerosols. In: Baron P, Willeke K, ed. Aerosol Measurement: Principle, Techniques and Applications. NY: Van Nostrand Reinhold.

Campbell Jr J, Fisher J. (2007). A PBPK modeling assessment of the competitive metabolic interactions of JP-8 vapor with two constituents, m-xylene and ethylbenzene. Inhalation Toxicol, 19, 265-273.

Chatterjee A, Babu R, Klausner M, Singh M. (2006). In vitro and in vivo comparison of dermal irritancy of jet fuel exposure using EpiDerm™(EPI-200) cultured human skin and hairless rats. Toxicol Lett, 167, 85-94.

Chavanne B. (2007). USAF Wants Fleet Certified For Synthetic Fuel Blend by 2011. Aviation Week: Aerospace Daily and Defense Report [Online] Available at:. [Online] Available at: http://www.aviationweek.com/aw/generic/story_channel.jsp?channel=defense&id=news/FUEL102907.xml. 29 October 2007.

ChemicalBook Inc. (2008a). 2-Methylnaphthalene (91-57-6). [Online] Available at: http://www.chemicalbook.com/ProductMSDSDetailCB5854626_EN.htm. Accessed August 11, 2009.

ChemicalBook Inc. (2008b). n-Tridecane (629-50-5). [Online] Available at: http://www.chemicalbook.com/ProductMSDSDetailCB3232426_EN.htm. Accessed August 11, 2009.

Cox SS, Zhao D, Little JC. (2001). Measuring partition and diffusion coefficients for volatile organic compounds in vinyl flooring. Atmos Environ, 35, 3823-3830.

Dennis JH, Stenton SC, Beach JR, Avery AJ, Walters EH, Hendrick DJ. (1990). Jet and ultrasonic nebuliser output: use of a new method for direct measurement of aerosol output. Thorax, 45, 728-32.

Dietzel K, Campbell J, Bartlett M, Witten M, Fisher J. (2005). Validation of a gas chromatography/mass spectrometry method for the quantification of aerosolized Jet Propellant 8. J Chromatogr A, 1093, 11-20.

Fechter L, Gearhart C, Fulton S, Campbell J, Fisher J, Na K, Cocker D, Nelson-Miller A, Moon P, Pouyatos B. (2007). JP-8 jet fuel can promote auditory impairment resulting from subsequent noise exposure in rats. Toxicol Sci, 98, 510-525.

Harris D, Sakiestewa D, Robledo R, Witten M. (1997). Immunotoxicological effects of JP-8 jet fuel exposure. Toxicol Ind Health, 13, 43-55.

Harris D, Sakiestewa D, Robledo R, Young R, Witten M. (2000). Effects of short-term JP-8 jet fuel exposure on cell-mediated immunity. Toxicol Ind Health, 16, 78.

Hemighaus G. (2007). Synthetic Fuels for Aviation. ASTM Stand News. ASTM International. [Online] Available at: http://www.astm.org/SNEWS/APRIL_2007/p_hemighaus_apr07.html. 17 July 2009.

Hernandez SAJ. (2007). SECAF certifies Fischer-Tropsch synthetic fuel blends for B-52H. Air Force Materiel Command - News. Air Force Materiel Command. [Online] Available at: http://www.afmc.af.mil/news/story.asp?id=123063849. 14 June 2009.

Jaeger RJ. (1994). Modular reversible-flow-past nasopulmonary respiratory dosing system for laboratory animals. Patent No. 5297502.

Keystone Automotive Industries. (2004). Material Safety Data Sheet. Product Name: 2.1 VOC Key Euro Clear Slow Activator. [Online] Available at: http://www.keystone-auto.com/bodyshops/msds/msds-keyC48.pdf. Accessed August 3, 2009.

Knave B, Persson H, Goldberg J, Westerholm P. (1976). Long-term exposure to jet fuel: an investigation on occupationally exposed workers with special reference to the nervous system. Scand J Work Environ Health, 2, 152-164.

Knave B, Olson B, Elofsson S, Gamberale F, Isaksson A, Mindus P, Persson H, Struwe G, Wennberg A, Westerholm P. (1978). Long-term exposure to jet fuel. II. A cross-sectional

epidemiologic investigation on occupationally exposed industrial workers with special reference to the nervous system. Scand J Work Environ Health, 4, 19-45.

Knave B, Mindus P, Struwe G. (1979). Neurasthenic symptoms in workers occupationally exposed to jet fuel. Acta Psychiatr Scand, 60, 39-49.

Mattie D, Alden C, Newell T, Gaworski C, Flemming C. (1991). A 90-day continuous vapor inhalation toxicity study of JP-8 jet fuel followed by 20 or 21 months of recovery in Fischer 344 rats and C57BL/6 mice. Toxicol Pathol, 19, 77-87.

May K. (1973). The Collison nebulizer: description, performance and application. J. Aerosol Sci, 4, 235-243.

McCallion O, Taylor K, Bridges P, Thomas M, Taylor A. (1996). Jet nebulisers for pulmonary drug delivery. Int J Pharm, 130, 1-11.

McDougal J, Garrett C, Amato C, Berberich S. (2007). Effects of brief cutaneous JP-8 jet fuel exposures on time course of gene expression in the epidermis. Toxicol Sci, 95, 495-510.

Monteiro-Riviere N, Inman A, Riviere J. (2001). Effects of short-term high-dose and low-dose dermal exposure to Jet A, JP-8 and JP-8+ 100 jet fuels. J Appl Toxicol, 21, 485-494.

Nordholm A. (1999). Repeated exposure of rats to JP-4 vapor induces changes in neurobehavioral capacity and 5-HT/5-HIAA levels. J Toxicol Environ Health, Part A, 56, 471-499.

Osgar M. (2009). Personal Communication. Savillex Corporation, Minnetonka MN.

Perleberg U, Keys D, Fisher J. (2004). Development of a physiologically based pharmacokinetic model for decane, a constituent of jet propellent-8. Inhalation Toxicology, 16, 771-783.

Porter H. (1990). Aviators intoxicated by inhalation of JP-5 fuel vapors. Aviation, space, and environmental medicine, 61, 654-656.

Potter TL, Simmons KE. (1998). Total Petroleum Hydrocarbon Criteria Working Group Series Volume 2: Composition of Petroleum Mixtures. Amherst Scientific Publishing. [Online] Available at: http://www.aehs.com/publications/catalog/contents/tph.htm. Accessed August 3, 2009.

Ramos G, Nghiem D, Walterscheid J, Ullrich S. (2002). Dermal application of jet fuel suppresses secondary immune reactions. Toxicol Appl Pharmacol, 180, 136-144.

Rau J. (2002). Design principles of liquid nebulization devices currently in use. Discussion. Respir Care, 47, 1257-1275.

Reboulet J. (2006). Personal Communication. Wright Patterson Air Force Base, Dayton, OH.

Rhodes A, LeMasters G, Lockey J, Smith J, Yiin J, Egeghy P, Gibson R. (2003). The Effects of Jet Fuel on Immune Cells of Fuel System Maintenance Workers. J Occup Environ Med, 45, 79-86.

Ritchie G, Rossi J, Nordholm A, Still K, Carpenter R, Wenger G, Wright D. (2001). Effects of repeated exposure to JP-8 jet fuel vapor on learning of simple and difficult operant tasks by rats. J Toxicol Environ Health, Part A, 64, 385-415.

Robledo R, Witten M. (1998). Acute pulmonary response to inhaled JP-8 jet fuel aerosol in mice. Inhalation Toxicol, 10, 531-553.

Robledo R, Young R, Lantz R, Witten M. (2000). Short-term pulmonary response to inhaled JP-8 jet fuel aerosol in mice. Toxicol Pathol, 28, 656.

Rossi J, Nordholm A, Carpenter R, Ritchie G, Malcomb W. (2001). Effects of repeated exposure of rats to JP-5 or JP-8 jet fuel vapor on neurobehavioral capacity and neurotransmitter levels. J Toxicol Environ Health, Part A, 63, 397-428.

Salem H, Katz S. (2006). Inhalation toxicology. CRC Press.

Savillex. (2005). C-Flow Nebulizer Installation Details. 300023. Savillex, Inc. Minnetonka, MN.

ScienceLab.com Inc. (2008). Material Safety Data Sheet. [Online] Available at: http://www.sciencelab.com. Accessed August 3, 2009.

Smith L, Bhattacharya A, Lemasters G, Succop P, II E, Medvedovic M, Joyce J. (1997). Effect of Chronic Low-Level Exposure to Jet Fuel on Postural Balance of US Air Force Personnel. J Occup Environ Med, 39, 623-632.

The Physical and Theoretical Chemistry Laboratory Oxford University. (2009). MSDS (Material Safety Data Sheet) Information. [Online] Available at: http://msds.chem.ox.ac.uk/. Accessed August 11, 2009.

Tillery MI, Wood GO, Ettinger HJ. (1976). Generation and characterization of aerosols and vapors for inhalation experiments. Environ Health Perspect, 16, 25-40.

Tremblay R, Martin S, Fechter L, Fisher J. (2008). A novel method for the chemical characterization of generated jet fuel vapor and aerosol for animal studies, 1100. The Toxicologist CD — An official Journal of the Society of Toxicology, 102, (S-1).

Tremblay R, Martin S, Fisher J. (2010a). In: Witten M, Ritchie G, Zeiger E, ed. Jet Fuel Toxicology. London: Taylor & Francis (*in press)*.

Tremblay RT, Martin SA, Fisher JW. (2010b). Feb. [Epub ahead of print]. Novel Characterization of the Aerosol and Gas Phase Composition for Aerosolized Jet Fuel Atmospheres. Inhalation Toxicology (in press), doi: 10.3109/08958370903456637.

Ullrich S. (1999). Dermal application of JP-8 jet fuel induces immune suppression. Toxicol Sci, 52, 61-67.

Whitman F, Hinz J. (2001). Sensory irritation study in mice: JP-4, JP-8, JP-8+100. IERA-RS-BR-SR-2001-0005. Risk Assessment Division, Air Force Institute for Operational Health,

Brooks City-Base, TX. IERA-RS-BR-SR-2001-0005. Risk Assessment Division AFIfOH, Brooks City-Base, TX.

Whitman F, Hinz J. (2004). Sensory irritation study in mice: JP-5, JP-TS, JP-7, DFM, JP-10. IOH-RS-BR-SR-2004-0001. Risk Assessment Division, Air Force Institute for Operational Health, Brooks City-Base, TX. IERA-RS-BR-SR-2004-0001. Risk Assessment Division AFIfOH, Brooks City-Base, TX.

Wolff R, Niven R. (1994). Generation of aerosolized drugs. J Aerosol Med, 7, 89-106.

Figure 2.1. University of Georgia Inhalation Exposure System

(A.) University of Georgia Inhalation Exposure System-A (UGIES-A). HEPA+Charcoal filtered air was pumped into a Collison Nebulizer, leading to generation of an aerosol:vapor exposure environment. The nebulizer design directs a fraction of the exposure air to the system, with the remainder recirculated into the liquid reservoir. The exposure air was passed through 60cm stainless steel tubing with a welded steel bung to allow addition of dilution air. A fraction was removed with a gate-valve and bellows pump, adding further control of the total concentration. Mixed chemical and dilution air was directed into the base of the nose-only chamber and expressed. The air was sampled via GC/FID with automated pneumatics and heated (200C) transfer-line to determine stability over time. Thermal-desorption tubes (TDS) were collected to quantify individual constituents and define the aerosol:vapor percentage for each constituent after GC/MS analysis. A 7-stage cascade impactor measured the droplet size distribution. Exhaust was removed to the fume hood for scrubbing and filtration. For further details refer to Materials and Methods section.

(B.) University of Georgia Inhalation Exposure System-B (UGIES-B).

HEPA+Charcoal filtered air was pumped into a single-pass nebulizer, leading to generation of an aerosol:vapor exposure environment. Nebulized jet fuel passed into a Scott-Type spray chamber (SC). The atmosphere was directed through a combination of stainless steel and fuel resistant tubing where it was mixed with dilution air. Sample collection progressed as per UGIES-A. For further details refer to Materials and Methods section.

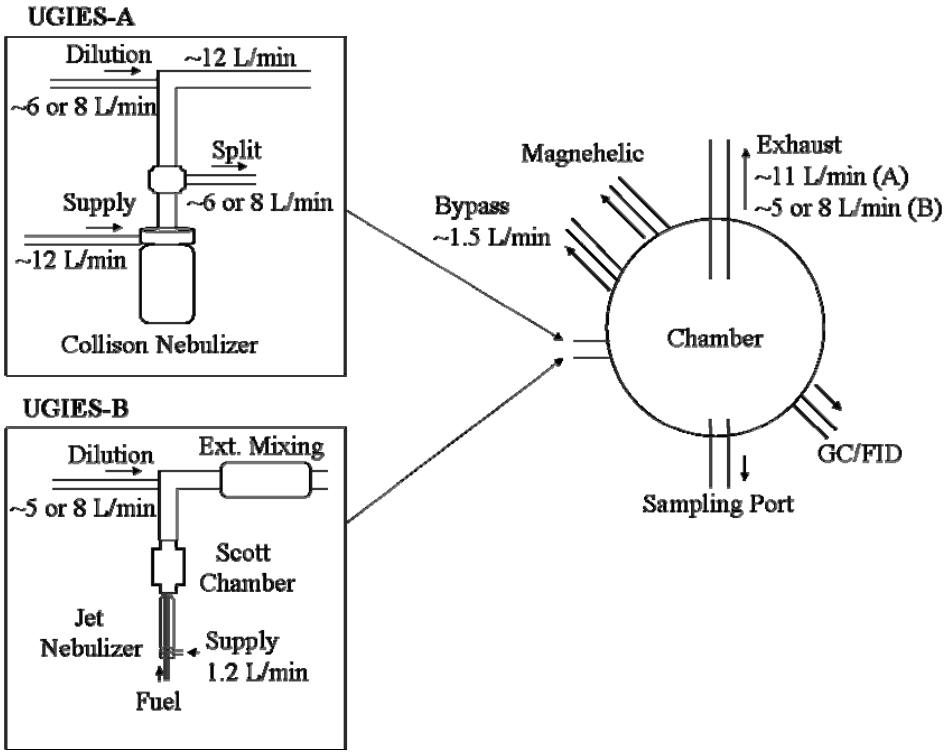
UGIES-A
Dilution
~12 L/min
~6 or 8 L/min
Split
Supply
~6 or 8 L/min
~12 L/min
Collison Nebulizer
UGIES-B
Dilution
Ext. Mixing
~5 or 8 L/min
Scott
Chamber
Jet
Nebulizer
Supply
1.2 L/min
Fuel
Magnehelic
Exhaust
~11 L/min (A)
~5 or 8 L/min (B)
Bypass
~1.5 L/min
Chamber
GC/FID
Sampling Port

Table 2.1. Properties of selected hydrocarbon constituents of n-alkane/PAH mixture and jet fuels

Chemical	**MW (g/mol)**	**Vapor Pressure (mm Hg)**	**Boiling Point (°C)**
Toluene [a]	92.1	22 (20C)	110.6
Ethylbenzene [a]	106.2	10 (20C)	136
m-Xylene [b]	106.2	6 (20C)	139.3
n-octane (C8) [b]	114.2	11 (20C)	125.6
1,2,4-Trimethylbenzene [c]	120.9	2.03 (25C)	168.89
Naphthalene [d]	128.2	0.05 (20C)	218
n-nonane (C9) [b]	128.3	3.22 (20C)	151
2-methylnaphthalene [e]	142.2	0.03 (25C)	241
n-decane (C10) [b,f]	142.3	0.89 (20C)	174
n-undecane (C11) [a]	156.3	<0.4 (20C)	196
n-dodecane (C12) [b,f]	170.3	0.074 (20C)	216.3
n-tridecane (C13) [g]	184.4	0.081 (25C)	235.4
n-tetradecane (C14) [b,f]	198.4	0.0071 (20C)	253.5
n-pentadecane (C15) [b,f]	212.4	0.0014 (20C)	270

a (The Physical and Theoretical Chemistry Laboratory Oxford University, 2009)
b (ScienceLab.com Inc., 2008)
c (Keystone Automotive Industries, 2004)
d (Acros Organics N.V., 2000)
e (ChemicalBook Inc., 2008b)
f (Cox et al., 2001)
g (ChemicalBook Inc., 2008a)

Table 2.2. Chamber sampling methods. Atmospheric concentration ($mg/m^3 \pm$ SD) with size distribution of aerosol droplets, stability across a 4-hour period as Coefficient of Variation (CV), and aerosol fraction (%) in all atmospheres.

System	Exposure	Mean Total Concentration ± Standard Deviation (SD) (mg/m^3), Coefficient of Variation (%)	Droplet Mass Median Aerodynamic Diameter (MMAD), Geometric Standard Deviation (GSD) (um)	Aerosol Fraction (%)
UGIES-A	**n-Alkane/PAH Mix (High)**	1337.8 ± 52.6, 4	2.22, 2.02	72
	n-Alkane/PAH Mix (Low)	644.7 ± 32.9, 5	3.21, 2.41	76
UGIES-B	**S-8**	1071.6 ± 34.5, 3 (TWA: 1037.5 ± 28.6)	1.38, 1.88	30
	JP-8	906.5 ± 38.49, 4 (TWA: 846.6 ± 34.1)	3.28, 2.50	36
	JP-8/S-8 Blend	188.5 ± 6.26, 3 (TWA: 182.6 ± 6.1)	0.96, 1.77	27

Table 2.3A. n-Alkane/PAH (1338 mg/m^3). Characterization of exposure air constituents with total, vapor, and aerosol concentration per chemical (mg/m^3± SD). Percent aerosol and vapor-phase of each constituent provided with coefficient of variation across 8 pairs of TD tubes collected at approximate 40 min intervals.

Hydrocarbon	**Total Conc. (mg/m^3) (SD, CV(%))**	**Vapor Conc. (mg/m^3) (SD, CV(%), fraction of total (%))**	**Aerosol Conc. (mg/m^3) (SD, CV(%), fraction of total (%))**
Decane	224.6 (14.7, 7)	152.4 (6.1, 4, 68)	72.2 (13.3, 18, 32)
Undecane	196.4 (11.5, 6)	95.8 (13.2, 14, 49)	100.6 (5.2, 5, 51)
Dodecane	164.9 (11.4, 7)	49.1 (7.90, 16, 30)	115.8 (4.8, 4, 70)
Tridecane	119.0 (6.6, 6)	15.7 (2.5, 16, 13)	103.3 (4.9, 5, 87)
Tetradecane	145.3 (19.5, 13)	5.90 (1.0, 17, 4)	139.4 (19.9, 14, 96)
Pentadecane	167.8 (23.9, 14)	2.0 (0.4, 22, 1)	165.8 (24.1, 15, 99)
2-methylnaphthalene	159.4 (10.7, 7)	16.0 (2.5, 16, 10)	143.4 (8.5, 6, 90)
Naphthalene	160.4 (5.3, 3)	33.9 (4.8, 14, 21)	126.5 (2.9, 2, 79)

Table 2.3B. n-Alkane/PAH (645 mg/m^3). Characterization of exposure air constituents with total, vapor, and aerosol concentration per chemical (mg/m^3± SD). Percent aerosol and vapor-phase of each constituent provided with coefficient of variation across 8 pairs of TD tubes collected at approximate 40 min intervals.

Hydrocarbon	**Total Conc. (mg/m^3) (SD, CV(%))**	**Vapor Conc. (mg/m^3) (SD, CV(%), fraction of total (%))**	**Aerosol Conc. (mg/m^3) (SD, CV(%), fraction of total (%))**
Decane	133.0 (6.4, 5)	94.1 (3.3, 4, 71)	38.9 (5.7, 15, 29)
Undecane	91.8 (3.5, 4)	48.2 (2.1, 4, 53)	43.6 (2.8, 6, 47)
Dodecane	76.4 (3.8, 5)	27.1 (0.7, 3, 35)	49.3 (3.3, 7, 65)
Tridecane	67.3 (6.5, 10)	13.0 (0.6, 4, 19)	54.3 (6.2, 11, 81)
Tetradecane	60.3 (5.3, 9)	4.8 (1.3, 27, 8)	55.5 (5.2, 9, 92)
Pentadecane	57.1 (12.1, 21)	2.4 (0.9, 37, 4)	54.7 (11.6, 21, 96)
2-methylnaphthalene	73.6 (2.9, 4)	10.2 (0.8, 8, 14)	63.4 (2.2, 3, 86)
Naphthalene	85.3 (3.9, 5)	20.3 (1.5, 7, 24)	65.0 (3.9, 6, 76)

Table 2.4A. JP-8 (907 mg/m^3). Characterization of exposure air constituents with total, vapor, and aerosol concentration per chemical. Percent aerosol and vapor-phase of each constituent provided with coefficient of variation across 5 pairs of TDS tubes collected at approximate 40 min intervals. Data are shown as mean ± standard deviation (mg/m^3).

Hydrocarbon	**Total Conc. (mg/m^3) (SD, CV(%))**	**Vapor Conc. (mg/m^3) (SD, CV(%), fraction of total (%))**	**Aerosol Conc. (mg/m^3) (SD, CV(%), fraction of total (%))**
Octane	12.4 (0.5, 4)	11.6 (0.3, 2, 94)	0.8 (0.6, 68, 6)
Nonane	16.1 (0.6, 4)	15.1 (0.5, 3, 94)	1.0 (0.3, 29, 6)
Decane	18.6 (0.4, 2)	16.2 (0.9, 6, 88)	2.4 (1.0, 44, 12)
Undecane	17.8 (0.7, 4)	12.4 (0.3, 2, 70)	5.4 (0.8, 15, 30)
Dodecane	13.9 (0.7, 6)	7.0 (0.2, 4, 50)	7.0 (0.8, 12, 50)
Tridecane	8.6 (0.3, 3)	2.5 (0.2, 8, 29)	6.1 (0.3, 5, 71)
Tetradecane	5.2 (0.1, 2)	2.9 (0.3, 12, 55)	2.3 (0.4, 16, 45)
Pentadecane	2.1 (0.2, 10)	0.1 (0.1, 140, 5)	2.0 (0.2, 11, 95)
2-methylnaphthalene	0.1 (<0.1, 16)	<0.1 (<0.1, 137, 12)	0.1 (<0.1, 30, 88)
Naphthalene	0.4 (0.2, 40)	0.2 (<0.1, 0.3, 39)	0.3 (0.2, 64, 61)

Table 2.4A. (Continued)

Toluene	4.6 (0.2, 4)	4.3 (0.1, 3, 93)	0.3 (0.1, 36, 7)
m-Xylene	7.0 (0.3, 4)	6.0 (0.3, 5, 87)	1.0 (0.3, 34, 13)
Ethylbenzene	2.8 (0.1, 3)	2.5 (0.1, 2, 90)	0.3 (0.1, 19, 10)
1,2,4-Trimethylbenzene	8.1 (0.4, 6)	6.0 (0.3, 4, 76)	2.0 (0.7, 32, 24)

Table 2.4B. S-8 (1072 mg/m^3). Characterization of atmosphere constituents with total, vapor, and aerosol concentration per chemical. Percent aerosol and vapor-phase of each constituent provided with coefficient of variation across 6 pairs of TD tubes collected at approximate 40 min intervals. Data are shown as mean ± standard deviation (mg/m^3).

Hydrocarbon	**Total Conc. (mg/m^3) (SD, CV(%))**	**Vapor Conc. (mg/m^3) (SD, CV(%), fraction of total (%))**	**Aerosol Conc. (mg/m^3) (SD, CV(%), fraction of total (%))**
Octane	41.4 (3.1, 8)	39.2 (2.6, 7, 95)	2.2 (2.9, 129, 5)
Nonane	51.9 (4.5, 9)	44.5 (3.2, 7, 86)	7.4 (5.5, 75, 14)
Decane	37.7 (3.3, 9)	28.1 (2.1, 7, 75)	9.6 (4.2, 43, 25)
Undecane	23.2 (1.6, 7)	14.0 (1.6, 11, 61)	9.2 (2.5, 27, 39)
Dodecane	15.0 (0.9, 6)	6.7 (0.8, 12, 45)	8.3 (1.6, 19, 55)
Tridecane	9.2 (0.6, 7)	2.1 (0.3, 13, 23)	7.1 (0.6, 8, 77)
Tetradecane	6.2 (0.7, 11)	2.6 (0.5, 19, 43)	3.5 (0.7, 21, 57)
Pentadecane	1.6 (0.5, 29)	<0.1 (0.1, 156, 3)	1.5 (0.5, 32, 97)

Table 2.4C. JP-8/S-8 (189 mg/m^3). Characterization of atmosphere constituents with total, vapor, and aerosol concentration per chemical. Percent aerosol and vapor-phase of constituents provided with coefficient of variation across 4 pairs of TD tubes collected at approximate 40 min intervals. Data shown as mean ± standard deviation (mg/m^3).

Hydrocarbon	**Total Conc. (mg/m^3) (SD, CV(%))**	**Vapor Conc. (mg/m^3) (SD, CV(%), fraction of total (%))**	**Aerosol Conc. (mg/m^3) (SD, CV(%), fraction of total (%))**
Octane	3.08 (0.35, 11)	2.70 (0.44, 16, 89)	0.38 (0.66, 175, 11)
Nonane	3.92 (0.44, 11)	3.31 (0.50, 15, 86)	0.61 (0.84, 139, 14)
Decane	3.39 (0.40, 12)	2.49 (0.37, 15, 75)	0.90 (0.69, 76, 25)
Undecane	2.59 (0.28, 11)	1.53 (0.28, 18, 60)	1.06 (0.52, 49, 40)
Dodecane	1.82 (0.17, 9)	0.71 (0.19, 27, 40)	1.12 (0.33, 30, 60)
Tridecane	1.18 (0.10, 9)	0.25 (0.12, 46, 22)	0.93 (0.19, 21, 78)
Tetradecane	0.75 (0.06, 9)	0.55 (0.24, 42, 75)	0.19 (0.26, 138, 25)
Pentadecane	0.25 (0.02, 8)	0.01 (<0.01, 56, 3)	0.24 (0.02, 8, 97)
2-methylnaphthalene	0.06 (0.01, 13)	0.01 (0.01, 56, 24)	0.04 (0.01, 29, 76)
Naphthalene	0.06 (0.01, 22)	0.02 (<0.01, 21, 36)	0.04 (0.01, 33, 64)
Toluene	0.36 (0.04, 11)	0.31 (0.04, 14, 87)	0.05 (0.07, 127, 13)
m-Xylene	0.52 (0.07, 13)	0.41 (0.06, 16, 80)	0.11 (0.11, 97, 20)

Table 4C. (Continued)

Ethylbenzene	0.24 (0.03, 11)	0.19 (0.03, 15, 80)	0.05 (0.05, 104, 20)
1,2,4-Trimethylbenzene	0.64 (0.07, 11)	0.40 (0.07, 17, 64)	0.24 (0.13, 54, 36)

CHAPTER 3

DEVELOPMENT OF A PHYSIOLOGICALLY-BASED PHARMACOKINETIC MODEL FOR JET FUELS IN THE RAT

Martin, S.A., Tremblay, R.T., Campbell, JL, Jr., Fisher, J.W. *To be submitted.*

INTRODUCTION

Approximately 5 billion gallons of kerosene-based aviation fuels were consumed by the U.S. Department of Defense in 2008. Jet Propellant 8 (JP-8) accounted for 50% of this total, with 2.5 billion/gal/year consumed by the U.S. Air Force and 1.3 billion/gallons/year of JP-8 and JP-5 consumed by the US Navy (DOD, 2008). JP-8 is a complex mixture consisting of aromatic and aliphatic hydrocarbons numbering in the hundreds. Military service personnel worldwide are commonly exposed to fuels while performing their duties (NRC, 2003). Exposures to jet fuels have been associated with reports of neurological, immune, and respiratory symptoms in pilots and flight line personnel (Knave *et al.*, 1979, Knave *et al.*, 1978, Knave *et al.*, 1976, Porter, 1990, Rhodes *et al.*, 2003b, Smith *et al.*, 1997b, Tunnicliffe *et al.*, 1999). However, the majority of the published inhalation toxicity data for jet fuels are derived from toxicity studies with rodents (Baldwin *et al.*, 2007, Harris *et al.*, 1997, Harris *et al.*, 2000, Ritchie *et al.*, 2001a).

In most of these inhalation toxicity studies with fuel only the total hydrocarbon concentrations (ie., mg/m^3) are reported for fuel vapors or aerosol droplets. Recently our laboratory evaluated the hydrocarbon composition of the rodent inhalation exposure chambers used for fuel toxicity testing at the University of Arizona (Dietzel *et al*., 2005). Since then we have constructed our own nose-only chamber exposure system for aerosolized jet fuel (Martin *et al.*, 2010, Tremblay *et al.*, 2010b). The hydrocarbon composition of inhaled aerosolized fuel was characterized and blood and tissues from rats were collected for the analysis of hydrocarbons to aid in the development of a PBPK model for jet fuels. A jet fuel PBPK model will provide a tool to better understand internal dosimetry for this complex mixture of hydrocarbons. The lack of detailed exposure characterization of inhaled jet fuels has precluded PBPK model development for jet fuels. Jet fuel toxicity studies have recently been conducted with aerosolized fuels

(Baldwin *et al*., 2007, Fechter *et al*., 2007, Wong *et al*., 2009, Wong *et al*., 2008), while older exposures utilized vaporized fuel (Ritchie *et al.*, 2001a, Rossi *et al.*, 2001). There is a need to reconcile both types of exposure into a single PBPK model and investigate similarities and differences in the resulting tissue kinetic behavior.

Pharmacokinetic studies were carried out with aerosolized petroleum derived jet fuel (JP-8) and a synthetic fuel (S-8), synthesized from natural gas by the Fischer-Tropsch process. Unlike JP-8, S-8 was free of aromatic hydrocarbons. Additionally, blend of JP-8 with S-8 has been found to be suitable for military aircraft operations and will be implemented in the coming decade (Chavanne, 2007). A fuel PBPK model was developed using 6 individual hydrocarbon markers for JP-8 and the blend, and 3 for S-8, then assigning the remaining fraction of fuel as 'lumps,' similar to the strategy implemented for modeling of gasoline exposures (Dennison *et al*., 2003).

Gasoline is composed of mid-range and light-end aliphatic and aromatic hydrocarbons, with constituent concentrations varying by blend. Dennison *et al.* (2003)developed a PBPK model for benzene, toluene, ethylbenzene, o-xylene (BTEX) and n-hexane alone, and in gasoline blends, to predict gas-uptake chamber concentration data during 6-hr exposures with initial concentrations of 100-1500ppm. A lumping approach was implemented to account for the remainder of the exposure air concentration and gauge the impact of competitive metabolic inhibition of the lump fraction on specific chemical "markers". At 500-1500ppm total metabolism of BTHEX and gasoline was reduced 1-28%.

PBPK models have also been published for n-decane vapor. Perleberg *et al* (2004) and Merrill *et al* (2008) developed models for exposure to 273-1200ppm decane vapor in the rat (Merrill *et al*., 2008, Perleberg *et al*., 2004). Hissink *et al* (2007) developed a model to describe

decane kinetics in 4-hour exposure to 100-820ppm white spirit vapor, where the concentration of decane was known. Metabolic parameters were fit to decane data without lumping the remaining constituents. Decane has not previously been described in a model for aerosolized or vaporized jet fuels. Tardif *et al* (1997) and Haddad *et al* (1999) developed PBPK models for exposure to 50-200ppm vapor exposures and evaluated the effect of inhibition of metabolism on chemicals in a ternary or quaternary mixture. Campbell and Fisher (2007) developed PBPK models for m-xylene and ethylbenzene using the pharmacokinetic data from Tardif *et al* (1997) and Haddad *et al* (1999). The model was then used to simulate data at three concentrations of JP-8 vapor, tracking both markers in exposed rats. A single lumped aromatic fraction was created to gauge the inhibitory potential of aromatic fuel constituents on metabolism of the markers. From low to high concentration exposures, the lumped fraction resulted in minimal to approximately 40% reduction in marker chemical metabolism, as interpreted by increases in area-under-the-curve (AUC) for blood time-course data.

No previous studies have investigated the pharmacokinetics of aerosolized n-octane, n-decane, n-tetradecane, toluene, ethylbenzene, or m-xylene, individually or in exposure to fuels. In this study systemic uptake of aerosol droplets and vapors are described in a jet fuel model for the rat.

MATERIALS AND METHODS

Animals

Adult male Fischer 344 rats (200-230g) were purchased from Charles River Inc. (Raleigh, NC) and maintained under 12-hour light:dark cycle (72±2°F, 50±10% humidity) with food (Purina Rat Chow) and water *ad libitum*. Food and water were not provided during

exposure. Prior to use, rats were conditioned in nose-only exposure cones by sequential insertion and removal for increasing time periods across 4 days (10, 30, 60, 120 minutes), as approved by the University of Georgia (UGA) Institutional Animal Care and Use Committee (IACUC). On the day of exposure, rats were inserted into nose-only tubes 10 minutes before studies were started. Rats were killed by CO_2 asphyxiation, tissues and blood removed, and stored in sealed vials at -80°C until time for analysis. All animal use was in compliance with policies of the UGA IACUC.

Chemicals

For tissue and atmospheric analysis, n-octane (C8), n-decane (C10), n-undecane (C11), n-dodecane (C12), n-tridecane (C13), n-tetradecane (C14), n-pentadecane (C15), naphthalene, o-ethyltoluene, ethylbenzene (EBZ), and trimethylbenzenes (TMBs) were at least 99 % purity and 1 and 2-methylnaphthalene, 97 % (Acros Organics, Morris Plains, NJ). n-Hexane (C6) was 95-97 % and toluene was +99% purity (JT Baker Phillipsburg, NJ). 2, 3 and 4-methyldecane were 99.5 %, 98.9 % and 98.7% purity, respectively (Chem Service, West Chester, PA). m, p, and o-Xylene were all 99+ % purity (Sigma-Aldrich, St. Louis, MO). PIONA-Mixture 1-Isoparaffines Standard (S-4136), used for all other aliphatic chemicals, was from Chiron AS, Trondheim, Norway. Jet propellant-8 (JP-8) (POSF 4658 with JP-8 additives) and Synthetic Jet Propellant-8 (S-8) (POSF 4734 Fischer-Tropsch Synthetic Fuel) were obtained from Wright-Patterson Air Force Base, Dayton, OH. “Marker” chemicals for PBPK model development were C8, C10, C14, TOL, EBZ, and m-XYL. Quantified non-marker chemicals were used only in development of PBPK model lumps, as will be described.

Experimental

Inhalation Exposures

All rat inhalation exposures were conducted with a 12-port directed-flow nose-only exposure system (CH Technologies, Westwood, NJ). Martin *et al.* (2010) describes in detail the inhalation exposure system and the techniques for generating atmospheric levels of hydrocarbons and Tremblay *et al.* (2010b) and Martin *et al.* (2010) describe the analytical methods used for characterizing the chamber atmosphere for aerosolized fuel exposures. With a limit on the number of rats that could be exposed at once (n=8), several inhalation exposures were carried out to construct each of 3 4-hour aerosolized jet fuel exposures; one with JP-8 (908 ± 18.09 mg/m^3; 28% aerosol), one with S-8 (1066 ± 48.87 mg/m^3; 35% aerosol) and another with a 50:50 blend of JP-8 and S-8 (186.5 ± 2.86 mg/m^3; 24% aerosol). Table 3.1 provides exposure information for each aerosolized fuel study. Droplet mass median aerodynamic diameter and geometric standard deviation (MMAD, GSD) were recorded for exposures to JP-8 (3.20, 2.62µm), S-8 (1.15, 1.55µm), and for the blend of JP-8 and S-8 (0.96, 1.77µm). Deposition fractions were predicted for the nasal passages, and for the tracheobronchial (TB) airways and lung (nasal, TB-lung), for exposure to JP-8 (0.53, 0.07), S-8 (0.08, 0.11), and the blend of JP-8 and S-8 (0.07, 0.11).

One 4-hour inhalation exposure was conducted by performing 3 4-hour aerosolized tetradecane inhalation exposures (89.5 ±10.6 mg/m^3 ; 84% aerosol). Adjusting the waste valve and dilution air controlled the tetradecane exposure concentration (Martin *et al.*, 2010). The total airflow rate was approximately 12 L/min. Droplet MMAD and GSD were 4.07 and 1.43µm, respectively. Predicted deposition fractions were 0.70 to the nasal passages and 0.10 to the tracheobronchial airways and lung.

Three 2-hour octane vapor inhalation exposures (C8, 90.3 ± 6.1, 996.2 ±22.0 and 4864 ± 99.6 ppm) were conducted using the nose-only inhalation chamber (Martin *et al.*, 2010). A fritted glass bubbler (Campbell Jr and Fisher, 2007) housed in a glass container with octane was used to generate the octane chamber concentrations. The total flow rate was approximately 12 L/min; consisting of octane vapor and dilution air. A gas transfer line, placed in one of the nose-only ports, was connected to a gas chromatograph equipped with a flame ionization detector. Concentrations of octane in the chamber were based on a calibration curve created using octane standards from a Tedlar bag (Perleberg *et al.*, 2004). Chamber concentrations were achieved through adjustment of bubbler and dilution flow rates. Before entering the chamber the aerosolized octane was passed through a 1L glass jar filled with glass wool to remove aerosol droplets.

Animal Exposures.

Twenty-four rats were used for the 4-hour JP-8 kinetic study with four rats killed at each time point. During the JP-8 exposure time points were at 2 hours and end of exposure and post exposure, 15, 30, 45 and 60 minutes. Thirty-two rats were used for the 4-hour S-8 kinetic study with four rats killed at each time point. During the S-8 exposure time points were at 2 hours and end of exposure and post exposure, 15, 30, 45 and 60 minutes and 24 and 48 hours. Sixteen rats were used for the 4-hour 50:50 blend of JP-8:S8 with four rats killed at each time point. During the fuel exposure time points were at 2 hours and end of exposure and post exposure 20 and 30 minutes. Twenty rats were used for the 4-hour tetradecane kinetic study with 4 rats killed at each time point. Rats were killed during exposure at 2 hours and end of exposure and post exposure at 15, 45, and 75 minutes. Twenty-four rats were used for the 2-hour octane vapor exposure.

Rats were killed only at the end of exposure for the 90 and 4864 ppm groups and for the 996 ppm group at the end of exposure and 5, 20 and 40 minutes. Tissues collected at sacrifice were liver, fat, lung, brain, and blood.

Determination of Blood and Tissue Concentration

Tissue and blood concentrations of hydrocarbons in jet fuel were quantified using a Solid Phase Microextraction coupled with Gas Chromatography/Mass Spectrometry (SPME-GC/MS) method reported by Campbell and Fisher (2007) (Table 3.3). The SPME-GC/MS system consisted of a COMBI Pal autosampler with SPME adaptor (CTC Analytics, Zwingen Switzerland) and a Saturn 2200 Ion Trap MS with a CP-3800 GC (Varian, Inc., Walnut Creek, CA) (Table 1). Individual 10 mL screw cap headspace vials (Supelco, Inc., Bellefone, PA) were filled with 3 mL of a sodium chloride solution (0.33 g/mL). Frozen tissues (0.5 g of liver, lung or brain) and blood (1.0 mL, heparinized) were added, then chopped with iris scissors, and vials capped. Fat (0.1 g) was mixed in the vial with 1 mL of the sodium chloride solution and 1 mL of a NaOH solution (2 M). Samples were vortexed for 1-hr at room temperature, then neutralized with 1 mL of HCl (2 M) and set aside for analysis. Quantification limits were found to be about 1 ng/g or mL for most compounds.

Extractions of the analytes in the headspace in each vial were performed using a 1 cm long 100 µm thickness polydimethylsiloxane (PDMS) SPME fiber. Analytes were desorbed for 1 min in a splitless mode inlet at 250oC. Analytes were resolved using a 50 m long HP-1 column (0.2 mm ID x 1.5 µm film thickness) with helium flow at 1 mL/min. Fibers were cleaned between each sample for 5-14 min at 250-275^{o}C.

For fuels, extraction durations were 16, 22, 22, 22 and 40 min for blood, brain, liver, lung and fat, respectively. Tissues were incubated under agitation for 45 min at 65°C. Analytes were desorbed for 1 min in a splitless mode inlet at 250°C. GC oven temperature programs were varied to minimize analysis time while maintaining good resolution. The oven was started at 35°C for 10 min, 2.0°C/min to 99°C, 7.0°C/min to 230°C, 20°C/min to 240°C, and held for 10 min.

For n-alkane (tetradecane, octane) extractions, a small number of parameters were modified from the fuel method described. Tetradecane exposed tissues were incubated under agitation at 65°C for 45 min. Extraction durations were unchanged compared to fuel analysis. The GC oven was started at 50°C, then ramped 7.0°C/min to 230°C, held 3 min, then 20°C/min to 240oC and held for 10 min. For octane samples, tissues were incubated under agitation for 25 min at 35°C. Extraction duration was 10 min for all octane samples. The GC oven was started at 50°C, then ramped 7.0°C/min to 230°C, then 20°C/min to 240°C and held for 3.8 min. The ion trap MS was set to scan from 45 to 260 m/z and an emission current of 45 μA was utilized to maximize signal.

PBPK Fuel Model

PBPK models for jet fuels were developed by relying on existing data collected in our laboratory for inhaled vapors of decane (Perleberg *et al.*, 2004), published PBPK models for m-xylene and ethyl benzene in JP-8 (Campbell Jr and Fisher, 2007), experimental studies reported in this paper and new PBPK models for individual hydrocarbons. Based on the composition of jet fuel, existing PBPK models and prevalence of hydrocarbons in liquid fuel and aerosolized fuel atmospheres, six representative hydrocarbons were selected as marker chemicals for JP-8 (n-

octane, n-decane, n-tetradecane, toluene, m-xylene, and ethylbenzene) and for S-8, 3 markers (n-octane, n-decane, and n-tetradecane). For the blended fuel mixture, the JP-8 PBPK model with the 6 hydrocarbon markers was used. Three PBPK models representing lump fractions of the fuel (Campbell Jr and Fisher, 2007) were used for JP-8 and 2 PBPK models for the lumped fractions of S-8.

Lumps for JP-8 and S-8 were derived from the GC/MS chromatogram for total aerosolized fuel by dividing the chromatogram into 3 sections for JP-8 and two sections for S-8 based on hydrocarbon retention time and aromatic content. JP-8 Lump 1 (L1) included aromatic hydrocarbons, representing 25% of total fuel concentration. Lump 2 (L2) represented primarily aliphatics C8 to C12 and Lump 3 (L3) represented aliphatics C-13 to C15. Naphthalene and substituted naphthalenes concentrations in the chamber were under 0.5 mg/m^3 and not included in the JP-8 PBPK fuel model. The JP-8:S-8 blend lumped PBPK models were identical to JP-8.

The PBPK models for JP-8 and S-8 were created for inhalation of aerosolized jet fuel, which contains both vapor and aerosol droplets. Each marker PBPK sub-model was composed of seven identical compartments representing the nasal tissue, lung, brain, liver, fat, and slowly perfused and rapidly perfused tissue groups. Tables 3.4 and 3.5 contain physiological and chemical specific model parameters for the sub-models.

Inhalation of Vapors and Aerosol Droplets

The deposition and systemic uptake of aerosol droplets were described for the nasal passage (respiratory and olfactory tissues) and tracheobronchial airways and lung similar to how inhaled manganese (Mn) deposition was described (Nong *et al.*, 2008, Teeguarden *et al.*, 2007). The

droplets deposited on the nasal passage and lung mucous layers. The lipophilic hydrocarbons in the droplet were assumed to dissolve and diffuse into the mucous layers of the nasal passages and tracheobronchial airways and lung. From the mucous layers, the hydrocarbons diffused into nasal, tracheobronchial and lung tissues, where the hydrocarbons were allowed to equilibrate and exchange with blood supplies perfusing these tissue groups. Inhalation of vapors was described using a simple algebraic blood/air equilibration (Campbell Jr and Fisher, 2007), which included the exhalation of volatile hydrocarbons derived from aerosol droplets in addition to inhaled vapors. The Multiple Path Particle Dosimetry Model (MPPD version 2.01, Hamner Institutes for Health Sciences, Research Triangle Park, NC) was used to determine the fraction of inhaled aerosol droplets deposited in the nasal passages or tracheobronchial airways, and lung (Fig. 1). 7-stage cascade impactor measurements were collected to determine the size of the aerosol droplets for use in the MPPD2 software (Martin *et al.*, 2010).

Chamber concentrations of individual hydrocarbon markers and lumped fractions of aerosolized fuel in the aerosol droplets and vapor (Table 3.1) or vapor only fuel exposures (Campbell and Fisher, 2007), were determined (Table 3.2). Exposure specific information was collected for JP-8, S-8, the blend of JP-8 and S-8, JP-8 vapors (Campbell Jr and Fisher, 2007) and white spirits (Hissink *et al.*, 2007, Lof *et al.*, 1999).

The deposition of hydrocarbon markers and associated lumped fractions found in aerosol droplets (either JP-8, S-8 or the blend of JP-8:S-8) in the nasal passage or tracheobronchial airways and lung were described with the following equations:

1) $$kdeposit\_{h,i}(mg/hr) = QP * CIA_{h,i} * fdeposit\_{h}$$

$Kdeposit_{h,I}$ equals the rate of deposition of inhaled hydrocarbon markers (i) and lumped chemicals (i) in either the nasal passages (h) or the tracheobronchial airways and lung (h), QP

equals the breathing rate (L/hr), $CIA_{h,i}$ is the concentration (mg/L) of aerosolized hydrocarbon for marker (i) and lumped chemical (i) for the nasal passages (h) or tracheobronchial airways and lung (h) and $fdeposit\_{h}$ is the MPPD2 calculated fractional deposition for either the nasal passages or tracheobronchial airways and lung.

$$2) \quad \frac{Rmucous\_{h,i}}{dt}(mg/hr) = kdeposit\_{h,i} - PA_{h,i} * Cmucous\_{h,i}$$

$Rmucous\_{h,i}$ equals the rate of change in the amount of hydrocarbon markers (i) and lumped chemicals (i) in the mucous of the nasal passages (h) and tracheobronchial airways and lung (h), $PA_{h,i}$ equals the permeability constant for transfer of hydrocarbon markers (i) and lumped compartments (i) into the mucous of the nasal passages (h) or tracheobronchial airways and lung (h), and $Cmucous\_{h,i}$ (mg/L) equals the concentration of hydrocarbon markers (i) and lumped compartments (i) in the mucous of the nasal passages (h) or tracheobronchial airways and lung (h).

$$3) \quad \frac{RA_{h,i}}{dt}(mg/hr) = Q_h * (CA_{h,i} - CV_{h,i}) + PA_{h,i} * Cmucous\_{h,i}$$

$RA_{h,I}$ equals the rate of change in the amount of hydrocarbon markers (i) and lumped chemicals (i) into the nasal tissue (h) or tracheobronchial airway and lung tissue (h), Q_h equals the blood flow rate (L/hr) to the nasal passages (h) or tracheobronchial airways and lung (h).

Development of Hydrocarbon Marker PBPK Sub-Models

Each PBPK model was composed of seven compartments: nasal passages, tracheobronchial airways and lung, brain, liver, fat, slowly perfused and rapidly perfused tissue groups (Figs. 2-4). Venous equilibration equations were used to describe the kinetics of the aromatics, m-xylene, toluene and ethylbenzene for most compartments, with diffusion limited

equations for nasal passages, tracheonchial airways and lung, and fat compartments. The kinetics of the n-alkanes, octane, decane and tetradecane were described using both diffusion limited equations (fat, liver, brain, nasal passages, tracheonchial airways and lung) and venous equilibration equations (rapidly perfused and slowly perfused). Metabolism of octane, decane and the aromatic hydrocarbon markers were described using hepatic Michaelis-Menten equations and n-tetradecane was assumed to have no appreciable metabolism, based on work by Anand *et al.* (2007). Metabolic parameters to describe L1 (aromatics) were from Campbell and Fisher (2007). Metabolic parameters for Lump 2 were taken from the mid-range n-alkane constituents and visually fit.

Metabolism

Mortensen *et al.* (2000) determined parameters for metabolic clearance of octane and decane n-alkanes using an in vitro headspace technique to expose rat liver slices. The reported Km and vmax were set as initial parameters for n-octane and n-decane prior to fitting.

Octane

Prior to this work, no detailed clearance data had been previously published for n-octane. Zahlsen *et al* (1992) conducted inhalation exposures to n-octane vapor and reported peak end of exposure blood and tissue concentrations. Male rats were exposed to 100ppm vapor for three days, 12-hr per day, prior to sacrifice and tissue collection.

Decane

Decane vapor kinetic data has been reported by Perleberg *et al.* (2004) in the rat. Exposures were conducted at 1200, 781, and 273ppm for a single 4 hr exposure period. For the 1200ppm exposure rats were sacrificed and tissues collected at 5, 30, 60, 120, 240 minutes post-exposure. For the 781 and 273ppm data collection occurred at 5 minutes post-exposure (Perleberg *et al.*, 2004). Similar to work with octane, Zahlsen *et al.* (1992) conducted exposures n-decane vapor. Male rats were exposed at 100 ppm vapor three days, 12-hr per day, prior to sacrifice and tissue collection (Zahlsen *et al.*, 1992). Nilsen *et al.* (1988) conducted exposures to n-decane vapor at 1369 ppm for a single 8 hour period. Tissues were collected at the end of exposure to determine peak concentration. No signs of overt toxicity were reported.

Tetradecane

Inhalation kinetics from exposure to n-tetradecane aerosol or vapor have not been previously reported in the literature. Tetradecane is a common constituent of jet fuels, diesel, and cutting oils and represents the higher molecular weight fraction of jet fuel.

Aromatics

Campbell and Fisher (2007) exposed male rats to JP-8 (Table 3.2). Exposures were conducted for 4 hours each, to one of three concentrations of JP-8 vapor, 384, 1100, or 2700 mg/m^3. Tissues were collected at 2 hours, end of exposure and 30 minutes post-exposure for the 2700 mg/m^3 exposure, and at 2 hours and end of exposure for both 1100 and 384 mg/m^3 exposures. PBPK models were developed for ethylbenzene and m-xylene using published individual chemical vapor exposure data (Haddad *et al.*, 1999, Tardif *et al.*, 1997). The models

were then compared to ethylbenzene and m-xylene data as components of JP-8 at the 3 exposure concentrations (Campbell Jr and Fisher, 2007). These vapor exposure models were adapted here to account for exposure to either aerosol+vapor or vapor-only chemical using the equations described earlier. Compartments for aerosol deposition and diffusion-limited fat were added.

Blood concentration data was collected from the literature for toluene. Haddad *et al.* (1999) and Tardif *et al.* (1997) exposed rats to toluene at 50, 100, 200ppm toluene vapor 4 hours. Tissues were collected at 5, 30, 60, 90, and 120 minutes post-exposure (Haddad *et al.*, 1999, Tardif *et al.*, 1997). Initial toluene metabolic parameters were from Haddad *et al*. (1999).

Additional Fuel Data

Additional unpublished JP-8 vapor exposure data was collected from earlier studies in our laboratory (Campbell Jr and Fisher, 2007) (Table 3.2). Exposure and pharmacokinetic data from the 4 hour 2700, 1100, and 384 mg/m^3 exposures was mined for use in the aromatic, n-alkane, and lump models.

Additional Complex Hydrocarbon Mixture Data

Exposure to decane has been reported in work with white spirit (WS) (Hissink *et al.*, 2007, Lof *et al.*, 1999). Lof *et al.* (Lof *et al.*, 1999) exposed rats to 400 or 800ppm dearomatized white spirit for 6hrs/day, 5 days per week, for 1, 2, or 3 weeks to collect pharmacokinetic data on the disposition of WS constituents in tissues. Rats were killed at end of exposure for the 1, 2, or 3 week exposure period and 120, 480, 360, and 1440 (24 hours) minutes post-exposure for the 3 week period.

Hissink *et al.* (2007) exposed rats to 600, 2400, and 4800mg/m^3 (102, 410, 820ppm) of traditional aromatic white spirit for 8 hours and collected kinetic data in support of PBPK model development. Tissues were collected at 2 and 4 hours during exposure, at end of exposure, and at 30, 60, 120, 240, and 480 minutes post-exposure. The neat white spirit was spiked with 1,2,4-trimethylbenzene and decane. The resulting aromatic constituent content was 25.6% of total concentration. After spiking, decane content was reported as 10% of the total concentration. Hissink *et al.* (2007) developed PBPK models for decane and 1,2,4-trimethylbenzene to describe the kinetics of an aromatic and n-alkane constituent in the presence of the mixture.

Models

All simulations were conducted using the ODEPACK solver in ACSLx (Advanced Continuous Simulation Language, v. 2.5.0.6, Mitchell and Gauthier Assoc., Huntsville, AL).

Octane

A PBPK model was created for octane using the octane pharmacokinetic studies reported in this paper with rats, partition coefficient values reported by Smith *et al.* (2005), and a Michaelis-Menten Km value for hepatic metabolism reported by Mortensen *et al.* (2000). The metabolic parameters were obtained by fitting the data sets obtained in this study (2 hours of exposure to octane vapors of 90, 996 and 4864 ppm). Km was initially increased 20% to 1.5 and vmax was visually fit then optimized. To optimize vmaxc, 3 starting values were used to ensure convergence around a single value, similar to work by Perleberg *et al.* (2004). The Nelder-Mead algorithm in the ACSLx Optimization Wizard (Advanced Continuous Simulation Language, v. 2.5.0.6, Mitchell and Gauthier Assoc., Huntsville, AL) was used with the heteroskedacity

parameter set to 1 and not allowed to vary. Vmaxc and the permeability area (PA) terms for fat and liver were optimized in this manner. Optimization of brain PA terms around the visually fit value was successful with data from 2 of 3 exposure concentrations with this tissue, but not when all 3 data sets were optimized together. The optimized value from 2 of 3 concentrations was used.

Another octane inhalation kinetic study by Zahlsen *et al.* (1992) was used to verify the n-octane model predictions. These authors conducted inhalation exposures with 100 ppm octane vapor for three days, 12 hours each day, and reported peak end of exposure blood and tissue concentrations. The octane model did not require alteration to fit blood and fat. The optimized value of the PA term for fat using the Zahlsen *et al.* (1992) data was similar to the initial model. Therefore the model PA term was not adjusted.

Decane

A PBPK model was created using pharmacokinetic data sets collected by Perleberg *et al.* (2004), partition coefficient values reported by Smith *et al.* (2005) and a Michaelis-Menten Km value for hepatic metabolism reported by Mortensen *et al.* (2000). The km value was held constant. Vmax and PA terms for tissue compartments were visually fit to data. Perleberg *et al.* (2004) exposed rats to decane vapors of 781 and 273 ppm with end of exposure collection of tissues and blood, and one time course study at 1200 ppm, where tissues were collected at multiple post-exposure time points. For model validation, decane inhalation studies from Zahlsen *et al.* (1992) and Nilsen *et al.* (1988) were simulated. The model was then used to simulate exposures to 3 aerosolized and 3 vaporized jet fuel concentrations. PA terms that best fit fuel data were used in preference over parameter values that only fit data from high

concentration exposures to decane, which were without the presence of potential metabolic inhibitors present in jet fuel.

Tetradecane

Inhalation kinetics from exposure to tetradecane aerosol or vapor has not been reported in the literature. A PBPK model was created using the exposure data collected in this study. The model structure described for octane and decane was retained, with the exception of a deep liver compartment included to account for limited diffusion between the deep tissue-lipid pool in the liver (2% of volume) and the shallow liver and blood. This behavior has been recognized and described with octamethylcyclotetrasiloxane (D4), another high molecular weight, lipid soluble chemical and Mn (Andersen *et al.*, 2001, Nong *et al.*, 2009, Sarangapani *et al.*, 2003, Yoon *et al.*, 2009) No in vitro determined partition coefficients were available. Comparison of model simulations to data, using predicted partition coefficients values resulted in poor fits to data (Smith *et al.*, 2005). Instead, tissue distribution ratios were used. Distribution ratios were calculated via the linear trapezoid method with tissue area–under-the-curve as described in Mirfazaelian et al (2006) using Sigma Plot software (Systat Software, Inc, San Jose, CA). The predicted blood:air partition coefficient was retained, as a best estimate. No appreciable metabolism has been reported (Anand *et al.*, 2007). PA terms were visually fit to blood and tissue data. Validation of the model with data from aerosolized jet fuel exposures was possible, as metabolic inhibition was not of concern. Model parameters were visually fit to best approximate both the single chemical and the jet fuel datasets, with preference for fuel data.

Ethylbenzene, and m-Xylene

Published PBPK models for ethylbenzene and for m-xylene (Campbell Jr and Fisher, 2007) were adapted to account for exposures as individual chemicals and as a constituents of jet fuels. Inhalation exposure and lump parameters were added as described for the n-alkanes. The PA term for aerosol exposure at the lung was visually fit to the aerosolized jet fuel exposure datasets. The PA term for nasal uptake was set to the value of the lung PA term. A diffusion limited fat compartment was added and the PA term fit to available fat and blood data from exposure to aerosolized and vaporized fuels. Metabolic parameters (vmaxc, km) were taken from the literature (Campbell Jr and Fisher, 2007). For model validation, ethylbenzene and m-xylene vapor inhalation studies from Haddad *et al.* (1999) and Tardif *et al.* (1997) at 50, 100, and 200ppm were simulated and compared to blood concentration data. For exposure to fuels, the sub-models were linked via the competitive metabolic inhibition equation in the liver compartments of each sub-model. To ensure the models retained the ability to fit individual chemical data, the models were re-initiated with concentrations of zero for other markers. To assess the pharmacokinetics of ethylbenzene and m-xylene in jet fuel exposures, simulations were conducted with 3 concentrations of vaporized and 3 concentrations of aerosolized fuels. Metabolic parameters for these markers in the presence of jet fuel were unchanged from values fit by Campbell and Fisher (2007).

Toluene

A PBPK model for exposure to toluene was developed to account for exposure to toluene as an individual chemical and as a constituent in aerosolized and vaporized fuels. Partition coefficients were collected from the literature (Haddad *et al.*, 1999). Determination of PA term

values for uptake and disposition was conducted as described previously for ethylbenzene and m-xylene. Metabolic parameters were initially equal to published values from Haddad *et al.* (1999) with a quarternary mixture of benzene, toluene, ethylbenzene, and xylene. Model simulations of vapor exposure were compared to blood concentration data at 50-200ppm from Haddad *et al.* (1999) and Tardif *et al.* (1997). As good simulation and data agreement was observed at all time points, the model was linked to the fuel model as described for the other marker constituents. The model simulations were compared to 3 concentrations of vaporized and 3 concentrations of aerosolized jet fuels.

Lumping

A lumping strategy was implemented to describe the remaining fuel mass. Aerosolized fuel exposure chromatograms were separated into three blocks of retention time ranges (comparable to molecular weight) using TDS-GC/MS data from aerosolized fuel exposures. Marker chemicals were identified to define each lump. The peak area of each lump was then manually integrated using HP Chemstation Software (Agilent Technologies, Inc, Santa Clara, CA). The total quantified aromatic content in aerosolized JP-8 fuel accounted for approximately 18% of total concentration. JP-8 aromatic content has been reported as 18-25% of total concentration (Ritchie *et al.*, 2001a). Lump 1 (L1) included all aromatic constituents and was assigned 25.0% of total concentration for JP-8 exposure, accounting for quantified and unquantified aromatic constituents. Lump 2 (L2) and Lump 3 (L3) represented 47.4% and 27.6% of total peak area, for quantified and non-quantified low to mid-range aliphatics up to dodecane, and higher molecular weight aliphatics tridecane through pentadecane to the end of the chromatogram (120 minutes), respectively. For aromatic-free S-8 exposures, L1 was set to

0% of the exposure concentration, L2 to 86.9%, and L3 to 13.1%. For the 50:50 blend of JP-8 and S-8, L1 was set to 12.5%, L2 to 72.3%, and L3 to 15.2% of total concentration. The fraction of total peak area for each lump was multiplied by total fuel concentration to define the lump exposure concentrations. Lumps were added to the model after accounting for marker concentrations. The final JP-8 model consisted of sub-models for 6 marker chemicals and 3 lump sub-models for the total exposure concentration. Sub-models were linked at the liver to describe competitive metabolic inhibition (Haddad *et al*, 1999).

For comparison to vaporized JP-8, lump concentrations were approximated using quantification data for 22 vapor constituents determined using charcoal adsorbent tubes (SKC, Inc., Eighty-Four, PA) and GC/FID data. L1 was set to 25% of total concentration (Campbell Jr and Fisher, 2007). L2 represented the remaining vapor exposure concentration, 74.9%. L3, the quantified concentrations of high molecular weight tridecane and tetradecane in vapor accounted for approximately 0.1% of total in all 3 JP-8 vapor exposure studies.

Lump models

Three lump sub-models were developed, based on model marker structures for the aromatic, mid-range n-alkane, and high molecular weight n-alkane markers previously described. L1 partition coefficients and metabolic parameters were obtained from the "lumped aromatic fraction" described by Campbell and Fisher (2007) and were not modified. L2 partition coefficients were set as the average of experimentally determined partition coefficients reported for octane, nonane, decane, undecane, and dodecane (Smith *et al.*, 2005); the prominent constituents of the lump. Km was the average of reported values for octane, nonane, and decane in the literature (Mortensen *et al.*, 2000). Vmax of L2 was fit to blood data from decane. PA

terms for L2 were set equal to the values of these parameters for decane. For L3, tissue distribution ratios from exposure to JP-8 aerosol were averaged for tridecane, tetradecane, and pentadecane. The predicted blood:air partition coefficients for these hydrocarbons were averaged to provide an estimate for blood:air partitioning (Smith *et al.*, 2005). Pentadecane was not tracked in JP-8 vapor or tissues, precluding use of JP-8 vapor data in calculation of distribution ratios for L3. PA terms were set to values from the tetradecane model as a representative of the lump. As with tetradecane, metabolic capacity for L3 was not included. For future extrapolations of the model to humans, PAc terms, Vmaxc values, pulmonary ventilation, nasal and tracheobronchial surface area, and cardiac output, were allometrically scaled to bodyweight ($BW^{3/4}$).

White Spirit (WS)

The fuel model was modified to simulate the kinetics of decane in a different complex hydrocarbon mixture. Time course data was collected for decane in two white spirit vapor exposure studies (Hissink *et al.*, 2007, Lof *et al.*, 1999). Hissink *et al.* (2007) exposed rats to white spirit for 8 hours at 600, 2400, and 4800 mg/m^3 (100, 410, 820ppm WS), for PBPK model development. The concentrations of decane were 10, 41, 82ppm, respectively.

Lof *et al* (1999) exposed rats to dearomatized WS vapor for 6 hrs each day 5 days each week, for up to 3 weeks, at 400 and 800ppm and collected blood, brain, and fat. The concentrations of decane were 66.4 and 132.8ppm, respectively.

Interactions

Metabolic interactions were assessed using the method of Campbell and Fisher (2007). In brief, the exposure concentration of the lumped fractions was set to zero and the model initiated without the potential for metabolic inhibition or other interactions. Then the defined lump exposure concentrations were included and the model initiated. The area-under-the-curve of the blood time course data was determined using Sigma Plot software (Systat Software, Inc, San Jose, CA). The increase in blood concentration, a measure of metabolic inhibition, was determined bycomparison of the two AUC values in terms of percent change. Data from the 3 vaporized and 3 aerosolized fuel studies was evaluated for octane, decane, toluene, ethylbenzene, and m-xylene in blood. Tetradecane was not evaluated as it is not subject to metabolism.

Sensitivity Analysis

A sensitivity analysis of predicted blood (CV) concentrations of each marker was performed using the method of Perleberg *et al.* (2004). The ACSLx Sensitivity Analysis Wizard v. 2.5.0.6 was used (Aegis Technologies, Huntsville, AL). The delta (change) value was set to 1%. The method of central differences was used. Results were log normalized and multiplied by the respective parameter value in the wizard. The markers were individually tested at 100ppm each, with all other chemical concentrations set to zero in the model. Coefficients were calculated for 2, 4, and 5-hours, covering the loading phase, peak concentration at end of exposure, and clearance phase, respectively.

RESULTS

Hydrocarbon Markers

Toluene simulations produced good agreement when compared to blood data collected from the literature (Haddad *et al.*, 1999) (Fig. 3.6a). EBZ and m-XYL vapor simulations also accurately predicted peak concentration and general clearance from blood (Fig. 3.7a, 3.8a). For octane, the fitted metabolic capacity (vmaxc) was 35.5mg/hr/kg$^{0.75}$ when accounting for diffusion limited movement. Simulations were in agreement with blood data from this study and Zahlsen *et al.* (1992) (Fig 3.9a,b).

The decane hydrocarbon marker sub-model adequately simulated the blood time course data from Perleberg et al (2004) for 1200ppm exposure group, but was less successful at lower concentration 781ppm (Fig. 3.10a,b). Comparison of observations and predictions of peak end of exposure blood data from Zahlsen *et al* (1992) and Nilsen *et al* (1988) were in very good agreement (Fig. 3.10c,d).

A PBPK model was developed to describe the time course of tetradecane aerosol exposure. Experimentally determined partition coefficients were not available. Tissue distribution ratios were calculated and applied to the model. Tissue data indicative of slow release from a reservoir of tetradecane within the rat prompted investigation of deep tissue compartments. Deep and shallow liver compartments were parameterized from the literature and fit to data. While capable of fitting the collected data, it was not possible to utilize the same parameter set (PA terms) to fit the individual chemical exposure and the fuels exposures. The model was refined and fit for the purpose of describing tetradecane in jet fuel. Consequently, while improved fits of tetradecane in fuel were observed, the fit model overpredicted exposure to

89 mg/m^3. However, simulations did maintain the general kinetic behavior of the data (Fig. 3.11a).

Jet Fuels

The individual chemical models were incorporated into the larger jet fuel model as hydrocarbon marker sub-models. The fuel model either accurately predicted or slightly overpredicted blood time course data for octane, decane, and tetradecane in vaporized and aerosolized JP-8, as well as in the aerosolized S-8 and blend of JP-8 and S-8 (Figs. 3.9-3.11). Simulations of toluene in blood and tissues also approximated, or somewhat over predicted, time course data in the presence of aerosolized and vaporized fuel (Fig. 3.6b-f). With the exception of m-xylene in blood (Fig. 3.7b) most simulations from the modified models from Campbell and Fisher (2007) were in agreement with blood concentration data from fuels.

Influence of Aerosol Droplets

Prediction of aerosolized fuel exposures has not been previously reported. Compartments for uptake of aerosol droplets were developed and parameterized with existing physiological constants and fit with permeability area terms. To gauge the importance of the aerosol and vapor fraction on blood kinetics, simulation of a hypothetical 100% aerosol and 100% vapor exposure was conducted with octane and tetradecane, at the exposure concentrations used to build the models. Results indicated that the difference in exposure method moderately affects the blood area-under-the-curve (AUC) when only the deposition parameters and form of exposure were modified. For an exposure to tetradecane at 90mg/m^3 the AUC values for a 100% aerosol and a 100% vapor exposure, was approximately 1%. If simulated using actual deposition parameters

from the aerosol study, 100% aerosol deposition in the lung increased AUC 15%, while 100% vapor increased the concentration 14%. For octane, a 28% reduction in AUC was observed between simulation of exposure at the actual 1000ppm vapor-only concentration and then at 1000ppm aerosol with 100% deposition in the lung.

Interactions

The effect of metabolic interactions on the concentration of metabolized chemicals was evaluated. Using percent change in area under the curve (AUC) when the chemical was simulated in the presence of fuel and without the fuel (see Methods). Predicted m-XYL blood area-under-the-curve (AUC) increased 32.8% at 900 mg/m^3 aerosolized JP-8 when lumped fractions were included and 38.6% and 22.1% for ethylbenzene and toluene respectively, at the same concentration. The model predicted an increased blood AUC for octane and decane of 32.5% and 21.6% at 900 mg/m^3 JP-8 aerosol. In the 1070 mg/m^3 S-8 exposure, the simulated AUC increased 15.5% and 17% for octane and decane, respectively when the lumps were included. For the JP-8:S-8 blend, m-xylene, ethylbenzene, and toluene increased 9, 12.3, and 12.2%, respectively. Octane and decane AUC increased 8.6% and 5.2%.

At 2700mg/m^3 vaporized JP-8, there was a 45.8% increase in toluene blood AUC, and a 62% and 60.9% increase for ethylbenzene and m-xylene, respectively, while octane and decane increase 28.8% and 9.7%. At 1100mg/m^3, there was a 24.4% increase in toluene blood AUC, and a 42.4% and 39.1% increase for ethylbenzene and m-xylene, respectively, while octane and decane increased 16.7% and 15.9%. At 400mg/m^3 vaporized JP-8 a 6.2% increase was observed for toluene, 16.3% for ethylbenzene, 15.1% for m-xylene, 7.0% for octane, and 5.7% for decane.

White Spirit

For exposure to aromatic white spirit, the concentration of L1 was set to 25.6% of total concentration for each study; as reported by the authors (Hissink *et al.*, 2007). The remainder of the vapor concentration (74.4%) was added to L2. L3 was set to zero, as white spirit contains predominately C7-C12 aliphatics, with minimal levels of constituents above C12 (IPCS, 1996). In comparison to blood decane concentrations from exposure to aromatic white spirit (Hissink *et al.*, 2007), simulations of peak blood concentration and early clearance were in agreement with data, though peak concentration was moderately overpredicted. The later time points were largely underpredicted (Fig 3.12a,b,c). For dearomatized white spirit exposures (Lof *et al.*, 1999) L1 and L3 were set to zero. After accounting for decane concentration (see methods), the remaining exposure concentration was added to L2 and simulations were conducted. Peak simulated decane concentrations in blood following exposure to dearomatized white spirit were in good agreement with data over a period of 3 weeks at 400 and 800 ppm (Fig. 3.12d,e)

DISCUSSION

The overarching goals of this work were the collection of rat pharmacokinetic data using aerosolized fuels and the development of predictive pharmacokinetic models to adequately assess the dosimetry of inhaled aerosol droplets and vapors for future use in fuel risk assessment. Individual alkane sub-models were developed for octane, decane, and tetradecane. Following model development, simulations were compared to data collected from our laboratory and from Zahlsen *et al* (1992) and Nilsen *et al* (1988). Submodels for aromatic ethylbenzene and m-xylene were adapted from Campbell and Fisher (2007), to accommodate aerosolized JP-8 and a blend of JP-8 and S-8. A sub-model for toluene was developed using published partition

coefficients and metabolic constants, with aerosol uptake and diffusion limitation in the fat compartment. The model was compared to data from Haddad *et al.* (1999) and achieved good agreement with blood time-course. Overall, the models were capable of predicting kinetic data from individual chemical vapor exposures and from exposures to aerosolized or vaporized jet fuels.

In order to predict the fuel data, the sub-models were combined into a larger PBPK model, using up to 6 marker chemicals and 3 lumped fractions to describe the total exposure (Fig. 3.5). The models were linked at the liver to describe competitive metabolic inhibition. Preference was given to fitting fuel mixture data over high concentration single chemical data.

For exposure to tetradecane it was not possible to fit the single chemical dataset and the fuel datasets with the same parameter set. This may be due to unknown concentration dependent transporters or other disposition issues with high molecular weight hydrocarbons that are not readily apparent at lower concentrations or in complex mixtures. The model generally predicted well the occupationally relevant concentrations or kinetic behavior of tetradecane, in both petroleum-based and synthetic fuels (Fig. 11b-e).

Fuel hydrocarbons share a common major metabolic pathway, as indicated in work with CYP450 2E1, though CYP`1A2 and 2B6 may also play a minor role (Anand *et al*., 2007, Edwards *et al*., 2005). Competitive metabolic inhibition has been reported as the most likely interaction mechanism for these constituents (Campbell Jr and Fisher, 2007, Haddad *et al*., 1999). The result of competitive inhibition of metabolism as it relates to jet fuel is the presence of higher concentrations of the marker constituents in blood and tissue, over a longer duration than would occur following individual chemical exposure. Depending on constituent of interest this could be toxicologically relevant for a parent chemical or metabolite.

As evidenced by earlier work, the influence of more readily metabolized constituents on the kinetics of similar constituents and on constituents with lower rates of metabolism is more pronounced at higher total exposure concentrations. Campbell and Fisher (2007) determined the effect on constituent blood concentration, as area under the curve (AUC). In that work total exposure concentration of 2700 mg/m^3 increased the blood time-course AUC of m-XYL by 40% and EBZ by 46% when the model included the lumped aromatic constituent of the fuel. Lower exposure concentrations of 1100 and 380 mg/m^3 produced increases in blood AUC of 9 and 5% respectively for m-XYL and 12 and 2.5% respectively for EBZ (Campbell Jr and Fisher, 2007). Development and integration of the total fuel lump models (L1-L3) in the current model allowed for assessment of the impact of the total fuel mixture on the kinetic behavior of the marker constituents.

The current fuel model predicted increases in blood concentration of 22-38% for m-xylene, ethylbenzene, and toluene, and 21-32% for octane and decane at an exposure of 900 mg/m^3 aerosolized JP-8 when lumped fractions were included. For S-8 exposures, aromatic constituents are not present in the fuel. The increase in n-alkane AUCs for octane and decane was consistent between the two chemicals at 16-17%. For the JP-8:S-8 blend m-xylene, ethylbenzene, and toluene AUC increased 9-12%, while octane and decane this range was 5-9%. The current model predicted AUC values for exposure to 2700 mg/m^3 vaporized JP-8 were somewhat higher for ethylbenzene (62%) and m-xylene (61%) compared to those reported in earlier work, at 46 and 40% respectively (Campbell and Fisher, 2007). This is most likely due to the inclusion of the three lumped compartments and a more defined atmospheric concentration. In particular, as L3 has no metabolic capability, the effect is likely due to the presence of the mid-range aliphatic fraction in L2, the largest fraction of the fuel chromatogram. Additionally,

the comparatively low concentration of a particular marker concentration compared to the total fuel, has been shown to play less of a role at low exposure concentrations than high.

The detailed atmospheric characterization from Martin *et al* (2010) and Tremblay *et al* (2010) allowed for more informed assessment of the aerosol and vapor phase contributions of marker constituents (Martin *et al*., 2009, Tremblay *et al*., 2009). The simulated dose was separated into one of the two phases and directed to either the gas-exchange or respiratory tract compartments, based on dosimetry predicted by the MPPD2 model. The importance of aerosol droplets in determining blood or lung kinetics can be determined through comparison of a 100% aerosol and a 100% vapor exposure. When deposition as vapor or as aerosol were adjusted and all other parameters held constant, a 28% change in octane blood AUC was observed, while a much smaller effect was seen for tetradecane. When deposition parameters from the actual model for tetradecane at 89 mg/m^3 were included, a 100% vapor exposure and 100% aerosol exposure resulted in an increase in the blood AUC of approximately 15%.

Fuel model predictions of the aerosolized JP-8 generally either provided good agreement with data or slightly overpredicted the chemical concentrations. However, even when overpredicted there was good agreement between simulations and the kinetic profile of the data. At lower concentrations, in particular for the JP-8:S-8 blend where exposure concentrations for some chemicals were near 1ppm, model simulations overpredicted later time points of the n-alkanes while accurately simulating the peak concentrations. The aerosol concentrations were calculated by subtraction of the vapor concentration of each constituent from the total exposure concentration. In the case of aromatic and low molecular weight constituents, when the vapor concentration was similar to the total concentration, the resulting aerosol concentration value is very low and would inherently have more potential for variability when the two larger values

have even small mean fluctations and variability. For higher molecular weight constituents with greater presence in the aerosol phase a similar effect would occur in relation to vapor concentration.

Tissue distribution ratios were used in the absence of in vitro determined partition coefficients for tetradecane. Tissue distribution ratios have been discussed in the literature (Mirfazaelian *et al.*, 2006, Nilsen *et al.*, 1988). Mirfazaelian *et al.* (2006) used tissue distribution ratios to describe the kinetics of deltamethrin. In work with animals exposed to n-alkane vapors, nonane through tridecane, Nilsen *et al*. (1988) determined that the brain to air tissue distribution ratio decreased with increasing carbon length; undecane at 16.0, dodecane at 4.3, and tridecane at <1.6 (as reported). Our use of distribution ratios with similar low values, at least in brain, are in line with the literature values for similar n-alkanes.

Dennison *et al*., (2003) conducted similar work with gasoline. A single lumped compartment was used to describe the remainder of the exposure concentration in closed-chamber gas uptake studies. Fitting the lump and marker constituents, benzene, toluene, ethylbenzene, o-xylene, and hexane, allowed for simulations of chamber loss consistent with observed data and reflected the potential for metabolic inhibition between the markers and the lump. In the current model, three lumps were created to describe the exposure. Metabolic activity was permitted in the aromatic (L1) and first aliphatic lump (L2). The description of the lumps enabled a more detailed investigation of the impact of the aromatic and aliphatic lumps on inhibition of marker chemical metabolism. Using this methodology, the model was capable of predicting peak and early blood concentrations of decane in rats exposed to 3 concentrations of aromatic white spirit (Hissink *et al.*, 2007) and 2 concentrations of dearomatized white spirit (Lof *et al.*, 1999). However, the lumps were described from reported concentrations rather than

chromatograms. The model overpredicted the rate of clearance from blood. Post-hoc use of the model to predict data from these mixture exposure is possible but required assumptions that internal chamber concentrations of decane were consistent with the reported concentrations spiked in the aromatic and de-aromatized white spirit and that other inhibitors not present in the jet fuel did not play a significant role in the kinetics of decane. Such complications may in part explain the overprediction of clearance in the later time points. Greater levels of metabolic inhibition from white spirit constituents could account for the extended duration of high concentrations of decane in blood. Similar agreement was observed in prediction of the 3 week exposure datasets from Lof et al, (1999). Further characterization of the white spirit exposure atmosphere could provide for improved simulation accuracy at the later time points.

It is imperative that investigations of the toxic potential of complex mixtures include detailed assessments of inhalation chamber chemical profiles. At present, there is a paucity of this data in the published literature for common complex hydrocarbon mixtures. Such information could aide in future model development as well identification of primary agents inducing toxicity observed in a mixture study. As humans are rarely exposed to only high concentrations of individual chemicals, increasing the relevance of rodent exposures and PBPK models for experimental exposures may be possible through detailed characterization of the exposure atmosphere.

This work represents the first PBPK model for the entire sample of jet fuel as aerosol and vapor, as well as for exposure to vapor phase-only JP-8. Future model refinements will include addition of several new markers to more fully define the time course of the fuel and broaden the range of chemicals that may be simulated in the presence of fuel. The key goals of the work were met with development of a modeling strategy capable of describing both types of fuel

exposures found in the literature. The first models for octane and tetradecane were developed using the first detailed time-course data for these n-alkanes that include several time points post-exposure. The kinetic data obtained from exposures to S-8 and the JP-8:S-8 blend are also the first reported data on these mixtures.

PBPK models are capable of predictions of internal dose across multiple exposure concentrations and for extrapolation across species. This model will aid in fuel risk assessment for JP-8, S-8, and the blended JP-8:S-8 fuel slated for use in the near future by the U.S. Department of Defense.

REFERENCES

Anand S, Campbell J, Fisher J. (2007). In Vitro Rat Hepatic Metabolism of n-Alkanes: Nonane, Decane, and Tetradecane. Int J Toxicol, 26, 325-329.

Andersen M, Sarangapani R, Reitz R, Gallavan R, Dobrev I, Plotzke K. (2001). Physiological modeling reveals novel pharmacokinetic behavior for inhaled octamethylcyclotetrasiloxane in rats. Toxicol Sci, 60, 214.

Baldwin C, Figueredo A, Wright L, Wong S, Witten M. (2007). Repeated Aerosol-vapor JP-8 Jet Fuel Exposure Affects Neurobehavior and Neurotransmitter Levels in a Rat Model. J Toxicol Environ Health, Part A, 70, 1203-1213.

Campbell Jr J, Fisher J. (2007). A PBPK modeling assessment of the competitive metabolic interactions of JP-8 vapor with two constituents, m-xylene and ethylbenzene. Inhalation Toxicol, 19, 265-273.

Chavanne B. (2007). USAF Wants Fleet Certified For Synthetic Fuel Blend by 2011. Aviation Week: Aerospace Daily and Defense Report [Online] Available at:. [Online] Available

at:
http://www.aviationweek.com/aw/generic/story_channel.jsp?channel=defense&id=news/FUEL102907.xml. 29 October 2007.

Csanady G, Filser J. (2007). A physiological toxicokinetic model for inhaled propylene oxide in rat and human with special emphasis on the nose. Toxicol Sci, 95, 37.

Dennison J, Andersen M, Yang R. (2003). Characterization of the pharmacokinetics of gasoline using PBPK modeling with a complex mixtures chemical lumping approach. Inhalation Toxicol, 15, 961-986.

DOD. (2008). Report to Congress on Synthetic Fuel Utilization. Department of Defense. http://www.dod.mil/ddre/doc/Jul08_Synthetic_Fuel_Utilization_Report_to_Congress.pdf.

Edwards J, Rose R, Hodgson E. (2005). The metabolism of nonane, a JP-8 jet fuel component, by human liver microsomes, P450 isoforms and alcohol dehydrogenase and inhibition of human P450 isoforms by JP-8. Chem-Biol Interact, 151, 203-211.

Fechter L, Gearhart C, Fulton S, Campbell J, Fisher J, Na K, Cocker D, Nelson-Miller A, Moon P, Pouyatos B. (2007). JP-8 jet fuel can promote auditory impairment resulting from subsequent noise exposure in rats. Toxicol Sci, 98, 510-525.

Haddad S, Tardif R, Charest-Tardif G, Krishnan K. (1999). Physiological modeling of the toxicokinetic interactions in a quaternary mixture of aromatic hydrocarbons. Toxicol Appl Pharmacol, 161, 249-257.

Harris D, Sakiestewa D, Robledo R, Witten M. (1997). Immunotoxicological effects of JP-8 jet fuel exposure. Toxicol Ind Health, 13, 43-55.

Harris D, Sakiestewa D, Robledo R, Young R, Witten M. (2000). Effects of short-term JP-8 jet fuel exposure on cell-mediated immunity. Toxicol Ind Health, 16, 78.

Hissink A, Krüse J, Kulig B, Verwei M, Muijser H, Salmon F, Leenheers L, Owen D, Lammers J, Freidig A. (2007). Model studies for evaluating the neurobehavioral effects of complex hydrocarbon solvents III. PBPK modeling of white spirit constituents as a tool for integrating animal and human test data. Neurotoxicology, 28, 751-760.

IPCS. (1996). Environmental Health Criteria 187. White Spirit (Stoddard Solvent). United Nations Environment Programme. International Labour Organisation. World Health Organization. International Programme On Chemical Safety (IPCS). [Online] Available at: http://www.inchem.org/documents/ehc/ehc/ehc187.htm. January 29, 2010.

Knave B, Persson H, Goldberg J, Westerholm P. (1976). Long-term exposure to jet fuel: an investigation on occupationally exposed workers with special reference to the nervous system. Scand J Work Environ Health, 2, 152-164.

Knave B, Olson B, Elofsson S, Gamberale F, Isaksson A, Mindus P, Persson H, Struwe G, Wennberg A, Westerholm P. (1978). Long-term exposure to jet fuel. II. A cross-sectional epidemiologic investigation on occupationally exposed industrial workers with special reference to the nervous system. Scand J Work Environ Health, 4, 19-45.

Knave B, Mindus P, Struwe G. (1979). Neurasthenic symptoms in workers occupationally exposed to jet fuel. Acta Psychiatr Scand, 60, 39-49.

Lof A, Lam H, Gullstrand E, Ostergaard G, Ladefoged O. (1999). Distribution of Dearomatised White Spirit in Brain, Blood, and Fat Tissue after Repeated Exposure of Rats. Pharmacol Toxicol, 85, 92.

Martin S, Brunson K, Kendrick C, Tremblay R, Fisher J. (2009). Characterization of a Nose-Only Inhalation Exposure System for Hydrocarbon Mixtures and Jet Fuels. Inhalation Toxicology (in press),

Martin SA, Tremblay RT, Brunson KF, Kendrick C, Fisher JW. (2010). Jan 28 [Epub ahead of print]. Characterization of a nose-only inhalation exposure system for hydrocarbon mixtures and jet fuels. Inhalation Toxicology (in press), doi:10.3109/08958370903456645.

Merrill E, Gearhart J, Sterner T, Robinson P. (2008). Improved Predictive Model for n-Decane Kinetics Across Species, as a Component of Hydrocarbon Mixtures. Inhalation Toxicol, 20, 851-863.

Mirfazaelian A, Kim K, Anand S, Kim H, Tornero-Velez R, Bruckner J, Fisher J. (2006). Development of a physiologically based pharmacokinetic model for deltamethrin in the adult male Sprague-Dawley rat. Toxicol Sci, 93, 432.

Mortensen B, Eide I, Zahlsen K, Nilsen O. (2000). Prediction of in vivo metabolic clearance of 25 different petroleum hydrocarbons by a rat liver head-space technique. Arch Toxicol, 74, 308-312.

Nilsen O, Haugen O, Zahlsen K, Halgunset J, Helseth A, Aarset H, Eide I. (1988). Toxicity of n-C9 to n-C13 alkanes in the rat on short term inhalation. Pharmacol Toxicol, 62, 259-266.

Nong A, Teeguarden J, Clewell 3rd H, Dorman D, Andersen M. (2008). Pharmacokinetic modeling of manganese in the rat IV: Assessing factors that contribute to brain accumulation during inhalation exposure. J Toxicol Environ Health A, 71, 413.

Nong A, Taylor M, Clewell III H, Dorman D, Andersen M. (2009). Manganese Tissue Dosimetry in Rats and Monkeys: Accounting for Dietary and Inhaled Mn with Physiologically based Pharmacokinetic Modeling. Toxicol Sci, 108, 22.

NRC. (2003). Toxicologic Assessment of Jet-Propulsion Fuel 8. National Research Council of the National Academies. Washington, DC. The National Academies Press.

Parent R. (1992). Comparative biology of the normal lung. CRC Press, Boca Raton.

Perleberg U, Keys D, Fisher J. (2004). Development of a physiologically based pharmacokinetic model for decane, a constituent of jet propellent-8. Inhalation Toxicol, 16, 771-783.

Porter H. (1990). Aviators intoxicated by inhalation of JP-5 fuel vapors. Aviation, space, and environmental medicine, 61, 654-656.

Rhodes A, LeMasters G, Lockey J, Smith J, Yiin J, Egeghy P, Gibson R. (2003). The effects of jet fuel on immune cells of fuel system maintenance workers. J Occup Environ Med, 45, 79-86.

Ritchie G, Rossi J, Nordholm A, Still K, Carpenter R, Wenger G, Wright D. (2001). Effects of repeated exposure to JP-8 jet fuel vapor on learning of simple and difficult operant tasks by rats. J Toxicol Environ Health, Part A, 64, 385-415.

Rossi J, Nordholm A, Carpenter R, Ritchie G, Malcomb W. (2001). Effects of repeated exposure of rats to JP-5 or JP-8 jet fuel vapor on neurobehavioral capacity and neurotransmitter levels. J Toxicol Environ Health, Part A, 63, 397-428.

Sarangapani R, Teeguarden J, Andersen M, Reitz R, Plotzke K. (2003). Route-specific differences in distribution characteristics of octamethylcyclotetrasiloxane in rats: analysis using PBPK models. Toxicol Sci, 71, 41.

Smith A, Campbell J, Keys D, Fisher J. (2005). Rat tissue and blood partition coefficients for n-alkanes (C8 to C12). Int J Toxicol, 24, 35-41.

Smith L, Bhattacharya A, Lemasters G, Succop P, II E, Medvedovic M, Joyce J. (1997). Effect of Chronic Low-Level Exposure to Jet Fuel on Postural Balance of US Air Force Personnel. J Occup Environ Med, 39, 623-632.

Tardif R, Charest-Tardif G, Brodeur J, Krishnan K. (1997). Physiologically based pharmacokinetic modeling of a ternary mixture of alkyl benzenes in rats and humans. Toxicol Appl Pharmacol, 144, 120-134.

Teeguarden J, Gearhart J, Clewell H, Covington T, Nong A, Andersen M. (2007). Pharmacokinetic modeling of manganese. III. Physiological approaches accounting for background and tracer kinetics. J Toxicol Environ Health Part A, 70, 1515-1526.

Thrall K, Gies R, Muniz J, Woodstock A, Higgins G. (2002). Route-of-entry and brain tissue partition coefficients for common superfund contaminants. J Toxicol Environ Health Part A, 65, 2075-2086.

Tremblay R, Martin S, Fisher J. (2009). Novel Characterization of the Aerosol and Gas Phase Composition for Aerosolized Jet Fuel Atmospheres. Inhalation Toxicology (in press),

Tremblay RT, Martin SA, Fisher JW. (2010). Feb. [Epub ahead of print]. Novel Characterization of the Aerosol and Gas Phase Composition for Aerosolized Jet Fuel Atmospheres. Inhalation Toxicology (in press), doi: 10.3109/08958370903456637.

Tunnicliffe W, O'Hickey S, Fletcher T, Miles J, Burge P, Ayres J. (1999). Pulmonary function and respiratory symptoms in a population of airport workers. Br Med J, 56, 118-123.

Whitman F, Hinz J. (2001). Sensory irritation study in mice: JP-4, JP-8, JP-8+100. IERA-RS-BR-SR-2001-0005. Risk Assessment Division, Air Force Institute for Operational Health, Brooks City-Base, TX. IERA-RS-BR-SR-2001-0005. Risk Assessment Division AFIfOH, Brooks City-Base, TX.

Whitman F, Hinz J. (2004). Sensory irritation study in mice: JP-5, JP-TS, JP-7, DFM, JP-10. IOH-RS-BR-SR-2004-0001. Risk Assessment Division, Air Force Institute for

Operational Health, Brooks City-Base, TX. IERA-RS-BR-SR-2004-0001. Risk Assessment Division AFIfOH, Brooks City-Base, TX.

Wong S, Vargas J, Thomas A, Fastje C, McLaughlin M, Camponovo R, Lantz R, Heys J, Witten M. (2008). In vivo comparison of epithelial responses for S-8 versus JP-8 jet fuels below permissible exposure limit. Toxicology, 254, 106-111.

Wong S, Thomas A, Barbaris B, Lantz R, Witten M. (2009). Pulmonary evaluation of permissible exposure limit of syntroleum S-8 synthetic jet fuel in mice. Toxicol Sci, 109, 312-320.

Yoon M, Nong A, Clewell III H, Taylor M, Dorman D, Andersen M. (2009). Evaluating placental transfer and tissue concentrations of manganese in the pregnant rat and fetuses after inhalation exposures with a PBPK model. Toxicol Sci, 112, 44.

Zahlsen K, Eide I, Nilsen A, Nilsen O. (1992). Inhalation kinetics of C6 to C10 aliphatic, aromatic and naphthenic hydrocarbons in rat after repeated exposures. Pharmacol Toxicol, 71, 144-149.

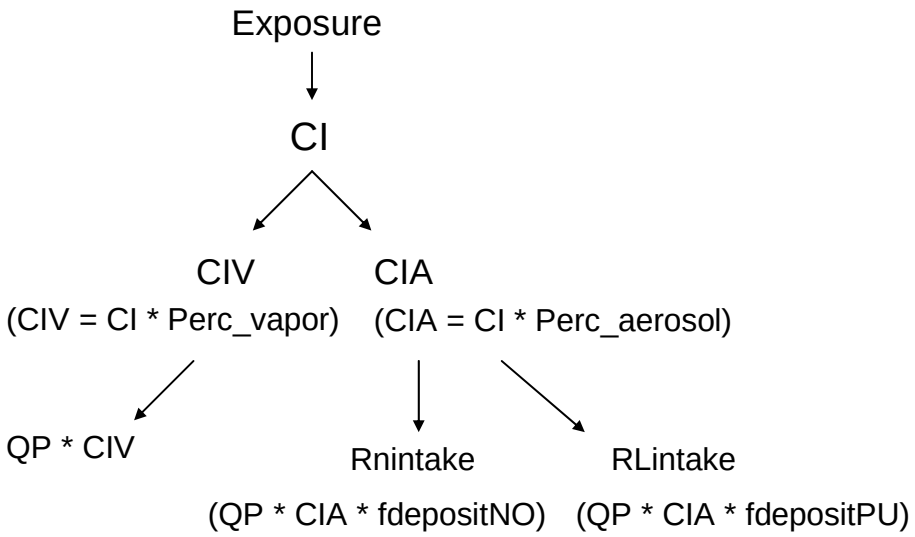

Figure 3.1. Aerosol and Vapor Deposition

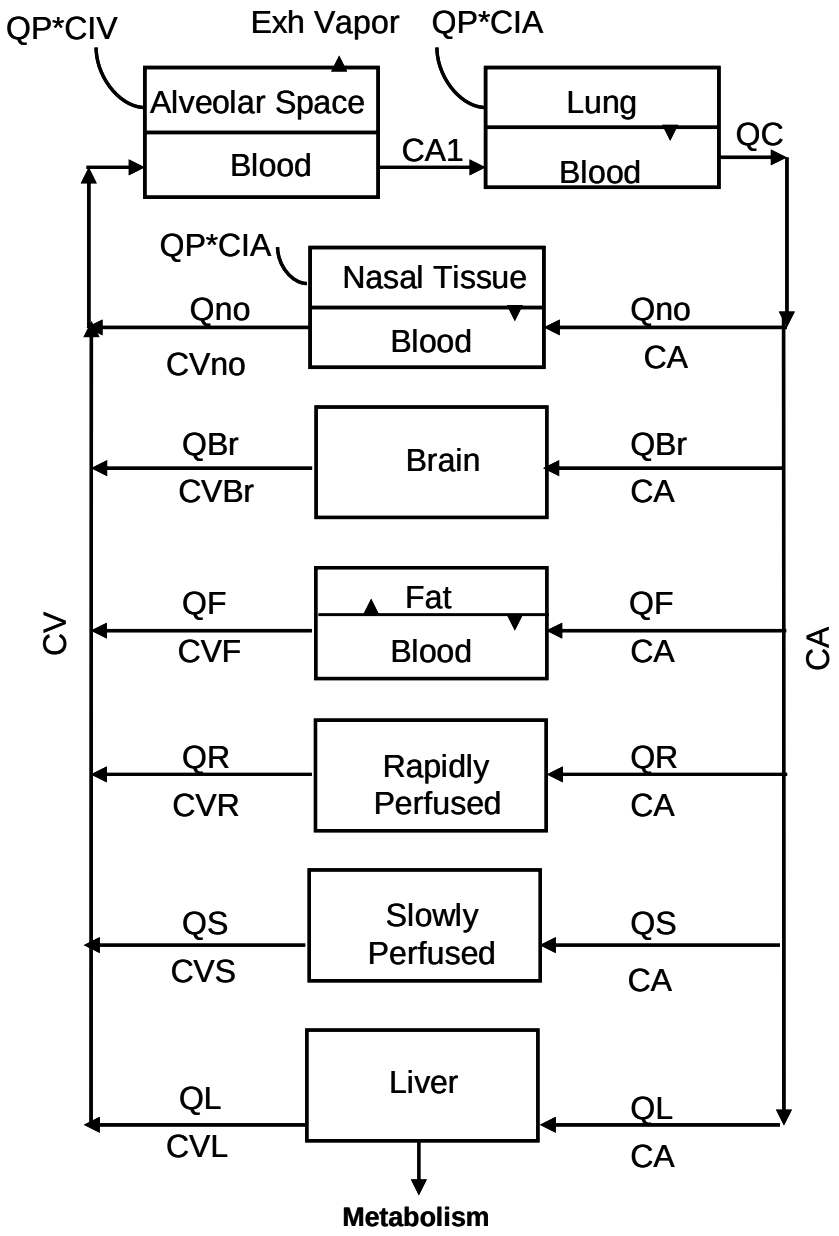

Figure 3.2. Schematic of PBPK Model for Aromatic Constituents and Lump 1 (L1).

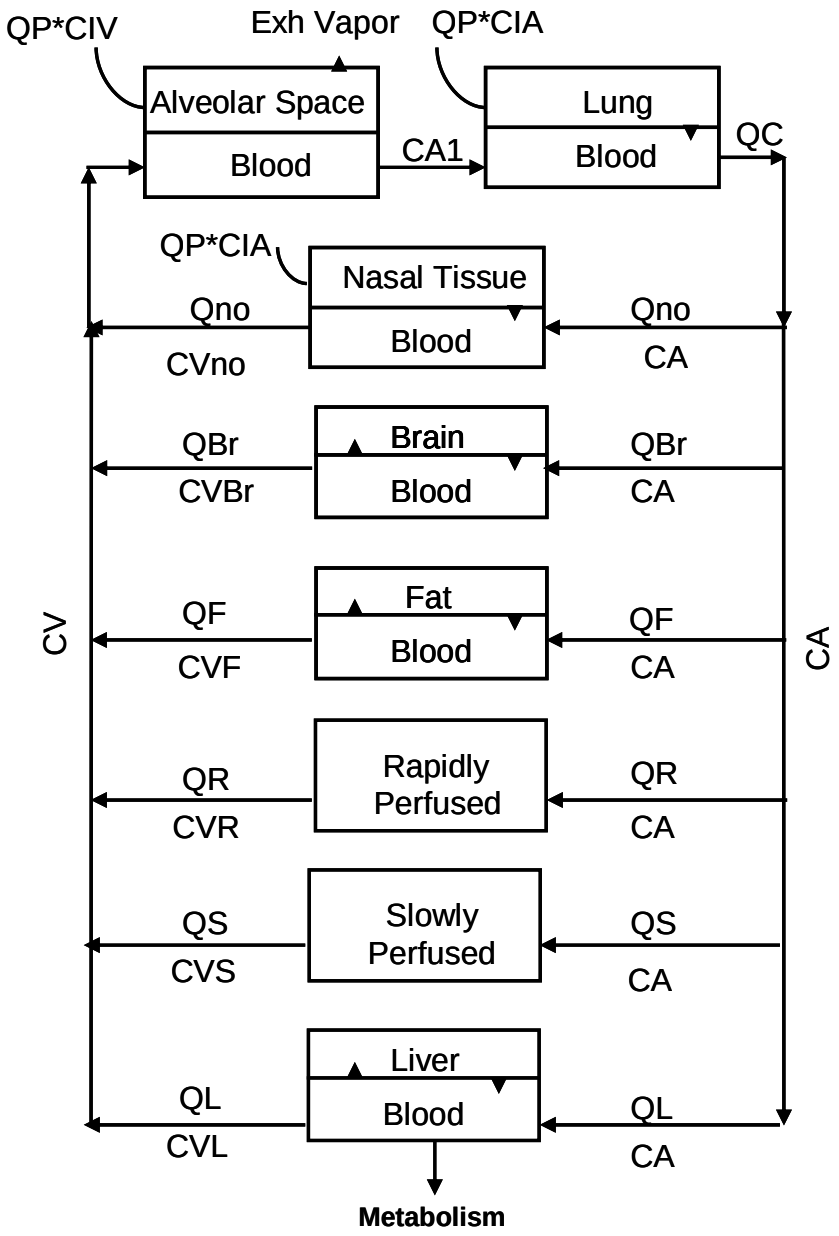

Figure 3.3. Schematic of PBPK model for Aliphatic Constituents and Lump 2 (L2).

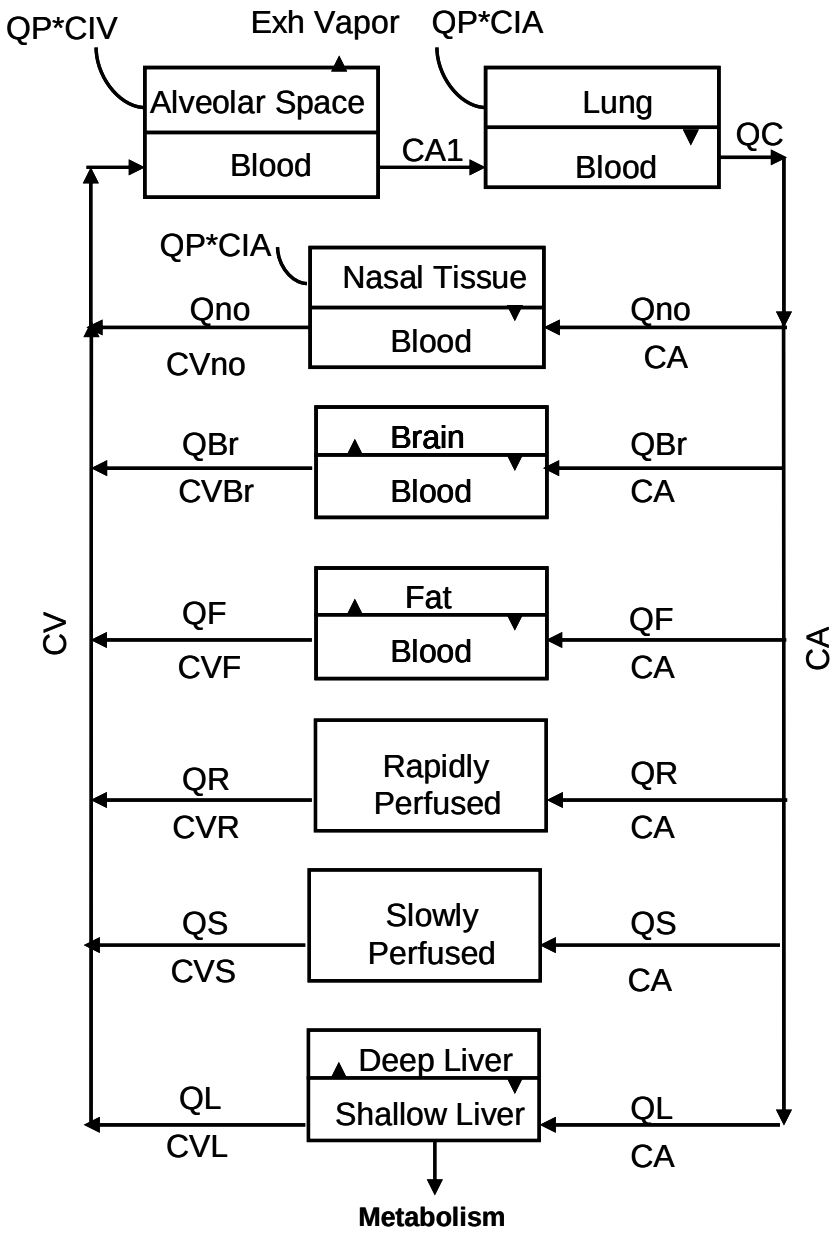

Figure 3.4. Schematic of PBPK Model for High Molecular Weight Aliphatics and Lump 3 (L3)

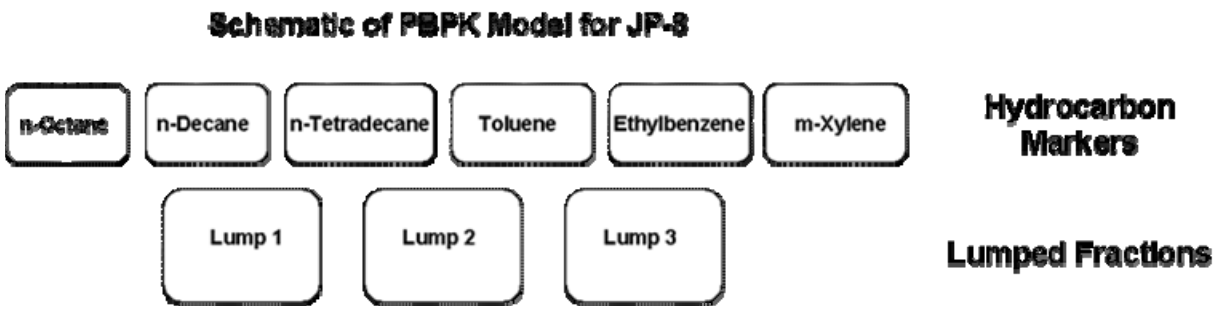

Figure 3.5. Schematic of PBPK Model for JP-8

Table 3.1 Aerosolized Jet Fuel Exposures

Hydrocarbon	**JP-8**			**S-8**			**JP-8:S-8**		
	Total Concentration (mg/m^3) (SD)	**Percent Vapor (%)**	**Percent Aerosol (%)**	**Total Concentration (mg/m^3) (SD)**	**Percent Vapor (%)**	**Percent Aerosol (%)**	**Total Concentration (mg/m^3) (SD)**	**Percent Vapor (%)**	**Percent Aerosol (%)**
Total Exposure	908.9 (18.1)	62.7	37.3	1066.5 (48.9)	69.6	30.4	186.5 (2.86)	73.4	26.6
Octane (C8)	13.4 (3.2)	88.4	11.6	51.4 (18.0)	80.7	19.3	3.83 (0.96)	90.95	9.05
Decane (C10)	19.2 (4.6)	79.0	21.0	41.0 (9.8)	65.9	34.1	4.23 (1.08)	91.06	8.94
Tetradecane (C14)	5.4 (1.3)	50.5	49.5	11.7 (8.7)	17.7	82.3	0.95 (0.28)	51.0	49.0
Toluene (TOL)	5.0 (1.2)	86.7	13.3	-	-	-	0.42 (0.1)	90.14	9.86
Ethylbenzene (EBZ)	3.0 (0.7)	81.9	18.1	-	-	-	0.28 (0.06)	91.07	8.93
m-Xylene (m-XYL)	7.3 (1.8)	79.8	20.2	-	-	-	0.62 (0.14)	91.6	8.40

Table 3.1 (continued)

Lump 1 (L1)	227.2	79.0	21.0	-	-	-	54.99	80.9	19.1
Lump 2 (L2)	431.07	83.0	16.0	931.86	73.4	26.6	104.78	83.9	16.14
Lump 3 (L3)	250.53	36.0	64.0	140.14	45.78	54.2	28.63	30.5	69.5

Table 3.2. Vaporized JP-8 Exposures (Campbell and Fisher, 2007)

Hydrocarbon	**JP-8 vapor (mg/m^3, SD)**		
Total Exposure	2681 (383.5)	1085.9 (18.9)	384.4 (243.5)
Octane (C8)	180.1 (22.9)	67.9 (3.51)	24.66 (14.8)
Decane (C10)	97.25 (16.01)	33.4 (2.31)	11.57 (8.22)
Tetradecane (C14)	0.27 (0.04)	0.10 (0.04)	0.04 (0.03)
Toluene (TOL)	84.31 (13.7)	115.0 (14.3)	36.02 (26.7)
Ethylbenzene (EBZ)	31.74 (3.72)	15.80 (0.06)	5.17 (3.69)
m-Xylene (m-XYL)	79.05 (17.01)	49.10 (1.39)	14.40 (11.98)
Lump 1 (L1)	83.78	271.5	96.11
Lump 2 (L2)	2008.1	813.3	287.95
Lump 3 (L3)	2.681	1.09	0.38

Table 3.3. SPME-GC/MS operating conditions JP-8, S-8, JP-8:S-8 fuels and C14, C8.

Pameter	Setting
Injection Mode:	SPME (splitless)
Sample Extraction:	
Agitator Temperature	Fuels and C14 (65°C) C8 (35°C)
Pre-Incubation Time	Fuels and C14 (45 min) C8 (25 min)
Fiber Extraction Time	Fuels and C14 (16 min - Blood, 22 min - brain and liver, and 40 min – fat) C8 (10 min)
Desorption Time	1.0 min
Fiber Clean Temperature	250-275°C
Fiber Bakeout Time	5-14 min
GC Parameters:	
Injector Temperature	250°C
Oven Program	Fuels (35°C start for 10 min, 2.0°C/min to 99°C, 7.0°C/min to 230°C, 20°C/min to 240°C hold for 10 min) C14 (50°C start, 7.0°C/min to 230°C, hold 3 min, then 20°C/min to 240°C hold for 10 min) C8 (50°C start, 7.0°C/min to 230°C, 20°C/min to 240°C hold for 3.8 min)
Column	HP-1 (0.2 mm x 50 m x 1.5 µm)
Helium Flow Rate	1.0 ml/min (constant flow)
MS Parameters:	
Transfer Line Temperature	230°C
Manifold Temperature	100°C
Ion Trap Temperature	200°C
Scan Range	45 – 260 m/z
Scan Time	0.33 seconds/scan
Emission Current	45 µamps

Table 3.4. Physiological Parameters

Body Weight (kg)	0.2	
QPC (Alveolar ventilation l/hr/kg^0.75)	15.6	Delp *et al*. 1991
QCC (Cardiac Output, l/hr/kg^0.75)	15.6	Delp *et al*. 1991
Blood Flows (% Cardiac Output)		
QLC (Liver)	17.4	Brown *et al*.1997
QFC (Fat)	2.0	Brown *et al*.1997
QBrC (Brain)	7	Brown *et al*.1997
QRC (Rapid)	0.78*QC-QL-QBr-Qno-Qtb	
QSC (Slow)	0.22*QC-QF	
Qno (Nose)	0.007	Csanady *et al*, 2007
Tissue Volume (% BW)		
VLC (Liver)	4.0	Schoeffner *et al*, 1999
VFC (Fat)	8.67	Schoeffner *et al*, 1999
VLuC (Lung)	0.47	Schoeffner *et al*, 1999
VBrC (Brain)	0.76	Schoeffner *et al*, 1999
VRC (Rapid)	0.12*BW -VBr-VLu-VNo-VTb-VL	
VSC (Slow)	0.80*BW - VF	
VnmucousC (Nasal mucous)	2.9e-5	Parent *et al*, 1992
Vno (Nasal)	2.2e-5	Csanady *et al*, 2007
Olfthick (cm)	7.0e-3	Csanady *et al*, 2007
Resthick (cm)	8e-3	Csanady *et al*, 2007
OlfSA (cm^2/kg)	2.5	Csanady *et al*, 2007
ResSA (cm^2/kg)	2.2	Csanady *et al*, 2007
VlmucousC (Lung mucous)	2.69e-4	Parent *et al*, 1992
VDLC (Deep Liver)	0.02*VL	
VSLC (Shallow Liver)	0.98*VL	

Table 3.4. Physiological Parameters (continued)

Blood Volume (% Tissue)		
Bvfc (Blood volume fat)	0.05	Brown *et al*,1997
Bvbrc (Blood volume brain)	0.03	Brown *et al*,1997
Bvlc (Blood volume liver)	0.21	Brown *et al*,1997
Bvluc (Blood volume lung)	0.36	Brown *et al*,1997

Table 3.5. Model Paramenters

Partition Coefficients	**TOL**[a]	**ETB**[a]	**m-XYL**[a]	**C8**[b]	**C10**[b]	**C14**[c]	**L1**[d]	**L2**[d]	**L3**[d]
PB (Blood:Air)	18.0	42.7	46.0	3.13	8.13	52.4[b]	36.7	12.408	52.4
PL (Liver:Blood)	4.64	1.96	1.98	1.92	1.97	0.29	2.89	1.77	0.19
PF (Fat:Blood)	56.7	36.4	40.4	246.6	328.12	48.75	46.4	520.78	16.45
PBr (Brain:Blood)	1.72[h]	1.41	0.8[g]	1.40	4.76	0.08	2.52	9.45	0.03
PS (Slow:Blood)	1.54	0.61	0.91	0.95	0.85	0.29	1.34	0.96	0.19
PR (Rapid:Blood)	4.64	1.41	1.98	1.92	1.97	0.29	2.89	1.77	0.19
PLu (Lung:Blood)	4.64	1.96	1.98	1.92	1.97	13	2.89	1.77	8.51
Pno (Nose:Blood)	4.64	1.96	1.98	1.92	1.97	13	2.89	1.77	8.51
VmaxC	3.44[e]	6.39[e]	6.49[e]	35.5[d]	10[d]	-	2.5[g]	10.22[d]	-
Km	0.13[e]	1.04[e]	0.45[e]	1.5[f]	1.5[f]	-	0.75[g]	1.6[d]	-
PABRinC[d]	-	-	-	5.5e-1	1.0E-03	3.5E-02	-	1.0E-03	3.5E-02
PABRoutC[d]	-	-	-	5.5e-1	3.0E-02	1.0E-01	-	3.0E-02	1.0E-01
PALinC[d]	-	-	-	8e-1	2.0E-01	1.0E-02	-	2.0E-01	1.0E-02
PALoutC[d]	-	-	-	8e-1	2.0E-01	1.0E-02	-	2.0E-01	1.0E-02
PAFinC[d]	0.95	0.658	0.56	4e-1	1.0E-01	7.6E-03	0.95	1.0E-01	7.6E-03
PAFoutC[d]	0.95	0.658	0.56	4e-1	9.0E-01	7.6E-03	0.95	9.0E-01	7.6E-03
PAC1, PACnose	1e-2	1e-2	1e-2	1e-1	2.3E-05	9.0E-04	1e-2	2.3E-05	9.0E-04

[a]Tardif *et al*., 1997
[b]Smith *et al*., 2004
[c]Distribution Ratio
[d]Estimated
[e]Haddad *et al* 1999
[f]Mortensen *et al*, 2000
[g]Campbell and Fisher, 2007
[h]Thrall *et al*, 2002

Table 3.6. Sensitivity Analysis

Octane	**2hr**	**4hr**	**5hr**
PB	0.35	0.31	**-3.31**
PSA	0.00	0.00	**3.82**
QPC	**0.72**	0.24	0.46
QCC	**-0.51**	**-0.52**	**-4.25**
BW	0.00	-0.34	**0.92**

Decane	**2hr**	**4hr**	**5hr**
PB	**0.97**	**0.97**	0.20
PSA	-0.03	0.01	**1.97**
QCC	0.00	0.00	**0.70**
QPC	0.12	-0.10	**1.07**
BW	**-0.01**	**-0.09**	**0.62**
VBRC	**-0.76**	**-0.76**	**-0.76**
QNOC	**-0.70**	**0.69**	**0.52**

Tetradecane	**2hr**	**4hr**	**5hr**
PB	0.45	**0.55**	**0.98**
PFA	**-0.57**	**0.60**	**0.82**
QPC	**0.55**	0.42	0.01
QNOC	**0.70**	**-0.70**	**-0.70**
VBRC	**-0.76**	**-0.76**	**-0.76**
PACLin	0.17	0.28	**0.88**
Toluene	**2hr**	**4hr**	**5hr**
PS	-0.12	-0.04	**0.82**
PB	0.40	0.50	**0.70**
QPC	**1.16**	**1.18**	**0.95**
QCC	-0.17	-0.14	**-0.89**
VBRC	**-0.76**	**0.72**	**0.76**
QLC	-0.25	-0.19	**-0.81**
Vmaxtlc	**-0.68**	**-0.83**	**-0.85**

Table 3.6. Sensitivity Analysis (continued)

Ethylbenzene	**2hr**	**4hr**	**5hr**
PF	-0.06	-0.11	**-0.55**
PS	-0.03	-0.01	**0.51**
QPC	**1.19**	**1.15**	**1.07**
QCC	-0.24	-0.20	**-0.65**
VBRC	**-0.76**	0.03	0.05
VFC	-0.06	-0.11	**-0.62**
VmaxcEBZ	**-0.72**	**-0.81**	**-1.06**
KmEBZ	0.30	0.33	**0.58**
QLC	-0.26	-0.22	**-0.77**

m-Xylene	**2hr**	**4hr**	**5hr**
PSA	-0.04	-0.01	**0.92**
QPC	**1.25**	**1.25**	**1.16**
QCC	-0.37	-0.34	**-1.28**
VFC	-0.04	-0.08	**-0.55**
VBrC	**-0.76**	0.03	0.04
Vmaxc	**-0.64**	**-0.77**	**-0.85**
QLC	-0.45	-0.41	**-1.16**
QNoC	-0.04	**0.70**	**0.70**

Figure 3.6. Model Simulations of Toluene (x-axis = Concentration (mg/L), y-axis = Time (hrs)

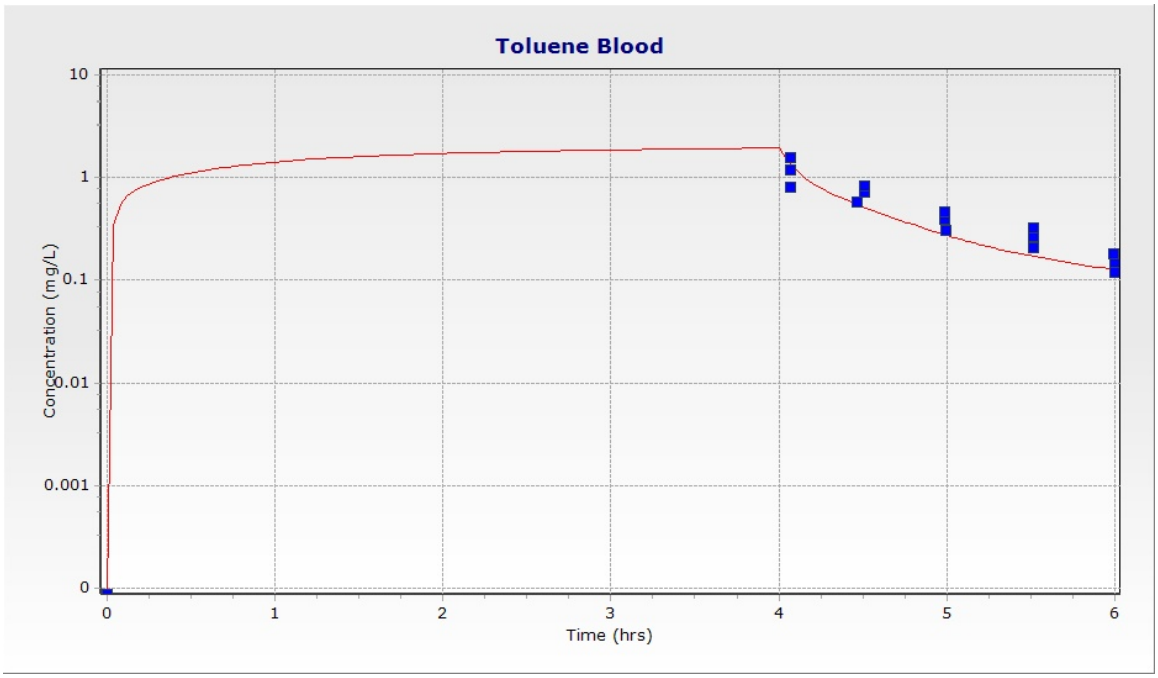

a.) Toluene vapor 100ppm 4hrs (Haddad, *et al.*, 1999)

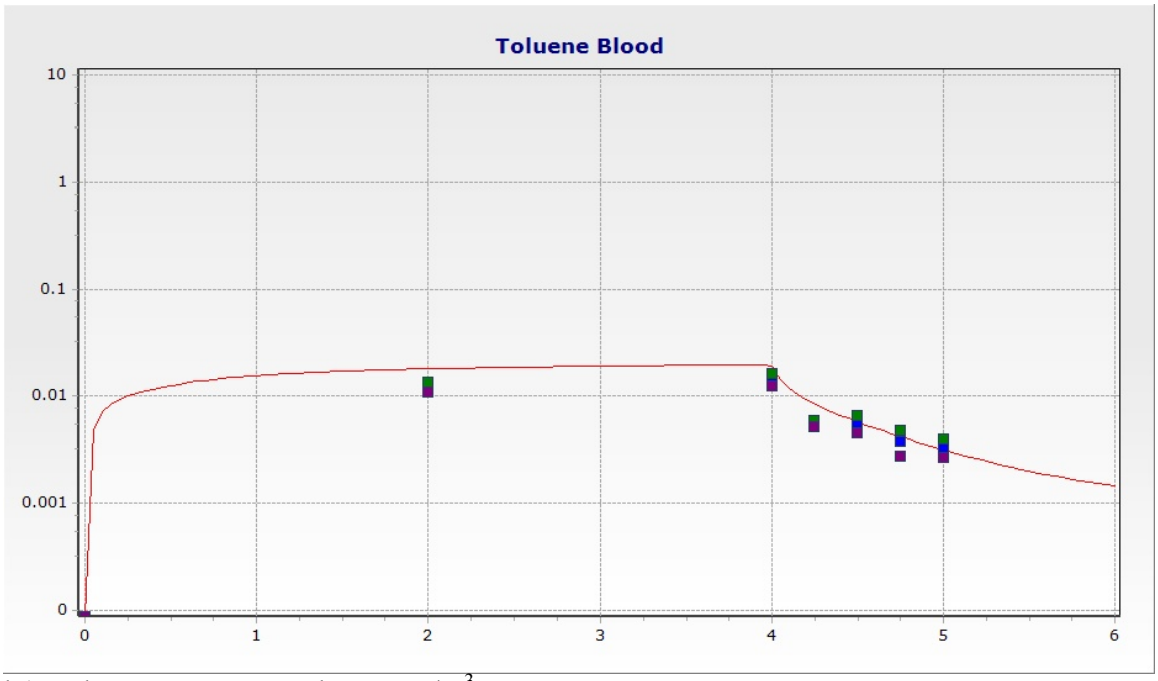

b.) Toluene JP-8 Aerosol 908 mg/m^3

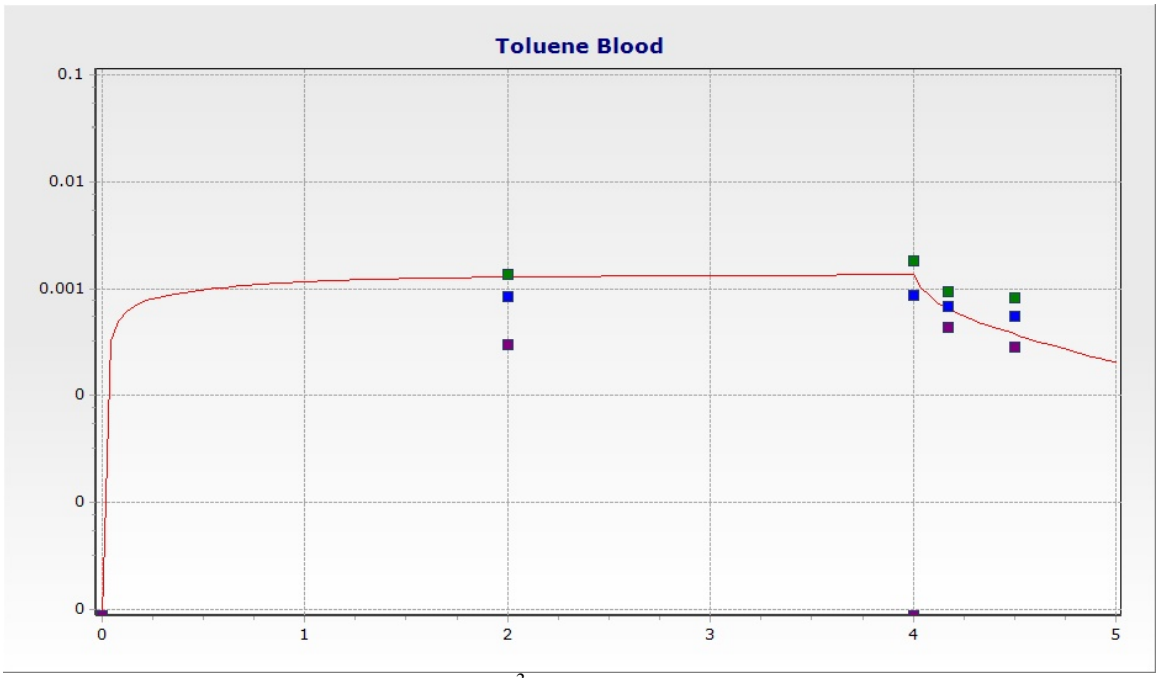

c.) Toluene JP-8:S-8 Aerosol 187 mg/m^3

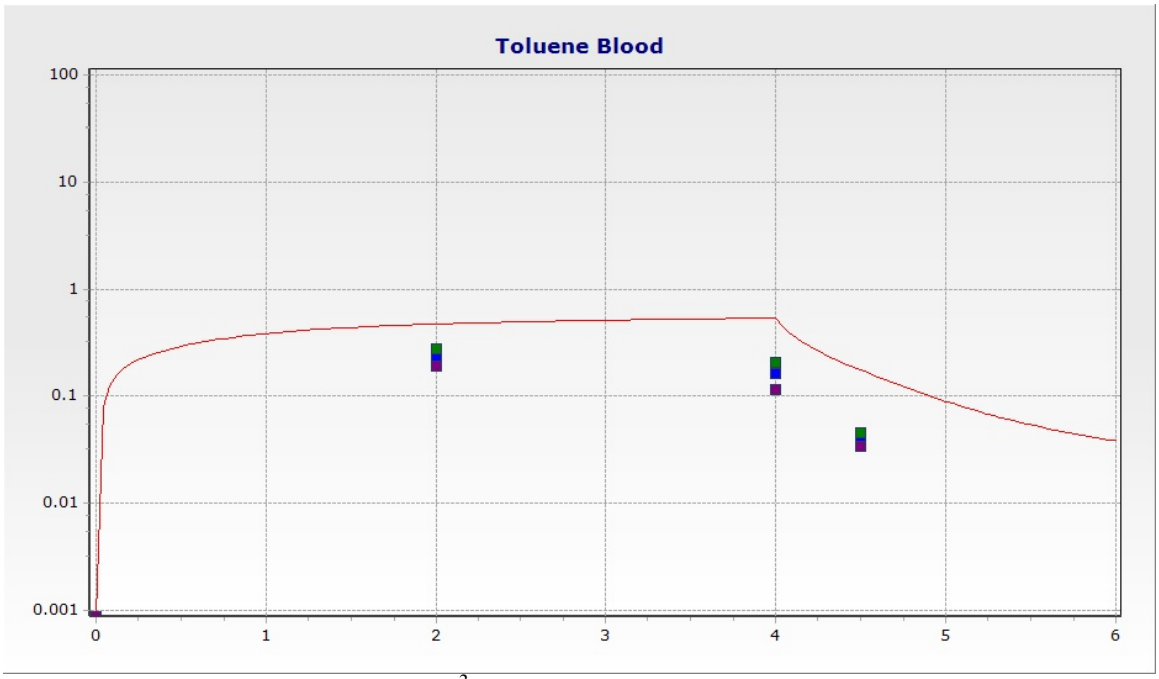

d.) Toluene JP-8 Vapor 2700 mg/m^3 4-hrs

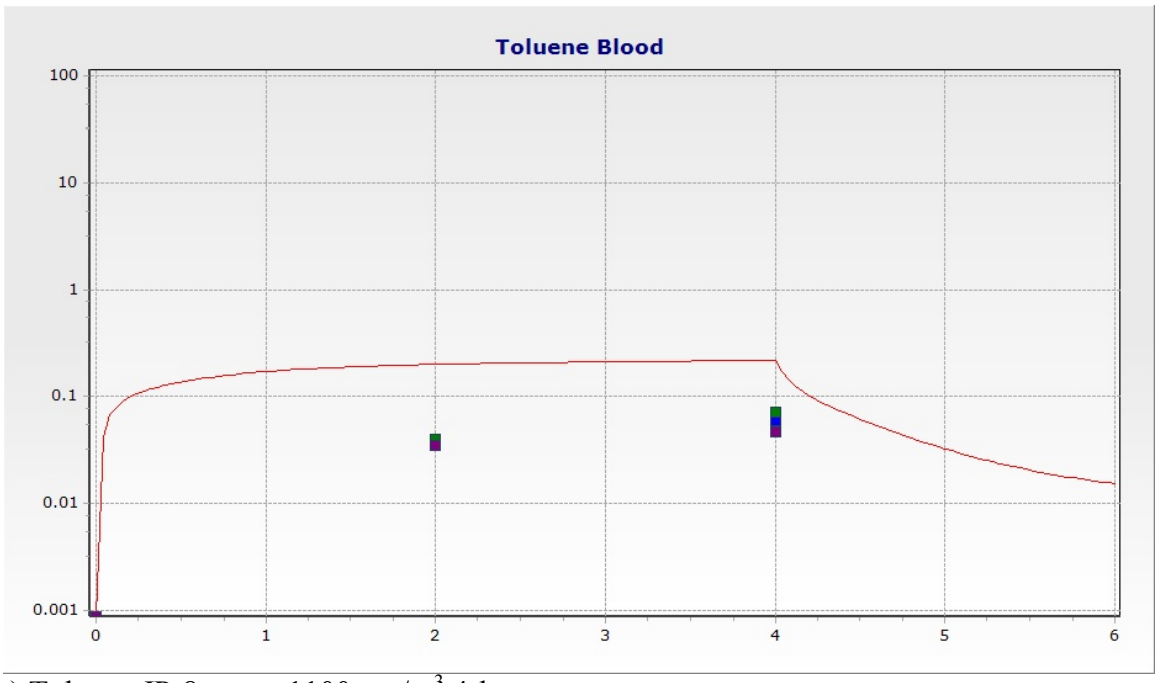

e) Toluene JP-8 vapor 1100 mg/m^3 4-hrs

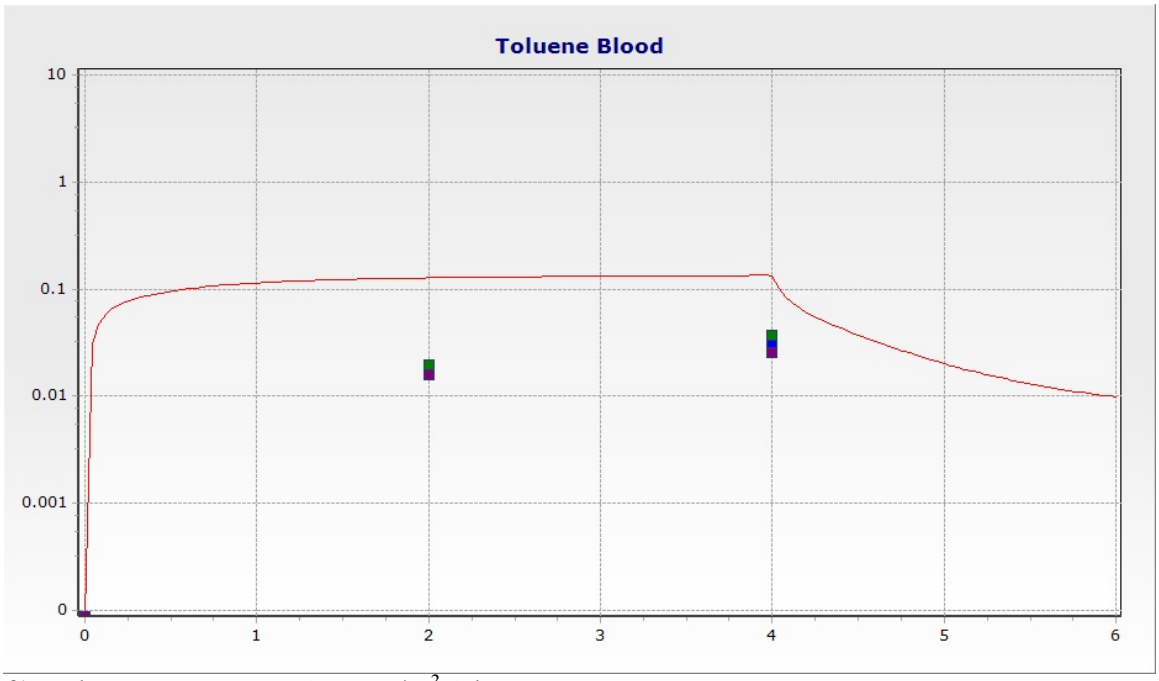

f.) Toluene JP-8 vapor 400 mg/m^3 4-hrs

Figure 3.7. Model Simulations of Xylene (x-axis = Concentration (mg/L), y-axis = Time (hrs)

a.) m-Xylene Vapor Blood 100 ppm, 4-hrs (Haddad *et al.*, 1999)

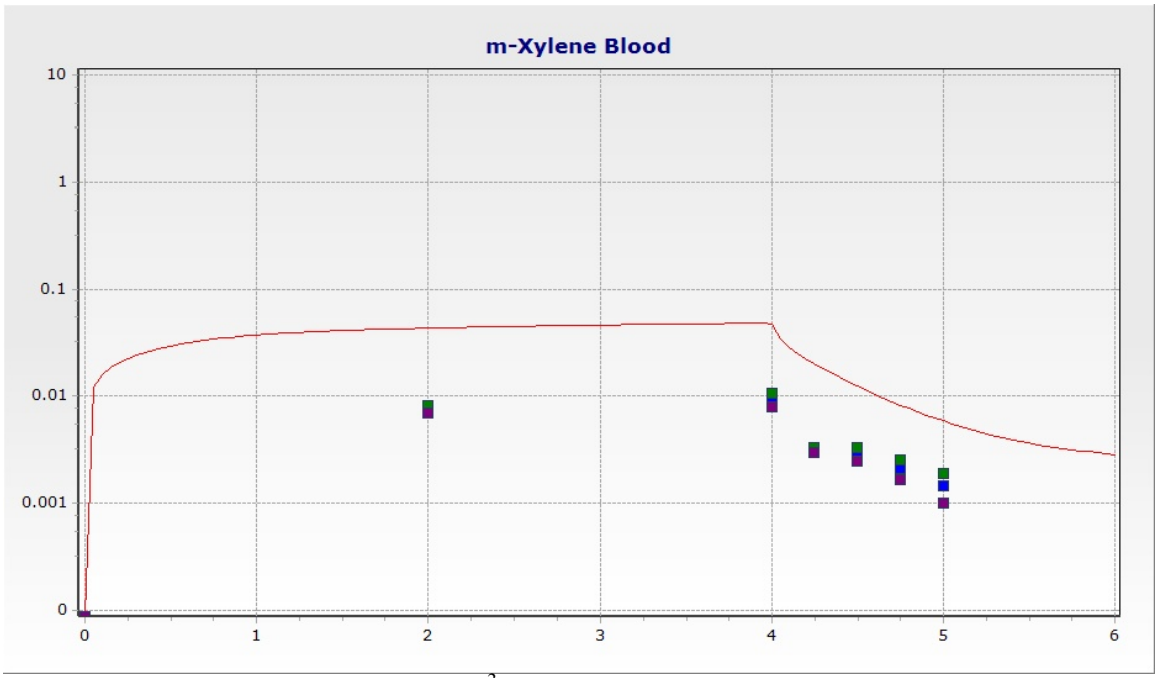

b.) JP-8 Aerosol m-Xylene 908 mg/m^3 4-hrs

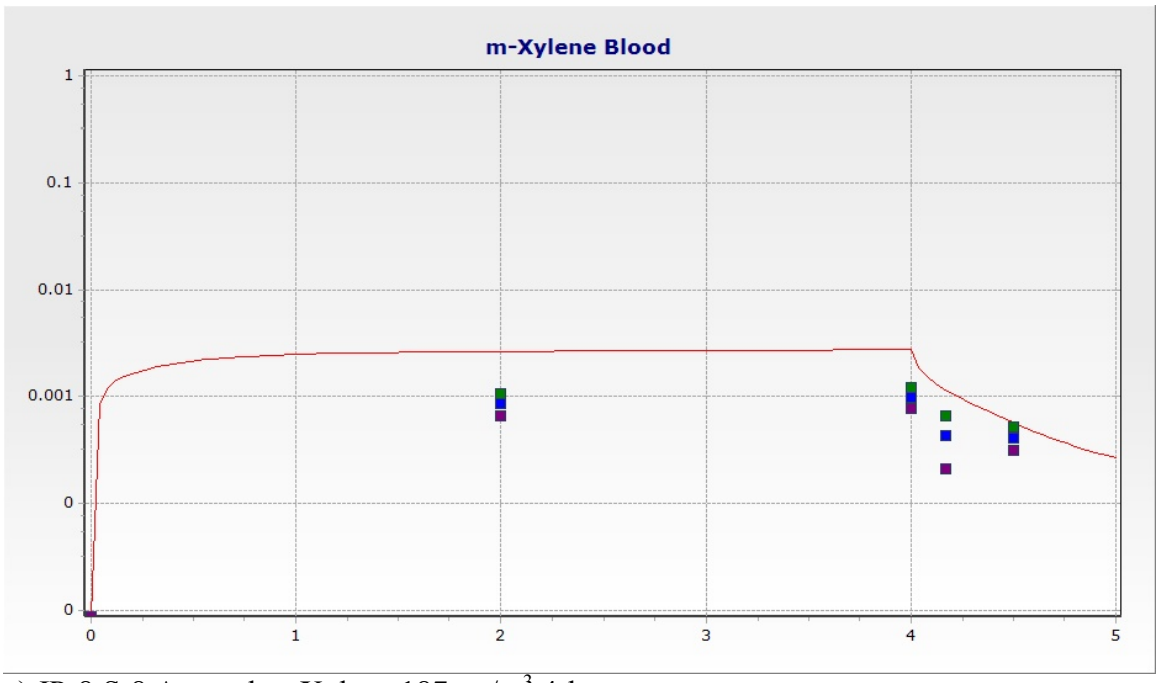

c.) JP-8:S-8 Aerosol m-Xylene 187mg/m^3 4-hrs

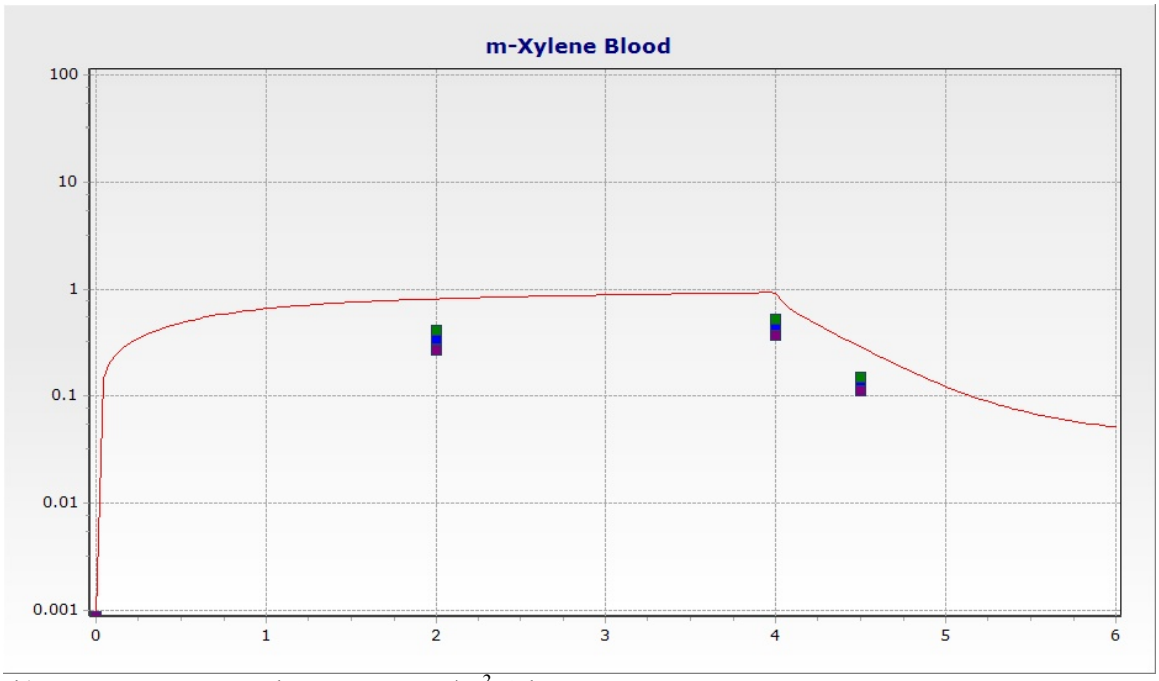

d.) JP-8 Vapor m-Xylene 2700 mg/m^3 4-hrs

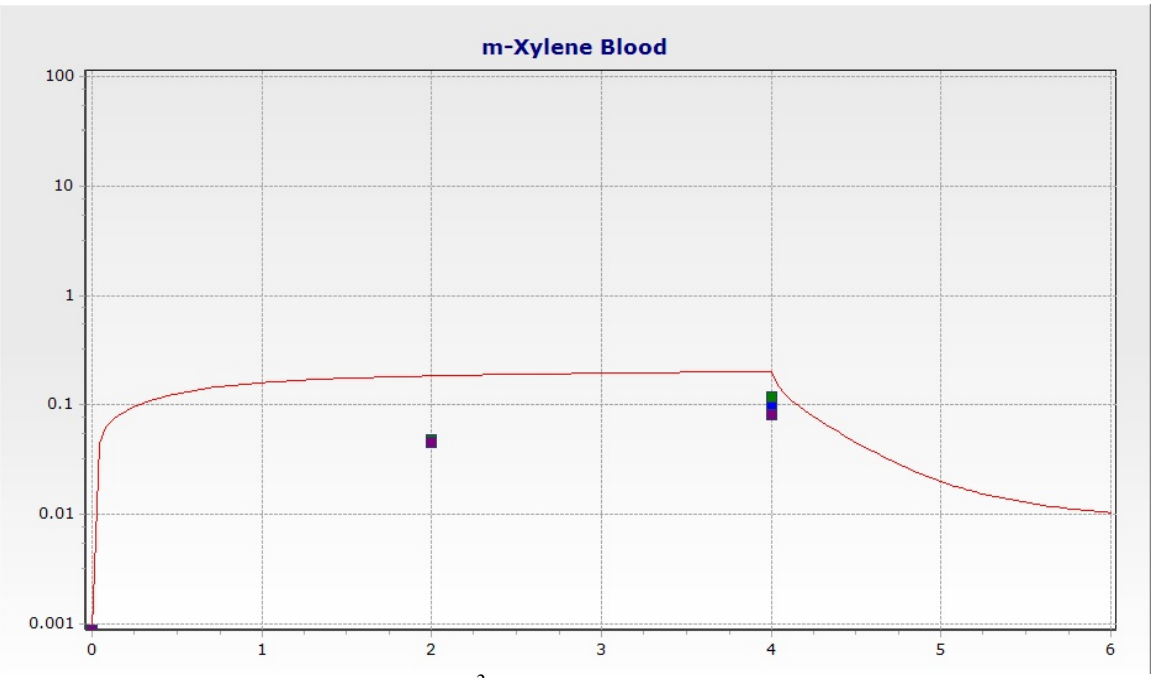

e.) JP-8 Vapor m-Xylene 1100 mg/m^3 4-hrs

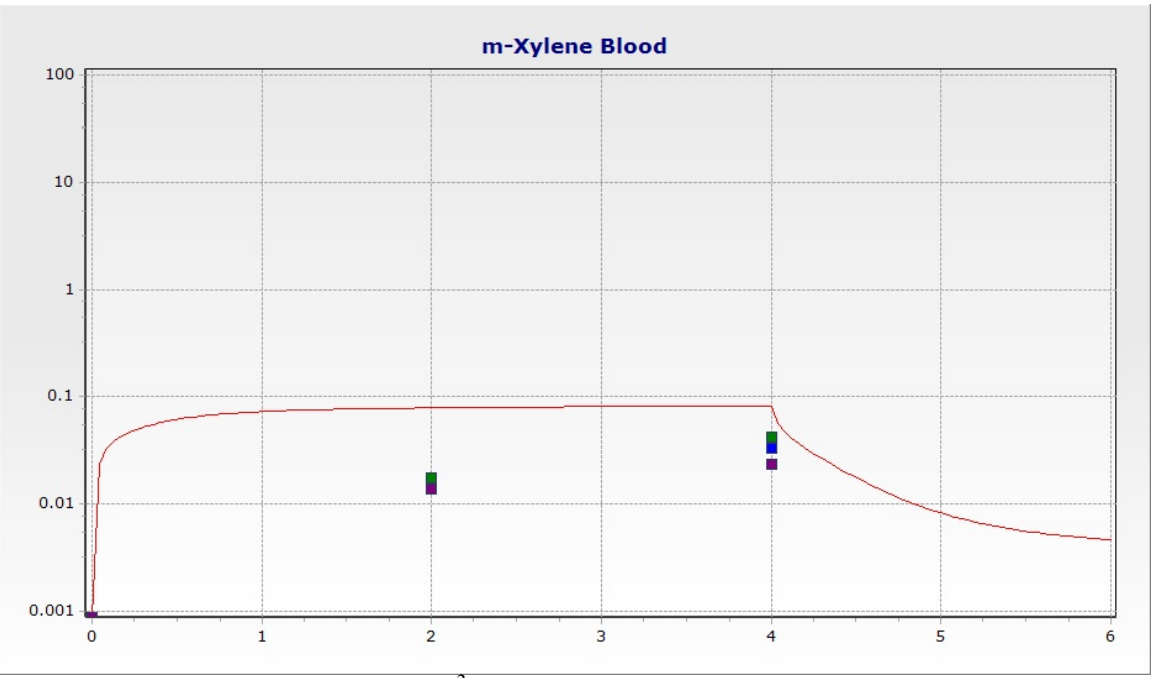

f.) JP-8 Vapor m-Xylene 400 mg/m^3 4-hrs

Figure 3.8. Simulations of Ethylbenzene (x-axis = Concentration (mg/L), y-axis = Time (hrs)

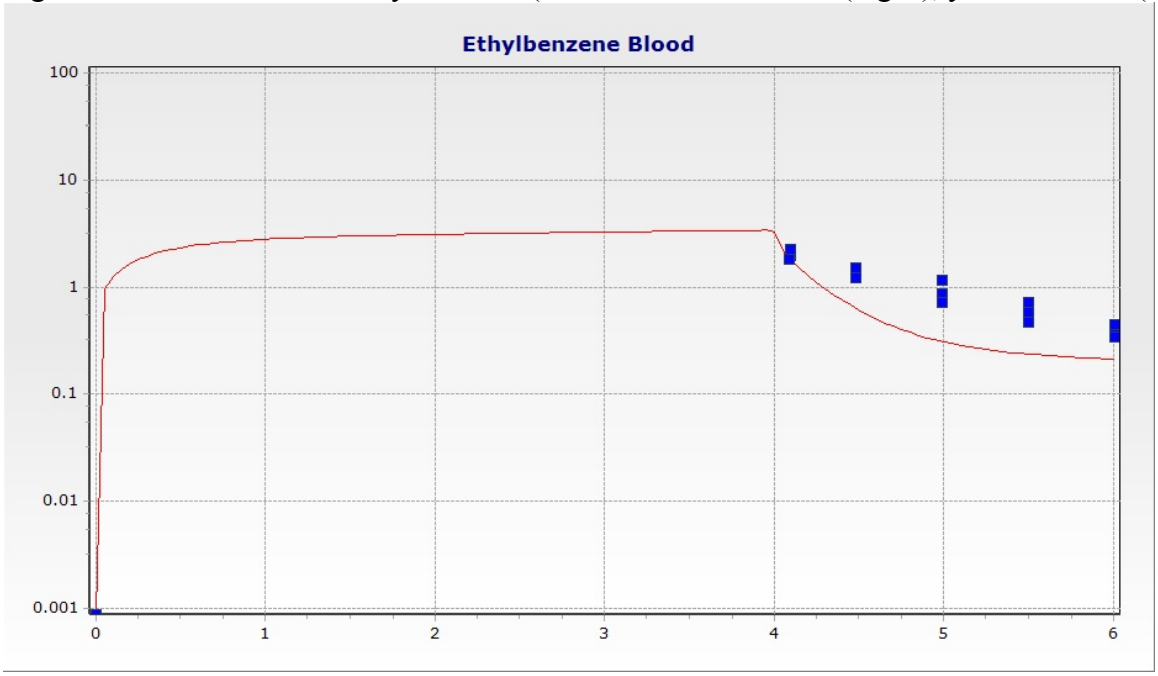

a.) Ethylbenzene 100ppm 4hrs (Haddad, *et al.*, 1999)

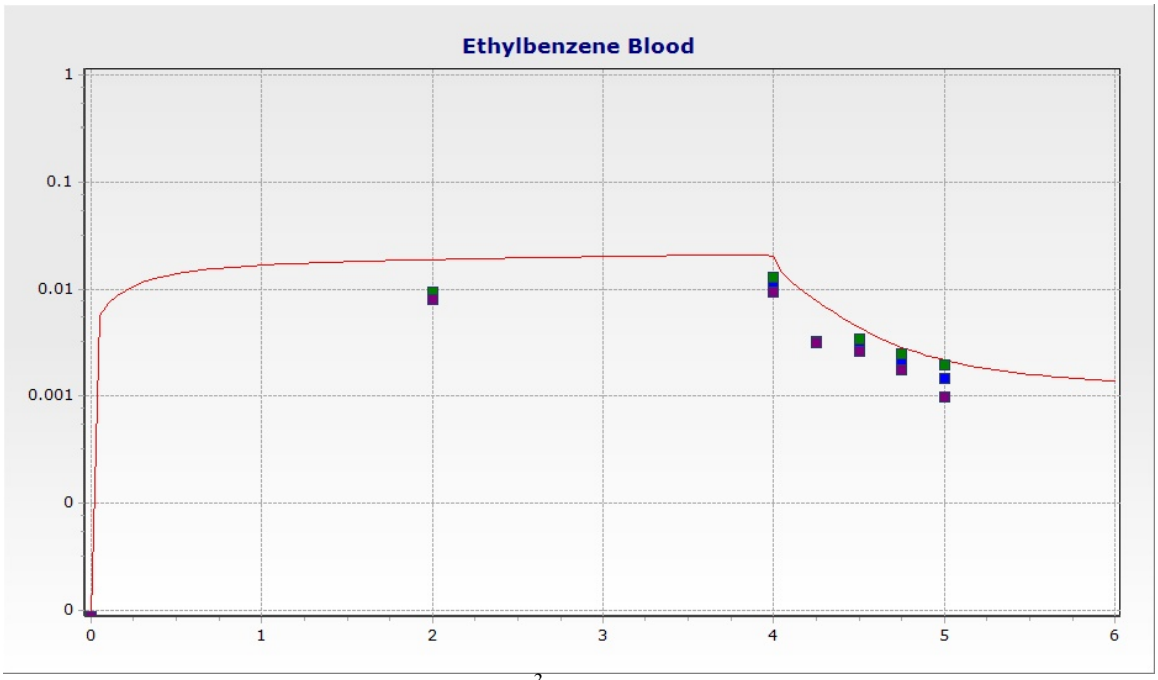

b.) Ethylbenzene Aerosol JP-8 908 mg/m^3

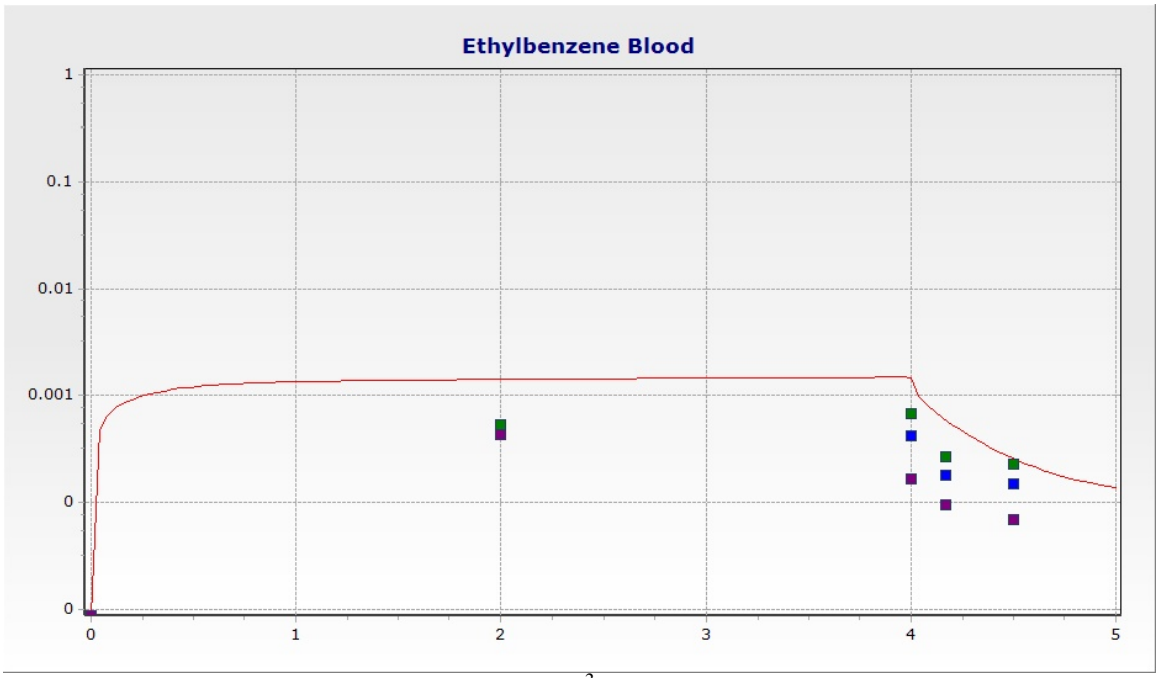

c.) Ethylbenzene JP-8:S-8 Aerosol 187 mg/m^3

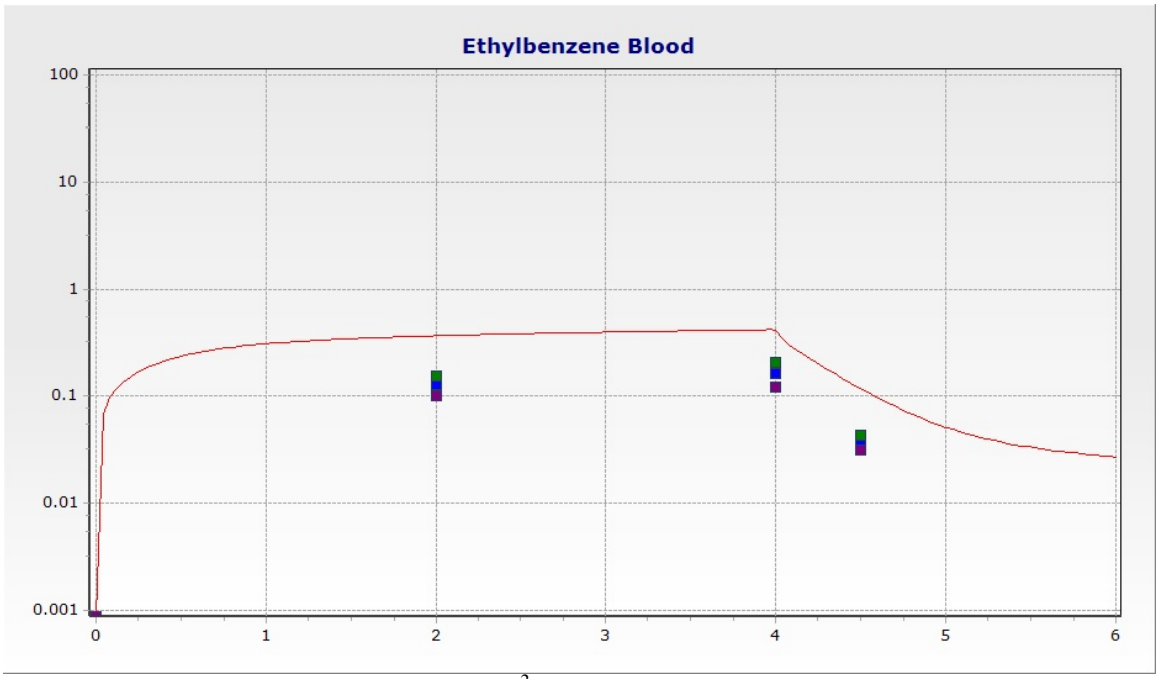

d.) Ethylbenzene JP-8 Vapor 2700mg/m^3 4hrs

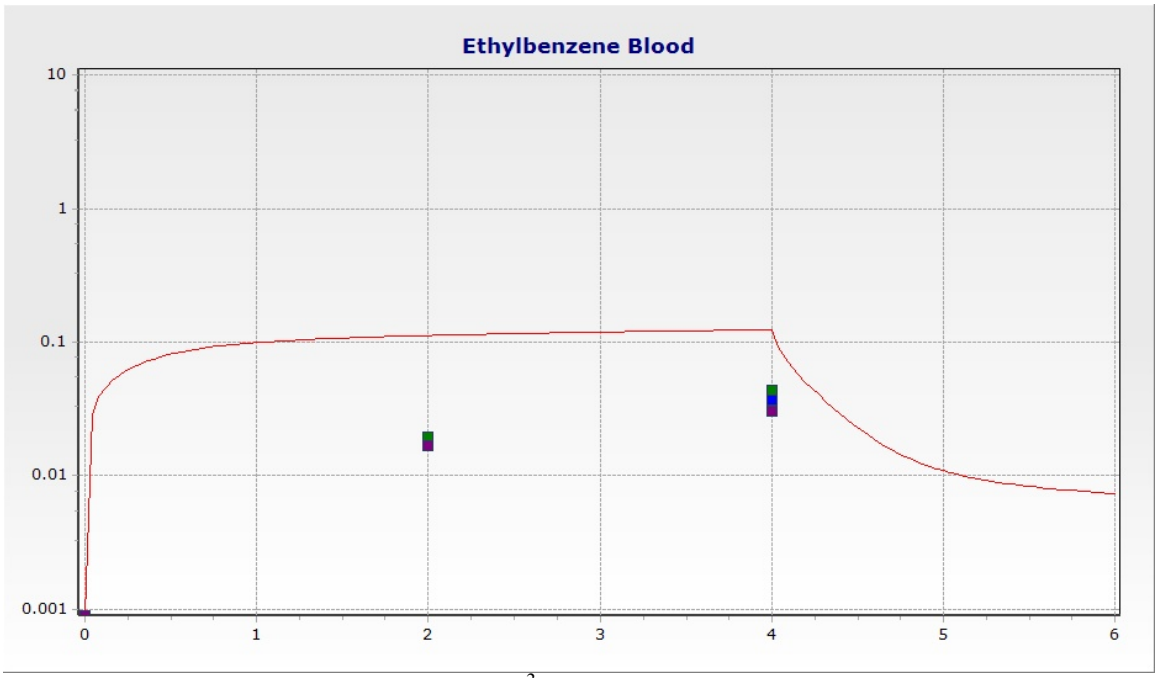

e.) Ethylbenzene JP-8 Vapor 1100 mg/m^3 4-hrs

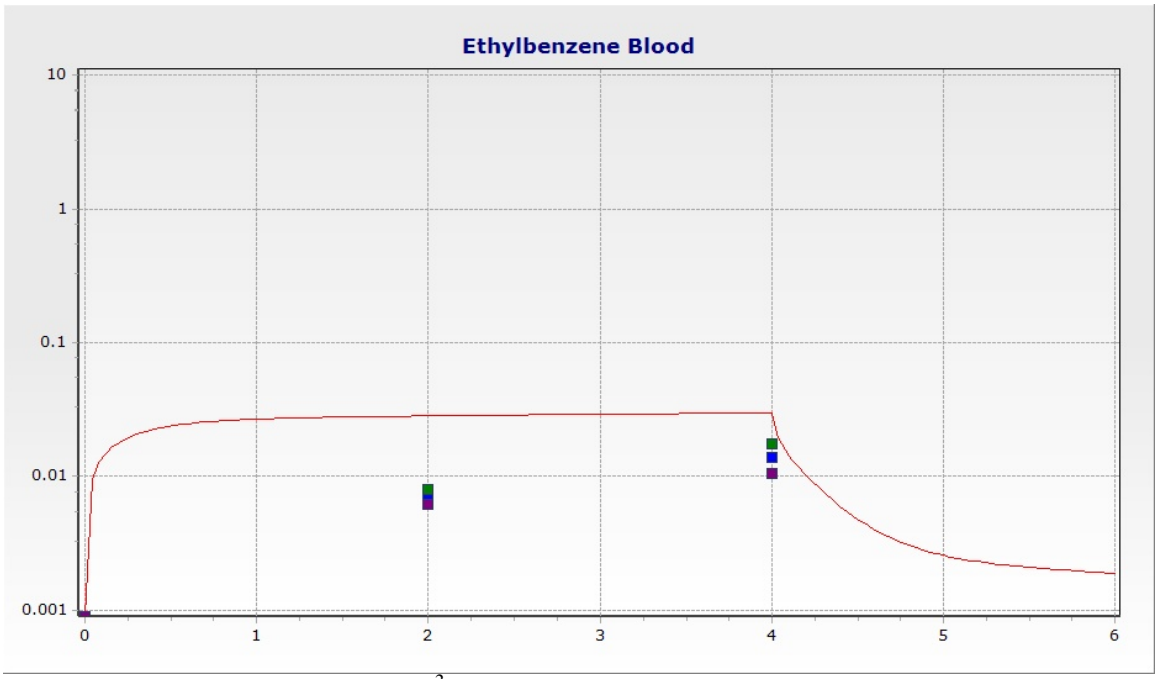

f.) Ethylbenzene vapor 400 mg/m^3 4-hrs

Figure 3.9. Model Simulations of Octane (x-axis = Concentration (mg/L), y-axis = Time (hrs)

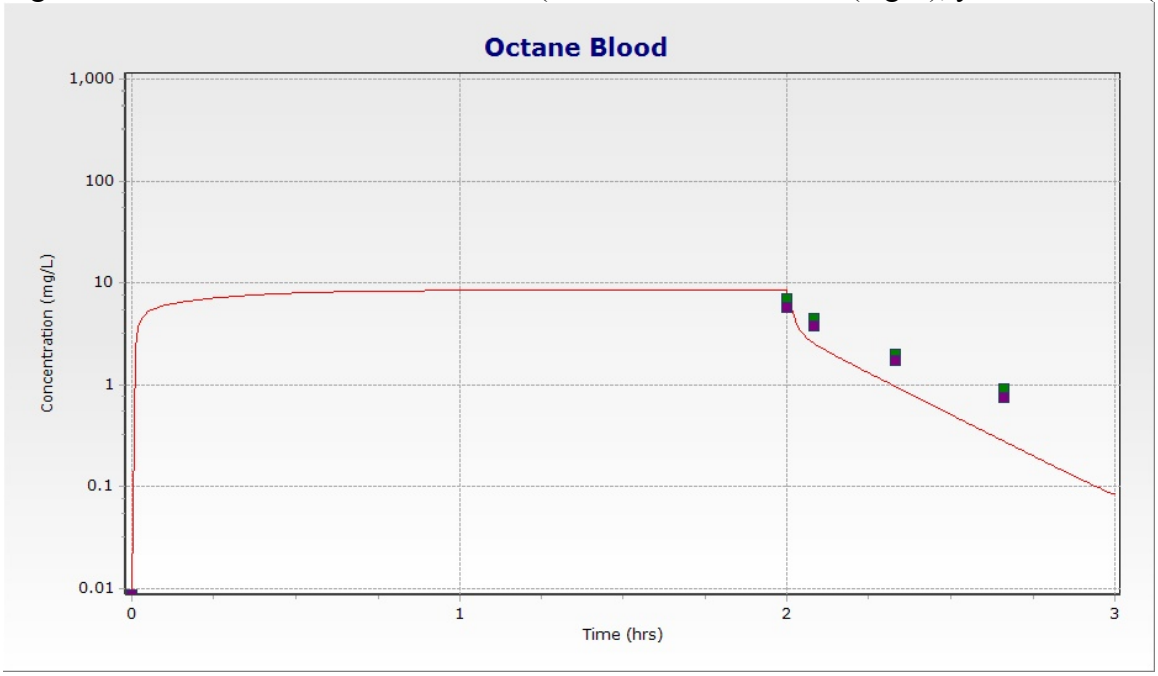

a.) Octane Vapor 1000ppm 2hrs

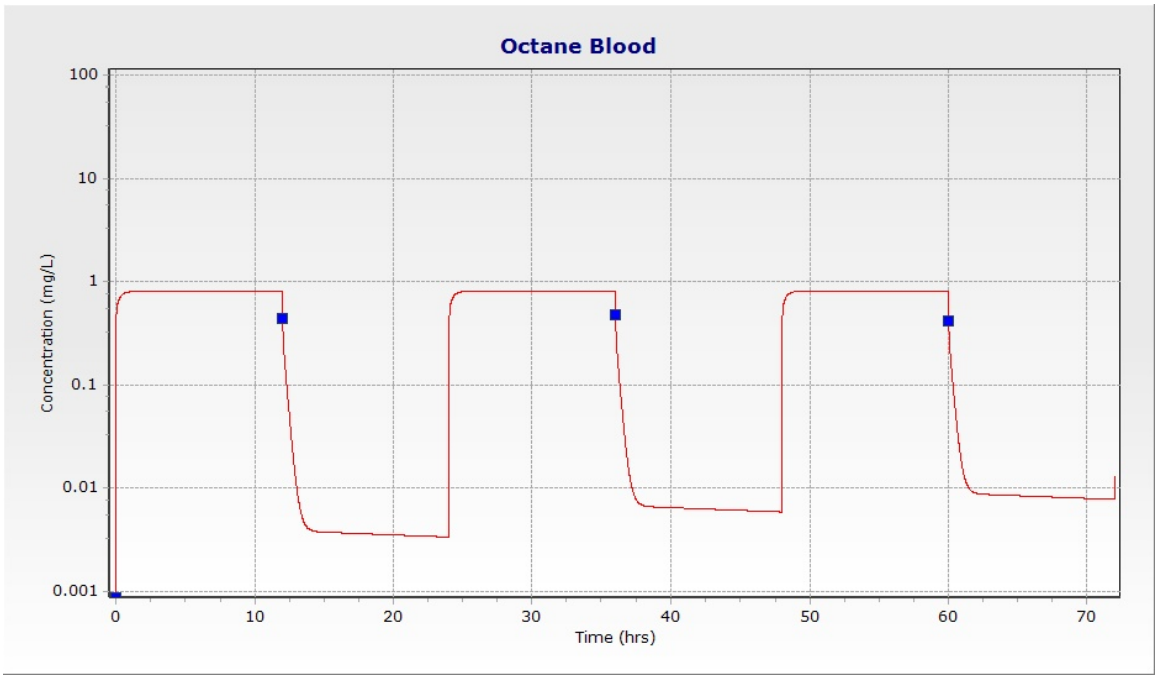

b.) Octane Vapor 100ppm 12hr/day/3 days (Zahlsen *et al*, 1992)

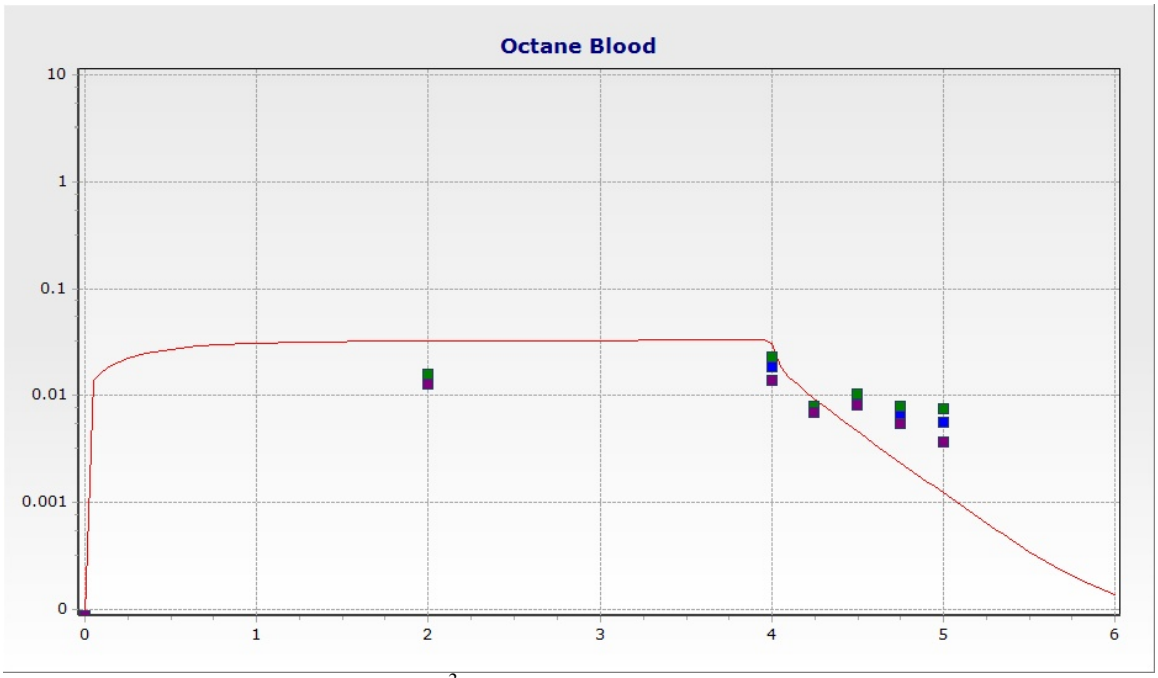

c.) Octane Aerosol JP-8 908 mg/m^3

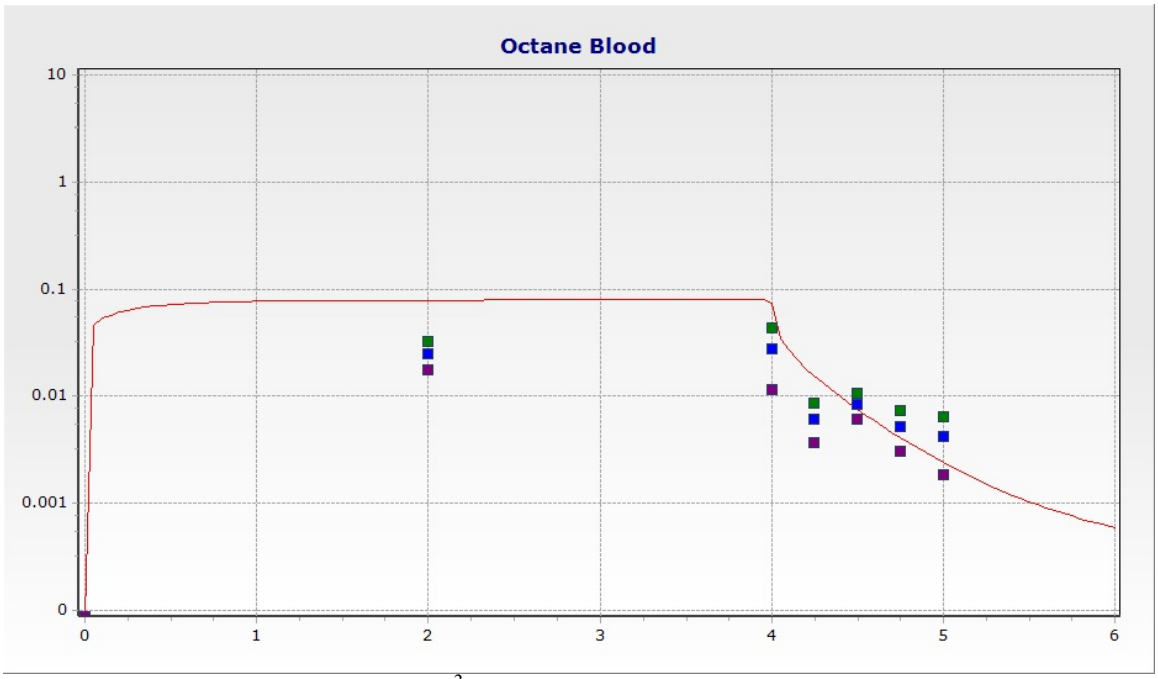

d.) Octane Aerosol S-8 1070 mg/m^3

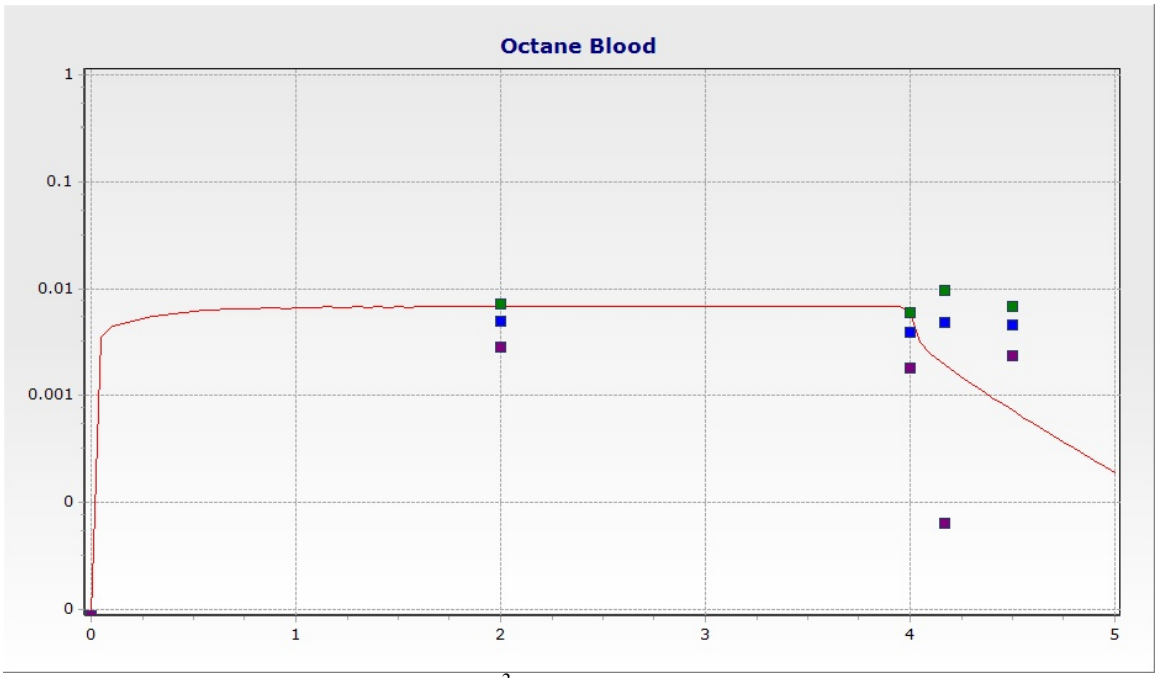

e.) Octane Aerosol JP-8:S-8 187 mg/m^3 4-hrs

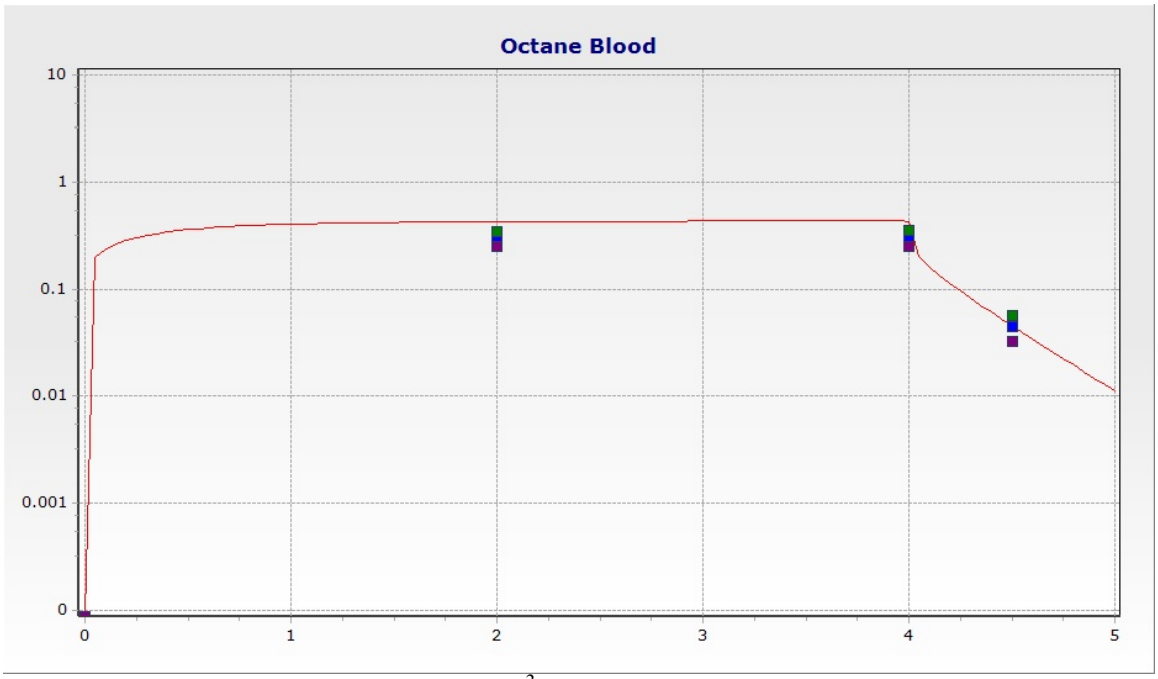

f.) Octane Vapor JP-8 Blood 2700 mg/m^3 4-hrs

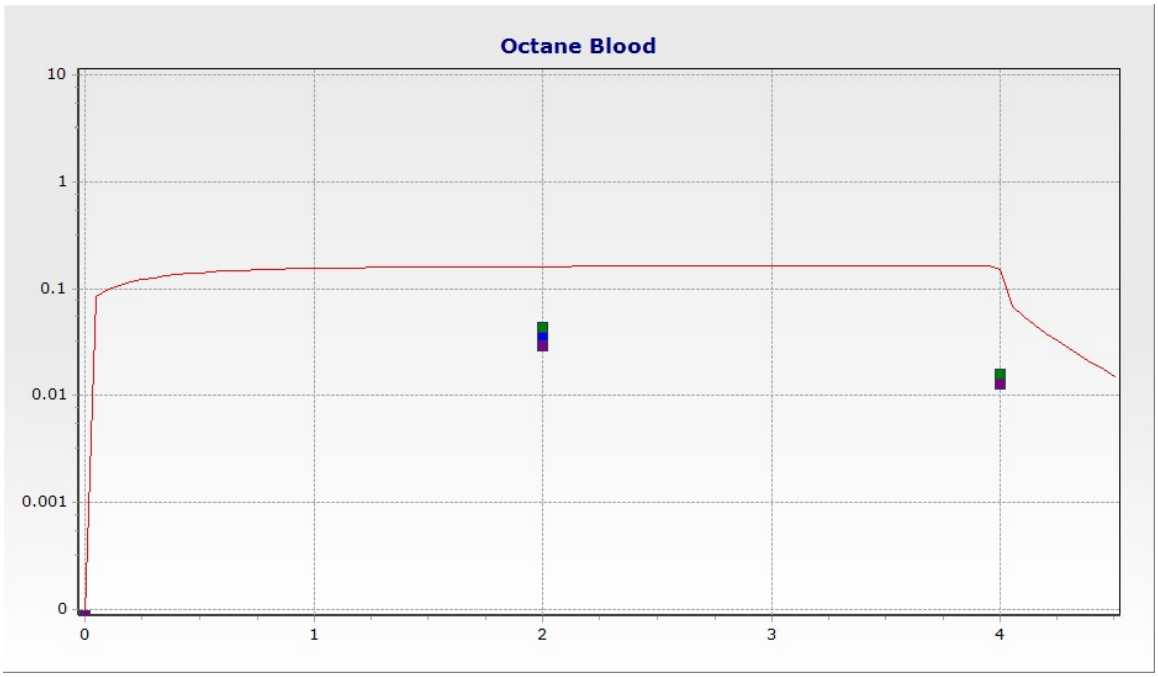

g.) Octane Vapor JP-8 Blood 1100 mg/m3 4-hrs

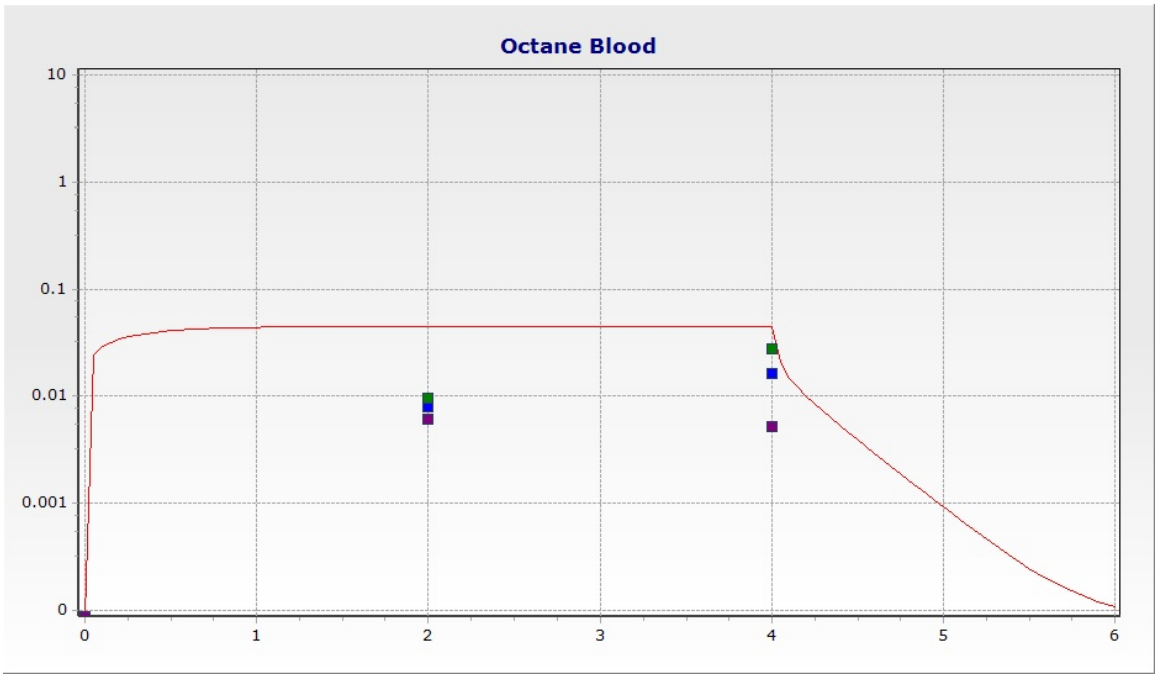

h.) Octane Vapor JP-8 Blood 400 mg/m3 4-hrs

Figure 3.10. Model Simulations of Decane (x-axis = Concentration (mg/L), y-axis = Time (hrs)

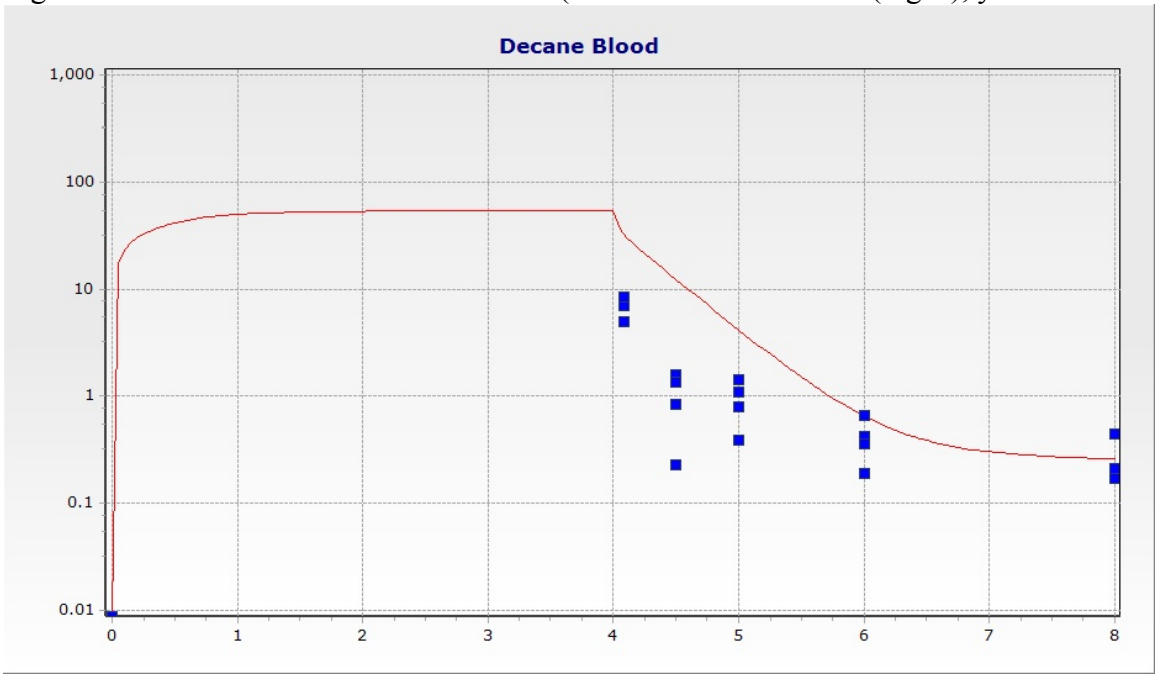

a.) Decane Vapor 1200 ppm 4-hrs (Perleberg *et al.*, 2004)

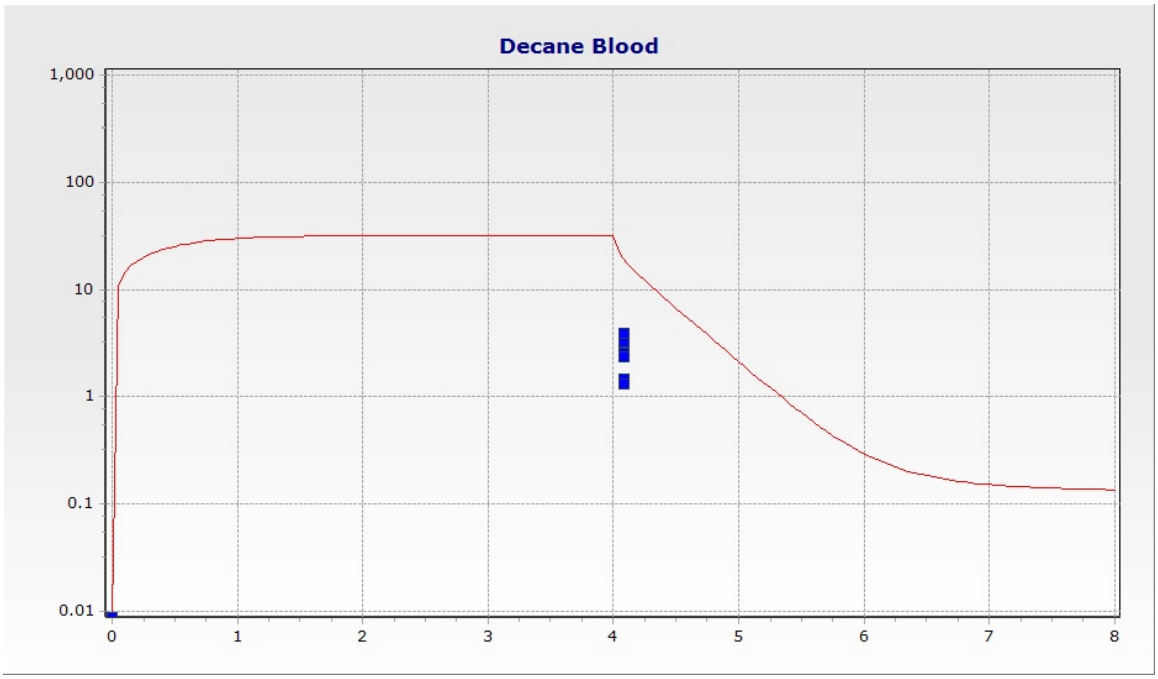

b.) Decane Vapor 781ppm 12hr/day/3 days 4-hrs (Perleberg *et al.*, 2004)

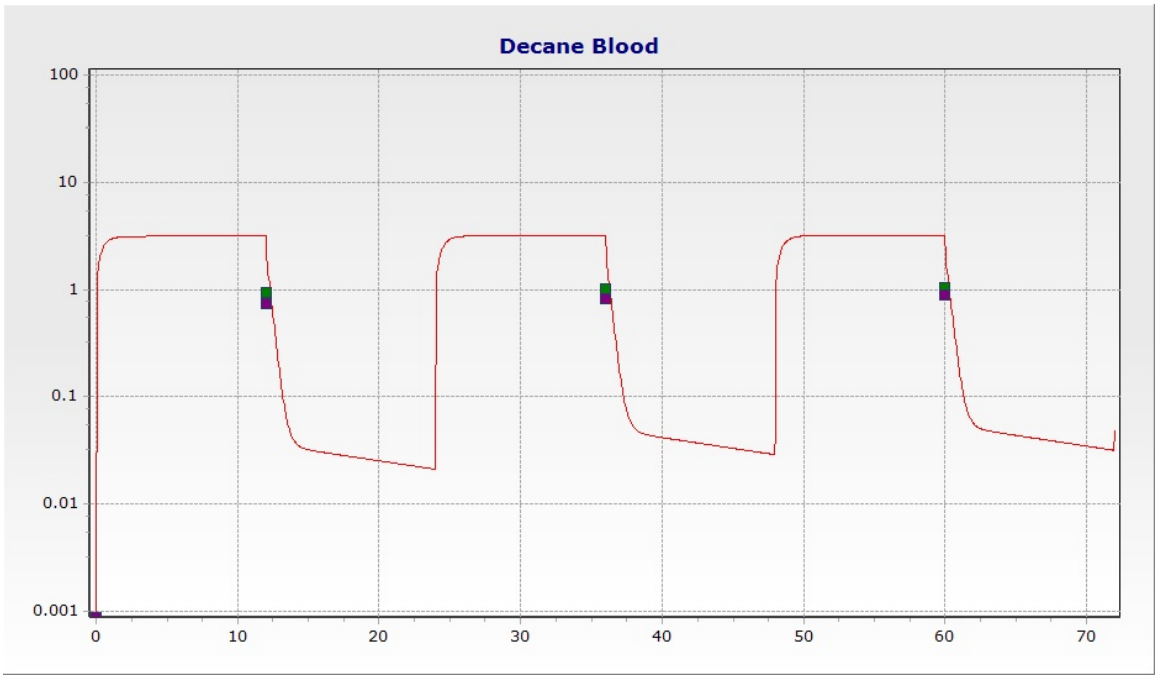

c.) Decane Vapor 100ppm 12hr/day/3 days (Zahlsen *et al*, 1992)

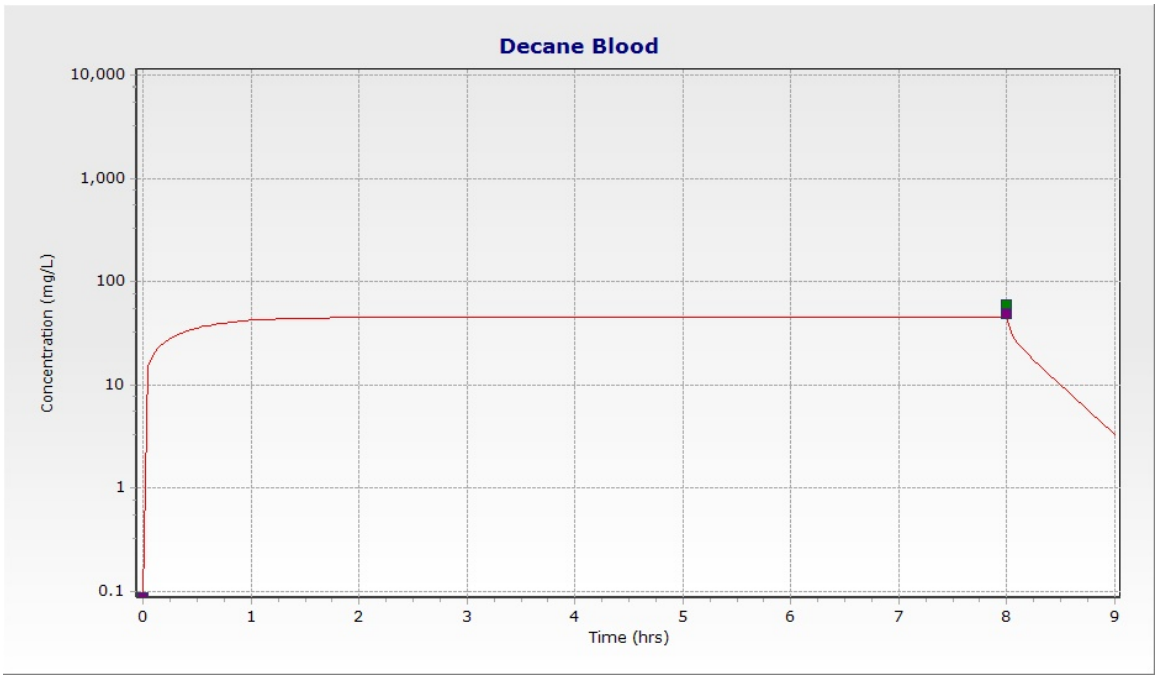

d.) Decane Vapor Blood 1369 ppm 8-hrs (Nilsen *et al.*, 1988)

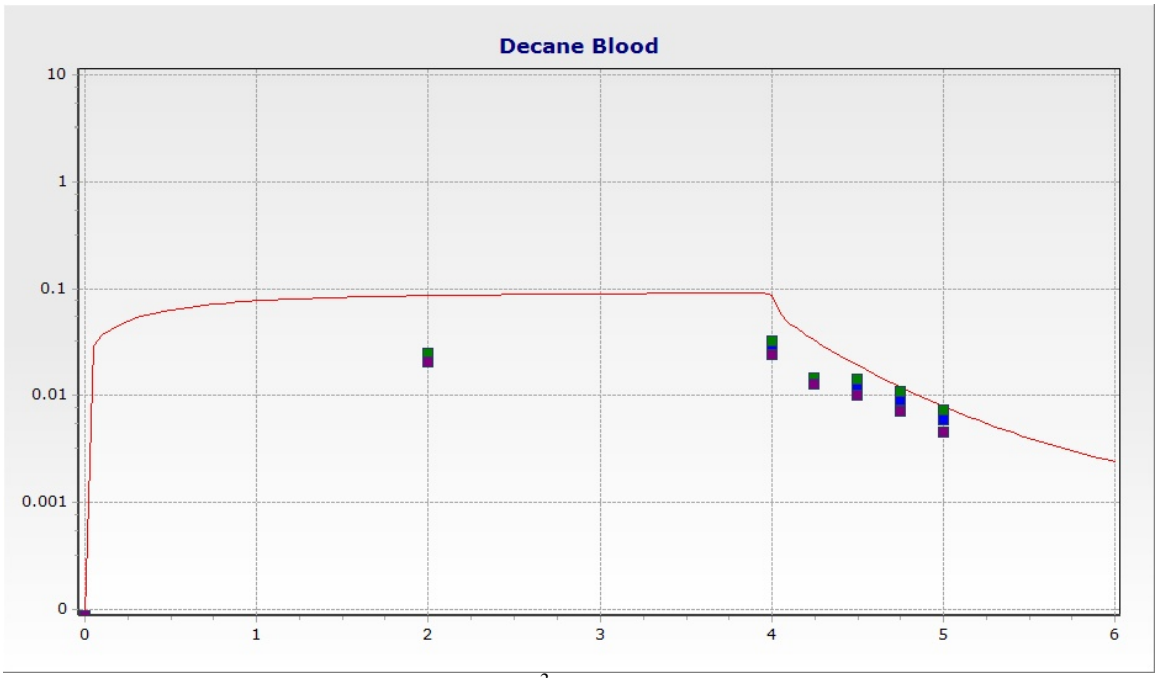

e.) Decane Aerosol JP-8 Blood 908 mg/m^3 4-hrs

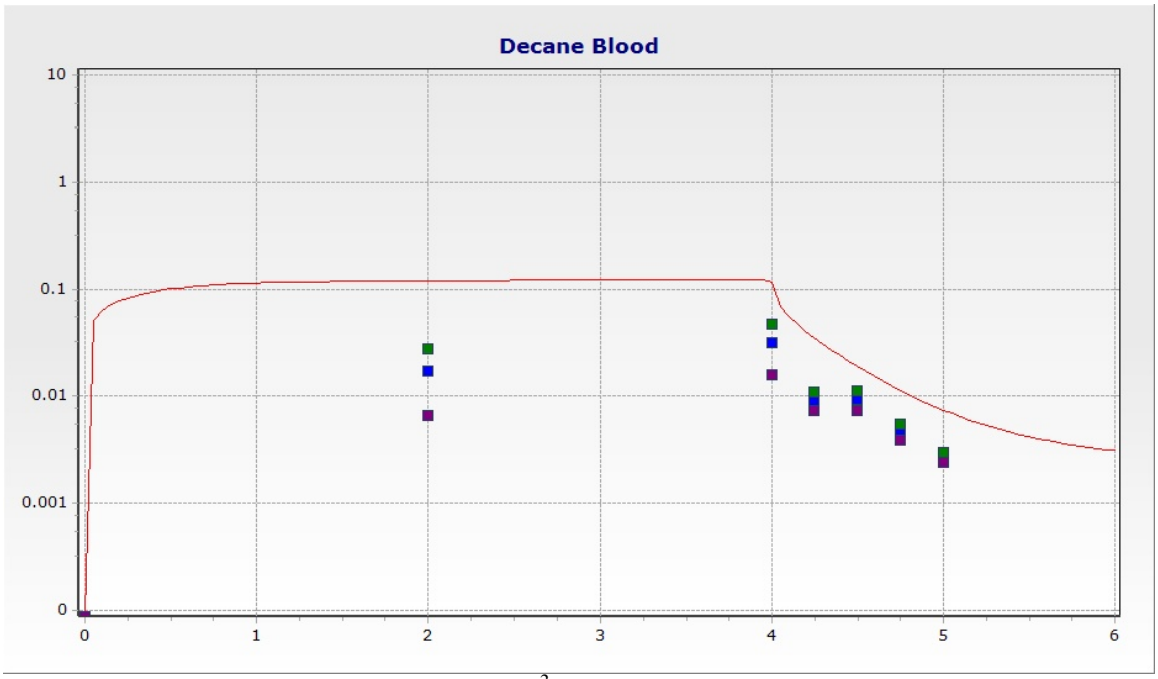

f.) Decane Aerosol S-8 Blood 1070 mg/m^3 4-hrs

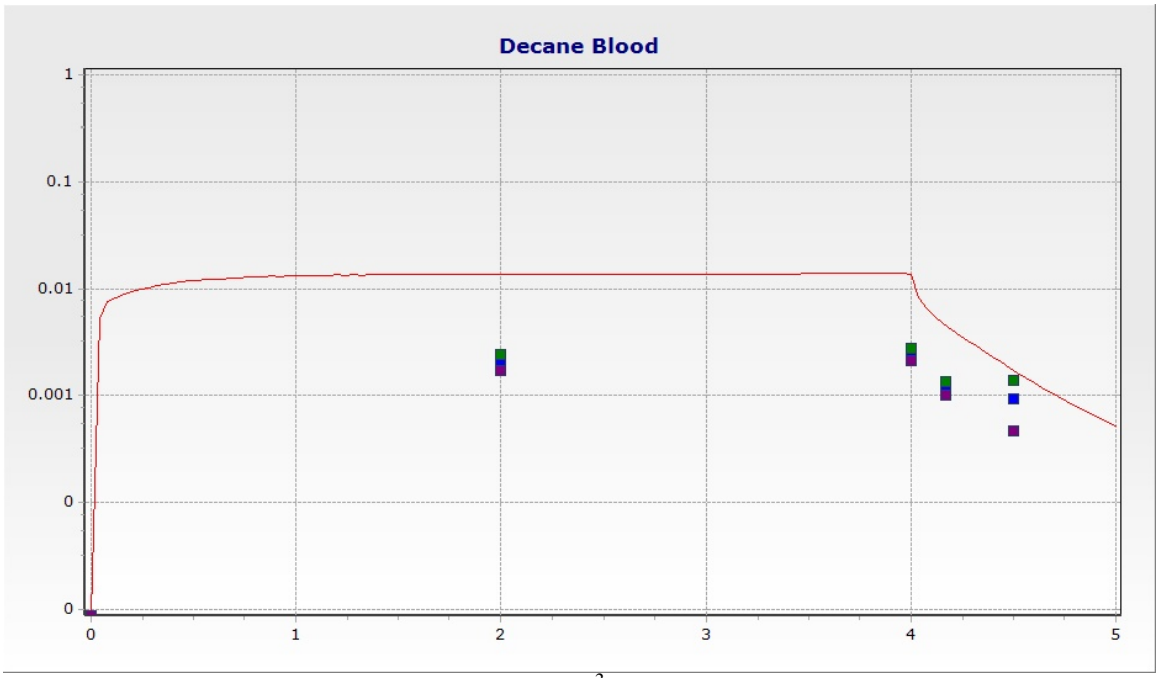

g.) Decane Aerosol JP-8:S-8 Blood 187 mg/m^3 4-hrs

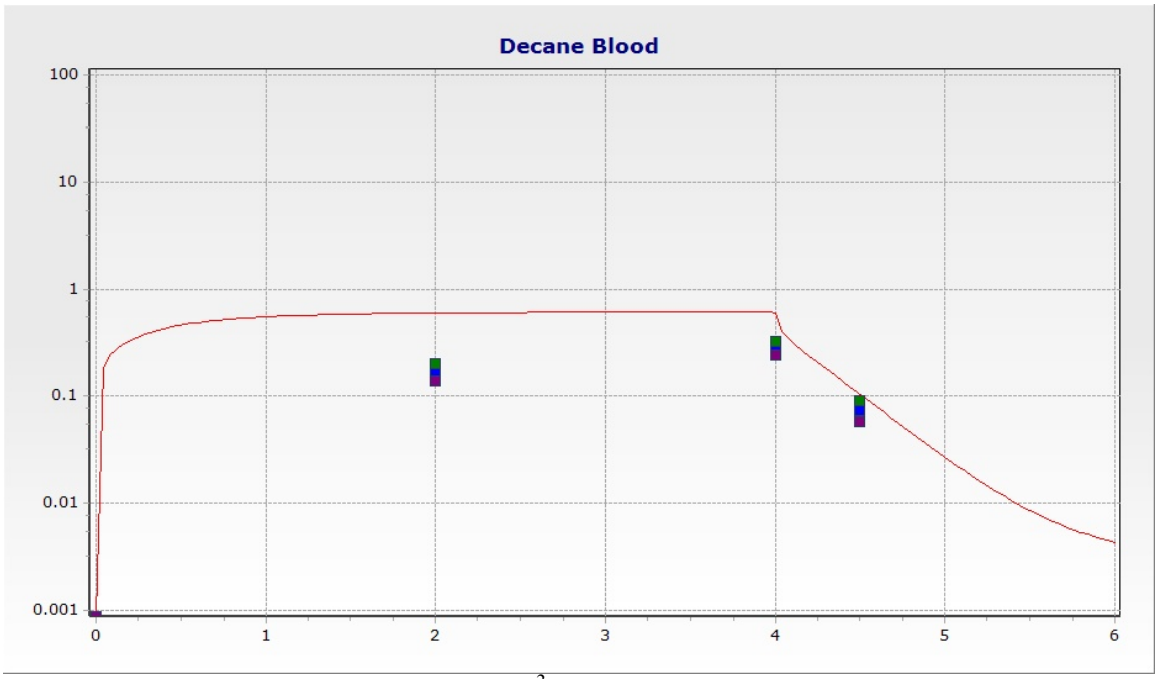

h.) Decane Vapor JP-8 Blood 2700 mg/m^3 4-hrs

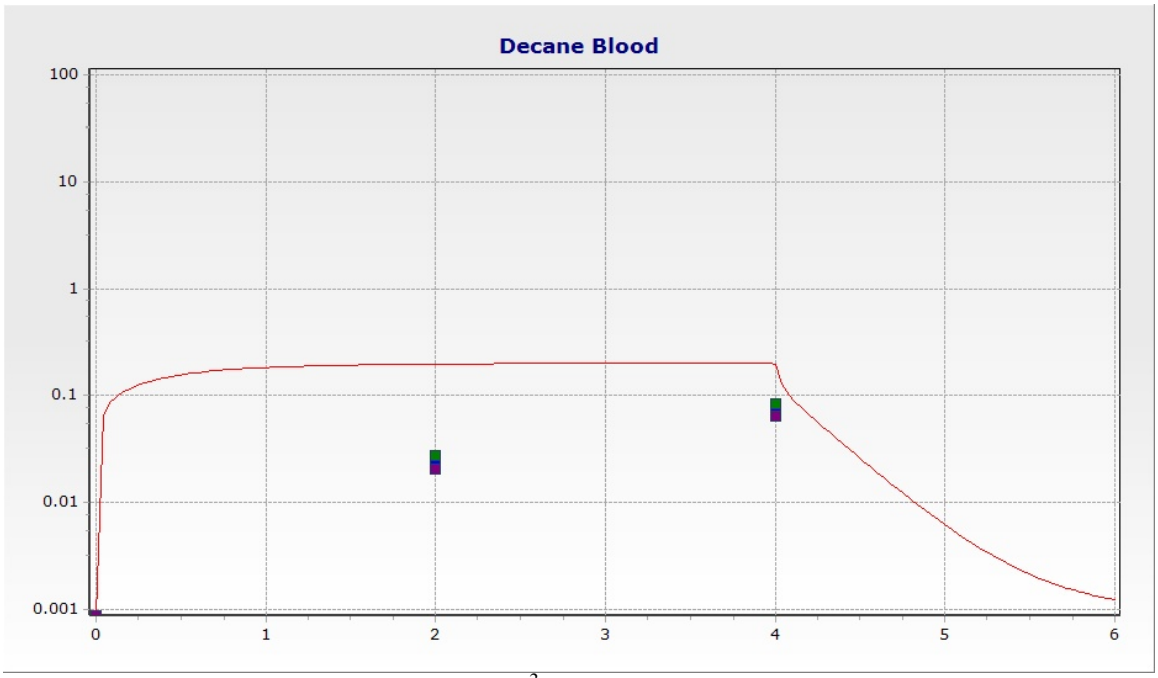

i.) Decane Vapor JP-8 Blood 1100 mg/m^3 4-hrs

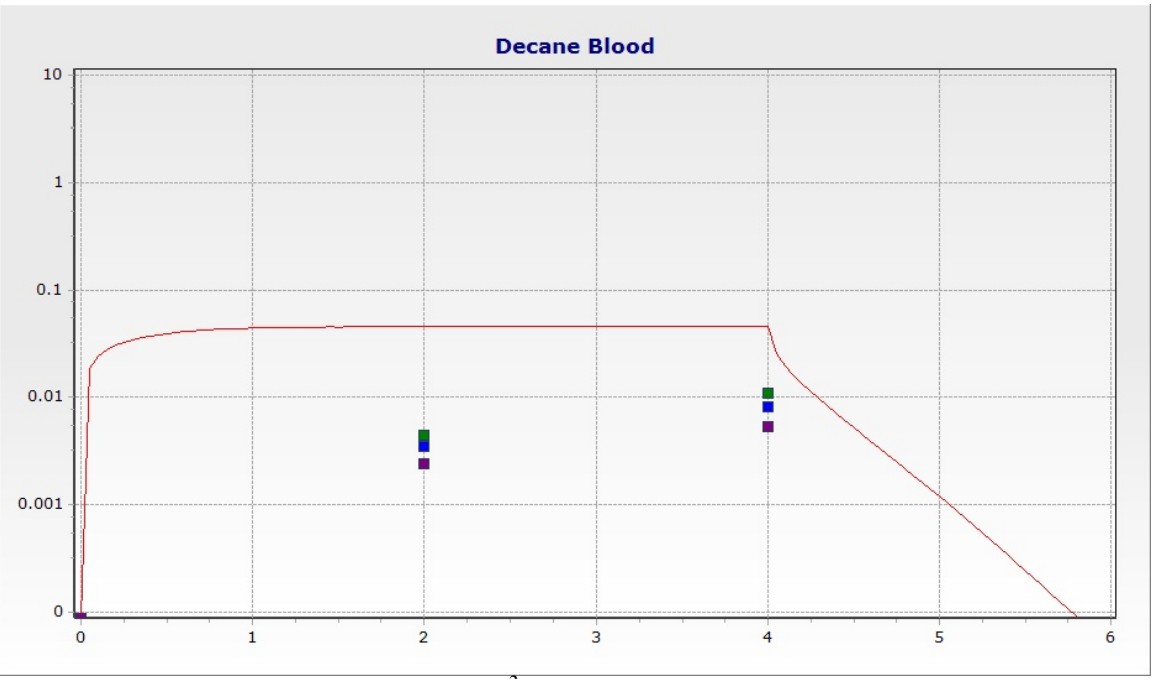

j.) Decane Vapor JP-8 Blood 400 mg/m^3 4-hrs

Figure 3.11. Model Simulations of Tetradecane (x-axis = Concentration (mg/L), y-axis = Time (hrs)

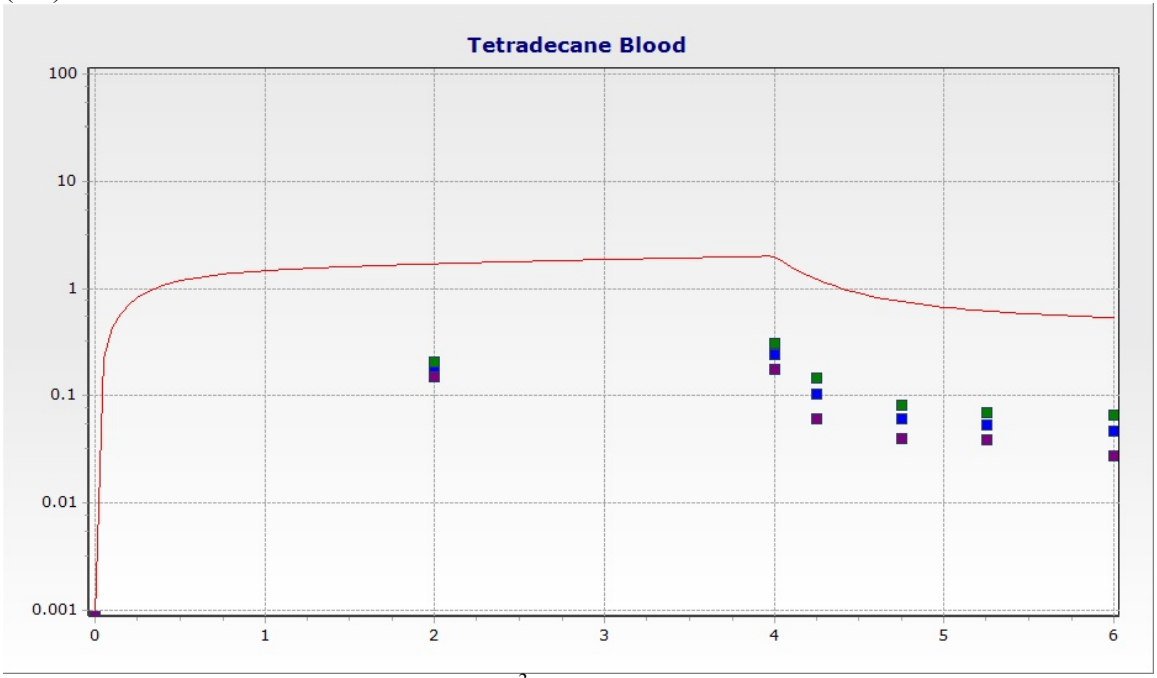

a.) Tetradecane Aerosol Blood 89 mg/m^3 4-hrs

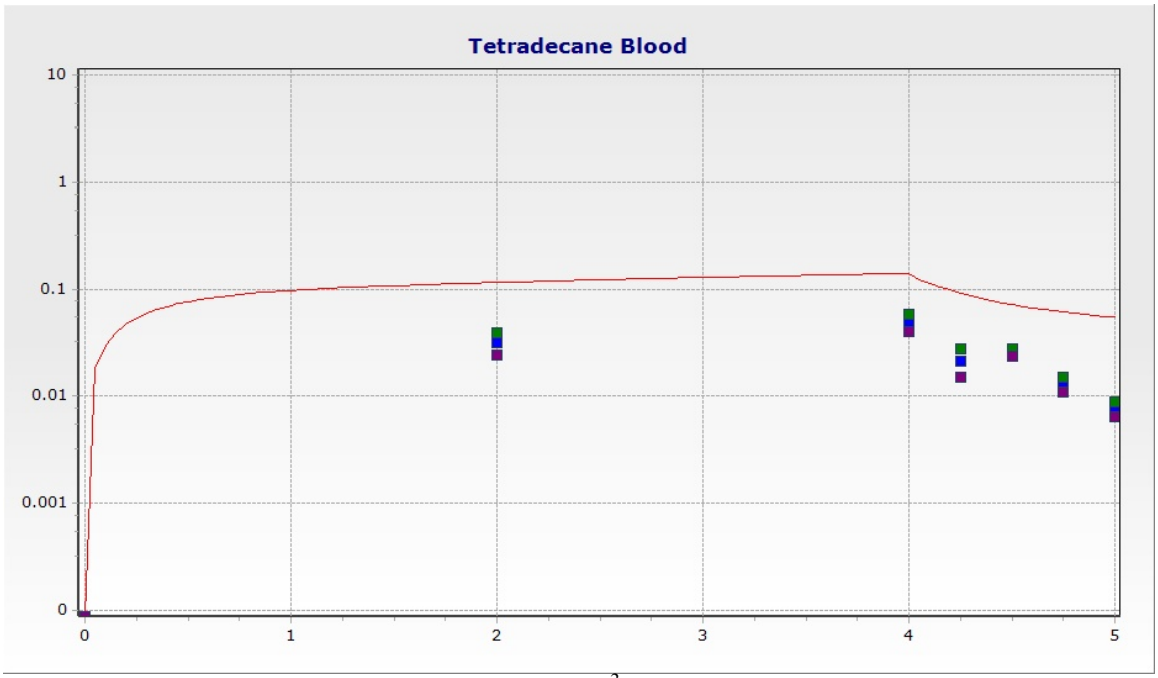

b.) Tetradecane Aerosol JP-8 Blood 908 mg/m^3 4-hrs

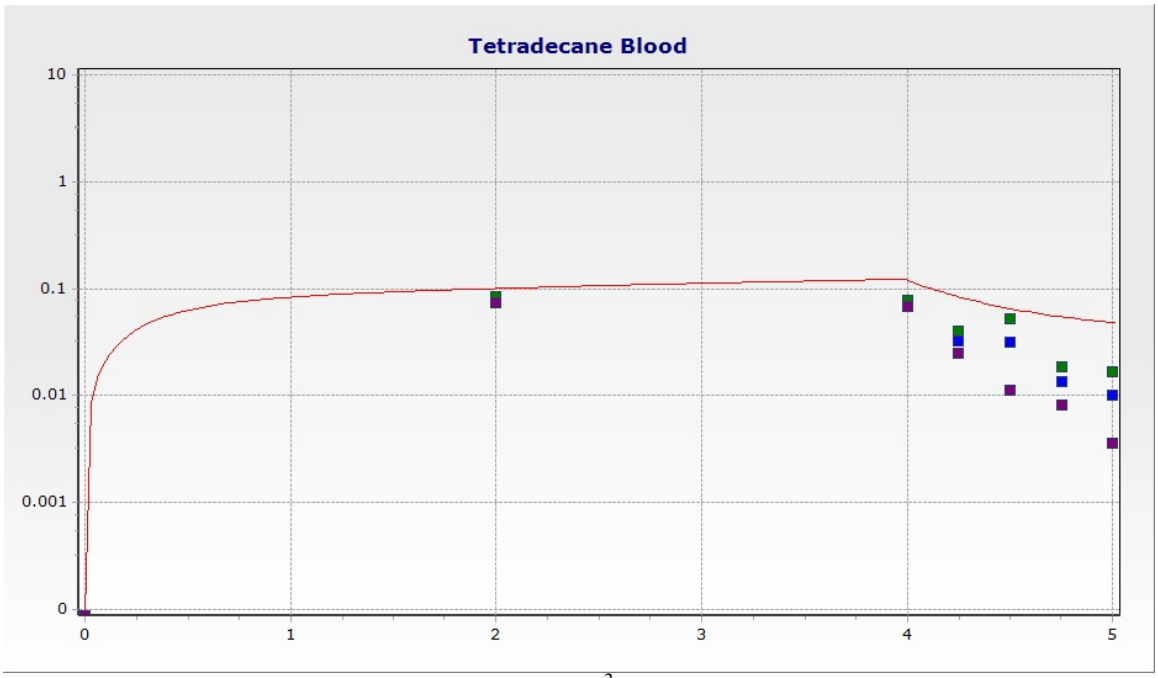

c.) Tetradecane Aerosol S-8 Blood 1070 mg/m^3 4-hrs

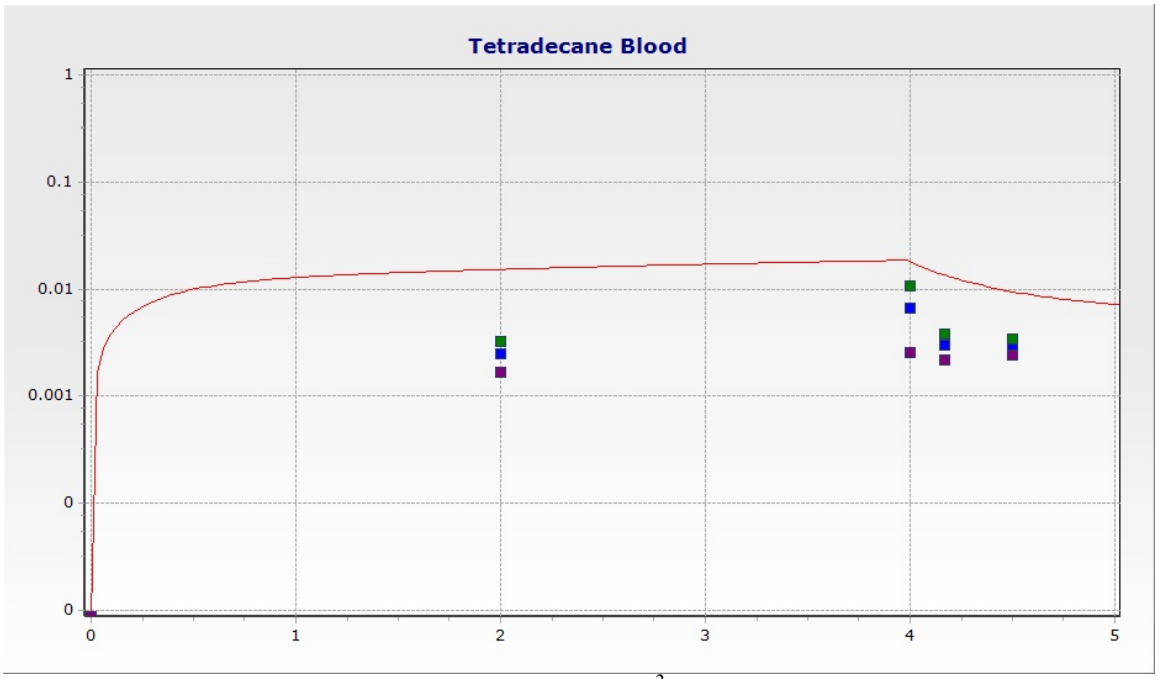

d.) Tetradecane Aerosol JP-8:S-8 Blood 187 mg/m^3 4-hrs

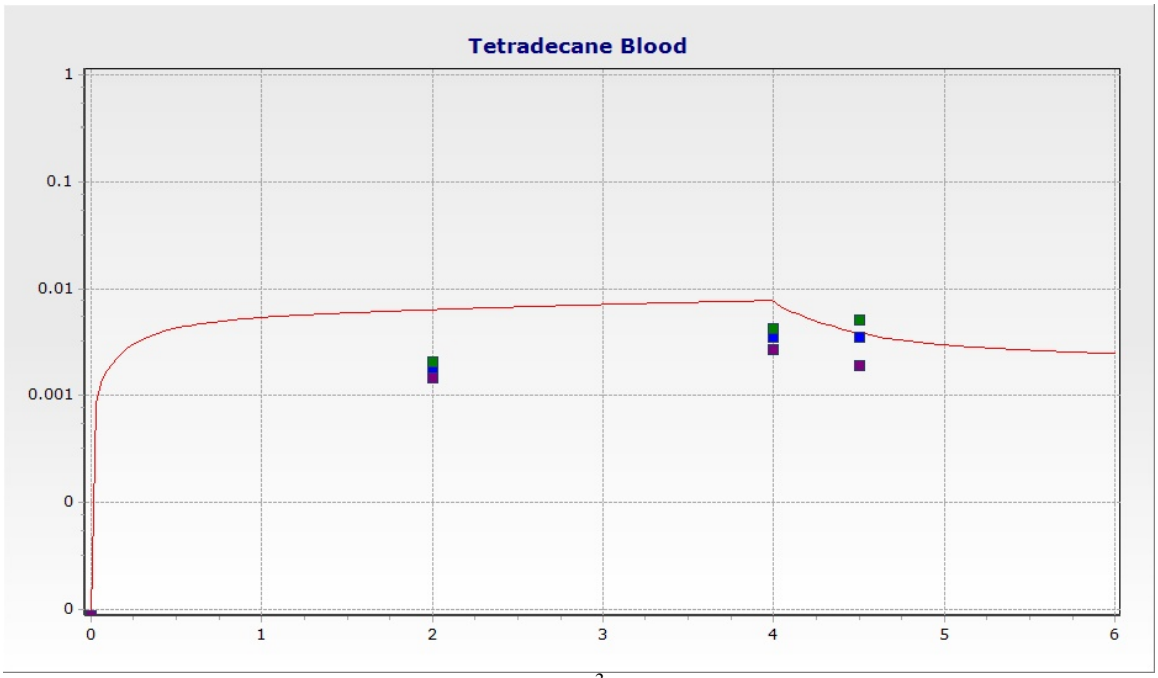

e.) Tetradecane Vapor JP-8 Blood 2700 mg/m^3 4-hrs

Figure 3.12. Application of the jet fuel model to predict White Spirit exposure (x-axis= Concentration (mg/L), y-axis = Time (hrs)

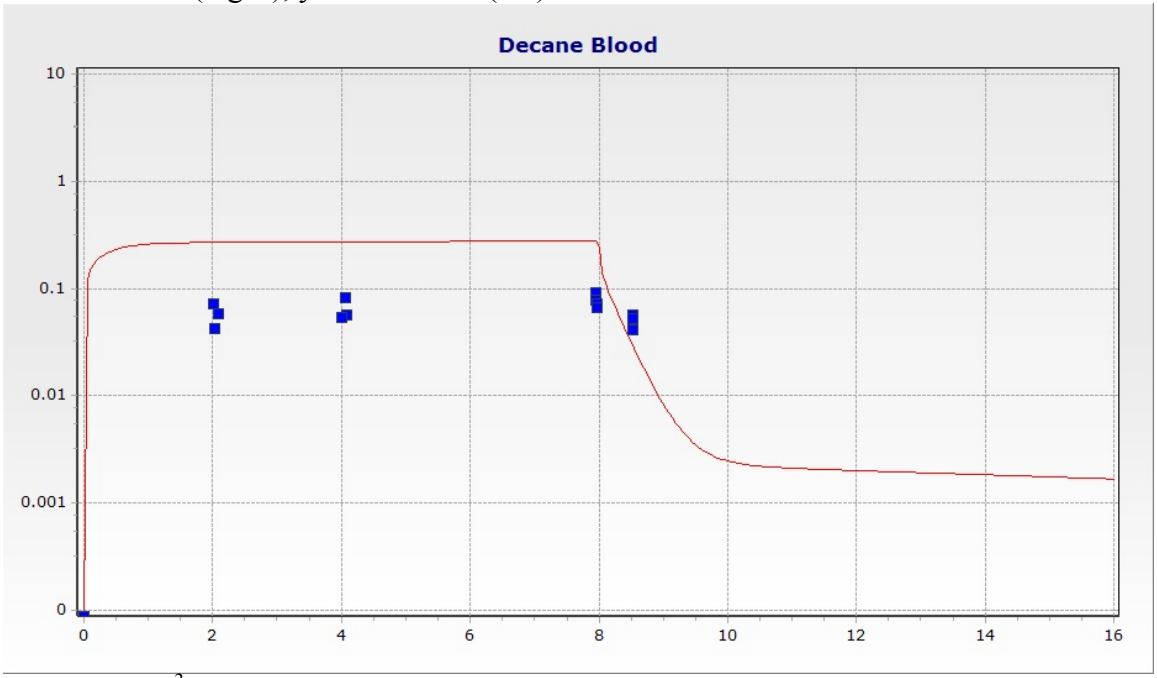

a.) 600 mg/m^3 White Spirit vapor (Hissink *et al*, 2007)

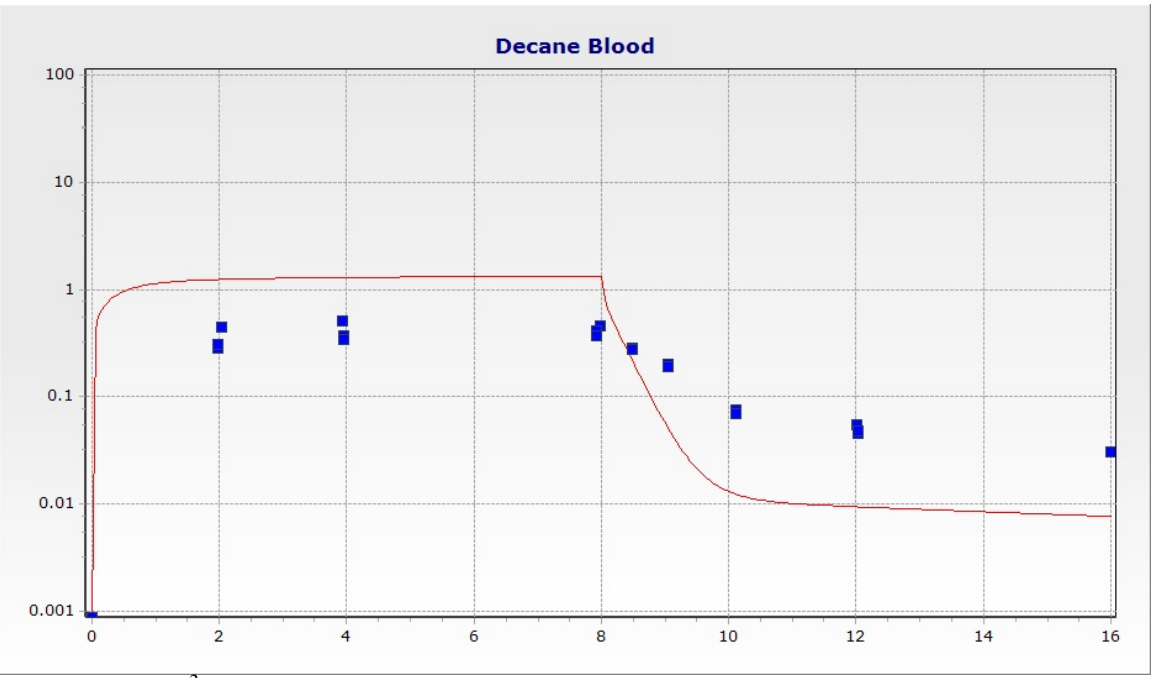

b.) 2400 mg/m^3 White Spirit vapor (Hissink *et al*, 2007)

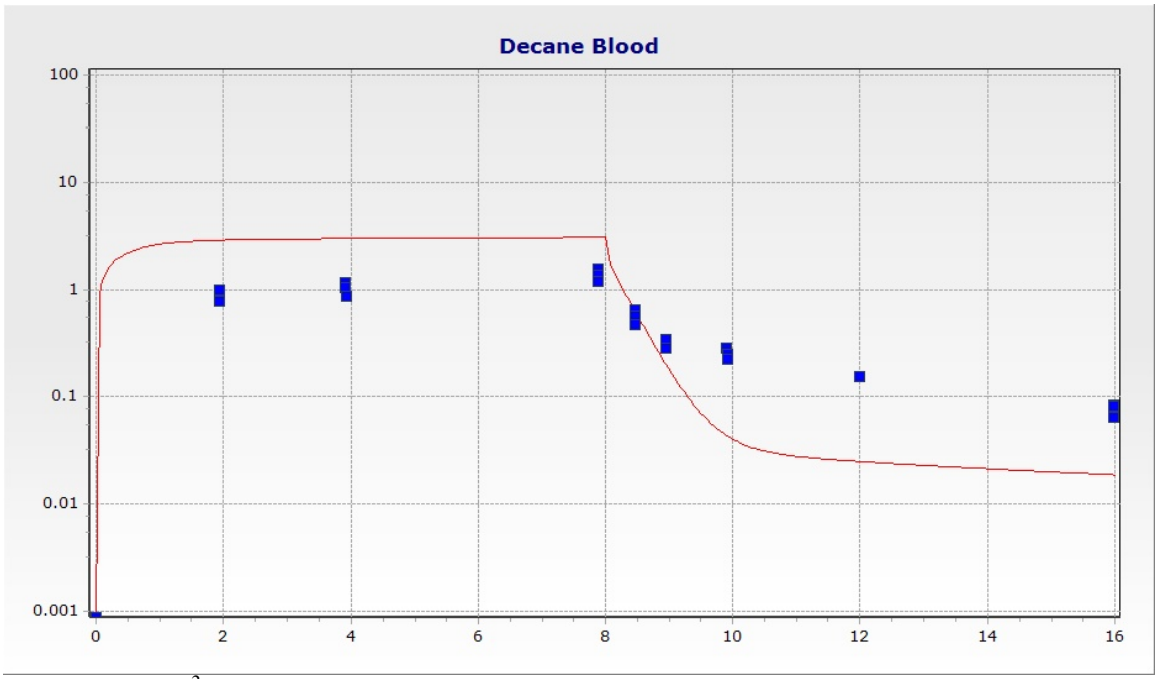

c.) 4800 mg/m^3 White Spirit vapor (Hissink *et al*, 2007)

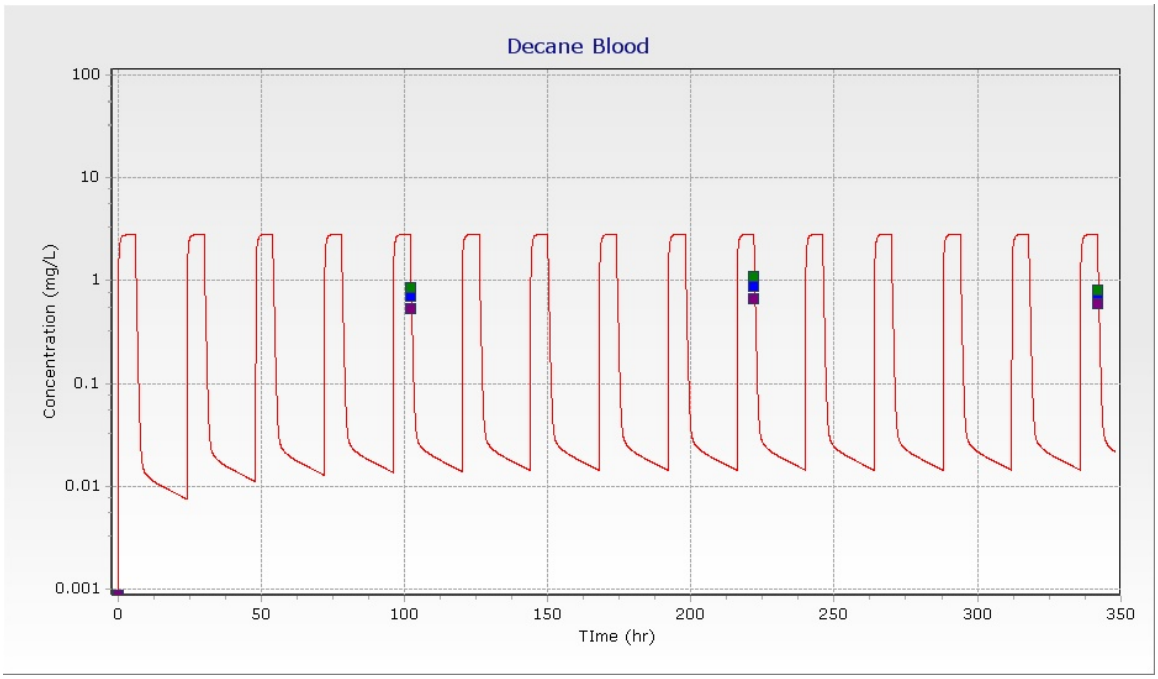

d.) 400 ppm White Spirit, Decane (Lof *et al*., 1999)

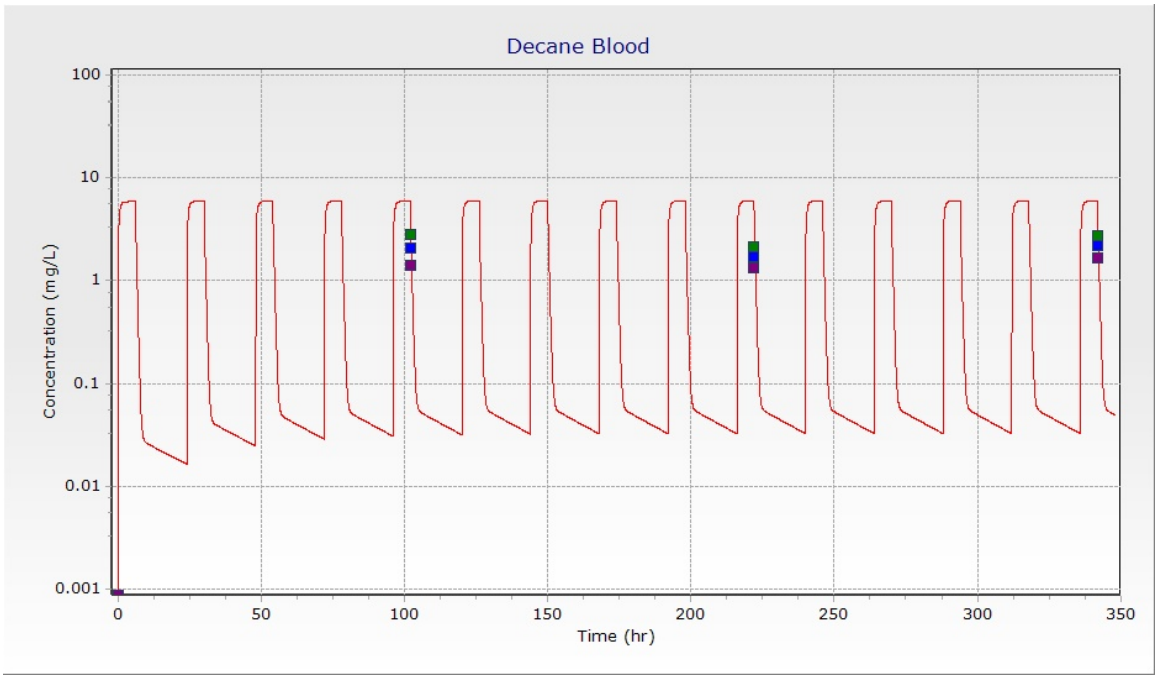

e.) 800 ppm White Spirit, Decane (Lof *et al*., 1999)

CHAPTER 4

ENVIRONMENTAL EXPOSURE OF A COMMUNITY TO AIRBORNE TRICHLOROETHYLENE

Martin S.A., Simmons M.B., Ortiz-Serrano M., Kendrick C., Gallo A., Campbell, Jr, J.L., Fisher J.W. *Arch Environ Occup Health.* 2005 Nov-Dec; 60(6):314-6. Reprinted here with permission of the publisher.

ABSTRACT

School officials and community citizens were concerned about airborne trichloroethylene (TCE) emanating from a nearby industrial facility that used TCE as a degreaser. No measurements of airborne TCE in the community were taken by public health officials or the industrial facility. Regulation of release of TCE from this facility was governed, in part, by mathematical model predictions of dispersion into the community. In support of community health concerns, a limited number of outdoor and indoor air samples were collected in the affected community for the analysis of TCE, including a school, a small business and 3 homes. The mean outdoor air concentration of TCE for all affected sites was 0.96 $\mu g/m^3$ with a peak TCE concentration of 4.59 $\mu g/m^3$. The mean indoor air concentration of TCE for all affected sites was 1.40 $\mu g/m^3$ with a peak TCE concentration of 4.66 $\mu g/m^3$. All air samples collected were below the guideline level of 5 μg TCE/m^3 of air used by the state of Georgia, USA, but were greater than large population studies of TCE in indoor and outdoor air in Minnesota, USA and Ottawa, Canada. Additional air samples are needed to better characterize exposure of the community to TCE.

INTRODUCTION

Trichloroethylene (TCE) is a chlorinated solvent used primarily as a degreaser by industry. The National Research Council of the National Academy of Sciences recently evaluated several key scientific human health issues with TCE (NRC, 2006). In the United States, TCE is recognized as a historic and widespread groundwater contaminant (NRC, 2006, Scott and Cogliano, 2000, Wu and Schaum, 2000). Airborne exposure to TCE has become a public health concern, primarily because of vapor intrusion into homes situated near contaminated soil and water (USEPA, 2001). Ambient levels of TCE in air have been reported in cities and rural areas since 1974 (Zhu *et al.*, 2005). In 2004-2005 indoor and outdoor source-

independent measurements of TCE were reported for residential settings with air concentrations ranging from 0.06 to 0.5 μg/m^3 for indoor air and 0.08 to 0.6 μg/m^3 for outdoor air (Adgate *et al.*, 2004, NRC, 2006, Sexton *et al.*, 2004, Zhu *et al.*, 2005). These studies were large population based studies involving hundreds of samplings in Minnesota, USA and Ottawa, Canada.

Unlike the population studies, this study reports on a limited number of air samples collected for analysis of TCE in a community near an industrial facility that uses TCE as a degreaser. According to the Toxic Release Inventory (TRI), this industrial facility was ranked eleventh in the United States for atmospheric release of TCE in 2004 (USEPA, 2006). The industrial facility is within 650m of a public middle school with 650 students, a small business and several homes. Some community members and school officials were concerned about health outcomes from exposure to airborne TCE. Unfortunately, no atmospheric measurements of TCE in the community or in the middle school were available. Health officials and the industrial facility officials relied on atmospheric dispersion models which predicted that the community exposure to TCE in air was likely below the level of concern (< 5 μg/m^3) (Manning, 2006). The primary purpose of this study was to determine if we could detect and quantify the concentration of TCE in air. These air sampling results could then be used by community members and school and public health officials to seek solutions for this environmental contaminant.

METHODS

Access was granted for five air sampling sites in the community near the industrial facility and one control site distant from the facility (approx. 14.5 Km) in Clark County, Georgia, USA. The community air sampling sites included a middle school, a small business, and 3 homes along with a control site at the University of Georgia. Site selection was based on

mathematical modeling projections of areas of likely contamination provided by the state regulatory body and upon permission received from property owners in the area. The 16 homes within a 1 km radius were separated into groups with 5 homes to the west, 6 homes to the south, and 5 homes to the east. Within a 2 km radius are three more neighborhoods, totaling approximately 50 homes. All sampled community sites were within 1 km of the emitting facility. The middle school, small business and one home (H2) were located east approximately 550 m, 500m, and 900m, respectively, from the facility. One home (H1) was located approximately 500 m west of the facility and another home (H3) south of the facility approximately 400 m. The resultant wind direction was from 230° (Southwest to Northeast) at average 9.25 km/h during the 2 month sampling period (USDOC, 2006).

To collect air samples, air pumps were deployed for 8 hours and TCE was trapped on charcoal tubes. For outdoor air samples, an SKC Airchek Model 224-PCXR8 low flow air pump (250 mL/min) was used with SKC 200/400 mg Anasorb CSC 226-09 charcoal tube. For indoor air samples, a Gilian Dual Mode Low Flow air pump (model LFS-113DC, 50 mL/min) was used with SKC 50/100 mg Anasorb CSC 226-01 charcoal tube. Air pumps were calibrated immediately prior to use with a Gilian Gillibrator 2. Though the facility is in operation 24 hours per day Monday through Friday, sampling was conducted one day per week throughout the two month study period (February 10 to April 5, 2006) between 8:00 AM and 5:00 PM. Five outdoor and 4 indoor samples were collected at the middle school, 2 outdoor and indoor samples at the small business and control site, and one outdoor and one indoor sample at the homes, with the exception of H1, at which 2 indoor samples were taken. For most visits both indoor and outdoor samples were collected at the same time.

In the laboratory, the samples were analyzed on an Agilent 6890N gas chromatograph (GC) equipped with a micro electron capture detector and a 7683 liquid autosampler after solvent desorption with carbon disulfide (Table 1). All samples were processed the day of sample collection. GC/mass spectroscopy was used for positive identification of TCE (Dietzel *et al.*, 2005). Charcoal from the tubes were transferred to 2 ml or 4 ml glass vials containing either 1ml or 1.5 ml of carbon disulfide, respectively, and held for 1 hour. Aliquots of the solvent containing TCE were then placed in autosampler vials for analysis. Calibration curves were generated each day that air samples were collected. The extraction efficiency for TCE removal from the charcoal was greater than 94% and the method limit of detection was 25 ng/m^3. The TCE air concentration was calculated by dividing the calculated mass of TCE extracted from the charcoal by the volume of air (m^3) metered through the charcoal tubes by the pumps.

RESULTS

TCE was detected in all of our air samplings in the community near the industrial facility and at our control site located 14.5 km distance from the facility. The lowest outdoor air concentrations of TCE (Table 2) were at our control site followed by the homes near the industrial facility. The school and small business air samples, although higher than the homes were all below the guideline concentration of 5 μg/m^3 used by the state of Georgia (Manning, 2006).

The indoor TCE air concentrations (Table 2) were similar compared to outdoor TCE concentrations for the middle school and small business (within a factor of 2.5). This was not the case for indoor air samples from two of the three homes and the control site which were

higher than the corresponding outdoor levels (47 to 155 fold greater) suggesting that indoor sources of TCE probably contributed to the indoor air TCE levels (Table 2).

The mean outdoor air concentration of TCE across all sites (±SE, n=10) and samplings was 0.96 ± 0.48 $\mu g/m^3$ with a peak value of 4.59 $\mu g/m^3$. The mean indoor air concentration of TCE across all sites (±SE, n =10) and samplings was 1.40 ± 0.47 $\mu g/m^3$ with a peak value of 4.66 $\mu g/m^3$.

DISCUSSION

Our findings demonstrate that airborne TCE is present in the community near an industrial facility that uses TCE as a degreaser. Before this study, there were no measurements of the TCE air concentrations in the community, only mathematical dispersion modeling projections. Although the number of samples was small in this study, the mean indoor and outdoor TCE concentrations were both greater in this study than those reported in large population studies in Ottawa, Canada (Zhu *et al.*, 2005) or Minnesota, USA (Adgate *et al.*, 2004, Sexton *et al.*, 2004). A more robust sampling design is needed near the industrial facility to better characterize exposure of the community to TCE.

The goal of this research project was to provide interested parties with preliminary airborne measurements of TCE that could be used to make informed public health decisions regarding the community. Public health officials, community members, middle school officials and representatives from the industrial facility were notified of our findings at a public meeting. Some community members expressed concern about their exposure to TCE. The public health solution for this community's exposure to TCE remains to be reconciled. With the recent evaluation of the health risks posed by exposure to TCE by the National Academy of

Sciences(NRC, 2006), the current exposure guideline value of 5 $\mu g/m^3$ may be reevaluated. The industrial faculty is trying to replace TCE with another cleaning product.

REFERENCES

Adgate J, Eberly L, Stroebel C, Pellizzari E, Sexton K. (2004). Personal, indoor, and outdoor VOC exposures in a probability sample of children. J Expo Anal Environ Epidemiol, 14 (Supplement 1), S4-S13.

Dietzel K, Campbell J, Bartlett M, Witten M, Fisher J. (2005). Validation of a gas chromatography/mass spectrometry method for the quantification of aerosolized Jet Propellant 8. J Chromatogr A, 1093, 11-20.

Manning R. (2006). Personal Communication. Georgia Environmental Protection Division, USA.

NRC. (2006). Assessing the Human Health Risks of Trichloroethylene: Key Scientific Issues. Committee on Human Health Risks of Trichloroethylene. http://www.nap.edu/catalog/11707.html.

Scott C, Cogliano V. (2000). Introduction, Trichloroethylene Health Risks-State of the Science. Environ Health Perspect, 108 (Supplement 2), 159-160.

Sexton K, Adgate J, Ramachandran G, Pratt G, Mongin S, Stock T, Morandi M. (2004). Comparison of personal, indoor, and outdoor exposures to hazardous air pollutants in three urban communities. Environ Sci Technol, 38, 423-430.

USDOC. 2006. National Climatic Data Center. Local Climatological Data. http://www.ncdc.noaa.gov/oa/ncdc.html.

USEPA. (2001). Trichloroethylene health risk assessment: synthesis and characterization. External review draft. EPA/600/P-01/002A. National Center for Environmental Assessment, U.S. Environmental Protection Agency. Washington, DC.

USEPA. 2006. TRI Explorer: Releases Facility Report. http://www.epa.gov/cgi-bin/broker?_SERVICE=oiaa&_PROGRAM=xp_tri.sasmacr.tristart.macro&VIEW=USFA&trilib=TRIQ0&TAB_RPT=1&sort=RE_TOLBY&FLD=E41&FLD=E51A&FLD=E51B&FLD=STONDISP&FLD=E1&FLD=E2&FLD=E3&FLD=E42&FLD=E52&FLD=E53A&FLD=E53B&FLD=E54&FLD=STOTHDIS&FLD=RELLBY&FLD=M81&FLD=M65&FLD=M64&FLD=STOFFDIS&FLD=M10&FLD=M41&FLD=M62&FLD=POTWMETL&FLD=M82&FLD=M66&FLD=M67&FLD=M73&FLD=M79&FLD=M90&FLD=M94&FLD=M99&FLD=STOTHOFF&FLD=TSFDSP&FLD=RE_TOLBY&ONDISPD=Y&OTHDISPD=Y&OFFDISPD=Y&OTHOFFD=Y&sort_fmt=2&INDUSTRY=ALL&STATE=ALL+STATES&COUNTY=All+counties&CHEMICAL=000079016&YEAR=2004&_TOP=11

Wu C, Schaum J. (2000). Assessment of Trichloroethylene Exposure, Trichloroethylene Health Risks-State of the Science. Environ Health Perspect, 108 (Supplement 2), 359-364.

Zhu J, Newhook R, Marro L, Chan C. (2005). Selected volatile organic compounds in residential air in the city of Ottawa, Canada. Environ Sci Technol, 39, 3964-3971.

Table 4.1. Analytical method for TCE analysis.

Injection Volume	1 µL
Injection Mode	Pulsed Splitless
Column Flow	2.5 mL/min (constant flow)
Column (Dimensions)	HP-5 (30 m x 0.53 mm)
Film Thickness	1.5 µm
Inlet Temperature	250°C
Oven Program:	30°C for 10 min.
	10°C/min to 70°C for 2 min.
	20°C/min to 280°C for 3.5 min.
Detector:	µ-ECD
Temperature	300°C
Makeup Gas	Nitrogen
Flow Rate	45.0 ml/min

Table 4.2. Individual measured concentrations of TCE in community outdoor and indoor air, except for the middle school which represents the mean ± SE.

School	Business	Home, H1	Home, H2	Home, H3	Control
TCE Concentration in Outdoor Air (µg/m^3)					
0.72 ± 0.46	4.59, 1.30	0.03	0.05	0.03	0.01, 0.01
TCE Concentration in Indoor Air (µg/m^3)					
0.92 ± 0.68	1.85, 0.59	1.62, 1.41	0.21	4.66	0.99, 1.02

CHAPTER 5

CONCLUSIONS: STATE OF THE SCIENCE AND GOALS FOR THE FUTURE

Complex hydrocarbon mixtures such as jet fuel, gasoline, and white spirit have the potential for a broad range of health effects. In particular, jet fuels represent a potential source of toxicity for both military and civilian flightline personnel (NRC, 2003). That exposures in the literature have been in both aerosolized and vaporized form, complicates assessments of the pharmacokinetics of the likely causative agents of this toxicity. Additionally, detailed investigation of exposure atmosphere characteristics and tissue pharmacokinetics is lacking in the literature.

Existing PBPK models for exposure to individual chemical vapors are present in the literature for several aromatic hydrocarbons such as ethylbenzene, toluene, m- and o-xylene, and benzene (Haddad *et al.*, 1999, Tardif and Charest-Tardif, 1999, Tardif *et al.*, 1997). Alternatively, there are few models for n-alkanes or other aliphatics (Merrill *et al.*, 2008, Perleberg *et al.*, 2004). Simple mixtures of various concentrations of 2 to 4 constituents have been constructed to test hypotheses surrounding types of metabolic interactions. As the majority of constituents of jet fuel share a common metabolizing enzyme, the most likely hypothesis of competitive inhibition has been reported and supported in work with these simple mixtures (Haddad *et al.*, 1999). The observable result of this inhibition would be an increase in the blood or tissue concentrations of the parent chemical. This may have implications for toxicity of parent chemicals or metabolites of concern.

Limited tissue data has been published for white spirits and jet fuel (Campbell Jr and Fisher, 2007, Hissink *et al.*, 2007). Gas-uptake chamber loss data has been reported for gasoline

(Dennison *et al.*, 2003). Using new and existing datasets PBPK models were reported for constituents of white spirit and jet fuel vapors. However, no one has previously investigated pharmacokinetics associated with the aerosol phase. Development of a PBPK model for vaporized and aerosolized jet fuels represents the next step in complex hydrocarbon mixture modeling and has implications for health risk assessments.

Chapter 2

A nose-only inhalation exposure system was designed and characterized to support PBPK model development. The atmospheric characterization data of aerosolized JP-8, S-8, and the 50:50 JP-8:S-8 blend are the first reported for these complex mixtures. This assessment of the dynamic aerosol and vapor atmosphere within the exposure chamber represents the most detailed description of air-phase chemical profiles to be reported in the fuel literature. Additionally, as very limited chamber characterization data has been reported with the published toxicity studies, it was a watershed moment in the understanding of aerosolized fuel chemistry and informed several aspects of PBPK model development that followed.

As droplets pass through an inhalation exposure chamber they evolve under the influence of the Kelvin effect. Volatile constituents evaporate from the droplet surface, resulting in a droplet with higher concentrations of chemicals with lower vapor pressure, compared to what was lost. Just as a vapor exposure atmosphere (depending on generation system) is not always representative of total fuel exposure, assessment of the kinetics of only the aerosol droplet would have a similar barrier to applicability. In order to fully understand the kinetics of jet fuel, one must account for both the aerosol and the vapor fraction in the chamber and in a PBPK model.

Chapter 3

The exposures and tissue time-course data collected for n-tetradecane and n-octane are the most detailed to be reported for these hydrocarbons. n-Decane exposure has been previously described in individual vapor and mixture studies (white spirit), but not in aerosolized jet fuels (Merrill *et al.*, 2008, Perleberg *et al.*, 2004). As it would not be possible to describe the kinetics of every constituent of a complex mixture, simplifications must be made. By tracking individual chemical "markers" that are representative of the major fuel constituents it is possible to approximate the kinetics of the whole fuel. Tetradecane represents a high molecular weight marker of the aerosolized, and to a lesser extent vaporized, exposure atmosphere. Octane is a mid-range n-alkane present at approximately equal levels in both aerosol and vapor-phase. n-Decane represents one of the largest percentage constituents of the fuel in both aerosol and vapor phase and is positioned in the middle of spectrum of fuel constituents. These three n-alkanes cover the breadth of the aliphatic content of JP-8 and S-8. The aromatics m-xylene, ethylbenzene, and toluene have been previously tracked either as individual constituents or in mixtures. They are also noted toxicants with influence on the kinetics of other fuel constituents. By tracking these aromatic and aliphatic constituents and designing "lumped" groups of the unquantified constituents a PBPK modeling based description of fuel kinetics can be created.

The fuel model describes the dynamic air phase kinetics within the rat respiratory tract, using a combination of chamber analytical data and predictions from aerosol dosimetry modeling software. Within model code all aspects of the aerosol and vapor phase chemical concentrations, and the predicted aerosol deposition fractions, were coded to interact simultaneously. Due to the inclusion of multiple model structures within the base model code, the chemical concentration of aerosol and/or vapor was directed toward either a single hydrocarbon model structure or into the

fuel model where it is combined with other fuel constituents. By coding the model in this manner, the ability to input defined chemical parameters from a vaporized or aerosolized gasoline, white spirit, or diesel exposure, in addition to jet fuel, becomes apparent. This cross-mixture applicability separates the current fuel model from earlier works with simple binary through quaternary mixtures. The model's lumping strategy and description of competitive metabolic inhibition on a scale not previously reported in the literature are also novel and set this work apart from other PBPK models. Future applications in risk assessment for fuels and other complex mixtures are envisioned.

Chapter 4

Trichloroethylene (TCE), a solvent emitted from a metal degreasing facility, was being emitted into the air of a community surrounding the facility. Within the community were several homes, and elementary school, stores, and other industrial facilities. Community members were concerned that levels of TCE were in excess of the state guideline value and could represent a threat to the health of children and community members. Air samples were collected on charcoal sorbent tubes and analyzed. Ambient and indoor concentrations were below the guideline value.

Air sampling and analytical skills were obtained in this work. These skills informed the student's development and sampling of the inhalation exposure chamber that supported the PBPK modeling work described. This project was the basis for the data collected and models completed.

Conclusion

As there are currently no models to assess dosimetry and pharmacokinetics of inhaled aerosolized jet fuel, we sought to meet this need in the toxicology and fuel mixture communities. The effort that followed was long and extremely time consuming, but the goals were met and will impact risk assessments for US military personnel. Over the course of this work several milestones were achieved. An inhalation exposure system was designed, characterized, and utilized. The most detailed assessment of aerosolized fuel exposure atmospheres was conducted and published. Tissue data was collected from rats exposed to individual hydrocarbons, simple mixtures, and jet fuels. Finally, a PBPK model for jet fuel was developed and utilized to predict pharmacokinetic data from both vaporized and aerosolized jet fuel exposure in the rat. The model was then extrapolated to another commonly used hydrocarbon mixture, white spirit.

STATE OF THE SCIENCE

While PBPK models have been developed to describe exposure to individual chemicals, simple mixtures, and a small number of complex mixtures, the study of mixture pharmacokinetics remains in its infancy. Considering the myriad exposures that humans are exposed to each moment, investigation of the kinetics and interactions between pharmaceuticals, endogenous chemicals, and xenobiotics represents an area of high relevance for our understanding of the complex pharmaco/toxicokinetic and dynamic processes occurring within mammals. Through the use of computational mixture models researchers have started to de-mystify processes governing metabolic interactions between mixture constituents or tissue specific induction of genetic or cytotoxic damage. At present, models for inhalation exposure have progressed to the level of regionally specific tissue doses associated with observable

responses. As examples, models for inhalation have provided detailed descriptions of respiratory tract tissue doses following exposure to reactive vapors or particles, as well as assessment of metabolic interactions at a common metabolic enzyme (Bogdanffy and Sarangapani, 2003, Campbell Jr and Fisher, 2007, Frederick *et al.*, 2001). The increased cross-talk and influence of computational fluid dynamics in the area of PBPK modeling for inhalation exposures is a step forward in the understanding of vapors, liquid droplets, and solid aerosol particles.

FUTURE DIRECTIONS

To address the kinetic profiles of constituents of complex hydrocarbon mixtures, including assessment of metabolic interactions, greater insight into the generation of biomarkers of exposure is needed, as well as more detailed characterization of exposure atmospheres of inhaled complex hydrocarbon mixtures in chambers and in the respiratory tract. Recent advances in the understanding of aerosol and vapor dosimetry, with investigation of localized cell specific toxicity in the respiratory tract, facilitate quantitative assessments of tissue dosimetry using PBPK models. Our understanding of the tissue dosimetry and resulting systemic disposition of jet fuels and individual hydrocarbons add to this body of work, describing the site of exposure and accounting for total fuel exposure through chemical lumping.

Metabolic interactions of fuel constituents may lead to modified toxicokinetic behavior of specific agents such as benzene, hexane, and others. Prior to this work there had been only a few complex hydrocarbon mixture assessments with regard to metabolic interactions. In the case of benzene, n-hexane, and naphthalene, where the metabolite is the toxic moiety, competitive inhibition reduces the production of the metabolite. However, with toluene the parent is the toxicant and inhibition of metabolism may promote toxicity.

For the future, it is hoped that the importance of characterization of exposure atmosphere composition will be more widely recognized. Without detailed information on the chamber constituents and vapor/aerosol phase profiles it would not have been possible to develop the PBPK models covered in this dissertation. An understanding of the constituents, their droplet size distributions, and percent contribution to the aerosol and vapor phase atmospheres is also required in order incorporate computational fluid dynamics in PBPK model development. In order to address the relevance of aerosol exposure and its effects on flightline personnel more work needs to be done with these workers. PBPK models for mixtures should continue to increase in number as more is learned about exposure profiles for different mixtures and tissue kinetic data becomes available. With renewed interest in biofuels from synthetic, biomass, and agricultural sources an additional layer of complexity will be added to modeling these mixtures based on the blend constituents. As the technology associated with computational software and analytical equipment continues to advance at a rapid pace, the future of computational modeling is wide open.

REFERENCES

Bogdanffy MS, Sarangapani R. (2003). Physiologically-based kinetic modeling of vapours toxic to the respiratory tract. Toxicol Lett, 138, 103-117.

Campbell Jr J, Fisher J. (2007). A PBPK modeling assessment of the competitive metabolic interactions of JP-8 vapor with two constituents, m-xylene and ethylbenzene. Inhalation Toxicol, 19, 265-273.

Dennison J, Andersen M, Yang R. (2003). Characterization of the pharmacokinetics of gasoline using PBPK modeling with a complex mixtures chemical lumping approach. Inhalation Toxicol, 15, 961-986.

Frederick C, Gentry P, Bush M, Lomax L, Black K, Finch L, Kimbell J, Morgan K, Subramaniam R, Morris J, Ultman J. (2001). A Hybrid Computational Fluid Dynamics and Physiologically Based Pharmacokinetic Model for Comparison of Predicted Tissue Concentrations of Acrylic Acid and Other Vapors in the Rat and Human Nasal Cavities Following Inhalation Exposure. Inhalation Toxicol, 13, 359-376. doi:10.1080/08958370117942.

Haddad S, Tardif R, Charest-Tardif G, Krishnan K. (1999). Physiological modeling of the toxicokinetic interactions in a quaternary mixture of aromatic hydrocarbons. Toxicol Appl Pharmacol, 161, 249-257.

Hissink A, Krüse J, Kulig B, Verwei M, Muijser H, Salmon F, Leenheers L, Owen D, Lammers J, Freidig A. (2007). Model studies for evaluating the neurobehavioral effects of complex hydrocarbon solvents III. PBPK modeling of white spirit constituents as a tool for integrating animal and human test data. Neurotoxicology, 28, 751-760.

Merrill E, Gearhart J, Sterner T, Robinson P. (2008). Improved Predictive Model for n-Decane Kinetics Across Species, as a Component of Hydrocarbon Mixtures. Inhalation Toxicol, 20, 851-863.

NRC. (2003). Toxicologic Assessment of Jet-Propulsion Fuel 8. National Research Council of the National Academies. Washington, DC. The National Academies Press.

Perleberg U, Keys D, Fisher J. (2004). Development of a physiologically based pharmacokinetic model for decane, a constituent of jet propellent-8. Inhalation Toxicol, 16, 771-783.

Tardif R, Charest-Tardif G, Brodeur J, Krishnan K. (1997). Physiologically based pharmacokinetic modeling of a ternary mixture of alkyl benzenes in rats and humans. Toxicol Appl Pharmacol, 144, 120-134.

Tardif R, Charest-Tardif G. (1999). The importance of measured end-points in demonstrating the occurrence of interactions: A case study with methylchloroform and m-xylene. Toxicol Sci, 49, 312.

APPENDIX A. JP-8 MODEL (.CSL CODE)

```
PROGRAM
! PBPK MODEL FOR EXPOSURE TO JP-8 AEROSOL AND VAPOR
! Sheppard A. Martin, Raphael T. Tremblay, Jeffrey W. Fisher
! M-Files contain code for Exposure Concentration, Metabolism, specific Partition Coefficients and PA Terms %Aerosol and Vapor
for exposures to fuel concentrations and white spirits in literature

        INITIAL

!----------------------[BODY WEIGHT]-------------------------------------------
CONSTANT BW   = 0.21                        ! body weight of rat, Kg

!-----------------------[BLOOD FLOWS]------------------------------------------
CONSTANT QCC= 15.6            ! cardiac output for rat, L/hr/kg bw  (Clewell et al.,, 2001)
CONSTANT QPC = 15.6           !  Ventilation Rate, l/hr/kg bw
CONSTANT QLC= 0.174           ! fraction of cardiac out that perfuses the liver,  (Brown et al., 1997), L/hr
CONSTANT QBrC = 0.02          ! fraction cardiac output to brain (Delp, et al.,, 1998)
CONSTANT QLuC = 1             ! cardiac output to lung
CONSTANT QFC = 0.07           ! Fat (Delp, et al.,, 1998)
CONSTANT QNoC = 0.007         ! Nasal blood flow (Csanady et al.,, 2006)
CONSTANT QTbC= 0.01           ! Tracheobronchial blood flow (Csanady et al.,, 2006)

!----------------------[TISSUE VOLUMES]----------------------------------------
CONSTANT VFC = 0.0867             ! fraction of BW, Fat (Schoeffner, et al.,, 1999), L/kg
CONSTANT VLC = 0.0397             ! fraction of BW, liver (Schoeffner, et al.,, 1999)
CONSTANT VBrC = 0.0076            ! brain (Schoeffner, et al.,, 1999)
CONSTANT VLuC = 0.0047            ! lung (Perleberg et al., 2005) L/kg
CONSTANT VnasmuclayerC = 2.9e-5 ! nasal mucous (Parent et al, 1992)
CONSTANT VtbmuclayerC = 2.69e-4 ! lung and tb lining fluid layer (Parent et al, 1992)
```

```
!----------------------[BLOOD VOLUMES]--------------------------------------
CONSTANT Bvfc  = 0.05            ! blood volume percent of fat, (Brown, 1997)
CONSTANT Bvbrc = 0.03            ! blood volume percent of brain, (Brown, 1997)
CONSTANT Bvlc  = 0.21            ! blood volume percent of liver (Brown, 1997)

!-------------------------[PARTITION COEFFICIENTS]-----------------------------------------------------

!C8 PC, Tissue:air, divide by blood:air PC
CONSTANT PLAc8  = 6.01           ! Liver:Air PC (Smith et al., 2005)
CONSTANT PFAc8  = 771.9          ! Fat:Air PC (Smith et al., 2005)
CONSTANT PBrAc8 =4.38            ! Brain:air PC  (Smith et al., 2005)
CONSTANT PSAc8  = 2.96           ! Slowly perfused tissue:air PC (Smith et al., 2005)
CONSTANT PRAc8  = 6.01           ! Rapidly perfused tissue air PC (set to liver)
CONSTANT PLuAc8 = 6.01           ! Lung:air PC (set to liver)
CONSTANT PBc8     = 3.13         ! Blood:air partition coefficient PC (Smith et al., 2005)
CONSTANT PNoac8  = 6.01          ! Nasal PC (set to liver)

!C10 Tissue:air, divide by blood:air PC
CONSTANT PLA = 16                ! Liver:air (Smith et al., 2005)
CONSTANT PFA =   2668            ! Fat:air (Smith et al., 2005)
CONSTANT PBRA = 39               ! Brain:air (Smith et al., 2005)
CONSTANT PSA = 6.92              ! Slowly perfused:air (Smith et al., 2005)
CONSTANT PRA = 16                ! Rapidly perfused:air, set to liver
CONSTANT PLUA = 16               ! Lung :air, set to liver
CONSTANT PB      = 8.13          !  Blood:air  (Smith et al., 2005)
CONSTANT PNOA = 16               ! Nasal:air, set to liver

!Tetradecane Distribution Ratios Distribution Ratios, Do Not divide by blood:air
CONSTANT PLAC14= 0.29            ! Liver Distribution Ratio
CONSTANT PFAC14 = 48.75          ! Fat Distribution Ratio
CONSTANT PBrAC14  =0.08          ! Brain Distribution Ratio
CONSTANT PSAC14 = 0.29           ! Slowly perfused tissue Distribution Ratio, set to liver
CONSTANT PRAC14 = 0.29           ! Rapidly perfused tissue Distribution Ratio, set to liver
```

```
CONSTANT PLuAC14= 13          ! Lung Distribution Ratio
CONSTANT PBC14   = 52.4       ! Blood :air partition coefficient (Smith et al., 2005)
CONSTANT PNoaC14  = 13        ! Nasal Distribution Ratio (set to lung)

!Partition Coefficients (Lumped Aromate component of Fuel vapor) divide by blood:air PC
CONSTANT   PWBlp =  36.7      ! Blood:air PC (Campbell and Fisher, 2007)
CONSTANT   PLlp  =  2.89      ! Liver:blood PC (Campbell and Fisher, 2007)
CONSTANT   PFlp  =  46.4      ! Fat:blood PC (Campbell and Fisher, 2007)
CONSTANT   PBrlp =   2.52     ! Brain tissue/blood PC (Campbell and Fisher, 2007)
CONSTANT   PSlp  =  1.34      ! Slowly perfused tissue:blood PC (set to liver)
CONSTANT   PRlp  =  2.89      ! Rapidly perfused tissue:blood PC (set to liver)
CONSTANT   Plulp=  2.89       ! Lung PC (set to liver)
CONSTANT   Pnolp=   2.89      ! Nasal PC (set to liver)

!Lump 2 PC, based on reported avg C8-C12 Tissue:air, divide by blood:air PC
CONSTANT PLALUMP  = 21.986   ! Liver:Air PC, average C8-C12 (Smith et al., 2005)
CONSTANT PFALUMP  = 6461.9   ! Fat:Air PC, average C8-C12 (Smith et al., 2005)
CONSTANT PBrALUMP =117.248 ! Brain:air PC, average C8-C12 (Smith et al., 2005)
CONSTANT PSALUMP   = 11.91    ! Slowly perfused tissue/air, muscle, average C8-C12 (Smith et al., 2005)
CONSTANT PRALUMP   = 21.986  ! Rapidly perfused tissue air, muscle, average C8-C12 (Smith et al., 2005)
CONSTANT PLuALUMP = 21.986  ! Lung partition coefficient, set to liver
CONSTANT PBLUMP      = 12.408 ! Blood/air partition coefficient (Smith et al., 2005)
CONSTANT PNoaLUMP  = 21.986 ! Nasal partition, set to liver

!Partition Coefficients (LUMP3) Distribution Ratios, Do not divide by blood:air
CONSTANT PLALUMP3     = 0.49   ! Liver
CONSTANT PFALUMP3     = 57.2   ! Fat
CONSTANT PBrALUMP3  =0.18     ! Brain
CONSTANT PSALUMP3     = 0.49   ! Slowly perfused tissue (set to liver)
CONSTANT PRALUMP3     = 0.49   ! Rapidly perfused tissue (set to liver)
CONSTANT PLuALUMP3  = 28.4    ! Lung
CONSTANT PBLUMP3      = 52.4    ! Blood:air partition coefficient (Smith et al., 2005)
CONSTANT PNoaLUMP3  = 28.4    ! Nasal
```

```
! m-Xylene Partition Coefficients, Tissue :Blood Already, do not divide by blood :air
CONSTANT   PWBmx =  46.0        ! Blood:air PC (Campbell and Fisher, 2007; Tardif et al., 1997)
CONSTANT   PLmx  =   1.976      ! Liver:blood partition coefficient (Campbell and Fisher, 2007; Tardif et al., 1997)
CONSTANT   PFmx  = 40.41        ! Fat :blood partition coefficient (Campbell and Fisher, 2007; Tardif et al., 1997)
CONSTANT   PBmx = 0.80          ! Brain tissue:blood partition (Campbell and Fisher, 2007)
CONSTANT   PSmx  =  0.911       ! Slowly perfused tissue :blood  partition (Campbell and Fisher, 2007; Tardif et al., 1997)
CONSTANT   PRmx  =  1.976       ! Rapidly perfused tissue:blood  partition (Campbell and Fisher, 2007; Tardif et al., 1997)
CONSTANT   plumx2008=1.976      ! Lung PC (set to liver)
CONSTANT   pnomx2008=1.976      ! Nasal PC (set to liver)

!Ethylbenzene Partition Coefficients, Tissue :Blood Already, do not divide by blood :air
CONSTANT   PWBebz =  42.7       ! Blood:air partition coefficient (Campbell and Fisher, 2007; Tardif et al., 1997)
CONSTANT   PLebz  =   1.96      ! Liver:blood partition coefficient (Campbell and Fisher, 2007; Tardif et al., 1997)
CONSTANT   PFebz  = 36.4        ! Fat:blood partition coefficient (Campbell and Fisher, 2007; Tardif et al., 1997)
CONSTANT   PBebz =  1.412       ! Brain tissue:blood partition (Campbell and Fisher, 2007)
CONSTANT   PSebz  =  0.609      ! Slowly perfused tissue:blood  partition (Campbell and Fisher, 2007; Tardif et al., 1997)
CONSTANT   PRebz  =  1.412      ! Rapidly perfused tissue:blood  partition (Campbell and Fisher, 2007; Tardif et al., 1997)
CONSTANT   Pluebz2008=1.96      ! Lung PC (set to liver)
CONSTANT   Pnoebz2008=1.96      ! Nasal PC (set to liver)

! Ttoluene Partition Coefficients, Tissue :Blood Already, do not divide by blood :air
CONSTANT   PWBtl =  18.         ! Blood:air partition coefficient (Tardif et al., 1997)
CONSTANT   PLtl  =   4.64       ! Liver :blood partition coefficient (Tardif et al., 1997)
CONSTANT   PFtl  = 56.7         ! Fat:blood partition coefficient (Tardif et al., 1997)
CONSTANT   PBtl =  1.72         ! Brain tissue :blood partition (Thrall etal 2002, Tardif et al., 1997)
CONSTANT   PStl  =  1.54        ! Slowly perfused tissue:blood  partition (set to liver)
CONSTANT   PRtl  =  4.64        ! Rapidly perfused tissue:blood  partition (set to liver)
CONSTANT   Plutol=4.64          ! Lung PC (set to liver)
CONSTANT   Pnotol=4.64          ! Nasal PC (set to liver)

!----------------------[MOLECULAR WEIGHTS]-----------------------------------------
CONSTANT   MWmx = 106.16        !m-xylene Molecular weight (g/mol)
```

```
CONSTANT   MWebz = 106.16       !ethylbenzene Molecular weight (g/mol)
CONSTANT   MWtl = 92.14         !Toluene Molecular weight (g/mol)
CONSTANT   MWC8 = 114.2         !C8 Molecular weight (g/mol)
CONSTANT   MW=142.29            !C10 Molecular weight (g/mol)
CONSTANT   MWC14= 198.39        !C14 Molecular weight (g/mol)
CONSTANT   MWLUMP= 167          !JP8 lUMP AVG MW  (g/mol)
CONSTANT   MWLP= 104.62         !JP8 LUMP-1 AVG MW  (g/mol)
CONSTANT   MWLUMP3=200          !JP8 lUMP-3 AVG MW  (g/mol)


!------------------------------[EXPOSURE TIMING]-----------------------------------------------
CONSTANT TCHNG = 4              ! Length of inhalation exposure - hrs
CONSTANT EXPTIME = 6            ! Total length pre- and post-exposure time points from tissues (hrs)

!------------------------------[RESPIRATORY PARAMETERS]---------------------------------
!Nasal and Tracheobronchial parameters
CONSTANT TBSA     = 7.1         ! Surface area of TB, cm/kg (Csanady et al., 2007)
CONSTANT TBthick  = 7.5e-3      ! Thickness of TB, cm (Csanady et al., 2007)
CONSTANT OlfSA    = 2.5         ! Surface area of nasal olf, cm2/kg (Csanady et al., 2007)
CONSTANT ResSA    = 2.2         ! Surface area of nasal res, cm2/kg (Csanady et al., 2007)
CONSTANT Olfthick = 7.0e-3      ! Thickness of nasal olf, cm (Csanady et al., 2007)
CONSTANT Resthick = 8e-3        ! Thickness of nasal resp, cm (Csanady et al., 2007)

!------------------------------[DEPOSITION PARAMETERS]---------------------------------
!standard values, values different per exposure
!Controlled in m-files
CONSTANT fdepositPU   = 0.05    ! Deposition in lung region, (MPPDv2.01 – Hammner Inst, RTP, NC)
CONSTANT fdepositTB = 0.05      ! Deposition in tracheobronchial region, (MPPDv2.01 – Hammner Inst, RTP, NC)
CONSTANT fdepositNO   = 0.7     ! Deposition in nasal region, (MPPDv2.01 – Hammner Inst, RTP, NC)

!----------------[PERCENT AEROSOL AND VAPOR]-----------------------------------
!Controlled in m-files
!Octane
```

```
CONSTANT perc_aerosolc8 =0.12 ! fraction total exposure that is aerosol
CONSTANT perc_vaporc8 = 0.88  ! fraction total exposure that is vapor

!Decane
CONSTANT perc_aerosol = 0.21     ! fraction total exposure that is aerosol
CONSTANT perc_vapor =  0.79      ! fraction total exposure that is vapor


!Tetradecane
CONSTANT perc_aerosolC14 = 0.16    ! fraction total exposure that is aerosol
CONSTANT perc_vaporC14 =  0.84     ! fraction total exposure that is vapor

!Lump 1
CONSTANT perc_aerosolLP =0.09       ! fraction total exposure that is aerosol
CONSTANT perc_vaporLP =  0.91       ! fraction total exposure that is vapor

!Lump 2
CONSTANT perc_aerosolLUMP =0.335 ! fraction total exposure that is aerosol
CONSTANT perc_vaporLUMP =  0.615 ! fraction total exposure that is vapor

!Lump 3
CONSTANT perc_aerosolLUMP3 =0.30 ! fraction total exposure that is aerosol
CONSTANT perc_vaporLUMP3 =  0.70 ! fraction total exposure that is vapor

!TOL
CONSTANT perc_aerosoltol =0.133       ! fraction total exposure that is aerosol
CONSTANT perc_vaportol =0.864         ! fraction total exposure that is vapor

!EBZ
CONSTANT perc_aerosolebz2008 =0.181 ! fraction total exposure that is aerosol
CONSTANT perc_vaporebz2008 = 0.819  ! fraction total exposure that is vapor

!m-XYLENE
```

```
CONSTANT perc_aerosolmx2008 =0.202 ! fraction total exposure that is aerosol
CONSTANT perc_vapormx2008 =0.798   ! fraction total exposure that is vapor



!-------------[EXPOSURE ATMOSPHERE CONCENTRATION]-----------------------------------
!Controlled in m-files

!Toluene
CONSTANT IconiTol= 0 !

!Ethylbenzene
CONSTANT IconiEbz2008= 0 !

!m-Xylene
CONSTANT IconiMX2008= 0 !

!Octane
CONSTANT IconiC8= 0 !

!Decane
CONSTANT Iconi = 0  !

!Tetradecane
CONSTANT IconiC14 = 0 !

!Lump 1
CONSTANT Iconilp = 0 !

!Lump 2
CONSTANT IconiLump= 0 !

!Lump 3
```

```
CONSTANT IconiLump3= 0  !


!--------------[PERMEABILITY AREA TERMS]-----------------------------------------------
!Lung PA Terms
CONSTANT PAC1tol=1E-2                   !Toluene
CONSTANT PAC1EBZ2008=1E-2               !Ethylbenzene
CONSTANT PAC1MX2008=1E-2                !m-Xylene
CONSTANT PAC1C8=1E-2                    !Octane
CONSTANT PAC1  = 9E-4                   !Decane
CONSTANT PAC1C14  = 9E-4                !Tetradecane
CONSTANT PAC1LP=1E-2                    !Lump 1
CONSTANT PAC1LUMP=1E-2                  !Lump 2
CONSTANT PAC1LUMP3=9E-4                 !Lump 3

! Nasal PA Terms
CONSTANT PACnosemx2008=1E-2             !m-Xylene
CONSTANT PACnoseEBZ2008=1E-2            !Ethylbenzene
CONSTANT PACnosetol=1E-2                !Toluene
CONSTANT PACnosec8=1E-2                 !Octane
CONSTANT PACnose  = 9e-5                !Decane
CONSTANT PACnoseC14  = 9e-4             !Tetradecane
CONSTANT PACnoseLP=1E-2                 !Lump 1
CONSTANT PACnoseLUMP=1E-2               !Lump 2
CONSTANT PACnoseLUMP3=1E-2              !Lump 3


!m-Xylene
CONSTANT PACFmx=0.56                    !m-xylene fat

!Ethylbenzene
CONSTANT PACFebz=0.658                  !ethylbenzene fat
```

```
!Toluene
CONSTANT PACFtl=0.95                    ! toluene fat

!Octane
CONSTANT PACBrinc8 = 3.5e-2             ! permeability area value (PA term)
CONSTANT PACBroutc8 = 1e-1              ! permeability area value (PA term)
CONSTANT PACfinc8 = 2e-2                ! permeability area value (PA term)
CONSTANT PACfoutc8 = 2e-2               ! permeability area value (PA term)
CONSTANT PACLinc8 = 1e-2                ! permeability area value (PA term)
CONSTANT PACLoutc8 =1e-2                ! permeability area value (PA term)

!Decane
CONSTANT PACBrin = 3.5e-2               ! permeability area value (PA term)
CONSTANT PACBrout = 1e-1                ! permeability area value (PA term)
CONSTANT PACfin = 2e-2                  ! permeability area value (PA term)
CONSTANT PACfout = 2e-2                 ! permeability area value (PA term)
CONSTANT PACLin = 1e-2                  ! permeability area value (PA term)
CONSTANT PACLout =1e-2                  ! permeability area value (PA term)
CONSTANT PACF = 2.35                    ! permeability area value (PA term)
CONSTANT PACL = 1.1                     ! permeability area value (PA term)

!Tetradecane
CONSTANT PACBrinC14 = 3.5e-2            ! permeability area value (PA term)
CONSTANT PACBroutC14 = 1e-1             ! permeability area value (PA term)
CONSTANT PACfinC14 = 7.57e-3            ! permeability area value (PA term)
CONSTANT PACfoutC14 = 7.57e-3           ! permeability area value (PA term)
CONSTANT PACLinC14 = 1e-2               ! permeability area value (PA term)
CONSTANT PACLoutC14 =1e-2               ! permeability area value (PA term)

!Lump 1
CONSTANT PACFlp=0.95                    ! permeability area value (PA term)

!Lump 2
```

```
CONSTANT PACBrinlump = 3.5e-2          ! permeability area value (PA term)
CONSTANT PACBroutlump = 1e-1           ! permeability area value (PA term)
CONSTANT PACfinlump = 2e-2             ! permeability area value (PA term)
CONSTANT PACfoutlump = 2e-2            ! permeability area value (PA term)
CONSTANT PACLinlump = 1e-2             ! permeability area value (PA term)
CONSTANT PACLoutlump =1e-2             ! permeability area value (PA term)

!Lump 3
CONSTANT PACBrinLUMP3 = 3.5e-2         ! permeability area value (PA term)
CONSTANT PACBroutLUMP3 = 1e-1          ! permeability area value (PA term)
CONSTANT PACfinLUMP3 = 7.6e-3          ! permeability area value (PA term)
CONSTANT PACfoutLUMP3 = 7.6e-3         ! permeability area value (PA term)
CONSTANT PACLinLUMP3 = 1e-2            ! permeability area value (PA term)
CONSTANT PACLoutLUMP3 =1e-2            ! permeability area value (PA term)


!----------------------[METABOLISM PARAMETERS]-----------------------------------------------
!Metabolism Parameters (m-Xylene)
CONSTANT Vmaxmxc = 8.75                ! vamxc, Campbell and Fisher, 2007, mg/hr/kg^0.75
CONSTANT Kmmx = 0.87                   ! km, Campbell and Fisher, 2007
CONSTANT Kimx = 0.87                   ! Interaction term, Set to km

!Metabolism Parameters (Ethylbenzene)
CONSTANT Vmaxebzc = 6.01               ! vamxc, Campbell and Fisher, 2007
CONSTANT Kmebz = 0.67                  ! km, Campbell and Fisher, 2007
CONSTANT Kiebz = 0.67                  ! Interaction term, set to km

!Metabolism Parameters (Toluene)
CONSTANT Vmaxtlc = 3.44                !vmaxc, Haddid et al., 1999
CONSTANT Kmtl = 0.13                   !km, Haddid et al., 1999
CONSTANT Kitl = 0.13                   !Interaction term, set to km

!Metabolism Parameters (C8)
```

```
CONSTANT vmaxCc8=35.5                !vmaxc, fit
CONSTANT kmc8=1.5                    !km, Fit
CONSTANT kic8=0.75                   !Interaction term, fit

!Metabolism Parameters (C10)
CONSTANT Vmaxc  = 10.0               ! vmaxc, fit
CONSTANT Km    = 1.5                 ! km,  Mortensen, et al 2000
CONSTANT Ki    = 1.5                 ! Interaction term, set to km

!Metabolism Parameters (C14)
CONSTANT VmaxcC14  = 0               ! No reported metabolism
CONSTANT KmC14    = 10000            ! No reported metabolism
CONSTANT KiC14    = 10000            ! No reported interactions

!Metabolism Parameters (Lump 1)
CONSTANT vmaxlpc = 2.50              ! vmaxc, Campbell and Fisher, 2007
CONSTANT Kmlp = 0.75                 ! km, Campbell and Fisher, 2007
CONSTANT Kilp = 0.75                 ! Interaction term, set to km

!Metabolism Parameters (Lump 2)
CONSTANT kmlump=1.6                  ! vmaxc, fit from decane
CONSTANT vmaxClump=10.22             ! km, fit from decane
CONSTANT kilump=1.6                  ! Interaction term, set to km

!Metabolism Parameters (Lump3)
CONSTANT vmaxClump3=0                ! No reported metabolism
CONSTANT kmlump3=10000               ! No reported metabolism
CONSTANT kilump3=10000               ! No reported interactions



END ! INITIAL
```

```
DYNAMIC

    ALGORITHM IALG = 14
    NSTEPS    NSTP = 1
    MAXTERVAL MAXT = 1.0e9
    MINTERVAL MINT = 1.0e-9
    CINTERVAL CINT = 0.04

    DERIVATIVE

! code for calulating the derivative goes here
!-----------------------[Flow Equations]-------------------------------------
Qbal = (QC-(QR+QS+QF+QL+Qno+Qbr))*100!+qf2 Q balance, 0.0 Jan 12, 2009
QC  = QCC*BW**0.75          ! Cardiac output - L/hr
QP  = QPC*BW**0.75          ! Pulmonary ventilation rate
QBr = QBrC*QC               ! Blood flow to brain
QL  = QLC*QC                ! Blood flow to liver
QF  = QFC*QC                ! Blood flow to fat
QLu = QLuC*QC               ! Blood flow to lungs
QR  = 0.78*QC-QL-QBr-QNo-Qtb   ! Q-fast
QS  = 0.22*QC-QF            ! Q-slow
Qno = Qnoc*QC               ! blood flow to nasal compartment (l/hr)
Qtb = Qtbc*QC               ! blood flow to tracheobronchial compartment (l/hr)

!-----------------------[TISSUE VOLUMES]-------------------------------------
!Volume Equations
Vbal = ((VL+VLU+VNO+VBR+VR+VF+VS+vtb)/BW)*100  ! Vol balance checking
VR  = 0.11*BW - VBr-Vlu-Vno-VL-vtb ! Rapidly Perfused
VS  = 0.80*BW - Vf                 ! Slowly Perfused
VF  = VFC*BW                       ! fat)
VL  = VLC*BW                       ! liver
```

```
VBr = VBrC*BW                    ! brain
VLu = VLuC*BW                    ! lung


NasSA = olfsa+ressa                    ! nasal mucosa SA
Nasthick=olfthick+resthick             ! nasal mucosa thickness
Vno = NasSA*(BW**0.75)*Nasthick/1000  ! nasal mucosa volume
Vtb = tbSA*(BW**0.75)*tbthick/1000  ! tb volume
Vnasmuclayer = VnasmuclayerC*BW   ! volume of mucous coating nasal passage rat
Vtbmuclayer =  VtbmuclayerC*BW      ! volume of lung and lung and tb lining fluid

!---------------[BLOOD VOLUMES]-----------------------------------------------
Bvbr = Bvbrc*VBr                   ! blood volume brain calculation (Perleberg et al., 2004)
Bvf  = Bvfc*VF                     ! fat
Bvl  = Bvlc*VL                     ! blood volume liver calculation

!-------------------[METABOLISM]-------------------------------------------------
VMAXC8=VMAXCC8*BW**0.75  !Octane
VMAX = vmaxc*BW**0.75   ! Decane
VMAXC14=VMAXCC14*BW**0.75  !Tetradecane (No reported metabolism)
VMAXmx = Vmaxmxc*BW**0.75  !m-Xylene
VMAXebz = Vmaxebzc*BW**0.75 !Ethylbenzene
VMAXtl = Vmaxtlc*BW**0.75  !Toluene
VMAXlp = Vmaxlpc*BW**0.75  !Lump 1
VMAXlump=VMAXCLUMP*BW**0.75  ! Lump 2
VMAXlump3=VMAXCLUMP3*BW**0.75  ! Lump 3 (No reported metabolism)

!----------------------[PERMEABILITY AREA TERMS]-------------------------------
!PA Terms for Fat for Aromatics and Lump1
PAFmx=PACFmx*BW**0.75 !
PAFebz=PACFebz*BW**0.75 !
PAFtl=PACFtl*BW**0.75 !
PAFlp=PACFlp*BW**0.75 !
```

```
!Decane
PABrin = PACBrin*BW**0.75       ! permeability area value "into" L/hr (PA term ) brain
PABrout = PACBrout*BW**0.75       ! permeability area value "into" L/hr (PA term ) brain
PALin = PACLin*BW**0.75       ! permeability area value "into" (PA term ) brain
PALout = PACLout*BW**0.75       ! permeability area value "out" (PA term ) brain
PAfin = PACfin*BW**0.75       ! permeability area value "into" (PA term ) brain
PAfout = PACfout*BW**0.75       ! permeability area value "out" (PA term ) brain
PA1  = PAC1*BW**0.75         ! permeability area
PAnose  = PACnose*BW**0.75        ! permeability area

!AROMATICS Lung PA
PA1tol=PAC1tol* BW **0.75                   ! permeability area
PA1ebz2008=PAC1ebz2008* BW **0.75  ! permeability area
PA1mx2008=PAC1mx2008* BW **0.75   ! permeability area

! Aromatics Nasal PA
PANOSEtol=PAcNOSetol*bw**0.75                   ! permeability area
PANOSEmx2008=PAcNOSemx2008*bw**0.75   ! permeability area
PANOSEebz2008=PAcNOSeebz2008*bw**0.75   ! permeability area

! Lump 1
PA1LP=PAC1LP*bw**0.75
PANOSElp=PACNOSElp*bw**0.75

!C8
PALinc8  =  PACLinc8*BW**0.75       ! permeability area value "into" (PA term) Liver
PALoutc8  =  PACLoutc8*BW**0.75       ! permeability area value "out" (PA term) Liver
PALuc8 =  PACLuc8*BW**0.75      ! permeability area value "into" (PA term) Lung
PABrinc8 = PACBrinc8*BW**0.75       ! permeability area value "in" L/hr (PA term ) brain
PABroutc8 = PACBroutc8*BW**0.75       ! permeability area value "out" L/hr (PA term ) brain
PAfinc8 = PACfinc8*BW**0.75   ! permeability area
PAfoutc8 = PACfoutc8*BW**0.75   ! permeability area
```

```
PANOSEc8=PAcNOSec8*bw**0.75   ! permeability area
PA1c8=PAC1c8*bw**0.75! permeability area

!C14
PALinC14  =  PACLinC14*BW**0.75       ! permeability area value "into" (PA term) Liver
PALoutC14  =  PACLoutC14*BW**0.75       ! permeability area value "into" (PA term) Liver
PALuC14 =  PACLuC14*BW**0.75      ! permeability area value "into" (PA term) Lung
PABrinC14 = PACBrinC14*BW**0.75       ! permeability area value "into" L/hr (PA term ) brain
PABroutC14 = PACBroutC14*BW**0.75       ! permeability area value "out" L/hr (PA term ) brain
PAfinC14 = PACfinC14*BW**0.75     ! permeability area
PAfoutC14 = PACfoutC14*BW**0.75    ! permeability area
PANOSEC14=PAcNOSeC14*bw**0.75   ! permeability area
PA1C14=PAC1C14*bw**0.75! permeability area

!LUMP 1
PALinLUMP1  =  PACLinLUMP1*BW**0.75       ! permeability area value "into" (PA term) Liver
PALoutLUMP1  =  PACLoutLUMP1*BW**0.75       ! permeability area value "out" (PA term) Liver
PALuLUMP1 =  PACLuLUMP1*BW**0.75      ! permeability area value "into" (PA term) Lung
PABrinLUMP1 = PACBrinLUMP1*BW**0.75       ! permeability area value "into" L/hr (PA term ) brain
PABroutLUMP1 = PACBroutLUMP1*BW**0.75       ! permeability area value "out" L/hr (PA term ) brain
PAfinLUMP1 = PACfinLUMP1*BW**0.75   ! permeability area
PAfoutLUMP1 = PACfoutLUMP1*BW**0.75   ! permeability area
PANOSELUMP1=PAcNOSeLUMP1* BW **0.75   ! permeability area
PA1LUMP1=PAC1LUMP1* BW **0.75! permeability area

!LUMP 2
PABrinlump = PACBrinlump*BW**0.75       ! permeability area value "into" L/hr (PA term ) brain
PABroutlump = PACBroutlump*BW**0.75       ! permeability area value "into" L/hr (PA term ) brain
PALinlump = PACLinlump*BW**0.75       ! permeability area value "into" L/hr (PA term ) brain
PALoutlump = PACLoutlump*BW**0.75       ! permeability area value "into" L/hr (PA term ) brain
PAFlump  = PACFlump*BW**0.75        ! permeability area value "into" L/hr (PA term ) fat
PAfinlump = PACfinlump*BW**0.75       ! permeability area value "into" L/hr (PA term ) brain
PAfoutlump = PACfoutlump*BW**0.75       ! permeability area value "into" L/hr (PA term ) brain
```

```
PANOSELUMP=PAcNOSELUMP*BW**0.75    ! permeability area
PA1LUMP=PAC1LUMP*bw**0.75   ! permeability area

!LUMP3
PALinLUMP3  =  PACLLUMP3*BW**0.75       ! permeability area value "into" (PA term) Liver
PALoutLUMP3  =  PACLoutLUMP3*BW**0.75       ! permeability area value "into" (PA term) Liver
PASinLUMP3= PACSinLUMP3*BW**0.75
PASoutLUMP3 = PACSoutLUMP3*BW**0.75
PALuCLUMP3 =  PACLuLUMP3*BW**0.75      ! permeability area value "into" (PA term) Lung
PABrinLUMP3 = PACBrinLUMP3*BW**0.75       ! permeability area value "into" L/hr (PA term ) brain
PABroutLUMP3 = PACBroutLUMP3*BW**0.75       ! permeability area value "into" L/hr (PA term ) brain
PAfinLUMP3 = PACfinLUMP3*BW**0.75
PAfoutLUMP3 = PACfoutLUMP3*BW**0.75
PANOSELUMP3=PAcNOSeLUMP3*bw**0.75
PA1LUMP3=PAC1LUMP3*bw**0.75


!-----------------------------[PARTITION COEFFICIENTS]-----------------------
!C8
PLc8  =  (PLAc8/PBc8)          ! Liver : blood partition coefficient
PFc8  = (PFAc8/PBc8)           ! Fat : Blood partition coefficient
PBrc8 = (PBrAc8/PBc8)     ! Brain:Blood PC unpublished
PSc8  = (PSAc8/PBc8)      ! Slowly perfused tissue:blood, muscle
PRc8  = (PRAc8/PBc8)      ! Rapidly perfused tissue:blood partition, liver
PLuc8 = (PLuAc8/PBc8)         ! Lung : blood partition coefficient (set to same as liver then fit, as per Reiko Decane
Pnoc8 = (PLuAc8/PBc8)         ! P nose set to lung PC
Ptbc8 = (PLuAc8/PBc8)          ! P tb set to lung PC

!C10
PL  =  (PLA/PB)                  ! Liver : blood partition coefficient
PF  = (PFA/PB)                   ! Fat : Blood partition coefficient
PBr = (PBrA/PB)                  ! Brain:Blood PC
PS  = (PSA/PB)                   ! Slowly perfused tissue:blood, muscle
```

```
PR  = (PRA/PB)                  ! Rapidly perfused tissue:blood partition, liver
PLu = (PLuA/PB)                 ! Lung : blood partition coefficient (set to same as liver then fit, as per Reiko Decane
Pno = (PLuA/PB)                 ! P nose set to lung PC
Ptb = (PLuA/PB)                 ! P tb set to lung PC

!C14
PLc14  =  (PLAc14)        ! Liver : blood partition coefficient
PFc14  = (PFAc14)         ! Fat : Blood partition coefficient
PBrc14 = (PBrAc14)          ! Brain:Blood PC unpublished
PSc14  = (PSAc14)  ! Slowly perfused tissue:blood, muscle
PRc14  = (PRAc14)  ! Rapidly perfused tissue:blood partition, liver
PLuc14 = (PLuAc14)    ! Lung : blood partition coefficient (set to same as liver then fit, as per Reiko Decane
Pnoc14 = (PLuAc14)  ! P nose set to lung PC
Ptbc14 = (PLuAc14) ! P tb set to lung PC
 PdL2bc14 =(PFAc14)


!Lump 2
PLLUMP  =  (PLALUMP/PBLUMP)          ! Liver : blood partition coefficient
PFLUMP  = (PFALUMP/PBLUMP)  ! Fat : Blood partition coefficient
PBrLUMP = (PBrALUMP/PBLUMP)     ! Brain:Blood PC unpublished
PSLUMP  = (PSALUMP/PBLUMP)   ! Slowly perfused tissue:blood, muscle
PRLUMP  = (PRALUMP/PBLUMP)! Rapidly perfused tissue:blood partition, liver
PLuLUMP = (PLuALUMP/PBLUMP)! Lung : blood partition coefficient (set to same as liver then fit, as per Reiko Decane
PnoLUMP = (PLuALUMP/PBLUMP)! P nose set to lung PC
PtbLUMP = (PLuALUMP/PBLUMP)! P tb set to lung PC

!LUMP3
PLLUMP3  = PLALUMP3         ! Liver : blood partition coefficient
PFLUMP3  = PFALUMP3          ! Fat : Blood partition coefficient
PBrLUMP3 = PBrALUMP3     ! Brain:Blood PC unpublished
PSLUMP3  = PSALUMP3          ! Slowly perfused tissue:blood, muscle
PRLUMP3  = PRALUMP3       ! Rapidly perfused tissue:blood partition, liver
```

```
PLuLUMP3 = PLuALUMP3     ! Lung : blood partition coefficient
PnoLUMP3 = PLuALUMP3     ! P nose set to lung PC
PtbLUMP3 = PLuALUMP3      ! P tb set to lung PC
 PdL2bLUMP3 =PFALUMP3    !
!---Shep toluene aerosol phase----------------------------------------
kInhPUtol =  QP * CIatol * (fdepositPU+fdepositTB)       ! mppd2 Pulmonary (Lung+TB)
kInhNOtol = QP * CIatol * (fdepositNO)       ! nasal region
kIvtol =  QP * CIvtol       ! vapor

!{Exposure parameters tol}
 !exposure =  pulse(0.0,exptime, tchng)
CIXtol = (ICONitol*MWTL/24450)    ! Inhaled concentration to mg/L
CIvtol = (CIXtol*perc_vaportol)*exposure      ! Turn on vapor inhalation
CIatol = ((CIXtol*perc_aerosoltol)* exposure)!      ! Turn on aerosol in MPPD2
CItol=CIvtol+CIatol

!{Nasal Compartment}
!transfer of chemical across mucous layer in nasal
Rnintaketol=kinhnotol
Rnmucoustol = (Rnintaketol-PAnosetol*Cnmucoustol)
anmucoustol = integ(rnmucoustol,0.0)
cnmucoustol = anmucoustol/vnasmuclayer
!nasal tissue
Rnasalttol = (PAnosetol*cnmucoustol) + Qno*(catol-cvnotol)
anasalttol= integ(rnasalttol,0.0)
cnasalttol=anasalttol/vno
cvnotol = cnasalttol/pnotol
Atnotol = anasalttol!

!Nasal Compartment Mass Balance
mbnotol = (anaslost2tol+anoseintol) - (anasalttol+anoseouttol)
rnoseintol=qno*ca1tol
anoseintol=integ(rnoseintol,0.0)
```

```
rnoseouttol=qno*cvnotol
anoseouttol=integ(rnoseouttol,0.0)
rnaslost2tol=panose*cnmucoustol
anaslost2tol=integ(rnaslost2tol,0.0)

!{Lung Compartment}
!transfer of chemical across mucous layer in conducting lung
RLintaketol=kinhputol
RLmucoustol = (RLintaketol-PA1tol*CLmucoustol)
aLmucoustol = integ(rLmucoustol,0.0)
CLmucoustol = aLmucoustol/vtbmuclayer
!Lung tissue
Rlungtol = (QC*(Ca1tol-Catol)+(PA1tol*clmucoustol))
alungttol= integ(rlungtol,0.0)  !
clungttol=alungttol/vlu !
catol = clungttol/plutol !

CA1tol = (QC*Cvtol+Qp*Civtol)/(QC+(QP/PwBtl))
      CXtol = CA1tol/PwBtl
      rAXtol = QP*CXtol
axtol=integ(raxtol,0.0)
CXPPMtol=(0.7*cxtol+0.3*citol)*24450/MWTL

Atputol =alungttol

!Lung Compartment Mass Balance
mblungstol = (alunglost2tol+alungintol) - (alungttol+alungouttol)
rlungintol=qc*ca1tol
alungintol=integ(rlungintol,0.0)
rlungouttol=qc*catol
alungouttol=integ(rlungouttol,0.0)
rlunglost2tol=pa1*clmucoustol
alunglost2tol=integ(rlunglost2tol,0.0)
```

```
rlungvaportol=QP*CIVtol
alungvaportol=integ(rlungvaportol,0.0)


!CV = Mixed venous blood concentration (mg/l)'
        CVtol = (QF*CVFtol+QL*CVLtol+QS*CVStol+QR*CVRtol+QBr*CVBrtol+qno*cvnotol)/QC
        CVAUCtol= integ(cvtol,0.)

!AX = Amount inhaled (mg)'
        RAItol = QP*CItol
        AItol =integ(RAItol,0.)
        !doseinhtol= aitol-axtol

!AS = Amount in slowly perfused tissues (mg)'
        RAStol = QS*(CAtol-CVStol)
        AStol = INTEG(RAStol,0.)
        CVStol = AStol/(VS*PStl)
        CStol = AStol/VS

!AR = Amount in rapidly perfused tissues (mg)'
        RARtol = QR*(CAtol-CVRtol)
      ARtol = INTEG(RARtol,0.)
      CVRtol = ARtol/(VR*PRtl)
      CRtol = ARtol/VR

!AF = Amount in fat tissue (mg)

   RAVFtol= QF*(CAtol-CVFtol)+((PAFtl*CFtol)/PFtl)-(PAFtl*CVFtol)
        AVFtol=INTEG(RAVFtol,0.)
        CVFtol=AVFtol/(BVF*VF)

        RAFtol=PAFtl*CVFtol-(PAFtl*CFtol)/PFtl
        AFtol=INTEG(RAFtol,0.)
```

```
        CFtol=AFtol/((1-BVF)*VF)
   AUCFtol=INTEG(CFtol,0.)

!AB = Amount in brain tissue
     RABrtol = QBr*(CAtol-CVBrtol)
     ABtol = INTEG(RABrtol,0.)
     CVBrtol = ABtol/(VBr*PBtl)
     CBrtol = ABtol/VBr

!AL = Amount in liver tissue (mg)'
     RALtol = QL*(CAtol-CVLtol)-RAMtol
          ALtol=INTEG(RALtol,0.)
          CVLtol=ALtol/(PLtl*VL)
          CLtol=ALtol/VL

     !MASS = mass balance (mg)
      MASStol = AFtol+ALtol+AStol+ARtol+AXtol+ABtol+amtol+atnotol+alungttol
     masbaltol=aitol-masstol
mb5tol=(alunglost2tol+anaslost2tol+alungvaportol)-masstol


!---------- EBZ Aerosol Phase----------------------------------------------
!ethylbenzene code
kInhPUebz2008 =  QP * CIaebz2008 * (fdepositPU+fdepositTB)       ! mppd2 Pulmonary (Lung+TB)
kInhNOebz2008 = QP * CIaebz2008 * (fdepositNO)       ! nasal region
kIvebz2008 =  QP * CIvebz2008       ! vapor

!{Exposure parameters tol}
 !exposure =  pulse(0.0,exptime, tchng)
CIXebz2008 = (ICONiebz2008*MWEBZ/24450)                          ! Inhaled concentration, converts ppm to mg/L ,conversion is
mg/L=(Xppm)(MW)/24450, 0.798 is total retention for C14-only
CIvebz2008 = (CIXebz2008*perc_vaporebz2008)*exposure      ! Turn on vapor inhalation
CIaebz2008 = ((CIXebz2008*perc_aerosolebz2008)* exposure)!*ff      ! Turn on aerosol in MPPD2
```

```
CIebz2008=CIvebz2008+CIaebz2008

!{Nasal Compartment}
!transfer of chemical across mucous layer in nasal
Rnintakeebz2008=kinhnoebz2008
Rnmucousebz2008 = (Rnintakeebz2008-PAnoseebz2008*Cnmucousebz2008)
anmucousebz2008 = integ(rnmucousebz2008,0.0)
cnmucousebz2008 = anmucousebz2008/vnasmuclayer
!nasal tissue
Rnasaltebz2008 = (PAnoseebz2008*cnmucousebz2008) + Qno*(caebz2008-cvnoebz2008)
anasaltebz2008= integ(rnasaltebz2008,0.0)
cnasaltebz2008=anasaltebz2008/vno
cvnoebz2008 = cnasaltebz2008/pnoebz2008
Atnoebz2008 = anasaltebz2008!

!Nasal Compartment Mass Balance
Mbnoebz2008 = (anaslost2ebz2008+anoseinebz2008) - (anasaltebz2008+anoseoutebz2008)
rnoseinebz2008=qno*ca1ebz2008
anoseinebz2008=integ(rnoseinebz2008,0.0)
rnoseoutebz2008=qno*cvnoebz2008
anoseoutebz2008=integ(rnoseouebz2008,0.0)
rnaslost2ebz2008=panose*cnmucousebz2008
anaslost2ebz2008=integ(rnaslost2ebz2008,0.0)

!{Lung Compartment}
!transfer of chemical across mucous layer in conducting lung
RLintakeebz2008=kinhpuebz2008
RLmucousebz2008 = (RLintakeebz2008-PA1ebz2008*CLmucousebz2008)
aLmucousebz2008 = integ(rLmucousebz2008,0.0)
CLmucousebz2008 = aLmucousebz2008/vtbmuclayer
!Lung tissue
Rlungebz2008 = (QC*(Ca1ebz2008-Caebz2008)+(PA1ebz2008*clmucousebz2008))
alungtebz2008= integ(rlungebz2008,0.0)  !
```

```
clungtebz2008=alungtebz2008/vlu !
caebz2008 = clungtebz2008/pluebz2008 !


CA1ebz2008 = (QC*Cvebz2008+Qp*Civebz2008)/(QC+(QP/PwBebz))
      CXebz2008 = CA1ebz2008/PwBebz
      rAXebz2008 = QP*CXebz2008
axebz2008=integ(raxebz2008,0.0)
CXPPMebz2008=(0.7*cxebz2008+0.3*ciebz2008)*24450/MWEBZ

Atpuebz2008 =alungtebz2008

!Lung Compartment Mass Balance
mblungsebz2008 = (alunglost2ebz2008+alunginebz2008) - (alungtebz2008+alungoutebz2008)!
rlunginebz2008=qc*ca1ebz2008
alunginebz2008=integ(rlunginebz2008,0.0)
rlungoutebz2008=qc*caebz2008
alungoutebz2008=integ(rlungoutebz2008,0.0)
rlunglost2ebz2008=pa1 ebz2008*clmucousebz2008
alunglost2ebz2008=integ(rlunglost2ebz2008,0.0)
rlungvaporebz2008=QP*CIVebz2008
alungvaporebz2008=integ(rlungvaporebz2008,0.0)

!CV = Mixed venous blood concentration (mg/l)'
         CVebz2008 =
(QF*CVFebz2008+QL*CVLebz2008+QS*CVSebz2008+QR*CVRebz2008+QBr*CVBrebz2008+Qno*CVnoebz2008)/QC
         CVAUCebz2008= integ(cvebz2008,0.)

!AX = Amount exhaled (mg)'
         RAIebz2008 = QP*CIebz2008
         AIebz2008 =integ(RAIebz2008,0.)
         !doseinhebz2008= aiebz2008-axebz2008
```

```
!AS = Amount in slowly perfused tissues (mg)'
        RASebz2008 = QS*(CAebz2008-CVSebz2008)
        ASebz2008 = INTEG(RASebz2008,0.)
        CVSebz2008 = ASebz2008/(VS*PSebz)
        CSebz2008 = ASebz2008/VS

!AR = Amount in rapidly perfused tissues (mg)'
        RARebz2008 = QR*(CAebz2008-CVRebz2008)
      ARebz2008 = INTEG(RARebz2008,0.)
      CVRebz2008 = ARebz2008/(VR*PRebz)
      CRebz2008 = ARebz2008/VR

!AF = Amount in fat tissue (mg)
  RAVFebz2008= QF*(CAebz2008-CVFebz2008)+((PAFebz*CFebz2008)/PFebz)-(PAFebz*CVFebz2008)
        AVFebz2008=INTEG(RAVFebz2008,0.)
        CVFebz2008=AVFebz2008/(BVF*VF)

        RAFebz2008=PAFebz*CVFebz2008-(PAFebz*CFebz2008)/PFebz
        AFebz2008=INTEG(RAFebz2008,0.)
        CFebz2008=AFebz2008/((1-BVF)*VF)
  AUCFebz2008=INTEG(CFebz2008,0.)

        !RAFebz = QF*(CAebz-CVFebz)
        !AFebz=INTEG(RAFebz,0.)
        !CVFebz=AFebz/(PFebz*VF)
        !CFebz=AFebz/VF

!AB = Amount in brain tissue diffusion limited(mg)'
     RABrebz2008 = QBr*(CAebz2008-CVBrebz2008)
     ABebz2008 = INTEG(RABrebz2008,0.)
     CVBrebz2008 = ABebz2008/(VBr*PBebz)
     CBrebz2008 = ABebz2008/VBr
```

```
!AL = Amount in liver tissue (mg)'
     RALebz2008 = QL*(CAebz2008-CVLebz2008)-RAMebz2008
           ALebz2008=INTEG(RALebz2008,0.)
           CVLebz2008=ALebz2008/(PLebz*VL)
           CLebz2008=ALebz2008/VL

     !MASS = mass balance (mg)
      MASSebz2008 =
AFebz2008+ALebz2008+ASebz2008+ARebz2008+AXebz2008+ABebz2008+amebz2008+atnoebz2008+alungtebz2008
     massbalebz2008=aiebz-massebz2008
mb5ebz2008=(alunglost2ebz2008+anaslost2ebz2008+alungvaporebz2008)-massebz2008


!---------------------- m-Xylene Aerosol Phase Model-------------------------------
!ethylbenzene code
kInhPUmx2008  =  QP * CIamx2008  * (fdepositPU+fdepositTB)       ! mppd2 Pulmonary (Lung+TB)
kInhNOmx2008  = QP * CIamx2008  * (fdepositNO)       ! nasal region
kIvmx2008  =  QP * CIvmx2008         ! vapor

!{Exposure parameters tol}
 !exposure =  pulse(0.0,exptime, tchng)
CIXmx2008  = (ICONimx2008 *MWMX/24450)                              ! Inhaled concentration, converts to mg/L
 CIvmx2008  = (CIXmx2008 *perc_vapormx2008 )*exposure      ! Turn on vapor inhalation
CIamx2008 = ((CIXmx2008 *perc_aerosolmx2008 )* exposure)!*ff      ! Turn on aerosol in MPPD2
CImx2008 =CIvmx2008 +CIamx2008

!{Nasal Compartment}
!transfer of chemical across mucous layer in nasal
Rnintakemx2008 =kinhnomx2008
Rnmucousmx2008  = (Rnintakemx2008 -PAnosemx2008 *Cnmucousmx2008 )
anmucousmx2008  = integ(rnmucousmx2008 ,0.0)
cnmucousmx2008  = anmucousmx2008 /vnasmuclayer
!nasal tissue
```

```
!Rnasalt = (ff*(PAnose*cnmucous) + Qno*(ca1-cvno))
Rnasaltmx2008  = (PAnosemx2008 *cnmucousmx2008 ) + Qno*(camx2008 -cvnomx2008)
anasaltmx2008 = integ(rnasaltmx2008 ,0.0)
cnasaltmx2008 =anasaltmx2008 /vno
cvnomx2008  = cnasaltmx2008 /pnomx2008
Atnomx2008  = anasaltmx2008 !

!Nasal Compartment Mass Balance
Mbnomx2008 = (anaslost2mx2008+anoseinmx2008) - (anasaltmx2008+anoseoutmx2008)
rnoseinmx2008=qno*ca1mx2008
anoseinmx2008=integ(rnoseinmx2008,0.0)
rnoseoutmx2008=qno*cvnomx2008
anoseoutmx2008=integ(rnoseoutmx2008,0.0)
rnaslost2mx2008=panose mx2008*cnmucousmx2008
anaslost2mx2008=integ(rnaslost2mx2008,0.0)

!{Lung Compartment}
!transfer of chemical across mucous layer in conducting lung
RLintakemx2008 =kinhpumx2008
RLmucousmx2008  = (RLintakemx2008 -PA1mx2008 *CLmucousmx2008 )
aLmucousmx2008  = integ(rLmucousmx2008 ,0.0)
CLmucousmx2008 = aLmucousmx2008 /vtbmuclayer
!Lung tissue
Rlungmx2008  = (QC*(Ca1mx2008 -Camx2008 )+(PA1mx2008 *clmucousmx2008))    !!!+(QP*CIV))!-((cLungt/plua)*QP))!-
(PA2*(clungt/PLU))
alungtmx2008 = integ(rlungmx2008 ,0.0)  !
clungtmx2008=alungtmx2008/vlu !
camx2008  = clungtmx2008 /plumx2008  !

CA1mx2008  = (QC*Cvmx2008 +Qp*Civmx2008 )/(QC+(QP/PwBmx))
      CXmx2008  = CA1mx2008 /PwBmx
      rAXmx2008  = QP*CXmx2008
axmx2008 =integ(raxmx2008 ,0.0)
```

```
CXPPMmx2008 =(0.7*cxmx2008 +0.3*cimx2008 )*24450/MWMX

Atpumx2008  =alungtmx2008  !



!Lung Compartment Mass Balance
mblungsmx2008 = (alunglost2mx2008+alunginmx2008) - (alungtmx2008+alungoutmx2008)!
rlunginmx2008=qc*ca1mx2008
alunginmx2008=integ(rlunginmx2008,0.0)
rlungoutmx2008=qc*camx2008
alungoutmx2008=integ(rlungoutmx2008,0.0)
rlunglost2mx2008=pa1mx2008*clmucousmx2008
alunglost2mx2008=integ(rlunglost2mx2008,0.0)
rlungvapormx2008=QP*CIVmx2008
alungvapormx2008=integ(rlungvapormx2008,0.0)


!CV = Mixed venous blood concentration (mg/l)'
        CVmx2008 =
(QF*CVFmx2008+QL*CVLmx2008+QS*CVSmx2008+QR*CVRmx2008+QBr*CVBrmx2008+Qno*CVnomx2008)/QC
        CVAUCmx2008= integ(cvmx2008,0.)

!AX = Amount exhaled (mg)'
        RAImx = QP*CImx
        AImx =integ(RAImx,0.)
        !doseinhmx= aimx-axmx

!AS = Amount in slowly perfused tissues (mg)'
        RASmx2008 = QS*(CAmx2008-CVSmx2008)
        ASmx2008 = INTEG(RASmx2008,0.)
        CVSmx2008 = ASmx2008/(VS*PSmx)
        CSmx2008 = ASmx2008/VS
```

```
!AR = Amount in rapidly perfused tissues (mg)'
      RARmx2008 = QR*(CAmx2008-CVRmx2008)
      ARmx2008 = INTEG(RARmx2008,0.)
      CVRmx2008 = ARmx2008/(VR*PRmx)
      CRmx2008 = ARmx2008/VR

!AF = Amount in fat tissue (mg)
   RAVFmx2008= QF*(CAmx2008-CVFmx2008)+(PAFmx*CFmx2008)/PFmx-PAFmx*CVFmx2008
         AVFmx2008=INTEG(RAVFmx2008,0.)
         CVFmx2008=AVFmx2008/(BVF*VF)

         RAFmx2008=PAFmx*CVFmx2008-(PAFmx*CFmx2008)/PFmx
         AFmx2008=INTEG(RAFmx2008,0.)
         CFmx2008=AFmx2008/((1-BVF)*VF)
   AUCFmx2008=INTEG(CFmx2008,0.)


!AB = Amount in brain tissue diffusion limited(mg)'
           RABrmx2008 = QBr*(CAmx2008-CVBrmx2008)
     ABmx2008 = INTEG(RABrmx2008,0.)
     CVBrmx2008 = ABmx2008/(VBr*PBmx)
     CBrmx2008 = ABmx2008/VBr

!AL = Amount in liver tissue (mg)'
     RALmx2008 = QL*(CAmx2008-CVLmx2008)-RAM1mx2008
           ALmx2008=INTEG(RALmx2008,0.)
           CVLmx2008=ALmx2008/(PLmx*VL)
           CLmx2008=ALmx2008/VL

     !MASS = mass balance (mg)
```

```
      MASSmx2008 =
AFmx2008+ALmx2008+ASmx2008+ARmx2008+AXmx2008+ABmx2008+am1mx2008+atnomx2008+alungtmx2008
masbalmx=aimx-massmx2008
mb5mx2008=(alunglost2mx2008+anaslost2mx2008+alungvapormx2008)-massmx2008

!----------------------------------[LUMP 1]-------------------------------------------------------
kInhPULP =  QP * CIaLP * (fdepositPU+fdepositTB)       ! mppd2 Pulmonary (Lung+TB)
kInhNOLP = QP * CIaLP * (fdepositNO)       ! nasal region
kIvLP =  QP * CIvLP       ! vapor
!{Exposure parameters LUMP}
 !exposure =  pulse(0.0,exptime, tchng)
CIXLP = (ICONiLP*MWLP/24450)                    ! Inhaled concentration, converts to mg/L
CIvLP = (CIXLP*perc_vaporLP)*exposure      ! Turn on vapor inhalation
CIaLP = ((CIXLP*perc_aerosolLP)* exposure)     ! Turn on aerosol in MPPD2
CILP=CIvLP+CIaLP                                ! Total, is used for cxppm calculation

!{Nasal Compartment LUMP}
!transfer of chemical across mucous layer in nasal
RnintakeLP=kinhnoLP
RnmucousLP = (RnintakeLP-PAnoseLP*CnmucousLP)
anmucousLP = integ(rnmucousLP,0.0)
cnmucousLP = anmucousLP/vnasmuclayer
!nasal tissue
RnasaltLP = (PAnoseLP*cnmucousLP) + Qno*(calp-cvnoLP)
anasaltLP= integ(rnasaltLP,0.0)
cnasaltLP=anasaltLP/vno
cvnoLP = cnasaltLP/pnoLP

AtnoLP = anasaltLP!

!Nasal Compartment Mass Balance
Mbnolp = (anaslost2lp+anoseinlp) - (anasaltlp+anoseoutlp)
rnoseinlp=qno*ca1mlp
```

```
anoseinlp=integ(rnoseinlp,0.0)
rnoseoutlp=qno*cvnolp
anoseoutlp=integ(rnoseoutlp,0.0)
rnaslost2lp=panoselp*cnmucouslp
anaslost2lp=integ(rnaslost2lp,0.0)

!{Lung Compartment}
!transfer of chemical across mucous layer in conducting lung
RLintakeLP=kinhpuLP
RLmucousLP = (RLintakeLP-PA1LP*CLmucousLP)
aLmucousLP = integ(rLmucousLP,0.0)
CLmucousLP = aLmucousLP/vtbmuclayer
!Lung tissue
RlungLP = (QC*(Ca1LP-CaLP)+(PA1LP*clmucousLP))    !!!+(QP*CIV))!-((cLungt/plua)*QP))!- (PA2*(clungt/PLU))
alungtLP= integ(rlungLP,0.0)  !
clungtLP=alungtLP/vlu !
caLP = clungtLP/pluLP  !

CA1LP = (QC*CvLP+Qp*CivLP)/(QC+(QP/PwBLP))
      CXLP = CA1LP/PwBLP
      rAXLP = QP*CXLP
axLP=integ(raxLP,0.0)
CXPPMLP=(0.7*cxLP+0.3*ci)*24450/MWLP

AtpuLP =alungtLP ! removed mucus

!CV = Mixed venous blood concentration (mg/l)'
         CVlp = (QF*CVFlp+QL*CVLlp+QS*CVSlp+QR*CVRlp+QBr*CVBrlp+Qno*cvnolp)/QC
         CVAUClp= integ(cvlp,0.)

!AX = Amount exhaled (mg)'
         !CXlp = CAlp/PWBlp !
         !RAXlp = QP*CXlp !
```

```
          !AXlp = INTEG(RAXlp, 0.) !
          RAIlp = QP*CIlp
          AIlp =integ(RAIlp,0.)
          !doseinhlp= ailp-axlp

!AS = Amount in slowly perfused tissues (mg)'
          RASlp = QS*(CAlp-CVSlp)
          ASlp = INTEG(RASlp,0.)
          CVSlp = ASlp/(VS*PSlp)
          CSlp = ASlp/VS

!AR = Amount in rapidly perfused tissues (mg)'
          RARlp = QR*(CAlp-CVRlp)
       ARlp = INTEG(RARlp,0.)
       CVRlp = ARlp/(VR*PRlp)
       CRlp = ARlp/VR

!AF = Amount in fat tissue (mg)

   RAVFlp= QF*(CAlp-CVFlp)+((PAFlp*CFlp)/PFlp)-(PAFlp*CVFlp)
          AVFlp=INTEG(RAVFlp,0.)
          CVFlp=AVFlp/(BVF*VF)

          RAFlp=PAFlp*CVFlp-(PAFlp*CFlp)/PFlp
          AFlp=INTEG(RAFlp,0.)
          CFlp=AFlp/((1-BVF)*VF)
   AUCFlp=INTEG(CFlp,0.)


!AB = Amount in brain tissue diffusion limited(mg)'
     RABrlp = QBr*(CAlp-CVBrlp)
     ABrlp = INTEG(RABrlp,0.)
     CVBrlp = ABrlp/(VBr*PBrlp)
```

```
    CBrlp = ABrlp/VBr

!AL = Amount in liver tissue (mg)'
    RALlp = QL*(CAlp-CVLlp)-RAMlp
        ALlp=INTEG(RALlp,0.)
        CVLlp=ALlp/(PLlp*VL)
        CLlp=ALlp/VL

    !MASS = mass balance (mg)
     MASSlp = AFlp+AVFlp+ALlp+ASlp+ARlp+AXlp+ABrlp+amlp+atnolp+alungtlp
    massballp=ailp-masslp
mb5lp=(alunglost2lp+anaslost2lp+alungvaporlp)-masslp


!-------------[OCTANE MODEL]------------------------------------------------------
kInhPUc8 =  QP * CIac8 * (fdepositPU+fdepositTB)       ! mppd2 Pulmonary (Lung+TB)
kInhNOc8 = QP * CIac8 * (fdepositNO)       ! nasal region
kIvc8 =  QP * CIvc8        ! vapor

!{Exposure parameters LUMP}
 !exposure =  pulse(0.0,exptime, tchng)
CIXc8 = (ICONic8*MWC8/24450)                                    ! Inhaled concentration, converts to mg/L
CIvc8 = (CIXc8*perc_vaporc8)*exposure      ! Turn on vapor inhalation
CIac8 = ((CIXc8*perc_aerosolc8)* exposure)    ! Turn on aerosol in MPPD2
CIc8=CIvc8+CIac8

![SHALLOW + DEEP BLOOD octane]
CVC8 =((QF*CVFc8 + QL*CVLc8 + QS*CVSc8 + QR*CVRc8 + QBr*CVBrc8 + qno*cvnoc8)/QC)!  venous
CVAUC_c8 = integ(CVc8,0.0) !

!{Nasal Compartment}
!transfer of chemical across mucous layer in nasal
Rnintakec8=kinhnoc8
```

```
Rnmucousc8 = (Rnintakec8-PAnosec8*Cnmucousc8)
anmucousc8 = integ(rnmucousc8,0.0)
cnmucousc8 = anmucousc8/vnasmuclayer
!nasal tissue
!Rnasalt = (ff*(PAnose*cnmucous) + Qno*(ca1-cvno))
Rnasaltc8 = (PAnosec8*cnmucousc8) + Qno*(cac8-cvnoc8) !Qno*(ca1-cvno)
anasaltc8= integ(rnasaltc8,0.0)
cnasaltc8=anasaltc8/vno
cvnoc8 = cnasalt/pno

Atnoc8 = anasaltc8!

!Nasal Compartment Mass Balance
mbnoc8 = (anaslost2+anosein) - (anasalt+anoseout)
rnoseinc8=qno*ca1c8
anoseinc8=integ(rnoseinc8,0.0)
rnoseoutc8=qno*cvnoc8
anoseoutc8=integ(rnoseoutc8,0.0)
rnaslost2c8=panosec8*cnmucousc8
anaslost2c8=integ(rnaslost2c8,0.0)

!{Lung Compartment}
!transfer of chemical across mucous layer in conducting lung
RLintakec8=kinhpuc8
RLmucousc8 = (RLintakec8-PA1c8*CLmucousc8)
aLmucousc8 = integ(rLmucousc8,0.0)
CLmucousc8 = aLmucousc8/vtbmuclayer
!Lung tissue
Rlungc8 = (QC*(Ca1c8-Cac8)+(PA1c8*clmucousc8))    !!!+(QP*CIV))!-((cLungt/plua)*QP))!- (PA2*(clungt/PLU))
alungtc8= integ(rlungc8,0.0)  !
clungtc8=alungtc8/vlu !
cac8 = clungtc8/pluc8  !
```

```
CA1c8 = (QC*Cvc8+Qp*Civc8)/(QC+(QP/PBc8))
      CXc8 = CA1c8/PBc8
      rAXc8 = QP*CXc8
axc8=integ(raxc8,0.0)
CXPPMc8=(0.7*cxc8+0.3*cic8)*24450/MWC8

Atpuc8 =alungtc8 ! removed mucus

!Lung Compartment Mass Balance
mblungsc8 = (alunglost2c8+alunginc8) - (alungtc8+alungoutc8)!-(alunglost4)
rlunginc8=qc*ca1c8
alunginc8=integ(rlunginc8,0.0)
rlungoutc8=qc*cac8
alungoutc8=integ(rlungoutc8,0.0)
rlunglost2c8=pa1c8*clmucousc8
alunglost2c8=integ(rlunglost2c8,0.0)
rlungvaporc8=QP*CIVc8
alungvaporc8=integ(rlungvaporc8,0.0)

!{RAPID}
!Chemical in rapidly perfused tissue compartment (Perfusion)
 RARc8 = QR*(cac8-CVRc8)                                    !rate of change in rapidly perfused - mg/h
   ARc8 = integ(RARc8, 0.0)              !inital amount in viscera - mg
 CRc8 = ARc8/VR                        !viscera concentration - mg/L
 CVRc8 = CRc8/PRc8                             !concentration in venous capillary blood - mg/L

!Rapid Compartment Mass Balance
rapidmassbalc8=(arapidinc8)-(AR+arapidoutc8)
rarapidinc8=qr*cac8
arapidinc8 = integ(rarapidinc8,0.0)
rarapidoutc8=qr*cvrc8
arapidoutc8=integ(rarapidoutc8,0.0)
```

```
!{SLOW}
!Chemical in slowly perfused tissue compartment (Perfusion)
 RASc8 = QS*(cac8-CVSc8)                          !rate of change in slowly perfused  - mg/h
   ASc8 = integ(RASc8, 0.0)                !inital amount in slowly perfused tissue - mg
 CSc8 = ASc8/VS                          !slowly perfused tissue concentration - mg/L
 CVSc8 = CSc8/PSc8                             !concentration in venous blood - mg/L
astotc8 = asc8 !

!Slow Compartment Mass Balance
slowmassbalc8=(aslowinc8)-(ASc8+aslowoutc8)
raslowinc8=qs*cac8
aslowinc8 = integ(raslowinc8,0.0)
raslowoutc8=qs*cvsc8
aslowoutc8=integ(raslowoutc8,0.0)

!{BRAIN}
!chem brain blood (Diffusion)
RABrbc8 = ((QBr*(cac8-CVBrc8)) - (PABrinc8*CVBrc8) + (PABroutc8*(CBrc8/PBrc8)))  !rate of change in brain blood amount -
mg/h made 1st + not
  ABrbc8 = integ(RABRbc8, 0.0)                    !initial amount in blood - mg
 CVBrc8= ABrbc8/Bvbr                          !concentration in brain blood
!chem in brain tissue (Diffusion)
RABrc8 = (PABrinc8*CVBrc8) - (PABroutc8*(CBrc8/PBrc8))          !rate of change in brain tissue
   ABrc8 = integ(rABrc8, 0.0)                    !initial amount in tissue
 CBrc8 = ABr/(VBr-Bvbr)                         !concentration in brain tissue
abrtotc8= abrc8+abrbc8                          !total brain

!Brain Compartment Mass Balance
brainmassbalc8=(abraininc8+abraindiffinc8)-(Abrc8+abrainoutc8+abraindiffoutc8)
rabraininc8=qbr*cac8
abraininc8 = integ(rabraininc8,0.0)
rabrainoutc8=qbr*cvbrc8
abrainoutc8=integ(rabrainout,0.0)
```

```
rabraindiffinc8 =(PABrin*CVBr)
abraindiffinc8 =integ (rabraindiffinc8,0.0)
rabraindiffoutc8= PABroutc8*(CBrc8/PBrc8)
abraindiffoutc8=integ(rabraindiffoutc8,0.0)

!{FAT}
!chem in fat blood (Diffusion)
RAFbc8 = (QF*(cac8-CVFc8) - (PAFinc8*CVFc8) + (PAFoutc8*(CFc8/PFc8)))  !rate of change in fat blood amount - mg/h made
add PAinf*cf/pf
AFbc8 = integ(Rafbc8,0.0)                    !initial amount in blood - mg
CVFc8 = AFbc8/Bvf                            !concentration in fat blood

!chem in shall fat tissue (Diffusion)
RAFc8 = (PAFinc8*CVFc8) - (PAFoutc8*(Cfc8/Pfc8))!
AFc8 = integ(Rafc8,0.0)       !initial amount in fat
CFc8 = Afc8/(vf-bvf)          !concentration in fat tissue

aftotc8=afc8+afbc8                           !total fat amount

!Fat Compartment 1 Mass Balance
fatmassbalc8=(afatinc8+afatdiffinc8)-(AFc8+afatoutc8+afatdiffoutc8)
rafatinc8=qf*cac8
afatinc8 = integ(rafatinc8,0.0)
rafatoutc8=qf*cvfc8
afatoutc8=integ(rafatoutc8,0.0)
rafatdiffinc8 =(PAfinc8*CVfc8)
afatdiffinc8 =integ (rafatdiffinc8,0.0)
rafatdiffoutc8= PAfoutc8*(Cfc8/Pfc8)
afatdiffoutc8=integ(rafatdiffoutc8,0.0)

 !{LIVER} rk-df liver
!Chemical in liver blood (Diffusion)
RALbc8 = QL*(Cac8-CVLc8) - (PALinc8*CVLc8) + (PALoutc8*(CLc8/PLc8))-RAMETc8   !
```

```
 ALbc8 =integ(Ralbc8, 0.0)
 CVLc8 = ALbc8/BvL
 !concentration in liver blood
RALc8=(PALinc8*CVLc8) - (PALoutc8*(CLc8/PLc8))
ALc8 =integ(Ralc8, 0.0)
 CLc8 = ALc8/(VL-BvL)
ALtotc8 = ALbc8+ALc8

!Liver Compartment Mass Balance
livermassbalc8=(aliverinc8+aliverdiffinc8)-(Alc8+aliveroutc8+aliverdiffoutc8+ametc8)
raliverinc8=ql*cac8
aliverinc8 = integ(raliverinc8,0.0)
raliveroutc8=ql*cvlc8
aliverout=integ(raliveroutc8,0.0)
raliverdiffinc8=(PALinc8*(CLc8/plc8))
aliverdiffinc8 =integ (rafatdiffinc8,0.0)
raliverdiffoutc8= PAloutc8*(CLc8/plc8))
aliverdiffoutc8=integ(raliverdiffoutc8,0.0)
raliverdiffoutc8= PAloutc8*(Clc8/Plc8)



!Mass balance for c8 inhalation
   Massc8  = AFtotc8 + AStotc8 + ARc8 + ALtotc8+ ABrtotc8 + axc8 + Atpuc8 +atnoc8 !
mb5c8=(alunglost2c8+anaslost2c8+alungvaporc8)-massc8


!--------------------[ DECANE MODEL CODE]---------------------------------
!{Exposure parameters, C10 model }
!INHALATION FOR C10
kInhPU =  QP * CIa * (fdepositPU+fdepositTB)        ! mppd2 Pulmonary (Lung+TB)
kInhNO = QP * CIa * (fdepositNO)        ! nasal region
kIv =  QP * CIv        ! vapor
```

```
 exposure =  pulse(0.0,exptime, tchng)
CIX = (ICONi*MW/24450)                                  ! Inhaled concentration, converts to mg/L ,conversion is
mg/L=(Xppm)(MW)/24450, 0.798 is total retention for C14-only
CIv = (CIX*perc_vapor)*exposure      ! Turn on vapor inhalation
CIa = ((CIX*perc_aerosol)* exposure)!*ff      ! Turn on aerosol in MPPD2
CI=CIv+CIa                                  ! Total, is used for cxppm calculation


CV =((QF*CVF + QL*CVL + QS*CVS + QR*CVR + QBr*CVBr + qno*cvno)/QC)!     ! venous
CVAUCc8 = integ(CVc8,0.0) !

!{Nasal Compartment}
!transfer of chemical across mucous layer in nasal
Rnintake=kinhno
Rnmucous = (Rnintake-PAnose*Cnmucous)
anmucous = integ(rnmucous,0.0)
cnmucous = anmucous/vnasmuclayer
!nasal tissue
!Rnasalt = (ff*(PAnose*cnmucous) + Qno*(ca1-cvno))
Rnasalt = (PAnose*cnmucous) + Qno*(ca-cvno) !Qno*(ca1-cvno)
anasalt= integ(rnasalt,0.0)
cnasalt=anasalt/vno
cvno = cnasalt/pno

Atno = anasalt!

!Nasal Compartment Mass Balance
mbno = (anaslost2+anosein) - (anasalt+anoseout)
rnosein=qno*ca1
anosein=integ(rnosein,0.0)
rnoseout=qno*cvno
anoseout=integ(rnoseout,0.0)
```

```
rnaslost2=panose*cnmucous
anaslost2=integ(rnaslost2,0.0)

!{Lung Compartment}
!transfer of chemical across mucous layer in conducting lung
RLintake=kinhpu
RLmucous = (RLintake-PA1*CLmucous)
aLmucous = integ(rLmucous,0.0)
CLmucous = aLmucous/vtbmuclayer
!Lung tissue
Rlung = (QC*(Ca1-Ca)+(PA1*clmucous))    !!!+(QP*CIV))!-((cLungt/plua)*QP))!- (PA2*(clungt/PLU))
alungt= integ(rlung,0.0)  !
clungt=alungt/vlu !
ca = clungt/plu !

CA1 = (QC*Cv+Qp*Civ)/(QC+(QP/PB))
      CX = CA1/PB
      rAX = QP*CX
ax=integ(rax,0.0)
ai=qp*ci

 CXPPM=(0.7*cx+0.3*ci)*24450/MW

Atpu =alungt ! removed mucus

!Lung Compartment Mass Balance
mblungs = (alunglost2+alungin) - (alungt+alungout)
rlungin=qc*ca1
alungin=integ(rlungin,0.0)
rlungout=qc*ca
alungout=integ(rlungout,0.0)
rlunglost2=pa1*clmucous
alunglost2=integ(rlunglost2,0.0)
```

```
rlungvapor=QP*CIV
alungvapor=integ(rlungvapor,0.0)

!{RAPID}
!Chemical in rapidly perfused tissue compartment (Perfusion)
 RAR = QR*(ca-CVR)                                  !rate of change in rapidly perfused - mg/h
   AR = integ(RAR, 0.0)                !inital amount in viscera - mg
 CR = AR/VR                              !viscera concentration - mg/L
 CVR = CR/PR                            !concentration in venous capillary blood - mg/L

!Rapid Compartment Mass Balance
rapidmassbal=(arapidin)-(AR+arapidout)
rarapidin=qr*ca
arapidin = integ(rarapidin,0.0)
rarapidout=qr*cvr
arapidout=integ(rarapidout,0.0)

!{SLOW}
!Chemical in slowly perfused tissue compartment (Perfusion)
 RAS = QS*(ca-CVS)                              !rate of change in slowly perfused  - mg/h
   AS = integ(RAS, 0.0)                !inital amount in slowly perfused tissue - mg
 CS = AS/VS                              !slowly perfused tissue concentration - mg/L
 CVS = CS/PS                            !concentration in venous blood - mg/L
astot = as !

!Slow Compartment Mass Balance
slowmassbal=(aslowin)-(AS+aslowout)
raslowin=qs*ca
aslowin = integ(raslowin,0.0)
raslowout=qs*cvs
aslowout=integ(raslowout,0.0)

!{BRAIN}
```

```
!chem brain blood (Diffusion)
RABrb = ((QBr*(ca-CVBr)) - (PABrin*CVBr) + (PABrout*(CBr/PBr)))  !
  ABrb = integ(RABRb, 0.0)                          !initial amount in blood - mg
 CVBr = ABrb/Bvbr                                   !concentration in brain blood
!chem in brain tissue (Diffusion)
RABr = (PABrin*CVBr) - (PABrout*(CBr/PBr))          !rate of change in brain tissue
   ABr = integ(rABr, 0.0)                           !initial amount in tissue
 CBr = ABr/(VBr-Bvbr)                               !concentration in brain tissue
abrtot= abr+abrb                                    !total brain

!Brain Compartment Mass Balance
brainmassbal=(abrainin+abraindiffin)-(Abr+abrainout+abraindiffout)
rabrainin=qbr*ca
abrainin = integ(rabrainin,0.0)
rabrainout=qbr*cvbr
abrainout=integ(rabrainout,0.0)
rabraindiffin =(PABrin*CVBr)
abraindiffin =integ (rabraindiffin,0.0)
rabraindiffout= PABrout*(CBr/PBr)
abraindiffout=integ(rabraindiffout,0.0)

!{FAT}
!chem in fat blood (Diffusion)
RAFb = (QF*(ca-CVF) - (PAFin*CVF) + (PAFout*(CF/PF)))  !rate of change in fat blood amount - mg/h made add PAinf*cf/pf
AFb = integ(Rafb,0.0)                               !initial amount in blood - mg
CVF = AFb/Bvf                                       !concentration in fat blood

!chem in shall fat tissue (Diffusion)
RAF = (PAFin*CVF) - (PAFout*(Cf/Pf))          !rate of change in fat tissue
AF = integ(Raf,0.0)           !initial amount in fat
CF = Af/(vf-bvf)              !concentration in fat tissue
!cvf=cf/pf
```

```
aftot=af+afb                              !total fat amount

!Fat Compartment 1 Mass Balance
fatmassbal=(afatin+afatdiffin)-(AF+afatout+afatdiffout)
rafatin=qf*ca
afatin = integ(rafatin,0.0)
rafatout=qf*cvf
afatout=integ(rafatout,0.0)
rafatdiffin =(PAfin*CVf)
afatdiffin =integ (rafatdiffin,0.0)
rafatdiffout= PAfout*(Cf/Pf)
afatdiffout=integ(rafatdiffout,0.0)


!{LIVER} rk-df liver
!Chemical in liver blood (Diffusion)
RALb = QL*(Ca-CVL) - (PALin*CVL) + (PALout*(CL/PL))-RAMET
 ALb =integ(Ralb, 0.0)                    !initial amount in liver blood - mg
 CVL = ALb/BvL
RAL=(PALin*CVL) - (PALout*(CL/PL))
AL =integ(Ral, 0.0)
 CL = AL/(VL-BvL)
ALtot = ALb+AL

  !Liver Compartment Mass Balance
livermassbal=(aliverin+aliverdiffin)-(Al+aliverout+ aliverdiffout+amet)
raliverin=ql*ca
aliverin = integ(raliverin,0.0)
raliverout=ql*cvl
aliverout=integ(raliverout,0.0)
raliverdiffin=(PALin*(CL/pl))
aliverdiffin =integ (rafatdiffin,0.0)
raliverdiffout= PAlout*(Cl/(cl/pl))
```

```
aliverdiffout=integ(raliverdiffout,0.0)
  Mass  = AFtot + AStot + AR + ALtot+ ABrtot + ax + amet + Atpu +atno !
mb5=(alunglost2+anaslost2+alungvapor)-mass



!-------------[C14 MODEL]-----------------------------------------------------------
CIXC14 = (ICONiC14*MWC14/24450)                                  ! Inhaled concentration, converts ppm to mg/L ,conversion is
mg/L=(Xppm)(MW)/24450, 0.798 is total retention for C14-only
CIvC14 = (CIXC14*perc_vaporC14)*exposure      ! Turn on vapor inhalation
CIaC14 = ((CIXC14*perc_aerosolC14)* exposure)!*ff      ! Turn on aerosol in MPPD2
CIC14=CIvC14+CIaC14                                          ! Total, is used for cxppm calculation

kInhPUC14 =  QP * CIaC14 * (fdepositPU+fdepositTB)        ! mppd2 Pulmonary (Lung+TB)
kInhNOC14 = QP * CIaC14 * (fdepositNO)        ! nasal region
kIvC14=  QP * CIvC14        ! vapor


!{Nasal Compartment}
!transfer of chemical across mucous layer in nasal
RnintakeC14=kinhnoC14
RnmucousC14 = (RnintakeC14-PAnoseC14*CnmucousC14)
anmucousC14 = integ(rnmucousC14,0.0)
cnmucousC14 = anmucousC14/vnasmuclayer
!nasal tissue
RnasaltC14 = (PAnoseC14*cnmucousC14) + Qno*(caC14-cvnoC14) !
anasaltC14= integ(rnasaltC14,0.0)
cnasaltC14=anasaltC14/vno
cvnoC14 = cnasaltC14/pnoC14

AtnoC14 = anasaltC14!

!Nasal Compartment Mass Balance
```

```
mbnoC14 = (anaslost2C14+anoseinC14) - (anasaltC14+anoseoutC14)
rnoseinC14=qno*ca1C14
anoseinC14=integ(rnoseinC14,0.0)
rnoseoutC14=qno*cvnoC14
anoseoutC14=integ(rnoseoutC14,0.0)
rnaslost2C14=panoseC14*cnmucousC14
anaslost2C14=integ(rnaslost2C14,0.0)

!{Lung Compartment}
!transfer of chemical across mucous layer
RLintakeC14=kinhpuC14
RLmucousC14 = (RLintakeC14-PA1C14*CLmucousC14)
aLmucousC14 = integ(rLmucousC14,0.0)
CLmucousC14 = aLmucousC14/vtbmuclayer
!Lung tissue
RlungC14 = (QC*(Ca1C14-CaC14)+(PA1C14*clmucousC14))
alungtC14= integ(rlungC14,0.0)  !
clungtC14=alungtC14/vlu !
caC14 = clungtC14/pluC14

!
CA1C14 = (QC*CvC14+Qp*CivC14)/(QC+(QP/PBC14))
      CXC14 = CA1C14/PBC14
      rAXC14 = QP*CXC14
axC14=integ(raxC14,0.0)

CXPPMC14=(0.7*cxC14+0.3*ciC14)*24450/MWC14

AtpuC14 =alungtC14 !

!Lung Compartment Mass Balance
mblungsC14 = (alunglost2C14+alunginC14) - (alungtC14+alungoutC14)!-(alunglost4)
rlunginC14=qc*ca1C14
```

```
alunginC14=integ(rlunginC14,0.0)
rlungoutC14=qc*caC14
alungoutC14=integ(rlungoutC14,0.0)
rlunglost2C14=pa1C14*clmucousC14
alunglost2C14=integ(rlunglost2C14,0.0)
rlungvaporC14=QP*CIVC14
alungvaporC14=integ(rlungvaporC14,0.0)


!{RAPID}
!Chemical in rapidly perfused tissue compartment (Perfusion)
 RARC14 = QR*(caC14-CVRC14)                                    !rate of change in rapidly perfused - mg/h
   ARC14 = integ(RARC14, 0.0)              !inital amount in viscera - mg
 CRC14= ARC14/VR                           !viscera concentration - mg/L
 CVRC14 = CRC14/PRC14                            !concentration in venous capillary blood - mg/L

!Rapid Compartment Mass Balance
rapidmassbalC14=(arapidinC14)-(AR+arapidoutC14)
rarapidinC14=qr*caC14
arapidinC14 = integ(rarapidinC14,0.0)
rarapidoutC14=qr*cvrC14
arapidoutC14=integ(rarapidoutC14,0.0)


!{SLOW}
!Chemical in slowly perfused tissue compartment (Perfusion)
 RASC14 = QS*(caC14-CVSC14)                              !rate of change in slowly perfused  - mg/h
   ASC14 = integ(RASC14, 0.0)              !inital amount in slowly perfused tissue - mg
 CSC14 = ASC14/VS                          !slowly perfused tissue concentration - mg/L
 CVSC14 = CSC14/PSC14                      !concentration in venous blood - mg/L

!Slow Compartment Mass Balance
slowmassbalC14=(aslowinC14)-(ASC14+aslowoutC14)
```

```
raslowinC14=qs*caC14
aslowinC14 = integ(raslowinC14,0.0)
raslowoutC14=qs*cvsC14
aslowoutC14=integ(raslowoutC14,0.0)

!{BRAIN}
!chem brain blood (Diffusion)
RABrbC14 = ((QBr*(caC14-CVBrC14)) - (PABrinC14*CVBrC14) + (PABroutC14*(CBrC14/PBrC14)))  !rate of change in brain
blood amount - mg/h made 1st + not
  ABrbC14 = integ(RABRbC14, 0.0)                    !initial amount in blood - mg
 CVBrC14 = ABrbC14/Bvbr                             !concentration in brain blood
!chem in brain tissue (Diffusion)
RABrC14 = (PABrinC14*CVBrC14) - (PABroutC14*(CBrC14/PBrC14))          !rate of change in brain tissue
   ABrC14 = integ(rABrC14, 0.0)                     !initial amount in tissue
 CBrC14 = ABrC14/(VBr-Bvbr)                         !concentration in brain tissue
abrtotC14= abrC14+abrbC14                           !total brain

!Brain Compartment Mass Balance
brainmassbalC14=(abraininC14+abraindiffinC14)-(AbrC14+abrainoutC14+abraindiffoutC14)
!brainmassbal=(abrainin)-(Abr+abrainout)
rabraininC14=qbr*caC14
abraininC14 = integ(rabraininC14,0.0)
rabrainoutC14=qbr*cvbrC14
abrainoutC14=integ(rabrainoutC14,0.0)
rabraindiffinC14 =(PABrinC14*CVBrC14)
abraindiffinC14 =integ (rabraindiffinC14,0.0)
rabraindiffoutC14= PABroutC14*(CBrC14/PBrC14)
abraindiffoutC14=integ(rabraindiffoutC14,0.0)

!{FAT}
!chem in fat blood (Diffusion)
RAFbC14 = (QF*(caC14-CVFC14) - (PAFinC14*CVFC14) + (PAFoutC14*(CFC14/PFC14)))  !
AFbC14 = integ(RafbC14,0.0)                 !initial amount in blood - mg
```

```
CVFC14 = AFbC14/Bvf                          !concentration in fat blood

!chem in shall fat tissue (Diffusion)
RAFC14 = (PAFinC14*CVFC14) - (PAFoutC14*(CfC14/PfC14))!
AFC14 = integ(RafC14,0.0)                    !initial amount in fat
CFC14 = AfC14/(vf-bvf) !                     !concentration in fat tissue
aftotC14=afC14+afbC14                        !total fat amount

!Fat Compartment 1 Mass Balance
fatmassbalC14=(afatinC14+afatdiffinC14)-(AFC14+afatoutC14+afatdiffoutC14)
!fatmassbal=(afatin)-(AF+afatout)
rafatinC14=qf*caC14
afatinC14 = integ(rafatinC14,0.0)
rafatoutC14=qf*cvfC14
afatoutC14=integ(rafatoutC14,0.0)
rafatdiffinC14 =(PAfinC14*CVfC14)
afatdiffinC14 =integ (rafatdiffinC14,0.0)
rafatdiffoutC14= PAfoutC14*(CfC14/PfC14)
afatdiffoutC14=integ(rafatdiffoutC14,0.0)


!Liver Compartment Mass Balance
livermassbalC14=(aliverinC14+aliverdiffinC14)-(AlC14+aliveroutC14+aogblC14+aliverdiffoutC14+ametC14)
!livermassbal=(aliverin)-(Al+aliverout+aogbl)
raliverinC14=ql*caC14
aliverinC14 = integ(raliverinC14,0.0)
raliveroutC14=ql*cvlC14
aliveroutC14=integ(raliveroutC14,0.0)

raliverdiffinC14 =(PAlinC14*(CdLC14/PdL2bC14))
!raliverdiffin=(PALin*(CL/pl))
aliverdiffinC14 =integ (rafatdiffinC14,0.0)
```

```
raliverdiffoutC14= PAloutC14*(ClC14/(PlaC14/pfaC14))
!raliverdiffout=(PALout*(CdL/PdL2b))
aliverdiffoutC14=integ(raliverdiffoutC14,0.0)

!raliverdiffout= PAlout*(Cl/Pl)
!raliverdiff2out=(PA2Lout*(CdL/PdL2b))
!aliverdiff2out=integ(raliverdiff2out,0.0)

!chem in liver tissue (Diffusion) shall
rALC14 = QL*(CaC14-cvlC14)+(PALinC14*(CdLC14/PdL2bC14))- PALoutC14*(clC14/(plaC14/pfaC14)) - RAMETC14!
ALC14 = integ(RalC14, 0.0)                          !initial amount in liver
 CLC14 = ALC14/(vsl)      !-bvl                        !concentration
cvlC14=clC14/plC14
!chem in liver tissue (Diffusion) deep
radlC14 = -(PALinC14*(CdLC14/PdL2bC14))+PALoutC14*(clC14/(plaC14/pfaC14))
adlC14= integ (radlC14, 0)
cdlC14 = adlC14/vdl

! tot
altotC14=alC14+adlC14

!Mass balance for c14 inhalation
   MassC14  = AFtotC14 + ASC14 + ARC14 + ALtotC14+ ABrtotC14 + axC14 + AtpuC14 +atnoC14 + AMetC14!!
   !Mass = AF + AS + AR + AL+ ABr + aEXHALE + AOGBL + Atno + Adeppu + atb !
   !mb    = ainhale - mass
mb5C14=(alunglost2C14+anaslost2C14+alungvaporC14)-massC14




!-------------[[LUMP 2]]-----------------------------------------------------------------------------------------
kInhPULUMP =  QP * CIaLUMP * (fdepositPU+fdepositTB)        ! mppd2 Pulmonary (Lung+TB)
!kInhLRT = QP * Cpaero * (fdepositpu)   !LRT
```

```
kInhNOLUMP = QP * CIaLUMP * (fdepositNO)        ! nasal region
kIvLUMP =  QP * CIvLUMP        ! vapor


!{Exposure parameters LUMP 2}
 !exposure =  pulse(0.0,exptime, tchng)
CIXLUMP = (ICONILUMP*MWLUMP/24450)     !
CIvLUMP = (CIXLUMP*perc_vaporLUMP)*exposure      ! Turn on vapor inhalation
CIaLUMP = ((CIXLUMP*perc_aerosolLUMP)* exposure)!*ff      ! Turn on aerosol in MPPD2
CILUMP=CIvLUMP+CIaLUMP                                    ! Total, is used for cxppm calculation

!{Nasal Compartment LUMP 2}
!transfer of chemical across mucous layer in nasal
RnintakeLUMP=kinhnoLUMP
RnmucousLUMP = (RnintakeLUMP-PAnoseLUMP*CnmucousLUMP)
anmucousLUMP = integ(rnmucousLUMP,0.0)
cnmucousLUMP = anmucousLUMP/vnasmuclayer
!nasal tissue
!Rnasalt = (ff*(PAnose*cnmucous) + Qno*(ca1-cvno))
RnasaltLUMP = (PAnoseLUMP*cnmucousLUMP) + Qno*(calump-cvnoLUMP)
anasaltLUMP= integ(rnasaltLUMP,0.0)
cnasaltLUMP=anasaltLUMP/vno
cvnoLUMP = cnasaltLUMP/pnoLUMP

AtnoLUMP = anasaltLUMP!

!{Lung Compartment Lump 2}
!transfer of chemical across mucous layer in conducting lung
RLintakeLUMP=kinhpuLUMP
RLmucousLUMP = (RLintakeLUMP-PA1LUMP*CLmucousLUMP)
aLmucousLUMP = integ(rLmucousLUMP,0.0)
CLmucousLUMP = aLmucousLUMP/vtbmuclayer
```

```
!Lung tissue lump 2
RlungLUMP = (QC*(Ca1LUMP-CaLUMP)+(PA1LUMP*clmucousLUMP))
alungtLUMP= integ(rlungLUMP,0.0)  !
clungtLUMP=alungtLUMP/vlu !
caLUMP = clungtLUMP/pluLUMP  !

CA1LUMP = (QC*CvLUMP+Qp*CivLUMP)/(QC+(QP/PBLUMP))
      CXLUMP = CA1LUMP/PBLUMP
      rAXLUMP = QP*CXLUMP
axLUMP=integ(raxLUMP,0.0)
CXPPMLUMP=(0.7*cxLUMP+0.3*ci)*24450/MWLUMP

AtpuLUMP =alungtLUMP ! removed mucus

!Venous Blood

CVLUMP=(QF*CVFLUMP + QL*CVLLUMP + QS*CVSLUMP + QR*CVRLUMP + QBr*CVBrLUMP +
QNO*CVNOLUMP)/QC
CVAUClump = integ(CVlump,0.0) !

!{RAPID LUMP 2}
!Chemical in rapidly perfused tissue compartment (Perfusion)
 RARlump = QR*(calump-CVRLUMP)                    !rate of change in rapidly perfused - mg/h
  ARlump = integ(RARLUMP, 0.0)          !inital amount in viscera - mg
 CRlump = ARLUMP/VR                  !viscera concentration - mg/L
 CVRLUMP = CRLUMP/PRLUMP                    !concentration in venous capillary blood - mg/L
 artotLUMP = arLUMP

![LIVER LUMP 2]
!Chemical in liver blood (Diffusion)
RALbLUMP = QL*(CaLUMP-CVLLUMP) - (PALinLUMP*CVLLUMP) + (PALoutLUMP*(CLLUMP/PLLUMP))-RAMLUMP

ALbLUMP =integ(RalbLUMP, 0.0)              !initial amount in liver blood - mg
```

```
 CVLLUMP = ALbLUMP/BvL                              !concentration in liver blood

RALLUMP=(PALinLUMP*CVLLUMP) - (PALoutLUMP*(CLLUMP/PLLUMP))
ALLUMP =integ(RalLUMP, 0.0)
 CLLUMP = ALLUMP/(VL-BvL)
ALtotLUMP = ALbLUMP+ALLUMP

!Liver Compartment Mass Balance
livermassballump=(aliverinlump+aliverdiffinlump)-(Allump+aliveroutlump +aliverdiffoutlump+ametlump)
raliverinlump=ql*calump
aliverinlump = integ(raliverinlump,0.0)
raliveroutlump=ql*cvllump
aliveroutlump=integ(raliveroutlump,0.0)
raliverdiffinlump=(PALinlump*(CLlump/pllump))
aliverdiffinlump =integ (rafatdiffinlump,0.0)
raliverdiffoutlump= PAloutlump*(Cllump/pllump)
aliverdiffoutlump=integ(raliverdiffoutlump,0.0)

!{Fat Perfusion LUMP 2}
!Chemical in fat tissue compartment
RAFbLUMP = (QF*(caLUMP-CVFLUMP) - (PAFinLUMP*CVFLUMP) + (PAFoutLUMP*(CFLUMP/PFlump)))  !
AFbLUMP = integ(RafbLUMP,0.0)                      !initial amount in blood - mg
CVFLUMP = AFbLUMP/Bvf                              !concentration in fat blood
RAFLUMP = (PAFinLUMP*CVFLUMP) - (PAFoutLUMP*(CfLUMP/PfLumP))!
AFLUMP = integ(RafLUMP,0.0)                        !initial amount in fat
CFLUMP = AfLUMP/(vf-bvf) !concentration in fat tissue
aftotLUMP=afLUMP+afbLUMP                           !total fat amount

!Fat Compartment 1 Mass Balance
fatmassbalLUMP=(afatinlump+afatdiffinlump)-(AFlump+afatoutlump+afatdiffoutlump)
rafatinLUMP=qf*calump
afatinLUMP = integ(rafatinLUMP,0.0)
rafatoutLUMP=qf*cvfLUMP
```

```
afatoutLUMP=integ(rafatoutLUMP,0.0)
rafatdiffinLUMP =(PAfinLUMP*CVfLUMP)
afatdiffinLUMP =integ (rafatdiffinLUMP,0.0)
rafatdiffoutLUMP= PAfoutLUMP*(CfLUMP/PfLUMP)
afatdiffoutLUMP=integ(rafatdiffoutLUMP,0.0)

!{SLOW, LUMP 2}
!Chemical in slowly perfused tissue compartment (Perfusion)
 RASLUMP = QS*(CALUMP-CVSLUMP)                          !rate of change in slowly perfused  - mg/h
   ASLUMP = integ(RASLUMP, 0.0)              !inital amount in slowly perfused tissue - mg
 CSLUMP = ASLUMP/VS                          !slowly perfused tissue concentration - mg/L
 CVSLUMP = CSLUMP/PSLump                     !concentration in venous blood - mg/L
astotLUmp = asLump !

!{Brain Perfusion LUMP 2}
!Chemical in rapidly perfused tissue compartment (Perfusion)
  RABrbLUMP = ((QBr*(caLUMP-CVBrLUMP)) - (PABrinLUMP*CVBrLUMP) + (PABroutLUMP*(CBrLUMP/PBrLumP)))
ABrbLUMP = integ(RABRbLUMP, 0.0)                  !initial amount in blood - mg
 CVBrLUMP= ABrbLUMP1/Bvbr                         !concentration in brain blood/PbRLUMP

RABrLUMP = (PABrinLUMP*CVBrLUMP) - (PABroutLUMP*(CBrLUMP/PBrLumP))
  ABrLUMP = integ(rABrLUMP, 0.0)                  !initial amount in tissue
 CBrLUMP = ABrlump/(VBr-Bvbr)                     !concentration in brain tissue
abrtotLUMP= abrLUMP+abrbLUMP                          !total brain

!Brain Compartment Mass Balance
brainmassbalLUMP=(abraininlump+abraindiffinlump)-(Abrlump+abrainoutlump+abraindiffoutlump)
rabraininLUMP=qbr*caLUMP
abraininLUMP = integ(rabraininLUMP,0.0)
rabrainoutLUMP=qbr*cvbrLUMP
abrainoutLUMP=integ(rabrainoutlump,0.0)
rabraindiffinLUMP =(PABrinlump*CVBrlump)
abraindiffinLUMP =integ (rabraindiffinLUMP,0.0)
```

```
rabraindiffoutLUMP= PABroutLUMP*(CBrLUMP/PBrLUMP)
abraindiffoutLUMP=integ(rabraindiffoutLUMP,0.0)

!Mass balance for lump 2 inhalation
MASSlump=AMetlump+AFTOTLUMP+ASTOTLUMP+ARTOTLUMP+ALTOTLUMP+ABRTOTLUMP+AXLUMP+ATNOLUM
P+ATPULUMP!
  !mblump    = ainhale - masslump
mb5lump=(alunglost2+anaslost2+alungvapor)-mass

!-------------[LUMP3 MODEL]-----------------------------------------------------------
CIXLUMP3 = (ICONiLUMP3*MWLUMP3/24450)                              ! Inhaled concentration, converts to mg/L
CIvLUMP3 = (CIXLUMP3*perc_vaporLUMP3)*exposure      ! Turn on vapor inhalation
CIaLUMP3 = ((CIXLUMP3*perc_aerosolLUMP3)* exposure)!*ff      ! Turn on aerosol in MPPD2
CILUMP3=CIvLUMP3+CIaLUMP3                                  ! Total, is used for cxppm calculation


kInhPULUMP3 =  QP * CIaLUMP3 * (fdepositPU+fdepositTB)        ! mppd2 Pulmonary (Lung+TB)
kInhNOLUMP3 = QP * CIaLUMP3 * (fdepositNO)        ! nasal region
kIvLUMP3=  QP * CIvLUMP3        ! vapor


![SHALLOW + DEEP BLOOD]
CVLUMP3 =((QF*CVFLUMP3 + QL*CVLLUMP3 + QS*CVSLUMP3 + QR*CVRLUMP3 + QBr*CVBrLUMP3 +
Qno*CvnoLUMP3)/QC)! venous
CVAUCLUMP3 = integ(CVLUMP3,0.0) !

!{Nasal Compartment}
!transfer of chemical across mucous layer in nasal
RnintakeLUMP3=kinhnoLUMP3
RnmucousLUMP3 = (RnintakeLUMP3-PAnoseLUMP3*CnmucousLUMP3)
anmucousLUMP3 = integ(rnmucousLUMP3,0.0)
cnmucousLUMP3 = anmucousLUMP3/vnasmuclayer
!nasal tissue
```

```
!Rnasalt = (ff*(PAnose*cnmucous) + Qno*(ca1-cvno))
RnasaltLUMP3 = (PAnoseLUMP3*cnmucousLUMP3) + Qno*(caLUMP3-cvnoLUMP3) !Qno*(ca1-cvno)
anasaltLUMP3= integ(rnasaltLUMP3,0.0)
cnasaltLUMP3=anasaltLUMP3/vno
cvnoLUMP3 = cnasaltLUMP3/pnoLUMP3

AtnoLUMP3= anasaltLUMP3!

!Nasal Compartment Mass Balance
mbnoLUMP3 = (anaslost2LUMP3+anoseinLUMP3) - (anasaltLUMP3+anoseoutLUMP3)
rnoseinLUMP3=qno*ca1LUMP3
anoseinLUMP3=integ(rnoseinLUMP3,0.0)
rnoseoutLUMP3=qno*cvnoLUMP3
anoseoutLUMP3=integ(rnoseoutLUMP3,0.0)
rnaslost2LUMP3=panoseC15*cnmucousLUMP3
anaslost2LUMP3=integ(rnaslost2LUMP3,0.0)

!{Lung Compartment}
!transfer of chemical across mucous layer in conducting lung
RLintakeLUMP3=kinhpuLUMP3
RLmucousLUMP3 = (RLintakeLUMP3-PA1LUMP3*CLmucousLUMP3)
aLmucousLUMP3 = integ(rLmucousLUMP3,0.0)
CLmucousLUMP3 = aLmucousLUMP3/vtbmuclayer
!Lung tissue
RlungLUMP3 = (QC*(Ca1LUMP3-CaLUMP3)+(PA1LUMP3*clmucousLUMP3))
alungtLUMP3= integ(rlungLUMP3,0.0)  !
clungtLUMP3=alungtLUMP3/vlu !
caLUMP3 = clungtLUMP3/pluLUMP3

!
CA1LUMP3 = (QC*CvLUMP3+Qp*CivLUMP3)/(QC+(QP/PBLUMP3))
      CXLUMP3 = CA1LUMP3/PBLUMP3
      rAXLUMP3 = QP*CXLUMP3
```

```
axLUMP3=integ(raxLUMP3,0.0)
CXPPMlump3=(0.7*cxlump3+0.3*cilump3)*24450/MWlump3

AtpuLUMP3 =alungtLUMP3 ! removed mucus



!Lung Compartment Mass Balance
mblungsLUMP3 = (alunglost2LUMP3+alunginLUMP3) - (alungtLUMP3+alungoutLUMP3)!-(alunglost4)
rlunginLUMP3=qc*ca1LUMP3
alunginLUMP3=integ(rlunginLUMP3,0.0)
rlungoutLUMP3=qc*caLUMP3
alungoutLUMP3=integ(rlungoutLUMP3,0.0)
rlunglost2LUMP3=pa1LUMP3*clmucousLUMP3
alunglost2LUMP3=integ(rlunglost2LUMP3,0.0)
rlungvaporLUMP3=QP*CIVLUMP3
alungvaporLUMP3=integ(rlungvaporLUMP3,0.0)

!{RAPID}
!Chemical in rapidly perfused tissue compartment (Perfusion)
 RARLUMP3 = QR*(caLUMP3-CVRLUMP3)                    !rate of change in rapidly perfused - mg/h
   ARLUMP3 = integ(RARLUMP3, 0.0)          !inital amount in viscera - mg
 CRLUMP3= ARLUMP3/VR                       !viscera concentration - mg/L
 CVRLUMP3 = CRLUMP3/PRLUMP3                    !concentration in venous capillary blood - mg/L

!Rapid Compartment Mass Balance
rapidmassbalLUMP3=(arapidinLUMP3)-(ARLUMP3+arapidoutLUMP3)
rarapidinLUMP3=qr*caLUMP3
arapidinLUMP3 = integ(rarapidinLUMP3,0.0)
rarapidoutLUMP3=qr*cvrLUMP3
arapidoutLUMP3=integ(rarapidoutLUMP3,0.0)
```

```
!{SLOW}
!Chemical in slowly perfused tissue compartment (Perfusion)
 RASLUMP3 = QS*(caLUMP3-CVSLUMP3)                    !rate of change in slowly perfused  - mg/h
   ASLUMP3 = integ(RASLUMP3, 0.0)              !inital amount in slowly perfused tissue - mg
 CSLUMP3 = ASLUMP3/VS                          !slowly perfused tissue concentration - mg/L
 CVSLUMP3 = CSLUMP3/PSLUMP3                        !concentration in venous blood - mg/L

!Slow Compartment Mass Balance
slowmassbalLUMP3=(aslowinLUMP3)-(ASLUMP3+aslowoutLUMP3)
raslowinLUMP3=qs*caLUMP3
aslowinLUMP3 = integ(raslowinLUMP3,0.0)
raslowoutLUMP3=qs*cvsLUMP3
aslowoutLUMP3=integ(raslowoutLUMP3,0.0)

!{BRAIN}
!chem brain blood (Diffusion)
RABrbLUMP3 = ((QBr*(caLUMP3-CVBrLUMP3)) - (PABrinLUMP3*CVBrLUMP3) +
(PABroutLUMP3*(CBrLUMP3/PBrLUMP3)))  !rate of change in brain blood amount - mg/h made 1st + not
  ABrbLUMP3 = integ(RABRbLUMP3, 0.0)                  !initial amount in blood - mg
 CVBrLUMP3 = ABrbLUMP3/Bvbr                          !concentration in brain blood
!chem in brain tissue (Diffusion)
RABrLUMP3 = (PABrinLUMP3*CVBrLUMP3) - (PABroutLUMP3*(CBrLUMP3/PBrLUMP3))          !rate of change in brain
tissue
   ABrLUMP3 = integ(rABrLUMP3, 0.0)                 !initial amount in tissue
 CBrLUMP3 = ABrLUMP3/(VBr-Bvbr)                     !concentration in brain tissue
abrtotLUMP3= abrLUMP3+abrbLUMP3                          !total brain

!Brain Compartment Mass Balance
brainmassbalLUMP3=(abraininLUMP3+abraindiffinLUMP3)-(AbrLUMP3+abrainoutLUMP3+abraindiffoutLUMP3)
!brainmassbal=(abrainin)-(Abr+abrainout)
rabraininLUMP3=qbr*caLUMP3
abraininLUMP3 = integ(rabraininLUMP3,0.0)
rabrainoutLUMP3=qbr*cvbrLUMP3
```

```
abrainoutLUMP3=integ(rabrainoutLUMP3,0.0)
rabraindiffinLUMP3 =(PABrinLUMP3*CVBrLUMP3)
abraindiffinLUMP3 =integ (rabraindiffinLUMP3,0.0)
rabraindiffoutLUMP3= PABroutLUMP3*(CBrLUMP3/PBrLUMP3)
abraindiffoutLUMP3=integ(rabraindiffoutLUMP3,0.0)


!{FAT}
!chem in fat blood (Diffusion)
RAFbLUMP3 = (QF*(caLUMP3-CVFLUMP3) - (PAFinLUMP3*CVFLUMP3) + (PAFoutLUMP3*(CFLUMP3/PFLUMP3)))  !
AFbLUMP3 = integ(RafbLUMP3,0.0)                    !initial amount in blood - mg
CVFLUMP3 = AFbLUMP3/Bvf                            !concentration in fat blood

!chem in shall fat tissue (Diffusion)
RAFLUMP3 = (PAFinLUMP3*CVFLUMP3) - (PAFoutLUMP3*(CfLUMP3/PfLUMP3))!
AFLUMP3 = integ(RafLUMP3,0.0)                      !initial amount in fat
CFLUMP3 = AfLUMP3/(vf-bvf)                         !concentration in fat tissue
aftotLUMP3=afLUMP3+afbLUMP3                              !total fat amount

!Fat Compartment 1 Mass Balance
fatmassbalLUMP3=(afatinLUMP3+afatdiffinLUMP3)-(AFLUMP3+afatoutLUMP3+afatdiffoutLUMP3)
rafatinLUMP3=qf*caLUMP3
afatinLUMP3 = integ(rafatinLUMP3,0.0)
rafatoutLUMP3=qf*cvfLUMP3
afatoutLUMP3=integ(rafatoutLUMP3,0.0)
rafatdiffinLUMP3 =(PAfinLUMP3*CVfLUMP3)
afatdiffinLUMP3 =integ (rafatdiffinLUMP3,0.0)
rafatdiffoutLUMP3= PAfoutLUMP3*(CfLUMP3/PfLUMP3)
afatdiffoutLUMP3=integ(rafatdiffoutLUMP3,0.0)


!chem in liver tissue (Diffusion) shall
```

```
rALLUMP3 = QL*(CaLUMP3-cvlLUMP3)+(PALinLUMP3*(CdLLUMP3/PdL2bLUMP3))-
PALoutLUMP3*(clLUMP3/(plaLUMP3/pfaLUMP3)) - RAMETLUMP3!!
ALLUMP3 = integ(RalLUMP3, 0.0)                          !initial amount in liver
 CLLUMP3 = ALLUMP3/(vsl)      !-bvl                        !concentration
cvlLUMP3=clLUMP3/plLUMP3

!chem in liver tissue (Diffusion) deep
radlLUMP3 = -(PALinLUMP3*(CdLLUMP3/PdL2bLUMP3))+PALoutLUMP3*(clLUMP3/(plaLUMP3/pfaLUMP3))
adlLUMP3= integ (radlLUMP3, 0)
cdlLUMP3 = adlLUMP3/vdl

! tot
altotLUMP3=alLUMP3+adlLUMP3

!Liver Compartment Mass Balance
livermassbalLUMP3=(aliverinLUMP3+aliverdiffinLUMP3)-(AlLUMP3+aliveroutLUMP3+aliverdiffoutLUMP3+ametLUMP3)
raliverinLUMP3=ql*caLUMP3
aliverinLUMP3 = integ(raliverinLUMP3,0.0)
raliveroutLUMP3=ql*cvlLUMP3
aliveroutLUMP3=integ(raliveroutLUMP3,0.0)

raliverdiffinLUMP3 =(PAlinLUMP3*(CdLLUMP3/PdL2bLUMP3))
!raliverdiffin=(PALin*(CL/pl))
aliverdiffinLUMP3 =integ (rafatdiffinLUMP3,0.0)

raliverdiffoutLUMP3= PAloutLUMP3*(ClLUMP3/(PlaLUMP3/pfaLUMP3))
!raliverdiffout=(PALout*(CdL/PdL2b))
aliverdiffoutLUMP3=integ(raliverdiffoutLUMP3,0.0)



!Mass balance for c14 inhalation
```

```
  MassLUMP3  = AFtotLUMP3 + ASLUMP3 + ARLUMP3 + ALtotLUMP3+ ABrtotLUMP3 + axLUMP3 + AtpuLUMP3
+atnoLUMP3 + AMetLUMP3!
  !mb    = ainhale - mass

mb5LUMP3=(alunglost2LUMP3+anaslost2LUMP3+alungvaporLUMP3)-massLUMP3




!--------------------[METABOLISM]----------------------------------------------------
!Octane
        RAMetc8 = (VMaxc8*CvLc8)/(CVLc8+ (Kmc8*chkmmc8LUi))
                AMetc8 = integ (RAMetc8, 0.0)

        chKmMC8LUi=1+((CVLtol/KiTL)+(CVLebz2008/KiEBZ)+(CVLmx2008/KiMX)+(CVLlp/KiLP)+(cvl/Ki)+(cvlump/KiLU
MP)+(cvlLUMP3/KiLUMP3)+(cvlC14/KiC14))

!Decane
        RAMet = (VMax*CvL)/(CVL+ (Km*chkmmc10LUi))
                AMet = integ (RAMet, 0.0)

        chKmMC10LUi=1+((CVLtol/KiTL)+(CVLebz2008/KiEBZ)+(CVLmx2008/KiMX)+(CVLlp/KiLP)+(cvlc8/KiC8)+(cvlump/
KiLUMP)+(cvlLUMP3/KiLUMP3)+(cvlC14/KiC14))

          !Lump 1
          RAMlp=(Vmaxlp*CVLlp)/(Kmlp*chKmlpi+CVLlp)
                  AMlp=INTEG(RAMlp,0.)


chKmLPi=1+((CVLebz2008/KiEBZ)+(CVLmx2008/KiMX)+(CVL/Ki)+(CVLtol/KiTL)+(cvlc8/KiC8)+(cvlLUMP/KiLUMP)+(cvlL
UMP3/KiLUMP3)+(cvlC14/KiC14)

!Shep, Lump 2
```

```
RAMetLUMP=(VmaxLUMP*CVLLUMP)/(KmLUMP*chKmLUMPi+CVLLUMP)
        AMLUMP=INTEG(RAMetLUMP,0.)

chKmLUMPi=1+((CVLebz2008/KiEBZ)+(CVLmx2008/KiMX)+(CVL/Ki)+(CVLtol/KiTL)+(CVLlp/KiLP)+(cvlc8/KMC8)+
(cvlLUMP3/KiLUMP3)+(cvlC14/KiC14))

! inhib m-xyl
RAM1mx2008=(Vmaxmx*CVLmx2008)/(Kmmx*chKmmx2008i+CVLmx2008)
        AM1mx2008=INTEG(RAM1mx2008,0.)

chKmMX2008i=1+((CVLebz2008/KiEBZ)+(CVL/Ki)+(CVLtol/KiTL)+(CVLlp/KiLP)+(cvlc8/KiC8)+(cvlump/KiLUMP)+(cvlLUM
P3/KiLUMP3)+(cvlC14/KiC14))


! EBZ inhib

RAMebz2008=(Vmaxebz*CVLebz2008)/(Kmebz*chKmebzi2008+CVLebz2008)
        AMebz2008=INTEG(RAMebz2008,0.)

chKmEBZi2008=1+((CVL/Ki)+(CVLmx2008/KiMX)+(CVLtol/KiTL)+(CVLlp/KiLP)+(cvlc8/KiC8)+(cvlump/KiLUMP)+
(cvlLUMP3/KiLUMP3)+(cvlC14/KiC14))

! TOL inhib
 RAMtol=(Vmaxtl*CVLtol)/(Kmtl*chKmtoli+CVLtol)
        AMtol=INTEG(RAMtol,0.)

chKmTOLi=1+((CVLebz2008/KiEBZ)+(CVLmx2008/KiMX)+(CVL/Ki)+(CVLLUMP3/KiLUMP3)+(CVLlp/KiLP)+(cvlc8/KiC8)+
(cvlump/KiLUMP)+(cvllump1/KiLUMP1)+(cvlC14/KiC14))

! SHEP C14 inhib
  RAMetC14=(VmaxC14*CVLC14)/(KmC14*chKmC14i+CVLC14)
        AMetC14=INTEG(RAMetC14,0.)
```

```
chKmC14i=1+((CVLebz2008/KiEBZ)+(CVLmx2008/KiMX)+(CVL/Ki)+(CVLtol/KiTL)+(CVLlp/KiLP)+(cvlc8/KiC8)+(cvlump/Ki
LUMP)+(cvLLUMP3/KiLUMP3))

! SHEP Lump 3 inhib
  RAMetLUMP3=(VmaxLUMP3*CVLLUMP3)/(KmLUMP3*chKmLUMP3i+CVLLUMP3)
                    AMetLUMP3=INTEG(RAMetLUMP3,0.)

chKmLUMP3i=1+((CVLebz2008/KiEBZ)+(CVLmx2008/KiMX)+(CVL/Ki)+(CVLtol/KiTL)+(CVLlp/KiLP)+(cvlc8/KiC8)+(cvlum
p/KiLUMP)+(cvlC14/KiC14))



END ! DERIVATIVE


                    ! Add discrete events here as needed
                    !  DISCRETE
                    !  END

                    ! code that is executed once at each communication interval goes here

                    CONSTANT TSTOP =8

                    TERMT (T .GE. TSTOP, 'ch2ecked on communication interval: REACHED TSTOP')

          END ! DYNAMIC


          TERMINAL
                    ! code that is executed once at the end of a simulation run goes here
          END ! TERMINAL
END ! PROGRAM
```

APPENDIX B. Generic Example of an m-file

(Note: data and concentration values not included, as they change per m-file of interest)

```
%m-file to run marker chemical model either alone or in the presence of hydrocarbon mixtures
%Sheppard A. Martin, Jeffrey W. Fisher

prepare t cvtol
%Exposure Concentrations
ICONITOL=X
ICONIEBZ2008=X
ICONIMX2008=X
ICONI=X  !c10
ICONIC8=X
ICONIC14=X
ICONILP=X
ICONILUMP=X
ICONILUMP3=X

%KI Terms
KIMX = X
KIEBZ = X
KITL = X
KILP = X
KIC8=X
KI    = X
KIC14    = X
KILUMP=X
KILUMP3=X
```

%Percent Aerosol and Vapor
%TOL
PERC_AEROSOLTOL =X
PERC_VAPORTOL =X

%EBZ
PERC_AEROSOLEBZ2008 =X
PERC_VAPOREBZ2008 = X

%m-XYLENE
PERC_AEROSOLMX2008 =X
PERC_VAPORMX2008 = X

% LUMP 1
PERC_AEROSOLLP =X
PERC_VAPORLP = X

% LUMP 2
PERC_AEROSOLLUMP =X
PERC_VAPORLUMP =X

% LUMP 3
PERC_AEROSOLLUMP3 =X
PERC_VAPORLUMP3 =X

%C8
PERC_AEROSOLC8 =X
PERC_VAPORC8 =X

%C10
PERC_AEROSOL =X
PERC_VAPOR =X

```
%C14
PERC_AEROSOLC14 =X
PERC_VAPORC14 =X

%Fractional Deposition
 FDEPOSITPU   =X
 FDEPOSITTB = X
 FDEPOSITNO   = X

TCHNG=4
EXPTIME=8
TSTOP=6

start @nocallback
cvtol_tol_UGA=[0 0 0 0 0 0
X       X       X       X       X       X
X       X       X       X       X       X
X       X       X       X       X       X
X       X       X       X       X       X
X       X       X       X       X       X
X       X       X       X       X       X
];

plot(_t,_cvtol,cvtol_tol_UGA(:,1),cvtol_tol_UGA(:,2), '+',cvtol_tol_UGA(:,3),cvtol_tol_UGA(:,4), '+',
cvtol_tol_UGA(:,5),cvtol_tol_UGA(:,6),'+', 'settingsTOL-BL.aps')
```